Controlled synchronization in networks of diffusively coupled dynamical systems

Controlled Synchronization in Networks of Diffusively Coupled Dynamical Systems

Carlos Gerardo Murguía Rendón

The research reported in this thesis is part of the research program of the Dutch Institute of Systems and Control (DISC). The author has successfully completed the educational program of the Graduate School DISC.

This research was partially supported by the National Council of Science and Technology (CONACYT) México.

A catalogue record is available from the Eindhoven University of Technology Library.
ISBN:978-90-386-3847-8

Cover Design: Donovan Alejandro Rodriguez.
Reproduction: Ipskamp Drukkers B.V., Enschede, The Netherlands.

Controlled Synchronization in Networks of Diffusively Coupled Dynamical Systems

PROEFSCHRIFT

ter verkrijging van de graad van doctor aan de
Technische Universiteit Eindhoven, op gezag van de
rector magnificus, prof.dr.ir. F.P.T. Baaijens, voor een
commissie aangewezen door het College voor
Promoties, in het openbaar te verdedigen
op maandag 18 mei 2015 om 16.00 uur

door

Carlos Gerardo Murguía Rendón

geboren te Mexico City, Mexico

Dit proefschrift is goedgekeurd door de promotoren en de samenstelling van de promotiecommissie is als volgt:

voorzitter	:	prof.dr. L.P.H. de Goey
promotor	:	prof.dr. H. Nijmeijer
copromotor	:	dr.ir. R.H.B. Fey
leden	:	prof.dr. C. van Leeuwen (Katholieke Universiteit Leuven)
	:	prof.dr. L. Marconi (Universita di Bologna)
	:	prof.dr. C. De Persis (Rijksuniversiteit Groningen)
	:	prof.dr. N. van de Wouw
	:	prof.dr. R.A. van Santen

Dedicated to my family:

Lupita, Mario, Paty, Lore, and Quique

To my beloved:

Laura

Contents

Summary

Controlled Synchronization in Networks of Diffusively Coupled Dynamical Systems

There are, at least, two crucial elements to be considered when studying synchronization in networks of dynamical systems. First, the dynamics of the individual systems; for instance, their input-output stability properties or their degree of homogeneity. Secondly, the exchange of information among the systems, i.e., how the systems in the network communicate information about their state to the systems they are connected to. This thesis studies the relation of these two elements to the occurrence of synchronous behavior in networks of coupled dynamical systems. Particularly, for some classes of systems, we investigate what network structures and coupling functions lead to synchronization of the interconnected systems. Additionally, because of the time needed to transmit data over the network, the use of networked communication to exchange information among the systems results in unavoidable time-delays. We analyze the effect of these networked-induced delays in the proposed synchronization schemes.

Firstly, we focus on synchronization in networks of *linear time-invariant systems*. Each system in the network is assumed to be *passive* and *detectable* with respect to the coupling variable (the measurable output). The systems are *time-delayed diffusively coupled*, i.e., they are coupled through weighted time-delayed differences of their outputs. Using the passivity property of the individual systems and Lyapunov-Krasovskii functionals, we derive conditions which ensure *ultimate boundedness* of the solutions of the coupled systems. Then, using the detectability assumption, we prove that under some mild conditions there always exists a region, referred to as the *synchronization region*, in the parameter space (coupling strength versus time-delay) such that if these parameters

belong to the region, the systems synchronize. Next, we propose *predictor-based diffusive dynamic couplings* to increase the time-delay that can be induced to the systems without compromising the synchronous behavior, i.e., by including predictors in the couplings, we prove that the synchronization regions may be increased. Additionally, we propose *observer-based diffusive dynamic couplings* to extend the class of systems under study. We show that by including observers in the loop, it is possible to remove the passivity assumption on the measurable output as long as this holds with respect to a different output function.

Secondly, we extend some of these results for a class of nonlinear systems. The notions of passivity and detectability of linear systems are replaced by *semipassivity* and *convergence* of the nonlinear case. We do not assume semipassivity plus convergence with respect to the measurable output, but this is supposed to hold with respect to a different output function which is not directly measured. However, if there exists a nonlinear observer which estimates the semipassive output from measurements of the available output, it can be used to construct an *observer-based diffusive dynamic coupling* to interconnect the systems. We develop a general tool for constructing the observer dynamics using ideas of *immersion and invariance*. Sufficient conditions on the systems, the couplings, the *convergence rate* of the observer, and the time-delays that guarantee boundedness of the solutions and synchronization of the coupled systems are derived.

We also study the possible emergence of *partial synchronization*. Partial synchronization is a phenomenon, in which some, at least two, systems in the network synchronize with each other but not with every system in the network. Using symmetries in the network, we identify linear invariant manifolds of the coupled systems. If these manifolds are attracting, the systems in the network may exhibit partial synchronization. We prove that a linear invariant manifold defined by a symmetry in the network is attracting, if the interaction among the systems is sufficiently strong and the rate of convergence of the observer is sufficiently fast. Next, we present a result on network synchronization in the case when the measurements of the outputs and the transmission of the controllers are subject to different time-delays. *Predictor-based diffusive dynamic couplings* based on the concept of *anticipating synchronization* are proposed to interconnect the systems. We show that these couplings are capable of increasing the time-delay that can be induced to the systems without compromising the synchronous behavior, i.e., by including the predictors, it is possible to significantly increase *the synchronization region*.

In the third part of the thesis, we present a set of experimental results on network synchronization using *static diffusive couplings* with time-delays. We employ an experimental setup with electronic circuit realizations of the Hindmarsh-Rose neuron model. Nevertheless, it is important to notice that in practical situations, the dynamics of the systems in the network cannot be expected to be perfectly identical. For instance, because the signals exchanged among the systems are contaminated with noise and/or there are small mismatches in the systems' parameters. Because of these inherent imperfections, we can not expect that the differences between the states of systems converge to zero. It is necessary to allow for a mismatch between them, which, of course, needs to be small enough in order to consider that the systems are "*practically synchronized*". To this end, we introduce the notion of *practical (partial) synchronization*, which states that the circuits may be called (partially) synchronized if the differences between their outputs are sufficiently small on a finite, long time-interval. First, practical synchronization of two diffusively coupled electronic Hindmarsh-Rose circuits is discussed. Next, we present three experimental studies on partial practical synchronization. Finally, we experimentally study the relation between the conditions for synchronization of symmetrically coupled systems and the network topology.

Chapter 1

Introduction

Abstract. The synchronization phenomenon, some historical notes, and practical applications of synchronization are introduced first in this chapter. Then, the objectives of the thesis, some technical preliminaries employed throughout the manuscript, and the used mathematical framework are presented. The chapter also discusses the motivation for this thesis and a detailed outline of the main contributions. The chapter ends with a list of the author's publications.

1.1 The Synchronization Phenomenon

The word synchronization is derived from the word "*synchronous*" which is originated from the Greek roots χρόνος (chronos, meaning time) and σύν (syn, meaning the same or common). Then, in a direct translation, "*synchronous*" means "*occurring at the same time*". Synchronization can be defined as a process in which "*events*" keep happening simultaneously for an extended period of time [139]. The emergence of synchronization in coupled dynamical systems is a fascinating topic in various scientific disciplines ranging from biology, physics, and chemistry to social networks and technological applications. The scientific interest in these phenomena can be traced back to Christiaan Huygens' seminal work *"an odd kind of sympathy"* between pendulum clocks, cf. [54, 102], and it continues to fascinate the scientific community to date. In 1665, the Dutch scientist, inventor of the pendulum clock, Christiaan Huygens, reported on *in-phase* and *anti-phase* synchronization of two pendulum clocks [54], see Figure 1.1. The description of the experiment, together with Huygens' explanation of the *sympathy of the clocks* is remarkable, since, at that time, differential calculus was still in its infancy. It was until the end of the 17^{th} century when Newton laid down the formal aspects of this theory. Huygens explained that the beam to which the clocks are attached serves as the medium for the possible emergence of anti-phase or in-phase synchroniza-

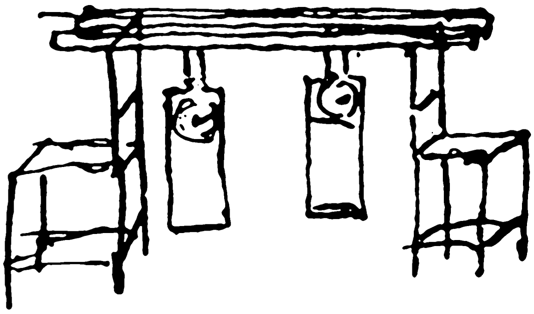

Figure 1.1 Original drawing of Christiaan Huygens illustrating his experiments with two pendulum clocks placed on a common support [54].

tion of the two pendulum clocks. Nowadays, a more accurate phrasing would be that the beam provides energy transfer from one clock to the other (and vice versa) through the beam. It is interesting to remark at this point that even today a complete mathematical theory describing the in-phase and anti-phase synchronous behavior of the two pendulum clocks is still missing. Some difficulties in this respect are the modeling of both the damping and the escapement mechanism and the particular nature of the beam that should be modeled as being flexible, thus making the overall model a combination of ordinary and partial differential equations [95, 96, 97, 98].

From the time of Huygens on, synchronous behavior among coupled dynamical systems has been encountered and investigated in many areas of science and engineering. For instance, in biology, clusters of synchronized pacemaker neurons regulating our heartbeat [101], synchronized neurons in the olfactory bulb that allow us to detect and distinguish among odors [45], and our circadian rhythm, which is synchronized to the 24-h day-night cycle [33, 145] are clear examples. In the animal kingdom, synchronized motion of bird flocks and fish schools, thousands of fireflies flashing simultaneously, synchronized attacks of killer whales, and groups of Japanese tree frogs (Hyla japonica) showing synchronous behavior in their calls are examples of *synchronized collective animal behavior*, see for instance [13, 62, 102, 139]. Animals in groups employ decentralized strategies and have limitations on sensing, computation, and actuation. Yet, at the level of the group, they are known to manage a variety of challenging tasks quickly, robustly, accurately, and adaptively in uncertain and changing environments. As pointed out by the authors in [62], nonlinear dynamics and control theory can be used to rigorously investigate mechanisms of feedback and interaction in high-performing animal groups. These tools can be translated into adaptive control laws for engineered applications. The study of synchronized motion in networks of individual mobile agents is receiving a rapidly growing interest in engineering [92, 103, 113, 123, 128]. Particularly, in [103, 123, 128], the authors address the *platooning problem*, i.e., the problem of designing intelligent vehicle/highway systems that can significantly increase safety and highway capacity. The general objective of the platooning problem is to pack the driving vehicles together as tightly as possible (with synchronized velocity, acceleration, braking, and steering) in order to increase traffic flow while preventing amplification of disturbances throughout the string. There are also several research groups studying synchronization in robotics, where multiple robots carry out tasks that cannot be achieved by a single one. For instance in [85, 116], the authors study synchronization of teleoperated systems, where one master system *guides* a slave system along the desired paths. Teleoperation is of use in various settings and contexts, like for instance, long distance tasks (e.g., cleaning at unsafe or inaccessible places or exploration at Mars), where the communication time-delay seriously challenges simple control schemes [38]. In other teleoperated tasks the challenge is extended with typical aspects regarding the human (at the master robot) and the environment (at the slave robot) [38, 50, 66]. In industrial applications like a distribution center or a luggage handling system at an airport, a (virtual) supervisor may assign tasks at a high level, and the *holons*, or robots in the distribution center have to arrange themselves in a synchronous manner such that the tasks are executed. Building such an environment, with sufficient room for optimal or sub-optimal performance, is an extremely interesting and challenging objective [9, 10, 11]. The range of engineering examples of network synchronization reaches beyond coordinated motion. For instance, control of the directional sensitivity of smart antennas [53] and synchronization of microelectromechanical systems (MEMS), which has promising applications such as neurocomputing [52] and improvements of signal-to-noise ratios [12].

Other applications are potentially foreseen in the *system of systems* context of which energy management (synchronization in power networks [39]) and the internet are a few examples. The goal in applications in such cases is often to achieve synchronous behavior with preferably a decentralized control structure where only neighbors' information is used in the feedback. Indeed, synchronous behavior of such a *system of systems* can be realized as a network synchronization problem. A key ingredient is that the systems in the network "*communicate*" information about their state to the systems they are connected to. This exchange of information may ultimately result in synchronization. The question is how the systems in the network should be connected and respond to the received information to achieve synchronous behavior. In other words, which network structures and what coupling functions lead to synchronization of the systems? Several more examples of synchronous behavior in physics, biology, and engineering can be found in, for instance, [27, 102, 139, 145] and references therein.

1.2 Controlled Synchronization

In this section, we formulate a coordinate-dependent definition of synchronization. This definition is a particular case of the coordinate-free definition given in [26]. Consider a network consisting of k input-output dynamical systems described by the following ordinary differential equations

$$\Sigma_{y_i} : \begin{cases} \dot{x}_i = f_i(x_i, u_i, t), \\ y_i = h_i(x_i, t), \quad i = 1, \ldots, k, \end{cases} \tag{1.1}$$

with state $x_i \in \mathbb{R}^{n_i}$, input $u_i \in \mathbb{R}^{m_i}$, output $y_i \in \mathbb{R}^{s_i}$, and functions $f_i : \mathbb{R}^{n_i} \times \mathbb{R}^{m_i} \times \mathbb{R} \to \mathbb{R}^{n_i}$ and $h_i : \mathbb{R}^{n_i} \times \mathbb{R} \to \mathbb{R}^{s_i}$. The interconnection among the systems is given through the input terms u_i. It is assumed that these terms are the outputs of some dynamical systems representing the dynamics of the couplings, i.e.,

$$\Sigma_{u_i} : \begin{cases} \dot{\eta}_i = \mathcal{N}_i(\eta_1, \ldots, \eta_k, y_1, \ldots, y_k, t), \\ u_i = \mathcal{U}_i(\eta_1, \ldots, \eta_k, y_1, \ldots, y_k, t), \quad i = 1, \ldots, k, \end{cases} \tag{1.2}$$

with state $\eta_i \in \mathbb{R}^{p_i}$, and functions $\mathcal{N}_i : \mathbb{R}^{p_1} \times \ldots \times \mathbb{R}^{p_k} \times \mathbb{R}^{s_1} \times \ldots \times \mathbb{R}^{s_k} \times \mathbb{R} \to \mathbb{R}^{m_i}$ and $\mathcal{U}_i : \mathbb{R}^{p_1} \times \ldots \times \mathbb{R}^{p_k} \times \mathbb{R}^{s_1} \times \ldots \times \mathbb{R}^{s_k} \times \mathbb{R} \to \mathbb{R}^{m_i}$. These dynamic couplings must satisfy the communication structure of the network, i.e., the functions $\mathcal{N}_i(\cdot)$ and $\mathcal{U}_i(\cdot)$ can only be constructed using the outputs of systems that are directly connected to system i in the communication network, see Figure 1.2.

Definition 1.1. *The k systems* (1.1) *interconnected through the dynamic couplings* (1.2) *are said to asymptotically synchronize (or simply synchronize) if the solutions of the coupled systems are well defined and $x_i(t) \to x_j(t)$ as $t \to \infty$ for all i, j.*

At this point, we distinguish two possibilities. On the one hand, if the coupling functions $\mathcal{N}_i(\cdot)$ and $\mathcal{U}_i(\cdot)$ are given, then the synchronization problem is one of *analysis*, i.e., for specific coupling functions, we study the possible emergence of synchronization of the coupled systems (1.1),(1.2). On the other hand, a more general case is when one should *synthesize* control algorithms to ensure synchronization. Designing coupling functions and/or network structures that lead to synchronization of the coupled systems is referred to as *controlled synchronization*.

Controlled synchronization has been extensively investigated in the literature. In particular, the study of synchronization in networks of *diffusively coupled systems* has received a lot attention, see, e.g., [20, 22, 23, 47, 91, 104, 132, 147, 151]. The k systems (1.1) are said to be *diffusively coupled*, if they interact through weighted differences of the form

$$u_i = \gamma \sum_{j \in \mathcal{E}_i} a_{ij}(y_j - y_i), \quad i = 1, \ldots, k, \tag{1.3}$$

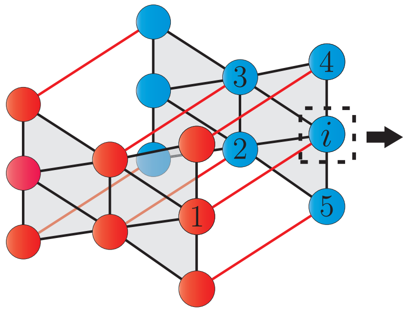

$$\begin{cases} \dot{x}_i = f_i(x_i, u_i, t), \\ y_i = h_i(x_i, t), \end{cases}$$

$$\begin{cases} \dot{\eta}_i = \mathcal{N}_i(\eta_1, \ldots, \eta_5, y_1, \ldots, y_5, t), \\ u_i = \mathcal{U}_i(\eta_1, \ldots, \eta_5, y_1, \ldots, y_5, t), \end{cases}$$

Figure 1.2 Network of coupled input-output dynamical systems.

where y_j denotes the output of a system j that is connected to system i, γ is a positive constant referred to as *the coupling strength*, $a_{ij} \geq 0$ are the weights of the interconnections, and $\mathcal{E}_i$ denotes the set of all systems j that are connected to system i. Moreover, since the coupling strength is encompassed in the constant γ, it is often assumed without loss of generality that $\max_{i \in \mathcal{I}} \sum_{j \in \mathcal{E}_i} a_{ij} = 1$.

Diffusive interaction is an important type of coupling. It is found in many fields of science and technology, e.g., networks of coupled neurons [24, 63, 93, 100, 126, 146], networks of biological systems [13, 33, 45, 62, 101, 139, 145], coupled mechanical systems [85, 86, 87, 116, 149], and electrical systems [12, 52, 82, 117]. For this reason, there are several technical results about synchronization in networks of *diffusively coupled* dynamical systems. For instance, in [19, 20, 22], the relation between synchronization in networks of coupled nonlinear systems and the network topology is investigated. A general method to determine the minimum coupling strength needed to achieve global synchronization is proposed. The derived bounds are explicitly linked with the average path length of the associated graph. In [47, 104, 147], the authors study synchronous behavior in *diffusively coupled networks* as a consequence of the inherent *dissipation* on the systems and the couplings. More recently, in [55], the output synchronization problem for networks of diffusively coupled heterogeneous nonlinear systems is considered. The authors apply nonlinear output regulation theory to force the output of each system of the network to robustly track the output of a prescribed nonlinear exosystem. In [35], the role of the internal model principle is investigated for the study of synchronization of relative-degree-one nonlinear systems. Assuming that the systems are incrementally (output-feedback) passive, the authors propose internal-model-based distributed control laws which guarantee output synchronization to an invariant manifold driven by autonomous synchronized internal models. The synchronization problem for a class of linear time-invariant systems interacting on time-varying topologies and interconnected through *observer-based diffusive dynamic couplings* is considered in [119, 144]. Using incremental dissipativity theory, the authors in [49] derive conditions on the coupling strength to achieve synchronization in networks of systems having a cyclic feedback structure. The method takes advantage of the incremental passivity properties of the subsystems in the network to reformulate the synchronization problem as one of achieving incremental stability by coupling. For a broad class of coupled nonlinear oscillators, in [40], a novel condition on the coupling functions ensuring network synchronization is presented. This condition can be stated in terms of the parameters of the individual subsystems and the topology of the underlying network. In [121], the authors develop analytical and numerical conditions to determine whether limit cycle oscillators synchronize in diffusively coupled networks. Two classes of systems are considered: reaction diffusion PDEs with Neumann boundary conditions, and compartmental ODEs, where compartments are interconnected through diffusion terms with adjacent compartments. The authors provide two time-scale averaging methods for certifying stability of spatially homogeneous time-periodic trajectories in the presence of sufficiently small or large diffusion and develop methods using structured singular values for the case of intermediate diffusion.

There are also some results addressing the problem of controlled synchronization of nonlinear systems interconnected through *diffusive time-delayed couplings*. This type of couplings arise naturally for interconnected systems since the transmission of signals can be expected to take some time. For instance, in [86, 87], the authors propose an *adaptive diffusive coupling* which solves the network synchronization problem for dynamical systems described by Euler-Lagrange equations and subject to time-delays. The authors in [91] give sufficient conditions for network synchronization in terms of Linear Matrix Inequalities (LMIs) for a class of nonlinear systems interconnected through *Pyragas-type* [110] time-delayed couplings. In [132], the authors consider the problem of network synchronization of diffusively time-delayed coupled *semipassive systems*. They prove that under some mild conditions, there always exists a region $\mathcal{S}$ in the parameter space (coupling strength γ versus time-delay τ) such that if $(\gamma, \tau) \in \mathcal{S}$, the systems synchronize. We refer the interested reader to [102, 140], the special issues [1, 2, 3, 4, 5, 6, 7, 8], and the references therein, where more recent results about controlled synchronization in networks of coupled dynamical systems can be found.

1.3 Objectives

This thesis aims to provide new insights into the study of synchronization in networks of coupled dynamical systems by means of analytical, numerical, and experimental analyses. Particularly, the purpose is to exploit some mathematical tools available in the literature to obtain results that are beyond the current understanding. The general objective of the thesis is to provide answers to the following questions: Given a set of input-output dynamical systems interacting on graphs with general topologies, what network structures and coupling functions lead to synchronization of the interconnected systems? Additionally, what is the effect of possible network-induced delays in the proposed synchronization schemes? And, is it possible to modify such an effect in order to increase robustness against time-delays in the network?

The authors in [104, 108] introduce a mathematical framework to analyze synchronization in networks of *diffusively coupled systems*. In this framework, it is assumed that each system has a property called *semipassivity*. A semipassive system is a system whose state trajectories remain bounded provided that the supplied energy is bounded[1]. Under this assumption, the authors prove that the solutions of diffusively coupled semipassive systems are ultimately bounded. Moreover, if the internal dynamics associated with the semipassive outputs are *exponentially convergent*[2], then there always exists a threshold such that if the coupling strength exceeds this threshold, the systems synchronize. This thesis extends the ideas presented in [104, 108]. Particularly, using the semipassivity-based framework, we study cases where the static diffusive couplings considered in [104, 108] fail to induce synchronization in networks of coupled systems. We propose different classes of couplings (both static and dynamic) to solve some particular problems of controlled synchronization.

The first situation to be considered is when the semipassive outputs are not available for feedback. If the measurable outputs are different state functions which do not have the desired properties (semipassivity and exponentially convergent internal dynamics), the results presented in [104, 108] cannot be applied. The first particular objective of the thesis is to design coupling functions that are capable of inducing network synchronization in this case. Such couplings must be constructed using the measurable non-semipassive outputs, the network structure, and the possible network-induced delays. On the one hand, general tools for constructing these coupling functions should be provided. On the other hand, we ought to guarantee that the solutions of the coupled systems exist and are ultimately bounded.

[1] A formal definition of semipassivity is presented in Section 1.4.2.
[2] Details are provided in Section 1.4.3.

The second objective is to design couplings which may enhance robustness against time-delays of the interconnected systems, i.e., these couplings must be capable of increasing the amount of time-delay that can be induced to the systems without compromising the synchronous behavior. We study the case when the measurements of the outputs and the transmission of the controllers are subject to different time-delays. The coupling functions must *predict* the future values of the semipassive outputs to compensate for the network-induced delays. We should guarantee that the designed couplings lead to ultimately bounded solutions of the interconnected systems.

Last but not least, the third particular objective is to illustrate some theoretical results by means of an experimental study. Particularly, in networks of *diffusively time-delayed coupled semipassive systems*, it is desired to test the theoretical results about *full synchronization*, *partial synchronization*, and *synchronization in relation to the network topology* presented in [132], [133], and [130], respectively. The goal is to verify the predictive value of these results using an experimental setup built around electronic circuit realizations of the Hindmarsh-Rose neuron model. However, the dynamics of the circuits cannot be expected to be perfectly identical. For instance, because the signals exchanged among the circuits are contaminated with noise and/or there are small mismatches in the circuits' components. Because of these inherent imperfections, we cannot expect that the circuits perfectly synchronize. It is necessary to allow for a mismatch between them, which, of course, needs to be small enough in order to consider that the circuits are "*practically synchronized*". The experiments with networks of coupled Hindmarsh-Rose circuits shall indicate when the aforementioned theoretical results, derived for identical systems and without any noise, (fail to) have sufficient predictive value in practice.

1.4 Mathematical Preliminaries and Framework

In this section, the notation, some definitions, and the mathematical framework used throughout the thesis are presented. Particularly, the notions of *semipassivity*, *convergent systems*, some basic terminology of *graph theory*, and the class of systems under study are introduced.

1.4.1 Notation

Unless otherwise stated, throughout this thesis the following notation is used: The symbol $\mathbb{R}_{>0}$ ($\mathbb{R}_{\geq 0}$) denotes the set of positive (nonnegative) real numbers.

Likewise, the symbol $\mathbb{C}_{>0}$ ($\mathbb{C}_{\geq 0}$) stands for the set of complex numbers with positive (nonnegative) real parts. The Euclidian norm in $\mathbb{R}^n$ is denoted simply as $|\cdot|$, $|x|^2 = x^T x$, where ^{T} defines transposition. The notation $\mathrm{col}(x_1, ..., x_n)$ stands for the column vector composed of the elements $x_1, ..., x_n$. This notation is also used in case the components x_i are vectors. The induced norm of a matrix $A \in \mathbb{R}^{n\times n}$, denoted by $\|A\|$, is defined as $\|A\| = \max_{x\in\mathbb{R}^n, |x|=1} |Ax|$. The $n \times n$ identity matrix is denoted by I_n or simply I if no confusion can arise. Likewise, $n \times m$ matrices composed of only ones and only zeros are denoted as $\mathbf{1}_{n\times m}$ and $\mathbf{0}_{n\times m}$, respectively, or simply $\mathbf{1}$ and $\mathbf{0}$ when their dimensions are evident. A function $V : \mathcal{X} \to \mathbb{R}_{>0}$ defined on a neighborhood $\mathcal{X}$ of $\mathbb{R}^n$ with $0 \in \mathcal{X}$ is positive definite if $V(x) > 0$ for all $x \in \mathcal{X}\backslash\{0\}$ and $V(0) = 0$, and it is radially unbounded if $\mathcal{X} = \mathbb{R}^n$. If $V(x) \to \infty$ as $|x| \to \infty$, then $V(\cdot)$ is called proper. If a quadratic form $x^T Px$ with a symmetric matrix $P = P^T$ is positive definite, then P is called positive definite. For positive definite matrices, we use the notation $P > 0$; moreover, $P > Q$ means that the matrix $P - Q$ is positive definite. The spectrum of a matrix A is denoted by $spec(A)$. For any two matrices A and B, the notation $A \otimes B$ (the Kronecker product) stands for the matrix composed of submatrices $A_{ij}B$, i.e.,

$$A \otimes B = \begin{pmatrix} A_{11}B & A_{12}B & \cdots & A_{1n}B \\ A_{21}B & A_{22}B & \cdots & A_{2n}B \\ \vdots & \vdots & \ddots & \vdots \\ A_{n1}B & A_{n2}B & \cdots & A_{nn}B \end{pmatrix},$$

where A_{ij}, $i, j \in \{1, ..., n\}$, stands for the ijth entry of the $n \times n$ matrix A. Let $\mathcal{X} \subset \mathbb{R}^n$ and $\mathcal{Y} \subset \mathbb{R}^m$. The space of continuous functions from $\mathcal{X}$ to $\mathcal{Y}$ is denoted by $\mathcal{C}(\mathcal{X}, \mathcal{Y})$. If the functions are (at least) $r \geq 0$ times continuously differentiable, then it is denoted by $\mathcal{C}^r(\mathcal{X}, \mathcal{Y})$. If the derivatives of a function of all orders ($r = \infty$) exist, the function is called smooth and if the derivatives up to a sufficiently high order exist the function is named sufficiently smooth. Time-delayed signals are denoted as $x(t)^\tau = x(t - \tau)$ with time-delay $\tau \in \mathbb{R}_{\geq 0}$. For simplicity of notation, we often suppress the explicit dependence of time t.

1.4.2 Semipassive Systems

The results presented in this thesis follow the same research line as [104, 108], where sufficient conditions for synchronization in networks of diffusively coupled *semipassive systems* are derived. Consider the system

$$\Sigma : \begin{cases} \dot{x} = f(x, u), \\ z = h(x), \end{cases} \tag{1.4}$$

with state $x \in \mathbb{R}^n$, input $u \in \mathbb{R}^m$, output $z \in \mathbb{R}^m$, and sufficiently smooth functions $f : \mathbb{R}^n \times \mathbb{R}^m \to \mathbb{R}^n$ and $h : \mathbb{R}^n \to \mathbb{R}^m$.

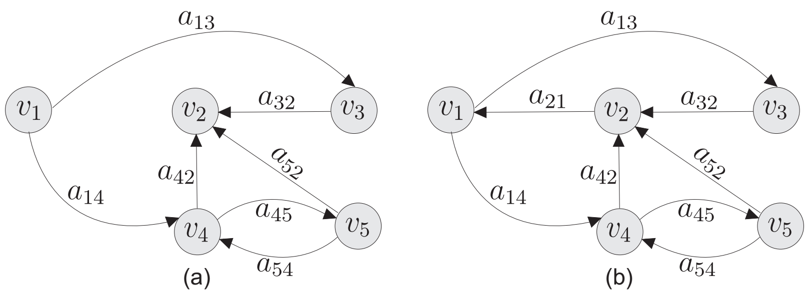

Figure 1.3 (a) Connected graph. (b) Strongly connected graph.

Definition 1.2. [108]. *The dynamical system* (1.4) *is called* $\mathcal{C}^r$*-semipassive if there exists a nonnegative function* $V \in \mathcal{C}^r(\mathbb{R}^n, \mathbb{R}_{\geq 0})$, $x \mapsto V(x)$*, called the storage function, such that* $\dot{V} \leq z^T u - H(x)$*, where the function* $H \in \mathcal{C}(\mathbb{R}^n, \mathbb{R})$ *is nonnegative outside some ball, i.e.,* $\exists\, \varphi > 0$ *s.t.* $|x| \geq \varphi \to H(x) \geq \varrho(|x|)$*, for some continuous nonnegative function* $\varrho(\cdot)$ *defined for* $|x| \geq \varphi$*. If the function* $H(\cdot)$ *is positive outside some ball, then the system* (1.4) *is said to be strictly* $\mathcal{C}^r$*-semipassive.*

Remark 1.3. *System* (1.4) *is* $\mathcal{C}^r$*-passive (strictly* $\mathcal{C}^r$*-passive) if it is* $\mathcal{C}^r$*-semipassive (strictly* $\mathcal{C}^r$*-semipassive) with* $H(\cdot)$ *being positive semidefinite (positive definite).*

In light of Remark 1.3, a (strictly) $\mathcal{C}^r$-semipassive system behaves like a (strictly) passive system for large $|x(t)|$. From a physical point of view, one may think of a semipassive system as a passive system with a limited amount of free energy. The class of strictly semipassive systems includes, e.g., the chaotic Lorenz system [104], the van der Pol oscillator [81], and many models that describe the action potential dynamics of individual neurons [136].

1.4.3 Convergent Systems

In the framework considered in [104, 108] (and also in this thesis), it is assumed that the internal dynamics of each subsystem in the network is a *convergent system*. Consider the system (1.4) and suppose $f(\cdot)$ is locally Lipschitz in x, $u(\cdot)$ is piecewise continuous in t, and takes values on some compact set $u \in U \subseteq \mathbb{R}^m$.

Definition 1.4. [37]. *System* (1.4) *is said to be convergent if and only if for any bounded signal* $u(t)$ *defined on the whole interval* $(-\infty, +\infty)$ *there is a unique bounded globally asymptotically stable solution* $\bar{x}_u(t)$ *defined in the same interval for which it holds that,* $\lim_{t\to\infty} |x(t) - \bar{x}_u(t)| = 0$*, for all initial conditions.*

For a *convergent system*, the limit solution is solely determined by the external excitation $u(t)$ and not by the initial condition. A sufficient condition for system (1.4) to be convergent obtained by Demidovich in [37] and later extended in [94] is presented in the following proposition.

Proposition 1.5. (Demidovich Condition [37, 94]). *If there exists a positive definite matrix $P \in \mathbb{R}^{n\times n}$ such that all the eigenvalues $\lambda_i(Q)$ of the symmetric matrix*

$$Q(x,u) = \frac{1}{2}\left(P\left(\frac{\partial f}{\partial x}(x,u)\right) + \left(\frac{\partial f}{\partial x}(x,u)\right)^T P\right), \tag{1.5}$$

are negative and separated from zero, i.e., there exists a constant $c \in \mathbb{R}_{>0}$ such that $\lambda_i(Q) \le -c < 0$, for all $i \in \{1,...,n\}$, $u \in U$, and $x \in \mathbb{R}^n$, then system (1.4) *is globally exponentially convergent. Moreover, for any pair of solutions $x_1(t), x_2(t) \in \mathbb{R}^n$ of* (1.4), *the following is satisfied*

$$\frac{d}{dt}\Big((x_1 - x_2)^T P(x_1 - x_2)\Big) \le -\alpha\,|x_1 - x_2|^2\,,$$

with constant $\alpha := \frac{c}{\lambda_{\max}(P)}$ and $\lambda_{\max}(P)$ being the largest eigenvalue of the symmetric matrix P.

1.4.4 Communication Graphs

Given a set of interconnected systems, the communication topology is encoded through a communication graph. The convention is that system i receives information from system j if and only if there is a directed link from node j to node i in the communication graph. Let $\mathcal{G} = (\mathcal{V}, \mathcal{E}, A)$ denote a weighted digraph (directed graph), where $\mathcal{V} = \{v_1, v_2, ..., v_k\}$ is the set of nodes, $\mathcal{E} \subseteq \mathcal{V}\times\mathcal{V}$ is the set of edges, and A is the weighted adjacency matrix with nonnegative elements a_{ij}. The neighbors of v_i is the set of directed edges to a node v_i and it is denoted as $\mathcal{E}_i$. If the graph does not contain self-loops, it is called simple. If two nodes have a directed edge in common, they are called *adjacent*. Assume that the network consists of k nodes, then the *adjacency matrix* $A \in \mathbb{R}^{k\times k} := a_{ij}$ with $a_{ij} > 0$, if $\{i,j\} \in \mathcal{E}$ and $a_{ij} = 0$ otherwise. We also introduce the *degree matrix* $D \in \mathbb{R}^{k\times k} := diag\{d_1, ..., d_k\}$ with $d_i = \sum_{j\in\mathcal{E}_i} a_{ij}$, and $L := D - A$, which is called the *Laplacian matrix* of the graph $\mathcal{G}$, see [29] for further details. In order to ensure that pieces of information may reach all nodes, the graph needs to be connected in some appropriate sense. Then, some notions of connectivity are introduced.

Definition 1.6. *A path from node $v_1 \in \mathcal{V}$ to node $v_\theta \in \mathcal{V}$ in a graph $\mathcal{G}$ is a sequence $\{v_1, ..., v_\theta\}$ with $\theta > 1$ of distinct nodes such that $(v_i, v_{i+1}) \in \mathcal{E}$, $i = \{1, ..., \theta - 1\}$. The length of the path is $\theta - 1$.*

Existence of a path from node $v_1 \in \mathcal{V}$ to node $v_\theta \in \mathcal{V}$ in some graph $\mathcal{G}$ implies that information can propagate from system v_1 to system v_θ.

Definition 1.7. *A graph $\mathcal{G} = (\mathcal{V}, \mathcal{E}, A)$ is called connected, if its set of nodes $\mathcal{V}$ contains at least one specific node v, called a centroid of $\mathcal{G}$, from which information can propagate to all other nodes along paths in $\mathcal{G}$. It is called strongly connected, if any node $v \in \mathcal{V}$ is a centroid of $\mathcal{G}$, i.e., there are paths connecting any two nodes.*

Proposition 1.8. [29, 129]. *The Laplacian matrix $L \in \mathbb{R}^{k\times k}$ of a connected graph $\mathcal{G}$ has an algebraically simple eigenvalue $\lambda_1 = 0$ with corresponding eigenvector $\mathbf{1}_{k\times 1}$ and all the other eigenvalues have positive real parts. Furthermore, if the graph $\mathcal{G}$ is strongly connected, then the left eigenvector ν corresponding to the zero eigenvalue of L has strictly positive real entries, i.e., $\nu^T L = 0$ with $\nu_i > 0$ for all i.*

Definition 1.9. *An independent strongly connected component* (iSCC) *of a directed graph $\mathcal{G} = (\mathcal{V}, \mathcal{E}, A)$ is an induced subgraph $\tilde{\mathcal{G}} = (\tilde{\mathcal{V}}, \tilde{\mathcal{E}})$ which is maximal, subject to being strongly connected, and satisfies $(v, \tilde{v}) \notin \mathcal{E}$ for any $v \in \mathcal{V}\backslash\tilde{\mathcal{V}}$ and $\tilde{v} \in \tilde{\mathcal{V}}$. Note that there is no edge in $\mathcal{E}$ with tail outside $\tilde{\mathcal{V}}$ and head in $\tilde{\mathcal{V}}$.*

The fact that there is no edge in $\mathcal{E}$ with tail outside $\tilde{\mathcal{V}}$ and head in $\tilde{\mathcal{V}}$ means that the systems represented by the nodes within the iSCC are not influenced by systems represented by nodes outside the iSCC. In order to illustrate the previous definitions, consider the graph depicted in Figure (1.3a). This graph is connected with centroid v_1, but it is not strongly connected since v_1 is the only centroid. However, adding a single edge from node v_2 to node v_1 makes the resulting graph (1.3b) strongly connected. Moreover, the iSCC in graph (1.3a) is just v_1 while in (1.3b) is the graph itself. Throughout this thesis, depending of the problem being tackled, it is assumed that the graph $\mathcal{G}$ encoding the communication topology is either connected or strongly connected.

1.4.5 Mathematical Framework

This section introduces the class of systems to be considered in this thesis. In particularly, the necessary input-output properties of each system in the network are specified. Consider k identical nonlinear systems of the form

$$\dot{x}_i = f(x_i) + Bu_i, \tag{1.6}$$

$$z_i = Cx_i, \tag{1.7}$$

$$y_i = Nx_i, \tag{1.8}$$

with $i \in \mathcal{I} := \{1, ..., k\}$, state $x_i \in \mathbb{R}^n$, input $u_i \in \mathbb{R}^m$, semipassive output $z_i \in \mathbb{R}^m$, measurable output $y_i \in \mathbb{R}^s$, sufficiently smooth function $f : \mathbb{R}^n \to \mathbb{R}^n$, matrices

C, N, and B of appropriate dimensions, and the matrix $CB \in \mathbb{R}^{m\times m}$ being similar to a positive definite matrix. It is assumed that:

(H1.1) Each system (1.6),(1.7) is strictly $\mathcal{C}^1$-semipassive with input u_i, output z_i, and radially unbounded storage function $V(x_i)$.

Then, there exists a globally defined coordinate transformation such that systems (1.6),(1.7) can be written in the following *normal form*, (this transformation is explicitly computed in [108]),

$$\dot{\zeta}_i = q(\zeta_i, z_i), \tag{1.9}$$

$$\dot{z}_i = a(\zeta_i, z_i) + CBu_i, \tag{1.10}$$

with internal state $\zeta_i \in \mathbb{R}^{n-m}$ and sufficiently smooth functions $q : \mathbb{R}^{n-m} \times \mathbb{R}^m \to \mathbb{R}^{n-m}$ and $a : \mathbb{R}^{n-m} \times \mathbb{R}^m \to \mathbb{R}^m$. It is further assumed that:

(H1.2) The internal dynamics (1.9) is an *exponentially convergent system*, i.e., there is a positive definite matrix $P \in \mathbb{R}^{(n-m)\times(n-m)}$ such that the eigenvalues of the symmetric matrix

$$Q(\zeta_i, z_i) = \frac{1}{2}\left(P\left(\frac{\partial q}{\partial \zeta_i}(\zeta_i, z_i)\right) + \left(\frac{\partial q}{\partial \zeta_i}(\zeta_i, z_i)\right)^T P\right), \tag{1.11}$$

are uniformly negative and bounded away from zero for all $\zeta_i \in \mathbb{R}^{n-m}$ and $z_i \in \mathbb{R}^m$.

Remark 1.10. *Assumption* (H1.2) *is employed to ensure that the internal states ζ_i asymptotically synchronize whenever the semipassive outputs z_i asymptotically synchronize. Indeed, there are some other methods to verify this, for instance, contraction theory* [68], *Lyapunov function approach to incremental stability* [15], *the quadratic* (QUAD) *inequality approach (a Lipschitz-like condition)* [36], *and differential dissipativity* [43], *which are all concepts that are closely related to notion of convergent systems* [94] *that we use here.*

We also refer the interested reader to Refs. [25, 36], where a fairly detailed comparison among some of these concepts can be found.

As mentioned before, the mathematical framework considered here is based on the one introduced in [104, 108], where synchronization in networks of diffusively coupled semipassive systems with exponentially convergent internal dynamics is studied. The authors in [104, 108] present sufficient conditions ensuring that the solutions of the coupled semipassive systems are ultimately bounded and asymptotically synchronize for sufficiently strong coupling. The main result of [108] can be summarized in the following theorem.

Theorem 1.11. [108]. *Consider k identical systems* (1.6),(1.7) *interconnected on a simple strongly connected graph through the diffusive static coupling*

$$u_i = \gamma \sum_{j \in \mathcal{E}_i} a_{ij}(z_j - z_i), \tag{1.12}$$

with $i \in \mathcal{I} := \{1, \ldots, k\}$, coupling strength $\gamma \in \mathbb{R}_{\geq 0}$, interconnection weights $a_{ij} = a_{ji} \in \mathbb{R}_{\geq 0}$ for all $i, j \in \mathcal{I}$, and $\mathcal{E}_i$ being the set of neighbors of system i. Let (H1.1) *be satisfied and assume that:*

(H1.3) *There exists a positive definite function $\mathcal{W} \in \mathcal{C}^2(\mathbb{R}^{n-m}, \mathbb{R}_{>0})$ such that for all $\zeta_i, \zeta_j \in \mathbb{R}^{n-m}$ and $z_i \in \mathbb{R}^m$ there is a constant $\alpha' \in \mathbb{R}_{>0}$ such that*

$$\nabla \mathcal{W}(\zeta_i - \zeta_j)^T \left(q(\zeta_i, z_i) - q(\zeta_j, z_i) \right) \leq -\alpha' \left| \zeta_i - \zeta_j \right|^2. \tag{1.13}$$

Then, the solutions of the coupled systems are ultimately bounded and there exists a positive constant γ' such that if $\gamma\lambda_2(L) > \gamma'$, where $\lambda_2(L)$ denotes the smallest nonzero eigenvalue of the symmetric Laplacian matrix, there exists a (globally) asymptotically stable subset of the diagonal set

$$\mathcal{M} := \{x := col(x_1, \ldots, x_k) \in \mathbb{R}^{kn} | x_i = x_j, \forall\, i, j \in \mathcal{I}\}.$$

Remark 1.12. *The notation γa_{ij} for the "effective" coupling strength (between systems i and j) looks a bit cumbersome at first sight. One might have expected simply γ_{ij} instead. The reason to use this notation is that, in this thesis, the networks are supposed to be given, i.e., the weights a_{ij} are supposed to be fixed and known. Then, for these fixed a_{ij}, conditions for synchronization are expressed in terms of the coupling strength γ.*

Proposition 1.13. [94]. *If the internal dynamics* (1.9) *satisfies* (H1.2) *for some positive definite matrix $P \in \mathbb{R}^{(n-m)\times(n-m)}$ and constant $\alpha \in \mathbb{R}_{>0}$, then* (H1.3) *in Theorem 1.11 is satisfied with $\mathcal{W}(\zeta_i - \zeta_j) = (\zeta_i - \zeta_j)^T P(\zeta_i - \zeta_j)$ and $\alpha' = \alpha$.*

The result stated in Theorem 1.11 amount to the following. Provided that (H1.1) and (H1.3) (or (H1.2)) are satisfied, the network topology is strongly connected and simple, and the coupling strength is sufficiently large, the solutions of the k diffusively coupled systems enter a compact invariant set in finite time and asymptotically synchronize. It is important to note that (H1.1) and (H1.3) are *independent* of the network. This implies that systems satisfying assumptions (H1.1) and (H1.3) *can* synchronize and this result does not depend of the specific network topology. Theorem 1.11 states that the systems synchronize if $\gamma\lambda_2(L)$ is sufficiently large. Here the network topology plays a role since $\lambda_2(L)$ denotes the smallest nonzero eigenvalue of the Laplacian of the network. The smallest nonzero eigenvalue of the Laplacian matrix is also known as the *algebraic connectivity* of the network [42].

1.5 Thesis Overview and Contributions

This thesis extends the ideas presented in [104, 108]. Particularly, using the semipassivity based framework introduced in Section 1.4.5, we study some cases where the result stated in Theorem 1.11 fails to provide a complete answer about the occurrence of synchronization in networks of coupled systems. There are some results in this direction already. For instance, in [129, 132], the authors analyze the case when the diffusive static coupling (1.12) is corrupted with network-induced time-delays. In other words, they tackle the problem of controlled network synchronization of semipassive systems interconnected through *diffusive static time-delayed couplings*. In the same spirit, in this thesis, we propose different classes of diffusive couplings (both static and dynamic) to solve some particular problems of controlled synchronization.

In Chapter 2, we consider the problem of controlled synchronization in networks of identical linear time-invariant systems of the form

$$\dot{x}_i = Ax_i + B_1u_i + B_2\omega, \tag{1.14}$$

$$y_i = C_1x_i, \tag{1.15}$$

$$z_i = C_2x_i, \tag{1.16}$$

with $i \in \mathcal{I} = \{1, ..., k\}$, state $x_i \in \mathbb{R}^n$, (measured) output $y_i \in \mathbb{R}^s$, passive output $z_i \in \mathbb{R}^m$, input $u_i \in \mathbb{R}^m$, matrices A, B_1, B_2, C_1, and C_2 of appropriate dimensions, and the matrix C_2B_1 being similar to a positive definite matrix. The systems are driven by some piecewise continuous bounded signal $\omega(t)$. This signal acts as either an external force or a reference signal that is applied to all the systems in the network. System (1.14),(1.16) is a particular form of system (1.6),(1.7) with $f(x_i) = Ax_i$, $C = C_2$, and the addition of the extra term $B_2\omega(t)$. Each system in the network is assumed to be *passive* and *detectable* with respect to the coupling variable $z_i = C_2x_i$. First, the systems are interconnected through *static time-delayed couplings* of the form

$$u_i = \gamma \sum_{j\in\mathcal{E}_i} a_{ij}(z_j^\tau - z_i), \tag{1.17}$$

$$u_i = \gamma \sum_{j\in\mathcal{E}_i} a_{ij}(z_j^\tau - z_i^\tau),\ i \in \mathcal{I}, \tag{1.18}$$

where $\tau \in \mathbb{R}_{>0}$ denotes the finite time-delay, u_i and $z_i^\tau := z_i(t-\tau)$ are the input and the time-delayed passive output of the system i, respectively, z_j^τ is the time-delayed passive output of system j to which system i is connected, $\gamma \in \mathbb{R}_{\geq 0}$ denotes the coupling strength, and $a_{ij} \in \mathbb{R}_{\geq 0}$ are the interconnection weights. It is not necessarily assumed that $a_{ij} = a_{ji}$. Although the systems are linear and time-invariant, the signal $\omega(t)$ may lead to complex oscillatory behavior without coupling. Due to this external signal and the time-delays, it is not immediate that the closed-loop system possesses bounded solutions. Using the passivity property of the individual systems and Lyapunov-Krasovskii functionals, we derive conditions which ensure *ultimate boundedness* of the solutions of the coupled systems. Then, using the detectability assumption of the pair (A, C_2), we prove that under some mild conditions there always exists a region $\mathcal{S}$, referred to as the *synchronization region*, in the parameter space (*coupling strength* γ *versus time-delay* τ) such that if $\gamma, \tau \in \mathcal{S}$, the coupled systems asymptotically synchronize. Next, we propose *predictor-based diffusive dynamic couplings* to increase the time-delay that can be induced to the systems without compromising the synchronous behavior, i.e., by including predictors in the couplings, we prove that the synchronization region $\mathcal{S}$ may be increased. In the results mentioned above, it is assumed that z_i (the passive output) is available for feedback. However, if the measurable output is a different state function $y_i = C_1 x_i$, which does not have the desired passivity properties, these results do not hold. Nevertheless, if the pair (A, C_1) is detectable, there exists an observer which reconstructs the retarded passive output z_i^τ from measurements of y_i^τ. Then, an *observer-based diffusive dynamic coupling* which only depends on the time-delayed measurable output y_i^τ can be constructed to interconnect the systems. The main results are illustrated by computer simulations. The contents of this chapter are published in [78].

In Chapter 3, for the nonlinear systems (1.6)-(1.8), we extend some of the results presented in Chapter 2. In the result stated in Theorem 1.11, it is assumed that the variables z_i that render the internal dynamics convergent, and for which each system is strictly $\mathcal{C}^1$-semipassive is available for feedback. Therefore, if the measurable output is a different state function $y_i = N x_i \in \mathbb{R}^s$, which does not have the desired properties, Theorem 1.11 cannot be applied. However, as in the linear case, if there exists a nonlinear observer which reconstructs z_i from measurements of y_i, then *diffusive dynamic couplings* which only depend on the measurable outputs y_i could be constructed to interconnect the systems. Such couplings are dynamical systems of the form

$$\dot{\eta}_i = l(\eta_i, y_i, u_i), \tag{1.19}$$

$$\hat{z}_i = \psi(\eta_i, y_i), \tag{1.20}$$

$$u_i = \gamma \sum_{j \in \mathcal{E}_i} a_{ij} \left(\hat{z}_j - \hat{z}_i \right), \tag{1.21}$$

with $i \in \mathcal{I}$, observer state $\eta_i \in \mathbb{R}^p$, $p \geq n - s$, input $u_i \in \mathbb{R}^m$, measurable output $y_i \in \mathbb{R}^s$, estimated semipassive output $\hat{z}_i \in \mathbb{R}^m$, sufficiently smooth functions $l : \mathbb{R}^p \times \mathbb{R}^s \times \mathbb{R}^m \to \mathbb{R}^p$ and $\psi : \mathbb{R}^p \times \mathbb{R}^s \to \mathbb{R}^m$, coupling strength $\gamma \in \mathbb{R}_{\geq 0}$, and interconnection weights $a_{ij} \in \mathbb{R}_{\geq 0}$. The dynamic diffusive coupling (1.19)-(1.21) is the combination of a nonlinear observer and an estimated version of the diffusive static coupling (1.12). Here, the observer is assumed to be given; therefore, the synchronization problem in networks of semipassive systems coupled through (1.19)-(1.21) is one of analysis. We derive sufficient conditions on the systems to be interconnected, the *convergence rate* of the observer, and the coupling strength γ such that the solutions of the coupled systems are uniformly bounded and synchronize. The results are illustrated by computer simulations of coupled FitzHugh-Nagumo neural oscillators. The contents of this chapter are published in [77].

In Chapter 4, we address and solve the *synthesis part* of a more general setting. Using ideas of *immersion and invariance* introduced in [17], a general tool for constructing the nonlinear observer (1.19),(1.20) is presented. Moreover, the effect of network-induced time-delays is also analyzed. We propose *observer-based diffusive time-delayed couplings* to interconnect the systems. Particularly, we propose dynamic couplings of the form

$$\begin{aligned} \dot{\eta}_i &= l(\eta_i, y_i, u_i), && (1.22)\\ \hat{z}_i &= \psi(\eta_i, y_i), && (1.23)\\ u_i &= \gamma \sum_{j \in \mathcal{E}_i} a_{ij} \left(\hat{z}_j^{\tau} - \hat{z}_i \right), && (1.24)\\ u_i &= \gamma \sum_{j \in \mathcal{E}_i} a_{ij} \left(\hat{z}_j^{\tau} - \hat{z}_i^{\tau} \right), && (1.25) \end{aligned}$$

with $i \in \mathcal{I}$, observer state $\eta_i \in \mathcal{C}([-\tau, 0], \mathbb{R}^p)$, $p \geq n - s$, $\mathcal{C}([-\tau, 0], \mathbb{R}^p)$ being a *Banach space* of continuous functions mapping the interval $[-\tau, 0]$ into $\mathbb{R}^p$, time-delay $\tau \in \mathbb{R}_{\geq 0}$, input $u_i \in \mathcal{C}([-\tau, 0], \mathbb{R}^m)$, measurable output $y_i \in \mathbb{R}^s$, estimated time-delayed semipassive output $\hat{z}_i^{\tau} \in \mathcal{C}([-\tau, 0], \mathbb{R}^m)$, coupling strength $\gamma \in \mathbb{R}_{\geq 0}$, interconnection weights $a_{ij} \in \mathbb{R}_{\geq 0}$, and to be designed mappings $l : \mathbb{R}^p \times \mathbb{R}^s \times \mathbb{R}^m \to \mathbb{R}^p$ and $\psi : \mathbb{R}^p \times \mathbb{R}^s \to \mathbb{R}^m$. As mentioned before, in this chapter, we give a methodology for constructing the functions $l(\cdot)$ and $\psi(\cdot)$ using the *immersion and invariance* techniques introduced in [17]. Sufficient conditions are derived on the systems to be interconnected, the network topology, the coupling dynamics, and the time-delay that guarantee boundedness and (global) state synchronization of the solutions of the coupled system. The results are illustrated by computer simulations of coupled chaotic FitzHugh-Nagumo neural oscillators. The contents of this chapter are based on [76].

In Chapter 5, using the delay-free observer-based couplings (1.19)-(1.21) introduced in Chapter 3, we study the possible emergence of *partial synchronization*. Partial synchronization is a phenomenon, in which some, at least two, systems in the network synchronize with each other but not with every system in the network. The result presented here is a direct extension of the results presented in [105, 106], where sufficient conditions for partial synchronization in networks of diffusively coupled semipassive systems are derived. Using symmetries in the network, we identify linear invariant manifolds of the coupled systems (1.6)-(1.8), (1.19)-(1.21). Note that the coupling (1.21) can be written in matrix form

$$u = -\gamma \left(L \otimes I_m \right) \hat{z}, \tag{1.26}$$

where $L \in \mathbb{R}^{k \times k}$ denotes the Laplacian matrix, $\hat{z} := \mathrm{col}(\hat{z}_1, ..., \hat{z}_k) \in \mathbb{R}^{km}$, and $u := \mathrm{col}(u_1, ..., u_k) \in \mathbb{R}^{km}$. If a network possesses certain symmetry, this symmetry must be present in the Laplacian matrix L. Particularly, the network may contain some repeated patterns when considering arrangements of the constants a_{ij} and hence the permutation of some elements would leave the network unchanged. In other words, the structure of the network is preserved after simultaneous swapping of (some of) the nodes of the network. The matrix representation of a permutation of the set $\mathcal{I} = \{1, ..., k\}$ is a permutation matrix $\Pi \in \mathbb{R}^{k \times k}$. We prove that, for a permutation matrix Π, if there is a solution $X \in \mathbb{R}^{k \times k}$ to the matrix equation

$$\left(I_k - \Pi \right) L = X \left(I_k - \Pi \right), \tag{1.27}$$

then the set $\ker \left(I - \Pi \otimes I \right)$ defines a linear invariant manifold for the coupled systems (1.6)-(1.8),(1.19)-(1.21). If these manifolds are attracting, the systems in the network may exhibit partial synchronization. We prove that a linear invariant manifold defined by a symmetry in a network is attracting, if the coupling strength γ is sufficiently large (but not large enough for having full synchronization) and the rate of convergence of the observer is sufficiently fast. The results are illustrated by computer simulations of coupled chaotic Hindmarsh-Rose neural oscillators. The contents of this chapter are published in [80].

In Chapter 6, we address the problem of constructing (reduced order) observers for general nonlinear systems when the output measurements are subject to constant time-delays. In Chapter 4, using the I&I techniques introduced in [56], we give a methodology for constructing the dynamic coupling (1.22)-(1.25). We remark that the observer dynamics (1.22)-(1.23) is independent of the time-delay, i.e., it is assumed that the measurements of y_i are not subject to time-delay and the delay in the dynamic coupling (1.22)-(1.25) is only induced when the estimated outputs $\hat{z}_i$ are transmitted. Under this assumption, it is possible to maintain a delay-free observer structure while analyzing the effect of transmission delays in the synchronous behavior. However, in some practical applications, the outputs y_i may also be corrupted with time-delays. For instance, when the measurement process intrinsically causes non-negligible time-delays or when the system is monitored through communication networks which results in unavoidable delays. In Chapter 6, we study the *immersion and invariance* techniques presented in [17, 56] for designing nonlinear observers. We show how these I&I ideas may be extended when the output measurements are corrupted by constant time-delays. Following the design method developed in [17], we derive a general tool for constructing I&I *observers* in the presence of time-delays. It is important to point out that, as it is the case in the delay-free setting considered in [17], the observer design relies on the existence of two mappings, $\beta(\cdot)$ and $\phi(\cdot)$, which must be selected to render the zero solution of the estimation error dynamics asymptotically stable. This stabilization problem may be difficult to solve, since, in general, it relies on the solution of a set of partial differential equations (or inequalities). However, as it is shown in the examples in Chapter 6, for some systems these equations turn out to be solvable. Throughout Chapter 6, the observer may play two different roles. On the one hand, it may be used to reconstruct a delayed version of the unmeasured state from measurements of the available delayed outputs. In this case, we refer to it as a *retarded immersion and invariance observer*. On the other hand, the observer may be used to reconstruct both the delay-free unmeasured state and the delay-free outputs from measurements of the delayed outputs. In this case, we refer to it as an *immersion and invariance predictor*. The tools given in Chapter 6 may be directly used to construct a more general version of the dynamic coupling (1.22)-(1.25), i.e., with these techniques, we may also consider time-delays at the level of the observer and not only when transmitting the estimated semipassive outputs. However, this case is not analyzed here and it is left as future research. The main results of this chapter are illustrated by computer simulations using the chaotic Lorenz system and the Duffing oscillator. The contents of this chapter are based on [75].

Chapter 7 focuses on controlled synchronization of identical semipassive systems interconnected through *predictor-based diffusive dynamic couplings*. An important element of our control scheme is the use of a communication network. Network communication is necessary in the study of synchronization to transmit and receive measurement and control data among the systems. Because of the time needed to transmit data over the network, the use of networked communication to exchange information results in unavoidable time-delays. These network-induced delays are undesirable because they may lead to the loss of synchrony in the network. Hence, when studying synchronization among dynamical systems with networked communication, it is important to design control algorithms which are robust with respect to time-delays. The results presented here follow the same research line as [132], where sufficient conditions for synchronization in networks of *diffusively time-delayed coupled* semipassive systems are derived. The authors in [132] prove that under some mild assumptions, there always exists a region $\mathcal{S}$ in the parameter space (coupling strength γ versus time-delay τ), such that if $(\gamma, \tau) \in \mathcal{S}$, the systems synchronize. Nevertheless, it is important to note that for this class of systems, once the network topology is specified, the region $\mathcal{S}$ is fixed. In other words, the time-delay that may be induced to the network without compromising the synchronous behavior is limited by the network topology [82]. The time-delay τ considered in the results presented in [132] can be realized as the sum of measurement and transmission time-delays. In this chapter, we make a clear distinction between these delays. The measurement time-delay $\tau_1 \in \mathbb{R}_{\geq 0}$ affects the outputs of the systems $y_i(t)$, resulting in time-delayed outputs $y_i(t-\tau_1)$ being available for control purposes. The transmission time-delay is encompassed in $\tau_2 \in \mathbb{R}_{\geq 0}$. It affects the control inputs $u_i(t)$, resulting in the time-delayed control signals $u_i(t-\tau_2)$ being applied to the systems. Notice that the total time-delay τ considered in [132] is simply given by the sum of the individual delays, i.e., $\tau = \tau_1 + \tau_2$. In this chapter, we show that by including predictors in the couplings, we may increase the total time-delay that can be induced. We propose *predictor-based diffusive dynamic couplings* based on the concept of *anticipating synchronization* [89] that on the one hand estimate future values $y_i(t+\tau)$ of the outputs $y_i(t)$, and on the other hand interconnect the systems through these time-ahead estimated signals. The proposed predictor-based couplings are dynamical systems of the form

$$\dot{\eta}_{1i} = q(\eta_{1i}, \eta_{2i}), \tag{1.28}$$

$$\dot{\eta}_{2i} = a(\eta_{1i}, \eta_{2i}) + CBu_i + \kappa \left(y_i(t-\tau_1) - \eta_{2i}(t-\tau) \right), \tag{1.29}$$

$$u_i = \gamma \sum_{j \in \mathcal{E}_i} a_{ij} \left(\eta_{2j} - \eta_{2i} \right), \tag{1.30}$$

$$\eta_i = \eta_{0i} \in \mathbb{R}^n, \quad t \in [-\tau, 0], \tag{1.31}$$

with $i \in \mathcal{I} = \{1, ..., k\}$, stacked state $\eta_i := \mathrm{col}(\eta_{1i}, \eta_{2i}) \in \mathcal{C}([-\tau, 0], \mathbb{R}^n)$, internal state $\eta_{1i} \in \mathcal{C}([-\tau, 0], \mathbb{R}^{n-m})$, actuated state $\eta_{2i} \in \mathcal{C}([-\tau, 0], \mathbb{R}^m)$, input $u_i \in \mathbb{R}^m$, smooth vectorfields $q(\cdot)$ and $a(\cdot)$ as in (1.9),(1.10), initial history η_{0i}, coupling strength $\gamma \in \mathbb{R}_{\geq 0}$, predictor gain $\kappa \in \mathbb{R}_{\geq 0}$, measurement time-delay $\tau_1 \in \mathbb{R}_{\geq 0}$, total time-delay $\tau \in \mathbb{R}_{\geq 0}$, and interconnection weights $a_{ij} = a_{ji} \geq 0$. The predictor dynamics is given by (1.28)(1.29) while (1.30) is a time-ahead estimated version of the diffusive static coupling (1.12). Notice that if $\kappa = 0$ and $u_i(t) = \mathbf{0}$, the predictor dynamics (1.28)(1.29) is the same as the individual systems dynamics (1.9),(1.10) with $u_i(t) = \mathbf{0}$. We construct the predictor in this way in order to take advantage of the stability properties of (1.9),(1.10), namely, *semipassivity* and *convergence*. By including the predictors in the loop, the new parameter κ comes into play. This κ plays the role of the *predictor gain*, i.e., it is a parameter of the predictors that can be tuned to make the *prediction error dynamics* converge to the origin. We derive sufficient conditions for global state synchronization of the interconnected systems. In particular, it is proved that under some assumptions, there always exists a region in the *extended parameter space* (coupling strength γ, total time-delay τ, and *predictor gain* κ), such that if γ, τ, and the new parameter κ belong to this region, the systems synchronize. Then, we provide a *local analysis*, in which the performance of our predictor-based control scheme is compared against the *diffusive static couplings* available in the literature. It is shown (locally) that the amount of time-delay that can be induced to the network may be increased by including the predictors in the loop. Finally, we present a simulation example that shows that indeed it is possible to extend the synchronization regions with the proposed control scheme. In this example, we notice that while the regions $\mathcal{S}$ obtained through the *diffusive static coupling* are strongly influenced by the network topology, the regions obtained with the predictor-based coupling are influenced by the network topology only for small coupling strength. As γ is increased, the upper bounds of these regions are solely determined by the predictor gain κ. The results are illustrated by computer simulations of coupled chaotic Hindmarsh-Rose neural oscillators. The contents of this chapter are based on [79].

Chapter 8 presents a set of experimental results on network synchronization using *diffusive static time-delayed couplings*. Particularly, we test some theoretical results about *full synchronization* [132], *partial synchronization* [133], and *synchronization in relation to the network topology* [130] in networks of coupled semipassive systems with time-delays. We employ an experimental setup with electronic circuit realizations of the Hindmarsh-Rose neuron model. It is important to notice that in practical situations, the dynamics of the systems in the network cannot be expected to be perfectly identical. For instance, because the signals exchanged among the systems are contaminated with noise and/or there are small mismatches in the systems' parameters. Because of these inherent imperfections, we cannot expect that the systems perfectly synchronize. It is necessary to allow for a mismatch between them, which, of course, needs to be small enough in order to consider that the systems are "*practically synchronized*". To this end, we introduce the notions of *practical synchronization* and *practical partial synchronization*, which states that circuits may be called (partially) synchronized if, after some transient, the differences between their outputs are sufficiently small on a long finite time interval. The experiments with networks of coupled Hindmarsh-Rose circuits indicate when the considered theoretical results, derived for identical systems and without any noise, (fail to) have sufficient predictive value in reality. The results presented in this chapter are based on [131].

All the chapters in this thesis are self-contained with their own introduction and conclusions. However, it is strongly advised to read first Section 1.4, where the notation, some definitions, and the mathematical framework used throughout the thesis are presented. In Figure 1.4, we show some important references to technical results about synchronization using the semipassivity-based framework. It is graphically indicated how these results have evolved from the original paper of Pogromsky in 1998 [104]. The position of this thesis among those results is also presented. Chapter 9 summarizes the most important conclusions of all chapters. Additionally, some recommendations for future research are given.

1.6 List of Publications

Refereed journal publications

- C. Murguía, R.H.B. Fey, and H. Nijmeijer. Network synchronization by dynamic diffusive coupling. International Journal of Bifurcation and Chaos, in Applied Sciences and Engineering, 23(4):1350076, 2013. (Chapter 3)
- C. Murguía, R.H.B. Fey, and H. Nijmeijer. Synchronization in networks of identical linear systems with time-delay. IEEE Transactions on Circuits and Systems-I. Vol. 61, 1801-1814, 2013. (Chapter 2)
- C. Murguía, R.H.B. Fey, and H. Nijmeijer. Network synchronization using invariant manifold based diffusive dynamic couplings with time-delay. Accepted in Automatica, 2014. (Chapter 4)
- C. Murguía, R.H.B. Fey, and H. Nijmeijer. Network synchronization of time-delayed coupled systems using predictor-based diffusive dynamic couplings. Chaos: An Interdisciplinary Journal of Nonlinear Science, 25:023108, 2015. (Chapter 7)
- E. Steur, C. Murguía, R.H.B. Fey and H. Nijmeijer. Synchronization and partial synchronization experiments with networks of time-delay coupled Hindmarsh-Rose neurons. Submitted to the International Journal of Bifurcation and Chaos, 2015. (Chapter 8)
- C. Murguía, R.H.B. Fey, and H. Nijmeijer. Immersion and invariance observers with time-delayed output measurements. Submitted to Communication in Nonlinear Science and Numerical Simulation, 2014. (Chapter 5)

Journal publications in preparation

- C. Murguía, J. Peña, R.H.B. Fey, and H. Nijmeijer. Partial antiphase synchronization between two complex networks using symmetry-based diffusive time-delayed couplings.
- C. Murguía, A. Denasi, R.H.B. Fey, and H. Nijmeijer. Controlled synchronization in networks of heterogeneous nonlinear system with prescribed performance.

Refereed proceedings

- C. Murguía and H. Nijmeijer. Controlled synchronization in networks of nonlinear systems via dynamic couplings, in Proceedings of the 3rd IFAC Conference on Analysis and Control of Chaotic Systems, Cancun, Mexico, 2012. (Chapter 3)
- H. Nijmeijer and C. Murguía. Cooperative mechanical systems: Past, present, and future, in Proceedings of the 56th Japan Joint Automatic Control Conference, pp. 1-4. Tokyo, Japan, 2013.
- T. Oguchi, H. Nijmeijer, C. Murguía, W.A.W.A. Oomen, Partial synchronization in Cartesian product networks of coupled nonlinear systems without/with delays, in Proceedings of the 56th Japan Joint Automatic Control Conference, pp. 1237-1242. Tokyo, Japan, 2013.
- C. Murguía, R.H.B. Fey, and H. Nijmeijer, Partial Network Synchronization and Diffusive Dynamic Couplings, in Proceedings of the IFAC World Conference, Cape Town, South Africa, 2014. (Chapter 6)
- C. Murguía, J. Peña, N. Jeurgens, R.H.B. Fey, T. Oguchi, and H. Nijmeijer, Synchronization in Cartesian-Product Networks of Time-Delay Coupled Systems. Submitted to the 4rd IFAC Conference on Analysis and Control of Chaotic Systems, Tokyo, Japan, 2015.

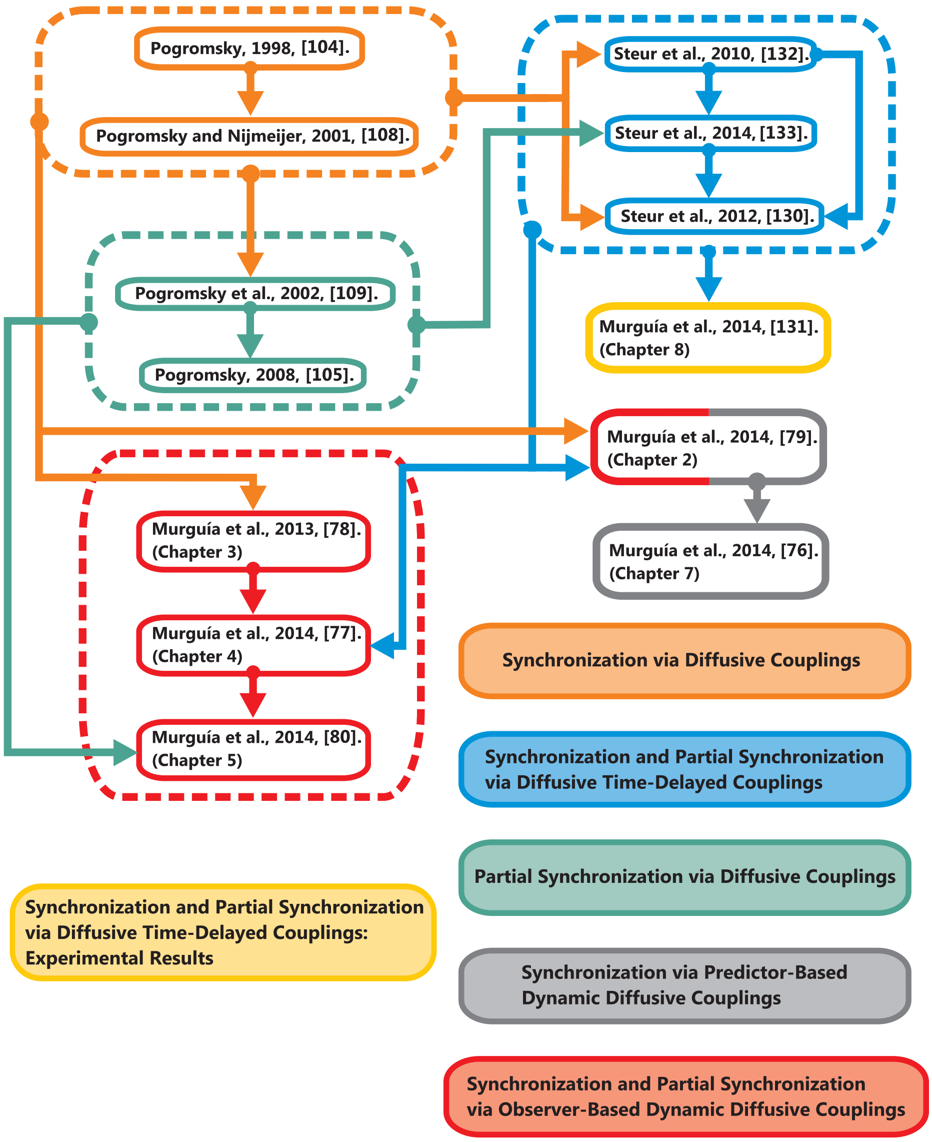

Figure 1.4 Flow chart of the results using the semipassivity-based framework.

Chapter 2

Synchronization of Diffusively Time-Delayed Coupled Linear Systems

Abstract. We study the problem of controlled network synchronization for a class of identical linear systems. The systems are interconnected through static and dynamic *diffusive couplings with time-delays*. In particular, we derive conditions on the systems, the couplings, the time-delay, and the network topology that guarantee global synchronization of the systems. Time-delayed dynamic diffusive couplings are constructed by combining linear observers and output feedback controllers. Using passivity properties of the individual systems, sufficient conditions for boundedness of the interconnected systems are derived. Moreover, predictor-based dynamic couplings are proposed in order to enhance robustness against time-delays in the network. The results are illustrated by numerical simulations.

2.1 Introduction

Synchronization, consensus, and coordination of dynamical linear systems have attracted the attention of many researchers during the last decades. For instance, in engineering, one of the most commonly cited examples for consensus and synchronization of linear systems is the problem of coordinated motion of individual mobile agents [92, 103, 113, 115, 123, 128]. Another example is speed synchronization of multiple induction motors during speed acceleration and load changes [34, 150], for instance, in distributed paper-making machines, continuous rolling mills, and manufacturing assemblies. Synchronization of wind turbines in wind parks is also an interesting example. This occurs when the blades of two different

This chapter is based on [78].

wind turbines have the same rotational speed, then the relative angle between their blades is constant [31, 32]. In this situation, the steady-state fluctuations of the electrical and mechanical variables of the wind turbines have the same values and they can produce significant positive effects on the electrical power system. Recently, consensus and synchronization have been used to control the segmented primary mirror of the *European Extremely Large Telescope* [118]. The controller must stabilize and maintain 984 segments composing the mirror in a fixed smooth surface. Measurements available for feedback are relative positions of neighboring segments, so the output is spatially localized. Distributed integral controllers based on measurements of the adjacent segments are proposed to solve the problem.

In this chapter, we study synchronization in networks of *diffusively coupled* linear systems. There are several technical results about *consensus* and *synchronization* of linear systems interconnected through static and dynamic *diffusive couplings*. In the *consensus* problem [64, 65, 73, 112, 114], the emphasis is on the communication constraints rather than the individual system dynamics. The dynamics of the individual systems are usually very simple (chains of integrators) and the evolution of the group is mostly determined by the network topology. Regarding *synchronization* [19, 43, 47, 84, 104, 147], the focus is not only on the network topology, but also on the individual system dynamics. In practical situations, time-delays caused by signal transmission affect the behavior of the interconnected systems. It is therefore important to study the effect of time-delays in existing synchronization and consensus schemes. In this chapter, we consider the problem of controlled synchronization for a class of identical linear systems in networks with general topologies. The systems are interconnected through either *static* or *dynamic diffusive time-delayed couplings*. Using Lyapunov-Razumikhin functions, we prove that under some mild assumptions there always exists a region $\mathcal{S}$ in the parameter space (*coupling strength* γ *versus time-delay* τ) such that if γ and τ belong to that region, the systems asymptotically synchronize. Moreover, we show that the systems synchronize provided that the *coupling strength* is sufficiently large, and the product of the coupling and the time-delay is sufficiently small, i.e., provided that the coupling is strong, we can always allow for a small time-delay and still end up in synchrony. There are some result in this direction already. In [92] and [28], the authors give estimations of the maximal delay that can be tolerated in the network without compromising the *consensus* behavior. They demonstrate that the maximal delay is inversely proportional to the largest eigenvalue of the Laplacian matrix. Using frequency-dependent and delay-dependent convex sets together with the *generalized Nyquist criterion*, in [74], the authors derive general set valued consensus conditions for linear systems. However, in these results, the dynamics of the individual systems are single, double, or higher dimensional chains of integrators. In [132], sufficient conditions for the existence of the region $\mathcal{S}$ are given for a class of nonlinear systems. In order to derive their results, the authors assume that the individual systems are *semipassive* [104] with respect to the coupling variable z_i and their corresponding internal dynamics have some desired stability properties (*convergent internal dynamics* [94]). In this chapter, we derive a similar result to the one presented in [132] for a class of linear systems. However, the requirements of *semipassivity* and *convergence* of the individual nonlinear systems amount to *passivity* and *detectability* in the linear case. Moreover, we propose *predictor-based dynamic diffusive couplings* in order to enhance robustness against time-delays in the network, i.e., by including some dynamics in the coupling, we may expand the synchronization region $\mathcal{S}$. Additionally, we let the systems be driven by some external piecewise continuous signal ω. Although the systems are linear and time-invariant, the signal ω may lead to oscillatory or even chaotic behavior without any coupling. The signal ω acts as either an external force or a reference signal that may be applied to all the systems. Due to this external signal and the time-delay, it is not immediate that the closed loop system possesses bounded solutions, [44, 122]. Hence, sufficient condition for boundedness of the solutions of the interconnected systems are also derived.

2.2 Systems Description and Time-delayed Couplings

In this section, we introduce the notion of *diffusive time-delayed coupling* together with the system description.

2.2.1 Systems Description

Consider k identical linear dynamical systems

$$\dot{x}_i = Ax_i + B_1 u_i + B_2 \omega, \tag{2.1}$$

$$y_i = C_1 x_i, \tag{2.2}$$

$$z_i = C_2 x_i, \tag{2.3}$$

with $i \in \mathcal{I} := \{1, ..., k\}$, state $x_i \in \mathbb{R}^n$, (measured) output $y_i \in \mathbb{R}^s$, passive output $z_i \in \mathbb{R}^m$, input $u_i \in \mathbb{R}^m$, matrices $A \in \mathbb{R}^{n\times n}, B_1 \in \mathbb{R}^{n\times m}, B_2 \in \mathbb{R}^{n\times w}$, $C_1 \in \mathbb{R}^{s\times n}, C_2 \in \mathbb{R}^{m\times n}$, and the matrix C_2B_1 being similar to a positive definite matrix. The systems are driven by some external signal $\omega(t) : \mathbb{R}_{\geq 0} \to \mathbb{R}^w$, which is assumed to be piecewise continuous and uniformly bounded for all t, i.e., $|\omega(t)| \leq \delta$ for some positive constant δ. The signal $\omega(t)$ acts as either an external force or a reference signal that is applied to all the subsystems. Throughout the chapter the following is assumed:

(H2.1) The system (A, B_1, C_2) is *passive*, i.e., there exists a positive definite matrix $P = P^T \in \mathbb{R}^{n\times n}$ such that

$$PA + A^T P \leq 0,\ B_1^T P = C_2. \tag{2.4}$$

Remark 2.1. *Notice that the nominal system (A, B_1, C_1) is not assumed to be passive. The passivity property is supposed to hold with respect to a state function $z_i = C_2 x_i$, which is not necessarily measured.*

2.2.2 Diffusive Time-Delayed Couplings

In practical situations, time delays caused by signal transmission affect the behavior of the interconnected systems. It is therefore important to study the effect of time-delays in existing synchronization schemes. Here, we consider two different types of *diffusive time-delayed couplings*

$$u_i = \gamma \sum_{j\in\mathcal{E}_i} a_{ij}(z_j^\tau - z_i), \tag{2.5}$$

$$u_i = \gamma \sum_{j\in\mathcal{E}_i} a_{ij}(z_j^\tau - z_i^\tau),\ i \in \mathcal{I}, \tag{2.6}$$

where $\tau \in \mathbb{R}_{>0}$ denotes the finite time-delay, u_i and $z_i^\tau := z_i(t-\tau)$ are the input and the time-delayed passive output of the system i, respectively, z_j^τ is the time-delayed passive output of system j to which system i is connected, $\gamma \in \mathbb{R}_{>0}$ denotes the coupling strength, and $a_{ij} \in \mathbb{R}_{\geq 0}$ are the weights of the interconnections. It is not necessarily assume that $a_{ij} = a_{ji}$. Moreover, since the coupling strength is encompassed in the constant γ, then it is assumed without loss of generality that $\max_{i\in\mathcal{I}} \sum_{j\in\mathcal{E}_i} a_{ij} = 1$. In coupling (2.5), the transmitted signal (the output of node j) is delayed by a factor τ and compared with the current output of node i. This type of coupling arises naturally for interconnected systems since the transmission signals can be expected to take some time. In case of coupling (2.6), both signals are time-delayed. Such a coupling may arise, for instance, when the systems are interconnected by a centralized control law. Couplings (2.6) and (2.5) can be written respectively in matrix form as follows

$$u = -\gamma\,(L \otimes I_m)\,z^\tau, \tag{2.7}$$

$$u = -\gamma\,(\mathcal{D} \otimes I_m)\,z + \gamma\,(\Lambda \otimes I_m)\,z^\tau, \tag{2.8}$$

where $u = \mathrm{col}(u_1, ..., u_k)$, $z = \mathrm{col}(z_1, ..., z_k)$, adjacency matrix $\Lambda \in \mathbb{R}^{k\times k}$, and diagonal degree matrix $\mathcal{D} \in \mathbb{R}^{k\times k}$. By definition any connected graph possesses one independent strongly connected component (iSCC), see Definition 1.9. Let

$\mathcal{V}_s = \{v_1, ..., v_{k_1}\}$ be the nodes forming the iSCC and $\mathcal{V}_c = \{v_{k_1+1}, ..., v_k\}$ the remaining nodes. It follows that the Laplacian matrix L of a connected graph can be written as follows

$$L = \begin{pmatrix} L_s & \mathbf{0} \\ \mathcal{F} & L_c \end{pmatrix}, \tag{2.9}$$

where the matrix $L_s \in \mathbb{R}^{k_1 \times k_1}$ denotes the Laplacian matrix of the iSCC of the graph, i.e., the Laplacian of the subgraph $\mathcal{G}_s = (\mathcal{V}_s, \mathcal{E}_s, A_s)$ where $\mathcal{E}_s \subseteq \mathcal{V}_s \times \mathcal{V}_s$ and $\Lambda_s \in \mathbb{R}^{k_1 \times k_1}$ the associated weighted adjacency matrix. The matrix $\mathcal{F} \in \mathbb{R}^{k_1 \times (k-k_1)}$ denotes the interconnection between the iSCC and the remaining nodes and $L_c \in \mathbb{R}^{(k-k_1)\times(k-k_1)}$ is a the matrix denoting the rest of the interconnection. If the systems interact on a simple connected graph, we can rewrite the couplings (2.7) and (2.8) as follows

$$\begin{pmatrix} u_s \\ u_c \end{pmatrix} = -\gamma \begin{pmatrix} L_s \otimes I_m & \mathbf{0} \\ \mathcal{F} \otimes I_m & L_c \otimes I_m \end{pmatrix} \begin{pmatrix} z_s^\tau \\ z_c^\tau \end{pmatrix}, \tag{2.10}$$

and

$$\begin{aligned} \begin{pmatrix} u_s \\ u_c \end{pmatrix} = & -\gamma \begin{pmatrix} \mathcal{D}_s \otimes I_m & \mathbf{0} \\ \mathbf{0} & \mathcal{D}_c \otimes I_m \end{pmatrix} \begin{pmatrix} z_s \\ z_c \end{pmatrix} \\ & + \gamma \begin{pmatrix} \Lambda_s \otimes I_m & \mathbf{0} \\ \mathcal{F} \otimes I_m & \Lambda_c \otimes I_m \end{pmatrix} \begin{pmatrix} z_s^\tau \\ z_c^\tau \end{pmatrix}, \end{aligned} \tag{2.11}$$

respectively, where $u = \text{col}(u_s, u_c) \in \mathbb{R}^{km}$ and $z = \text{col}(z_s, z_c) \in \mathbb{R}^{km}$. Moreover, $D_s := diag\{d_1, ..., d_{k_1}\} \in \mathbb{R}^{k_1 \times k_1}$, $\Lambda_s := \mathcal{D}_s - L_s$, $\mathcal{D}_c := diag\{d_{k_1+1}, ..., d_k\} \in \mathbb{R}^{k-k_1 \times k-k_1}$, and $\Lambda_c := \mathcal{D}_c - L_c$. The vectors z_s and z_c are partitions of the stacked vector z such that $z_s = \text{col}(z_1, ..., z_{k_1}) \in \mathbb{R}^{mk_1}$ and $z_c = \text{col}(z_{k_1+1}, ..., z_k) \in \mathbb{R}^{m(k-k_1)}$. The vector z_s stands for the stacked output of the iSCC and z_c is the stacked output of the remaining nodes.

2.3 Boundedness and Synchronization

Due to the external signal ω and the time-delay, it is not immediate that the closed-loop system possesses bounded solutions, [44, 122]. Moreover, even without time-delay, it is not trivial that systems interacting through diffusive couplings have bounded solutions. The diffusive coupling can make systems which have an asymptotically stable equilibrium in isolation to produce stable oscillations [107].

2.3.1 Boundedness

Let the k systems (2.1),(2.3) be interconnected via the *diffusive time-delayed coupling* (2.6). Notice that the closed-loop stacked system is written as follows

$$\dot{x} = (I_k \otimes A)x - \gamma(L \otimes B_1 C_2)x^{\tau} + (\mathbf{1}_{k\times 1} \otimes B_2)\omega. \tag{2.12}$$

with $x = \mathrm{col}(x_1, ..., x_k)$.

Lemma 2.2. *Consider the k passive systems* (2.1),(2.3) *with* $|\omega(t)| < \delta$ *for some constant* $\delta \in \mathbb{R}_{>0}$ *and positive definite matrix* $P = P^T \in \mathbb{R}^{n\times n}$ *satisfying* (2.4). *Let the systems be interconnected through the diffusive time-delayed coupling* (2.6) *with coupling strength* $\gamma \in \mathbb{R}_{>0}$ *on a simple connected graph. Assume that there exists a constant* $\beta \in \mathbb{R}_{>0}$ *such that the following Riccati inequality is satisfied*

$$PA + A^T P + \beta P B_2 B_2^T P + 2\gamma\bar{a} C_2^T C_2 \quad \leq \quad 0, \tag{2.13}$$

where $\bar{a} = 2\bar{d} + \|\mathcal{F}\| + \|L_c\|$ *and* $\bar{d} = max_{i\in\mathcal{I}} \sum_{j\in\mathcal{E}_i} a_{ij}$. *Let* γ_{max} *be the largest* γ *that satisfies inequality* (2.13), *then the solutions of the closed-loop system* (2.1),(2.3),(2.6) *are bounded for all finite* $\tau \geq 0$ *and* $\gamma \in \mathcal{I}_\gamma := [0, \gamma_{max}]$.

The proof of Lemma 2.2 can be found in the Appendix A.

Remark 2.3. *The result stated in Lemma 2.2 is independent of the time-delay. Therefore, if* (2.13) *is satisfied, the closed-loop system* (2.1),(2.3),(2.6) *is bounded for arbitrary large time-delay. However, it can be shown that if* (2.13) *is not satisfied for any* $\gamma \in \mathbb{R}_{>0}$, *but the inequality*

$$PA + A^T P + \beta P B_2 B_2^T P \leq 0, \tag{2.14}$$

is satisfied for some $\beta \in \mathbb{R}_{>0}$, *then the solutions may be bounded for some values of* (γ, τ) *in some set* $\mathcal{I}_{\gamma\tau}$. *That is, there may exist a delay-dependent region* $\mathcal{I}_{\gamma\tau}$ *where boundedness of the closed-loop system is guaranteed.*

Remark 2.4. *Using the Schur complement* [120], *the boundedness condition* (2.13) *can be rewritten as the following linear matrix inequality* (LMI)

$$\begin{pmatrix} PA + A^T P & PB_1 & PB_2 \\ B_1^T P & -\frac{1}{\gamma\bar{a}} I & \mathbf{0} \\ B_2^T P & \mathbf{0} & -\frac{1}{\beta} I \end{pmatrix} \leq 0. \tag{2.15}$$

It follows that the boundedness problem considered in Lemma 2.2 can be regarded as a feasibility problem of the LMI (2.15). *Then, for a given* γ, *constant* $\bar{a}$, *and matrix* P *satisfying* (2.4), *the solutions of the closed-loop system* (2.1),(2.3),(2.6) *are bounded, if there exists a constant* $\beta \in \mathbb{R}_{>0}$ *such that* (2.15) *is feasible. This condition is only satisfied for values of* γ *in some interval* $\mathcal{I}_\gamma$. *Then, the solutions of the closed-loop system are ensured to be bounded for* $\gamma \in \mathcal{I}_\gamma$

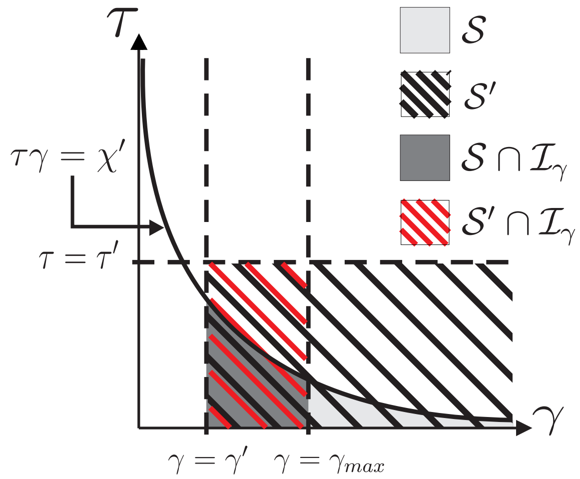

Figure 2.1 Extended region of attraction for synchronization $\mathcal{S} \cap \mathcal{I}_\gamma \subseteq \mathcal{S}'$.

Remark 2.5. *The result presented in Lemma 2.2 applies for systems interacting on a simple connected graph. If the systems interact on a simple strongly connected graph, it follows that $L = L_s$, $L_c = \mathbf{0}$, and $\mathcal{F} = \mathbf{0}$, i.e., the strongly connected component is the graph itself. Then, the condition for boundedness* (2.13) *amounts to*

$$PA + A^T P + \beta P B_2 B_2^T P + 4\gamma \bar{d} C_2^T C_2 \quad \leq \quad 0. \tag{2.16}$$

Now, let the k systems (2.1),(2.3) be interconnected through the *diffusive time-delayed coupling* (2.5). Note that, in this case, the closed-loop stacked system is written as

$$\dot{x} = (I_k \otimes A)x - \gamma(\mathcal{D} \otimes B_1 C_2)x + \gamma(\Lambda \otimes B_1 C_2)x^\tau + (\mathbf{1}_{k\times 1} \otimes B_2)\omega.$$

Lemma 2.6. *Consider the k identical passive systems* (2.1),(2.3) *with $|\omega(t)| < \delta$ for some constant $\delta \in \mathbb{R}_{>0}$ and positive definite matrix $P = P^T \in \mathbb{R}^{n\times n}$ satisfying* (2.4). *Let the systems be interconnected through the diffusive time-delayed coupling* (2.5) *with coupling strength $\gamma \in \mathbb{R}_{>0}$ on a simple connected graph. Assume that there exists a constant $\beta \in \mathbb{R}_{>0}$ such that the following Riccati inequality is satisfied*

$$PA + A^T P + \beta P B_2 B_2^T P + 2\gamma \bar{a} C_2 C_2^T \quad \leq \quad 0, \tag{2.17}$$

where $\bar{a} = max\,(\|\mathcal{F}\| + \|\Lambda_c\| - \underline{d}\ \ , \|\mathcal{F}\|)$ and $\underline{d} = min_{i\in(k_1+1,\ldots,k)} \sum_{j\in\mathcal{E}_i} a_{ij}$. Let γ_{max} be the largest γ that satisfies inequality (2.17), *then the solutions of the closed-loop system* (2.1),(2.3),(2.5) *are bounded for all finite $\tau \geq 0$ and $\gamma \in \mathcal{I}_\gamma = [0, \gamma_{max}]$.*

The proof is very similar to the proof Lemma 2.2 and it is omitted here.

Remark 2.7. *If the systems interact on a simple strongly connected graph, the condition for boundedness* (2.17) *is weakened to* (2.14)*, i.e., solutions are bounded for arbitrarily large γ as long as* (2.14) *holds.*

2.3.2 Synchronization

In this section, we derive sufficient conditions for synchronization of systems interacting through the *diffusive time-delayed couplings* described in the previous section. Passivity of (2.1),(2.3) and nonsingularity of the matrix C_2B_1 imply the existence of a coordinate transformation such that the systems can be written in the following normal form

$$\dot{\zeta}_i = N_1\zeta_i + N_2z_i + N_3\omega, \tag{2.18}$$

$$\dot{z}_i = M_1\zeta_i + M_2z_i + M_3\omega + C_2B_1u_i, \tag{2.19}$$

with $i \in \mathcal{I}$, internal state $\zeta_i \in \mathbb{R}^p$, $p := n - m$, matrices $N_1 \in \mathbb{R}^{p\times p}, N_2 \in \mathbb{R}^{p\times m}, N_3 \in \mathbb{R}^{p\times w}, M_1 \in \mathbb{R}^{m\times p}$, $M_2 \in \mathbb{R}^{m\times m}, M_3 \in \mathbb{R}^{m\times w}$, and C_2B_1 being nonsingular. In addition, if the pair (A, C_2) is detectable, then it can be shown that the coordinate transformation can be chosen such that the matrix N_1 is Hurwitz. For the sake of simplicity, we assume that $C_2B_1 = I_m$. Then, the stacked system is given by

$$\dot{\zeta} = (I_k \otimes N_1)\zeta + (I_k \otimes N_2)z + (I_k \otimes N_3)\omega, \tag{2.20}$$

$$\dot{z} = (I_k \otimes M_1)\zeta + (I_k \otimes M_2)z + (I_k \otimes M_3)\omega + u, \tag{2.21}$$

with $\zeta = \mathrm{col}(\zeta_1, ..., \zeta_k)$. Define the linear manifold

$$\mathcal{M} := \left\{\mathrm{col}(z,\zeta) \in \mathbb{R}^{kn} |\ z_j = z_i \text{ and } \zeta_j = \zeta_i\ \forall\, i,j\right\}.$$

The manifold $\mathcal{M}$ is often called the *synchronization manifold* or the *diagonal set*. In the following theorem, we give sufficient conditions for synchronization when the systems are interconnected via the time-delayed diffusive coupling (2.6).

Theorem 2.8. *Consider k identical systems* (2.1),(2.3) *interacting through the time-delayed diffusive coupling* (2.6) *on a simple connected graph. Assume that the pair (A, C_2) is detectable and the conditions of Lemma 2.2 are satisfied. Then, there exist positive constants $\gamma', \chi' \in \mathbb{R}_{>0}$ such that if $\gamma' < \gamma \leq \gamma_{max}$ (with γ_{max} being the maximal coupling strength for which boundedness of solutions is guaranteed) and $\gamma\tau < \chi'$, then the solutions of the closed-loop system* (2.1),(2.3),(2.6) *asymptotically converge to the diagonal set $\mathcal{M}$.*

The proof of Theorem 2.8 can be found in the Appendix A. Next, let the systems (2.1),(2.3) be interconnected through (2.5).

Theorem 2.9. *Consider k identical systems* (2.1),(2.3) *interacting through the time-delayed diffusive coupling* (2.5) *on a simple connected graph. Assume that the pair (A, C_2) is detectable and the conditions of Lemma 2.6 are satisfied. Then, there exist positive constants $\gamma', \chi' \in \mathbb{R}_{>0}$ such that if $\gamma' < \gamma \leq \gamma_{max}$ (with γ_{max} being the maximal coupling strength for which boundedness of solutions is guaranteed) and $\gamma\tau < \chi'$, then the solutions of the closed-loop system* (2.1),(2.3),(2.5) *asymptotically converge to the diagonal set $\mathcal{M}$.*

The proof is very similar to the proof of Theorem 2.8 and it is omitted here. The results stated in Theorem 2.8 and Theorem 2.9 amount to the following. If the conditions of the above theorems are satisfied, then there always exists a region $\mathcal{S} = \{\gamma, \tau \in \mathbb{R}_{\geq 0} | \gamma > \gamma' \text{ and } \gamma\tau < \chi'\}$, (lighter gray area in Figure 2.1), such that if $(\gamma, \tau) \in \mathcal{S} \cap \mathcal{I}_\gamma$, (darker gray area in Figure 2.1), the k diffusively interconnected systems synchronize. Note that if $\gamma_{max} < \gamma'$ synchronization can not be achieved.

Remark 2.10. *The results stated in Theorem 2.8 and Theorem 2.9 remain valid without the assumptions of Lemma 2.2 and Lemma 2.6, respectively, as long as the solutions of the whole network are bounded. Similar statements can be made for the subsequent results.*

In the above remark, we want to point out that all the synchronization results in this chapter are valid even if the systems are not passive and the Ricatti equations in all the the lemmas are not satisfied as long as the closed-loop system has bounded solutions. It may be that solutions are bounded for some values of (γ, τ) in some set $\mathcal{I}_{\gamma\tau}$, then the synchronization results can be applied in this set.

2.4 Diffusive Dynamic Time-Delayed Couplings

2.4.1 Observer-based Diffusive Dynamic Couplings

So far, it has been assumed that z_i (the passive output) is available for feedback. However, if the measurable output is a different state function $y_i = C_1 x_i$, which does not have the desired passivity properties, then the results stated in Theorem 2.8 and Theorem 2.9 cannot be used to conclude synchronization. Nevertheless, if the pair (A, C_1) is detectable, there exists an observer which reconstructs the retarded passive output z_i^τ from measurements of y_i^τ. Then, an *observer-based diffusive dynamic coupling* (ODDC), which only depends on the time-delayed measurable output y_i^τ can be constructed. Consider an observer of the form

$$\begin{aligned} \dot{\eta}_i &= A\eta_i + B_1 u_i^\tau + B_2 \omega^\tau + H(C_1\eta_i - y_i^\tau), \\ \hat{z}_i^\tau &= C_2 \eta_i(t). \end{aligned} \tag{2.22}$$

Define the estimation error $\epsilon_i := \eta_i - x_i^\tau$. Then, the estimation error dynamics is given by

$$\dot{\epsilon}_i = (A + HC_1)\,\epsilon_i. \tag{2.23}$$

It follows that the observer (2.22) exponentially reconstructs z_i^τ, if and only if the matrix $(A + HC_1)$ is Hurwitz. Then, combining (2.22) and an estimated version of (2.6), we construct the ODDC as follows

$$\begin{aligned} \dot{\eta}_i &= A\eta_i + B_1 u_i^\tau + B_2 \omega^\tau + H(C_1\eta_i - y_i^\tau), && (2.24)\\ u_i &= \gamma \sum_{j\in\mathcal{E}_i} a_{ij} C_2\,(\eta_j - \eta_i)\,,\ i \in \mathcal{I}. && (2.25) \end{aligned}$$

In the following lemma and theorem, we give sufficient conditions for boundedness and synchronization of the solutions of the closed-loop system (2.1),(2.2), (2.24),(2.25).

Lemma 2.11. *Consider the k identical passive systems* (2.1)-(2.3) *with $|\omega(t)| < \delta$ for some constant $\delta \in \mathbb{R}_{>0}$ and positive definite matrix $P = P^T \in \mathbb{R}^{n\times n}$ satisfying* (2.4). *Let the systems be interconnected through the* ODDC (2.24),(2.25) *with coupling strength $\gamma \in \mathbb{R}_{>0}$ on a simple connected graph. Suppose that the pair (A, C_1) is detectable and the observer gain H is such that $A + HC_1$ is Hurwitz. In addition, assume that there exists a constant $\beta \in \mathbb{R}_{>0}$ such that* (2.13) *is satisfied. Let γ_{max} be the largest γ that satisfies inequality* (2.13)*, then the solutions of the closed-loop system* (2.1),(2.2),(2.24),(2.25) *are bounded for all finite $\tau \geq 0$ and $\gamma \in \mathcal{I}_\gamma = [0, \gamma_{max}]$.*

Theorem 2.12. *Consider k identical systems* (2.1),(2.2) *interacting through the* ODDC (2.24),(2.25) *on a simple connected graph. Assume that the pairs (A, C_1) and (A, C_2) are detectable and the conditions of Lemma 2.11 are satisfied. Then, there exist positive constants $\gamma', \chi' \in \mathbb{R}_{>0}$ such that if $\gamma' < \gamma \leq \gamma_{max}$ (with γ_{max} being the maximal coupling strength for which boundedness of solutions is guaranteed) and $\gamma\tau < \chi'$, then the solutions of the closed-loop system* (2.1),(2.2),(2.24), (2.25) *asymptotically converge to the diagonal set $\mathcal{M}$.*

The proofs of Lemma 2.11 and Theorem 2.12 can be found in the Appendix A.

2.4.2 Predictor-based Diffusive Dynamic Couplings

Now, we study whether it is possible to enhance robustness against time-delays in the network by including some dynamics in the coupling. *Predictor-based diffusive dynamic couplings* (PDDC) that may increase the region of attraction for synchronization are proposed. Consider a predictor of the form

$$\begin{aligned} \dot{\varsigma}_i &= A\varsigma_i + B_1 u_i + B_2\omega + K_1(C_2\varsigma_i^\tau - z_i^\tau), && (2.26)\\ \hat{z}_i &= C_2\varsigma_i, \end{aligned}$$

with predictor state $\varsigma_i \in \mathbb{R}^n$ and predictor gain $K_1 \in \mathbb{R}^{n\times m}$. Define the prediction error $\varepsilon_i := \varsigma_i - x_i$, then

$$\dot{\varepsilon}_i = A\varepsilon_i + K_1 C_2 \varepsilon_i^\tau, \tag{2.27}$$

notice that $\varepsilon_i(t) \to 0$ implies that $\varsigma_i(t) \to x_i(t)$. The origin $\varepsilon_i = 0$ of (2.27) is exponentially stable if and only if the roots of the characteristic equation

$$\det\left(\lambda I - A - K_1 C_2 e^{-\lambda\tau}\right) = 0, \tag{2.28}$$

belong to the open left half of the complex plane, (see [72] for details). Then, system (2.26) is called a predictor for system (2.1),(2.3) if and only if there exists a gain K_1 such that all the roots of (2.28) possess negative real parts.

Remark 2.13. *The characteristic equation* (2.28) *is transcendental and has infinitely many solutions. Moreover, its exact region of stability as an explicit function of A, K_1, C_2, and τ is not known analytically. However, the purpose of this chapter is not to give a solution method to the spectrum assignment problem of* (2.27)*. There are several results dealing with approximating this stability region. For instance, in* [71]*, the authors propose a stabilization method for linear time-delayed systems, which consists in controlling the rightmost eigenvalue of the closed-loop system. They use the software package* DDE-BIFTOOL [41] *to approximate such an eigenvalue. In* [72]*, analytical methods and computational algorithms using a unified eigenvalue-based approach are presented. Finally, results based on* LMIs *can be found in, for instance,* [83] *and references therein.*

Combining (2.26) and a delay-free version of (2.6), we construct the PDDC as follows

$$\begin{aligned}
\dot{\varsigma}_i &= A\varsigma_i + B_1 u_i + B_2\omega + K_1(C_2\varsigma_i^\tau - z_i^\tau), &(2.29)\\
u_i &= \gamma \sum_{j\in\mathcal{E}_i} a_{ij} C_2\left(\varsigma_j - \varsigma_i\right), \quad i \in \mathcal{I}. &(2.30)
\end{aligned}$$

In the following lemma and theorem, we give sufficient conditions for boundedness and synchronization of the solutions of the closed-loop system (2.1),(2.3), (2.29),(2.30).

Lemma 2.14. *Consider the k identical passive systems* (2.1),(2.3) *with $|\omega(t)| < \delta$ for some constant $\delta \in \mathbb{R}_{>0}$ and positive definite matrix $P = P^T \in \mathbb{R}^{n\times n}$ satisfying* (2.4)*. Let the systems be interconnected through the* PDDC (2.29),(2.30) *with coupling strength $\gamma \in \mathbb{R}_{>0}$ on a simple connected graph. Suppose that the pair (A, C_2) is detectable and the predictor gain K_1 is such that all the roots of* (2.28) *belong to the open left half of the complex plane. In addition, assume that there exists a constant $\beta \in \mathbb{R}_{>0}$ such that* (2.13) *is satisfied with $\bar{a} = \|\mathcal{F}\| + \|L_c\|$. Let γ_{max} be the largest γ that satisfies inequality* (2.13)*, then the solutions of the closed-loop system* (2.1),(2.3),(2.29),(2.30) *are bounded for all finite $\tau \geq 0$ and $\gamma \in \mathcal{I}_\gamma = [0, \gamma_{max}]$.*

Theorem 2.15. *Consider k identical systems* (2.1),(2.3) *interacting through the* PDDC (2.29),(2.30) *on a simple connected graph. Assume that the pair (A, C_2) is detectable and the conditions of Lemma 2.14 are satisfied. Then, there exist positive constants $\gamma', \tau' \in \mathbb{R}_{>0}$ such that if $\gamma' < \gamma \leq \gamma_{max}$ (with γ_{max} being the maximal coupling strength for which boundedness of solutions is guaranteed) and $\tau < \tau'$, then the solutions of the closed-loop system* (2.1),(2.3),(2.29),(2.30) *asymptotically converge to the diagonal set $\mathcal{M}$.*

The proofs of Lemma 2.14 and Theorem 2.15 can be found in the Appendix A. Assume again that the passive output $z_i = C_2 x_i$ is not available for feedback. Next, a PDDC that may compensate for the time-delay in the network and estimate the passive output z_i from measurements of y_i^τ is proposed. Consider the following PDDC

$$\dot{\varsigma}_i = A\varsigma_i + B_1 u_i + B_2\omega + K_2(C_1\varsigma_i^\tau - y_i^\tau), \tag{2.31}$$

$$u_i = \gamma \sum_{j \in \mathcal{E}_i} a_{ij} C_2 \left(\varsigma_j - \varsigma_i\right), \quad i \in \mathcal{I}, \tag{2.32}$$

with predictor state $\varsigma_i \in \mathbb{R}^n$ and predictor gain $K_2 \in \mathbb{R}^{n \times s}$. Consider the error $\varepsilon_i = \varsigma_i - x_i$, then

$$\dot{\varepsilon}_i = A\varepsilon_i + K_2 C_1 \varepsilon_i^\tau. \tag{2.33}$$

The origin $\varepsilon_i = \mathbf{0}$ of (2.33) is exponentially stable if and only if the roots of the characteristic equation

$$\det\left(\lambda I - A - K_2 C_1 e^{-\lambda\tau}\right) = 0, \tag{2.34}$$

belong to the open left half of the complex plane. In the following lemma and theorem, we give sufficient conditions for boundedness and synchronization of the solutions of the coupled systems (2.1),(2.2),(2.31),(2.32).

Lemma 2.16. *Consider the k identical passive systems* (2.1)-(2.3) *with $|\omega(t)| < \delta$ for some constant $\delta \in \mathbb{R}_{>0}$ and positive definite matrix $P = P^T \in \mathbb{R}^{n \times n}$ satisfying* (2.4). *Let the systems be interconnected through the* PDDC (2.31),(2.32) *with coupling strength $\gamma \in \mathbb{R}_{>0}$ on a simple connected graph. Suppose that the pair (A, C_1) is detectable and the predictor gain K_2 is such that all the roots of* (2.34) *belong to the open left half of the complex plane. In addition, assume that there exists a constant $\beta \in \mathbb{R}_{>0}$ such that* (2.13) *is satisfied with $\bar{a} = \|\mathcal{F}\| + \|L_c\|$. Let γ_{max} be the largest γ that satisfies inequality* (2.13), *then the solutions of the closed-loop system* (2.1),(2.2),(2.31),(2.32) *are bounded for all finite $\tau \geq 0$ and $\gamma \in \mathcal{I}_\gamma = [0, \gamma_{max}]$.*

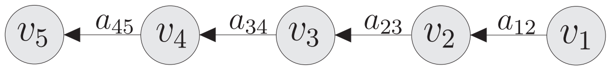

Figure 2.2 Graph of the interconnection.

Theorem 2.17. *Consider k identical systems* (2.1),(2.2) *interacting through the* PDDC (2.31),(2.32) *on a simple connected graph. Assume that the pairs (A, C_2) and (A, C_1) are detectable and the conditions of Lemma 2.16 are satisfied. Then, there exist positive constants $\gamma', \tau' \in \mathbb{R}_{>0}$ such that if $\gamma' < \gamma \leq \gamma_{max}$ (with γ_{max} being the maximal coupling strength for which boundedness of solutions is guaranteed) and $\tau < \tau'$, then the solutions of the closed-loop system* (2.1),(2.2),(2.31),(2.32) *asymptotically converge to the diagonal set $\mathcal{M}$.*

The proofs of Lemma 2.16 and Theorem 2.17 are very similar to the proofs of Lemma 2.14 and Theorem 2.15 and we omit them here. From Theorem 2.15 and Theorem 2.17, it can be concluded that if the predictor gains K_1 and K_2 are chosen appropriately, the region of attraction for synchronization may be increased with respect to the region $\mathcal{S}$. In other words, if the systems are interconnected either by (2.29),(2.30) or (2.31),(2.32), then there always exists a region $\mathcal{S}' = \{\gamma, \tau \in \mathbb{R}_{\geq 0} | \gamma > \gamma' \text{ and } \tau < \tau'\}$, indicated in Figure 2.1, such that if $(\gamma, \tau) \in \mathcal{S}' \cap \mathcal{I}_\gamma$, then the systems synchronize. Moreover, if the matrices K_1 and K_2 are chosen appropriately, it may be that $S \cap \mathcal{I}_\gamma \subseteq S' \cap \mathcal{I}_\gamma$.

2.5 Two Examples

2.5.1 Second Order Systems

A.1 Dynamical model

Consider k identical systems (2.1)-(2.3) with matrices

$$\begin{aligned} A &= \begin{pmatrix} 0 & a_1 \\ -a_2 & -a_3 \end{pmatrix}, \; B_1 = B_2 = \begin{pmatrix} 0 \\ 1 \end{pmatrix}, \\ C_1 &= \begin{pmatrix} 1 & 0 \end{pmatrix}, \; C_2 = \begin{pmatrix} 1 & \frac{2a_1}{a_3} \end{pmatrix}. \end{aligned} \tag{2.35}$$

with $a_1, a_2, a_3 \in \mathbb{R}_{>0}$. The above system represents the dynamics of a large class of linear systems, e.g., *Mass-Spring-Damper* systems or *RLC* circuits. See for instance

[149] and [67], respectively, for applications of networks of such systems. Define the function $\omega(t)$ as

$$\omega(t) = \text{sign}(\sin(2t) + \cos(t)), \tag{2.36}$$

with sign$(0) = 0$, which is piecewise continuous and bounded.

A.2 Passivity

The system (A, B_1, C_2) as in (2.35) is strictly-passive with positive definite matrix $P = P^T \in \mathbb{R}^{2\times 2}$ as follows

$$P = \begin{pmatrix} \frac{2a_2}{a_3} + \frac{a_3}{a_1} & 1 \\ 1 & \frac{2a_2}{a_3} \end{pmatrix}, \tag{2.37}$$

and

$$PA + A^T P = \begin{pmatrix} -2a_2 & 0 \\ 0 & -2a_1 \end{pmatrix}. \tag{2.38}$$

A.3 Network Topology and Diffusive Time-Delayed Coupling

Consider a network of five systems interconnected according to the graph depicted in Figure 2.2 with $a_{ij} = 1$ if $\{ij\} \in \mathcal{E}$ and $a_{ij} = 0$ otherwise. This network is *connected* and has a unique centroid v_1. Then, the Laplacian matrix $L \in \mathbb{R}^{5\times 5}$ is given by

$$L = \begin{pmatrix} 0 & 0 & 0 & 0 & 0 \\ -1 & 1 & 0 & 0 & 0 \\ 0 & -1 & 1 & 0 & 0 \\ 0 & 0 & -1 & 1 & 0 \\ 0 & 0 & 0 & -1 & 1 \end{pmatrix}. \tag{2.39}$$

Let the five systems be interconnected through the *time-delayed diffusive coupling* (2.6), i.e.,

$$u(t) = -\gamma L z(t - \tau), \tag{2.40}$$

with time-delay τ, input vector $u = \text{col}(u_1, ..., u_5)$, delayed output vector $z^\tau = \text{col}(z_1^\tau, ..., z_5^\tau)$, and coupling strength γ.

A.4 Boundedness

The system (A, B_1, C_2) as in (2.35) is *strictly-passive*, the external signal ω is uniformly bounded, and the graph depicted in Figure 2.2 is *connected*. Then, by Lemma 2.2, the solutions of the closed-loop system (2.1),(2.3),(2.35),(2.40) are bounded for arbitrary large time-delay, if inequality (2.13) is satisfied for a given coupling strength γ and some positive constant β. Taking $a_1 = a_2 = a_3 = 1$, inequality (2.13) takes the following form

$$Q(\beta, \gamma) = \begin{pmatrix} -2 + \beta + 2\gamma & 2(\beta + 2\gamma) \\ 2(\beta + 2\gamma) & -2 + 4\beta + 8\gamma \end{pmatrix} \leq 0. \tag{2.41}$$

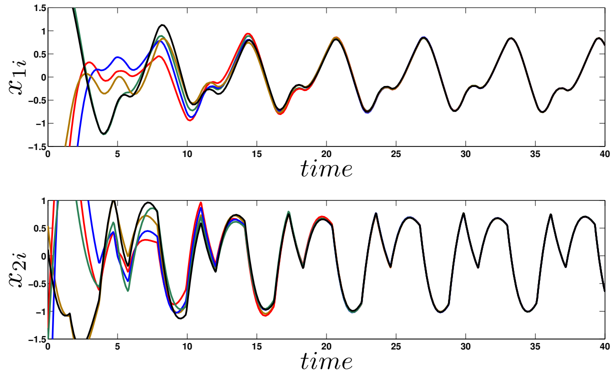

Figure 2.3 Synchronization of five systems, $x_i = (x_{1i}, x_{2i})^T$.

The above inequality is satisfied if the eigenvalues of the symmetric matrix $Q(\beta, \gamma)$ are nonpositive, i.e.,

$$\lambda(Q(\beta, \gamma)) = (-2, -2 + 5\beta + 10\gamma) \leq 0.$$

The constant β can be arbitrarily small as long as it is larger than zero. Maximizing γ in $\lambda(Q(\beta, \gamma))$ yields a maximal $\gamma_{max} = 0.2$. Therefore, the solutions of the closed-loop system are ensured to be bounded for $\gamma \leq \gamma_{max} = 0.2$ and $\tau \geq 0$. The result stated in Lemma 2.2 is just a sufficient condition, then it may be that boundedness is possible for larger values of γ. Actually, using computer simulation, we found that boundedness is guarantee for $\gamma \leq 0.23$. Moreover, the result in Lemma 2.2 is independent of the time-delay, then it may be that the closed-loop system possesses bounded solutions for some values of (γ, τ) in some set $\mathcal{I}_{\gamma\tau}$, i.e., there may exists a delay-dependent region where boundedness is guaranteed.

A.5 Synchronization

The conditions of Lemma 2.2 are satisfied and the pair (A, C_2) as in (2.35) is observable. Then by Theorem 2.8, the systems synchronize provided that $\gamma \leq \gamma_{max}$ is sufficiently large, and $\gamma\tau$ is sufficiently small. Figure 2.3 depicts the simulation results for $\tau = 2$ and $\gamma = 0.1$.

2.5.2 Linear Oscillators

B.1 Dynamical Model and Network Topology

Consider a group of k systems (2.1)-(2.3) with matrices

$$A = \begin{pmatrix} 0 & 1 & 0 \\ -1 & 0 & 0 \\ -1 & -1 & -1 \end{pmatrix}, \quad B_1 = \begin{pmatrix} 1 \\ 0 \\ 0 \end{pmatrix}, \tag{2.42}$$

$$B_2 = \begin{pmatrix} 0 \\ 0 \\ 1 \end{pmatrix}, \quad C_1 = B_2^T, \quad C_2^T = \begin{pmatrix} 1.21 \\ 0 \\ 0.18 \end{pmatrix}.$$

The function $\omega(t)$ is defined as

$$\omega(t) = \text{sign}(\sin(2t+5) + \cos(t)) + \cos(t)\sin(10t), \tag{2.43}$$

with sign$(0) = 0$, which is piecewise continuous and bounded. Consider a network of eight systems interconnected according to the graph depicted in Figure 2.4 with $a_{ij} = 1$ if $\{ij\} \in \mathcal{E}$ and $a_{ij} = 0$ otherwise. Then, the Laplacian matrix $L \in \mathbb{R}^{8\times 8}$ is given by

$$L = \begin{pmatrix} 2 & -1 & 0 & 0 & -1 & 0 & 0 & 0 \\ 0 & 1 & 0 & -1 & 0 & 0 & 0 & 0 \\ -1 & 0 & 1 & 0 & 0 & 0 & 0 & 0 \\ 0 & 0 & -1 & 2 & 0 & 0 & 0 & -1 \\ 0 & 0 & 0 & 0 & 1 & 0 & -1 & 0 \\ 0 & 0 & 0 & 0 & -1 & 1 & 0 & 0 \\ 0 & 0 & 0 & 0 & 0 & 0 & 1 & -1 \\ 0 & 0 & 0 & 0 & 0 & -1 & 0 & 1 \end{pmatrix}. \tag{2.44}$$

Again, this network satisfies the minimal connectivity requirements for achieving synchronization of the coupled systems, i.e., it is *simple* and *connected*.

B.2 Observer-based Dynamic Diffusive Coupling

The pairs (A, C_1) and (A, C_2) are observable, and the system (A, B_1, C_2) is passive with matrix P satisfying (2.4) given by

$$P = \begin{pmatrix} 1.21 & 0 & 0.18 \\ 0 & 1.02 & 0 \\ 0.18 & 0 & 0.18 \end{pmatrix}. \tag{2.45}$$

Next, assume that the measurable output y_i is subject to constant time-delay. Let the eight systems be interconnected through the ODDC (2.24),(2.25),(2.42) with observer gain $H = (2.6, 0.65, -2.6)^T$. The boundedness inequality (2.13) of Theorem 2.12 is not satisfied for any $P > 0$ and $\gamma, \beta \in \mathbb{R}_{>0}$, i.e., there does not exist a γ which ensures boundedness of the closed-loop system (2.1),(2.2),(2.24),(2.25), (2.42) for arbitrary large time-delay. However, since the condition (2.14) is satisfied, then it may be that the closed-loop system possesses bounded solutions for some values of (γ, τ) in some set $\mathcal{I}_{\gamma\tau}$. Moreover, according to Theorem 2.12,

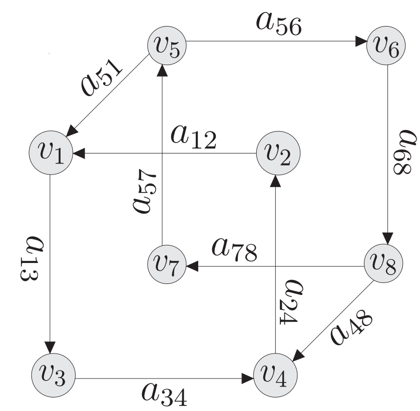

Figure 2.4 Graph of the interconnection.

there exists a region $\mathcal{S} = \{\gamma, \tau \in \mathbb{R}_{\geq 0} \,|\, \gamma > \gamma' \text{ and } \gamma\tau < \chi'\}$, such that if $(\gamma, \tau) \in \mathcal{S}$, then the systems synchronize. Therefore, the closed-loop system (2.1),(2.2),(2.24),(2.25),(2.42) possesses bounded solutions and all the systems synchronize if $(\gamma, \tau) \in \mathcal{I}_{\gamma\tau} \cap \mathcal{S}$. Figure 2.5 depicts the regions $\mathcal{I}_{\gamma\tau}$ and $\mathcal{S}$, which are obtained by computer simulation. Note that $\mathcal{S} \subset \mathcal{I}_{\gamma\tau}$ and therefore $\mathcal{I}_{\gamma\tau} \cap \mathcal{S} = \mathcal{S}$. Hence, boundedness and synchronization is achieved for $(\gamma, \tau) \in \mathcal{S}$.

B.3 Predictor-based Dynamic Diffusive Coupling

Finally, let the eight systems be interconnected through the PDDC (2.31),(2.32), (2.42). As mentioned before, the network is simple and connected, the pairs (A, C_1) and (A, C_2) are observable, the system (A, B_1, C_2) is passive and inequality (2.14) is satisfied. Then, given a predictor gain K_2 such that all the roots of the characteristic equation (2.34) belong to the open left half of the complex plane, it follows by Theorem 2.17 that the solutions of the closed-loop system (2.1),(2.2),(2.31),(2.32), (2.42) are bounded and there exist positive constants γ' and τ' such that if $\gamma > \gamma'$ and $\tau < \tau'$, then the systems synchronize. In Figure 2.6, the real parts of the roots λ of (2.34) with the largest real part (the rightmost characteristic root) for two different values of K_2 are shown. This figure is obtained using the software package DDE-BIFTOOL [41]. Notice that $\Re(\lambda)$ becomes positive for large time-delays. Figure 2.7 depicts the synchronization regions $\mathcal{S}_1' = \{\gamma, \tau \in \mathbb{R}_{\geq 0} \,|\, \gamma > 0 \wedge \tau < 2.86\}$ and $\mathcal{S}_2' = \{\gamma, \tau \in \mathbb{R}_{\geq 0} \,|\, \gamma > 0 \wedge \tau < 1.65\}$ obtained by computer simulation for the two predictor matrices $K_2 = (0.532, -0.779, -0.475)^T$ and $K_2 = (-0.231, -0.656, 0.522)^T$, respectively. Note that $\mathcal{S} \subseteq \mathcal{S}_1' \subseteq \mathcal{S}_2'$, the synchronization region $\mathcal{S}$ is increased for the given values of the predictor gains.

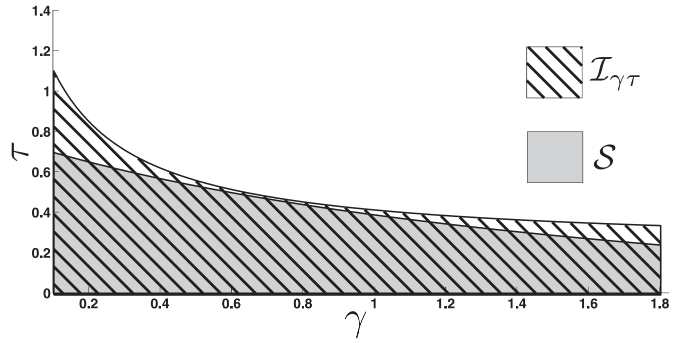

Figure 2.5 Boundedness region $\mathcal{I}_{\gamma\tau}$ and synchronization region $\mathcal{S}$.

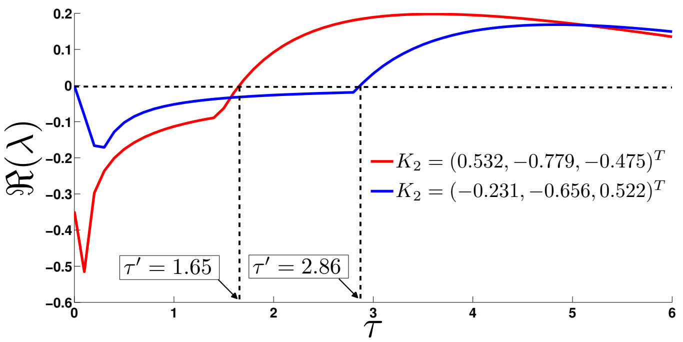

Figure 2.6 The rightmost characteristic root of (2.34) as a function of the delay τ.

2.6 Conclusions

We have presented analytical tools for studying synchronization of diffusively coupled linear systems interacting on networks with general topologies. We have proposed diffusive static and dynamic couplings with time-delays which, under some mild conditions, achieve asymptotic state synchronization of the interconnected systems. Sufficient conditions which ensure boundedness of the solutions of the coupled systems have been derived. We have constructed diffusive dynamic couplings by combining linear observers and output feedback controllers. Moreover, predictor-based diffusive dynamic couplings have been proposed to enhance robustness against time-delay in the network. The results are illustrated by numerical simulations.

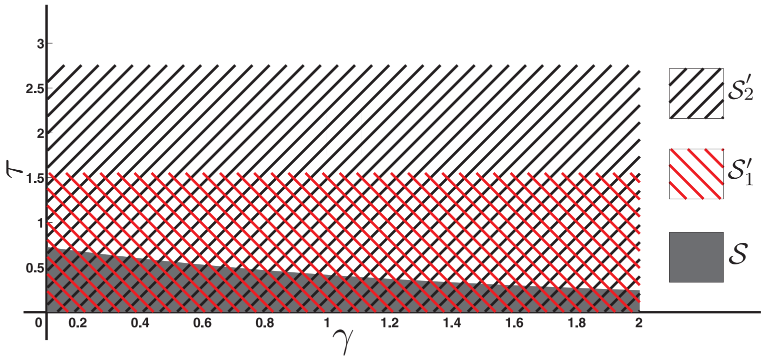

Figure 2.7 Synchronization regions $\mathcal{S} \subseteq \mathcal{S}_1' \subseteq \mathcal{S}_2'$.

Chapter 3

Synchronization via Observer-Based Diffusive Dynamic Couplings

Abstract. We address the problem of controlled synchronization in networks of nonlinear systems interconnected through *diffusive dynamic couplings*. These couplings can be realized as dynamic output feedback controllers constructed by combining nonlinear observers and feedback interconnection terms. Using Lyapunov-Krasovskii functionals and the notion of *semipassivity*, we prove that under some mild assumptions, the solutions of the interconnected systems are ultimately bounded. Sufficient conditions on the systems to be interconnected, the network topology, the coupling strength, and the rate of convergence of the observer that guarantee (global) state synchronization are derived. The stability of the synchronization manifold is proved using Lyapunov-Razumikhin methods. The results are illustrated by computer simulations of coupled FitzHugh-Nagumo neural oscillators.

3.1 Introduction

This chapter focuses on synchronization in networks of identical nonlinear systems. This thesis follows the same research line as [104, 108], where sufficient conditions for synchronization of *semipassive* systems interconnected through diffusive static couplings are presented. However, their results apply to systems which are *semipassive* and their internal dynamics are *convergent* with respect to the coupling variable (the measurable output). In this manuscript, we do not assume semipassivity plus convergence with respect to the measurable outputs y_i as in [104], but this is supposed to hold with respect to a different state function z_i,

This chapter is based on [77, 81].

which is not directly measured. However, if there exists a nonlinear observer which reconstructs z_i from measurements of y_i, a *diffusive dynamic coupling* which only depends on the measurable outputs y_i could be constructed to interconnect the systems. In this chapter, we start the *analysis part* of these ideas. Assuming that the observer is given, we derive sufficient conditions on the systems to be interconnected, the network topology, the coupling strength, and the rate of convergence of the observer ensuring network synchronization and ultimate boundedness of the solutions of the coupled systems. There are some results in this direction already. For instance, in [119, 144], the synchronization problem for a class of linear systems with time-varying topologies interconnected through *observer-based diffusive dynamic couplings* is considered. In [116], the authors propose a *dynamic output feedback controller* that solves the synchronization problem in networks of robot manipulators, in the case when position measurements are available only. Using *adaptive control methods*, the authors in [86, 87] construct diffusive dynamic couplings which solve the network synchronization problem for dynamical systems described by Euler-Lagrange equations and subject to time-delays. The remainder of the chapter is organized as follows. In Section 3.2, the system description and the motivation for this chapter are presented. The class of observers that are considered, the observer-based diffusive couplings that are used to interconnect the systems, and sufficient conditions for boundedness of the solutions of the closed-loop system are presented in Section 3.3. In Section 3.4, sufficient conditions for network synchronization are given. An illustrative example that shows step by step how to apply the results of Section 3.4 is presented in Section 3.5. Finally, conclusions are stated in Section 3.6.

3.2 System Description and Diffusive Static Couplings

The systems description, the result presented in [108], and the motivation for this chapter are presented in this section. Consider a network of k nonlinear systems of the form

$$\dot{x}_i = f(x_i) + Bu_i, \tag{3.1}$$

$$y_i = C_1 x_i, \tag{3.2}$$

$$z_i = C_2 x_i, \tag{3.3}$$

with $i \in \mathcal{I} := \{1, ..., k\}$, state $x_i \in \mathbb{R}^n$, input $u_i \in \mathbb{R}^m$, measurable output $y_i \in \mathbb{R}^s$, semipassive output $z_i \in \mathbb{R}^m$, sufficiently smooth function $f : \mathbb{R}^n \to \mathbb{R}^n$, matrices C_1, C_2, and B of appropriate dimensions, and the matrix $C_2 B \in \mathbb{R}^{m \times m}$ being similar to a positive definite matrix. The systems (3.1),(3.3) are assumed to be strictly semipassive and to have relative degree one. Then, there exists a globally defined coordinate transformation such that systems (3.1),(3.3) can be written in the following *normal form*, (this transformation is explicitly computed in [108]),

$$\dot{\zeta}_i = q(\zeta_i, z_i), \tag{3.4}$$

$$\dot{z}_i = a(\zeta_i, z_i) + C_2 B u_i, \tag{3.5}$$

with internal state $\zeta_i \in \mathbb{R}^{n-m}$ and sufficiently smooth vectorfields $q : \mathbb{R}^{n-m} \times \mathbb{R}^m \to \mathbb{R}^{n-m}$ and $a : \mathbb{R}^{n-m} \times \mathbb{R}^m \to \mathbb{R}^m$. For the sake of simplicity, it is assumed that $C_2 B = I_n$ (results for the general case with $C_2 B$ being similar to a positive definite matrix can easily be derived). The network is called *diffusively coupled* if the systems interact through weighted differences of the form

$$u_i = \gamma \sum_{j \in \mathcal{E}_i} a_{ij}(z_j - z_i), \;\; i \in \mathcal{I}, \tag{3.6}$$

where z_j is the output of system j to which system i is connected, $\gamma \in \mathbb{R}_{>0}$ denotes the coupling strength, $a_{ij} = a_{ji} \geq 0$ are the weights of the interconnections, and $\mathcal{E}_i$ is the set of neighbors of system i. Notice that the controller (3.6) can be written in matrix form as follows

$$u = -\gamma \, (L \otimes I_m) \, z, \tag{3.7}$$

with $z := \mathrm{col}(z_1, \ldots, z_k) \in \mathbb{R}^{km}$, $u := \mathrm{col}(u_1, \ldots, u_k) \in \mathbb{R}^{km}$, and Laplacian matrix $L = L^T \in \mathbb{R}^{k \times k}$. Define the linear manifold

$$\mathcal{M} := \{\mathrm{col}(z, \zeta) \in \mathbb{R}^{kn} | z_i = z_j \text{ and } \zeta_i = \zeta_j, \forall \, i, j \in \mathcal{I}\},$$

where $\zeta := \mathrm{col}(\zeta_1, \ldots, \zeta_k) \in \mathbb{R}^{k(n-m)}$. The manifold $\mathcal{M}$ is called the synchronization manifold or the diagonal set. The systems are said to synchronize, if the synchronization manifold $\mathcal{M}$ contains an asymptotically stable subset. The main result of [108] is given in the following theorem.

Theorem 3.1. [108]. *Consider k identical systems* (3.1),(3.3) *interconnected on a simple strongly connected graph through the diffusive static coupling* (3.6) *with coupling strength $\gamma \in \mathbb{R}_{\geq 0}$. Assume that:*

(H3.1) *Each system* (3.1),(3.3) *is strictly $\mathcal{C}^1$-semipassive with input u_i, output z_i, and radially unbounded storage function $V(x_i)$.*

(H3.2) *There exists a positive definite function $\mathcal{W} \in \mathcal{C}^2(\mathbb{R}^{n-m}, \mathbb{R}_{>0})$ such that for all $\zeta_i, \zeta_j \in \mathbb{R}^{n-m}$ and $z_i \in \mathbb{R}^m$ there is a constant $\alpha' \in \mathbb{R}_{>0}$ such that*

$$\nabla \mathcal{W}(\zeta_i - \zeta_j)^T \left(q(\zeta_i, z_i) - q(\zeta_j, z_i) \right) \leq -\alpha' \left| \zeta_i - \zeta_j \right|^2, \tag{3.8}$$

where $q(\cdot)$ is the vector field associated with the internal dynamics (3.4).

Then, the solutions of the coupled systems are ultimately bounded and there exists a positive constant γ' such that if $\gamma \lambda_2(L) > \gamma'$, where $\lambda_2(L)$ denotes the smallest nonzero eigenvalue of the symmetric Laplacian matrix, there exists a (globally) asymptotically stable subset of the diagonal set $\mathcal{M}$.

Proposition 3.2. [94]. *If there exists a positive definite matrix* $P \in \mathbb{R}^{(n-m)\times(n-m)}$ *such that the eigenvalues of the symmetric matrix*

$$Q(\zeta_i, z_i) = \frac{1}{2}\left(P\left(\frac{\partial q}{\partial \zeta_i}(\zeta_i, z_i)\right) + \left(\frac{\partial q}{\partial \zeta_i}(\zeta_i, z_i)\right)^T P\right), \tag{3.9}$$

are negative and separated away from zero, i.e., there exists a constant $c \in \mathbb{R}_{>0}$ *such that* $\lambda_l(Q) \leq -c < 0$, *for all* $l \in \{1, ..., n-m\}$, $\zeta_i \in \mathbb{R}^{n-m}$, *and* $z_i \in \mathbb{R}^m$; *then, the internal dynamics* (3.4) *is an exponentially convergent system and* (H3.2) *in Theorem* 3.1 *is satisfied with* $\mathcal{W}(\zeta_i - \zeta_j) = (\zeta_i - \zeta_j)^T P(\zeta_i - \zeta_j)$ *and* $\alpha' = \frac{c}{\lambda_{\max}(P)}$, *where* $\lambda_{\max}(P)$ *denotes the largest eigenvalue of the symmetric matrix* P.

Remark 3.3. *In Proposition 3.2, we present a general tool for verifying assumption* (H3.2) *in Theorem 3.1 using the concept of convergent systems. This assumption is employed to ensure that the internal states* ζ_i *asymptotically synchronize whenever the semipassive outputs* z_i *asymptotically synchronized. Indeed, there are some other methods to verify this, for instance, contraction theory* [68], *Lyapunov function approach to incremental stability* [15], *the quadratic (*QUAD*) inequality approach (a Lipschitz-like condition)* [36], *and differential dissipativity* [43], *which are all concepts that are closely related to notion of convergent systems* [94] *that is used here.*

We also refer the interested reader to [25, 36], where a fairly detailed comparison among some of these techniques can be found.

In the result stated in Theorem 3.1, it is assumed that the variable z_i that renders the internal dynamics convergent, and for which each system is strictly $\mathcal{C}^1$-semipassive is available for feedback. Hence, if the measurable output is a different state function y_i, which does not have the desired properties, Theorem 3.1 cannot be applied. It is therefore interesting to extend these results to the case when the variable z_i is not measurable, but there exists a (nonlinear) observer which reconstructs z_i from the measurable output y_i. Then, a natural question arises, "is it possible to interconnect the systems using an estimated variable $\hat{z}_i$ and still achieve synchronization and boundedness of the solutions?" In order to answer this question, we first need to make some stability assumptions on the observer dynamics.

3.3 Boundedness and Diffusive Dynamic Couplings

In this section, the class of observers that are considered and the observer-based diffusive couplings that are used to interconnect the systems are introduced. Moreover, sufficient conditions for boundedness of the closed-loop system are derived.

3.3.1 Nonlinear Observer

Consider the k nonlinear systems (3.1)-(3.3). Assume that for any initial condition $x_i(0) \in \mathbb{R}^n$ and every input signal u_i, the corresponding solution $x_i(t)$ is defined for all $t \geq 0$, i.e., the system is *forward complete* [16]. Consider (nonlinear) observers of the form

$$\begin{cases} \dot{\eta}_i = l(\eta_i, y_i, u_i), \\ \hat{z}_i = \beta(\eta_i, y_i), \end{cases} \tag{3.10}$$

with $i \in \mathcal{I}$, state $\eta_i \in \mathbb{R}^p$, $p \geq n - s$, estimated semipassive output $\hat{z}_i \in \mathbb{R}^m$, and sufficiently smooth functions $l : \mathbb{R}^p \times \mathbb{R}^s \times \mathbb{R}^m \to \mathbb{R}^p$ and $\beta : \mathbb{R}^p \times \mathbb{R}^s \to \mathbb{R}^m$ designed such that $\hat{z}_i$ asymptotically converges to the actual value of z_i. Associated with the observer (3.10), we have the estimation error $\epsilon_i \in \mathbb{R}^m$ defined as

$$\epsilon_i := \hat{z}_i - z_i = \beta(\eta_i, y_i) - z_i. \tag{3.11}$$

Then, the estimation error dynamics is given by

$$\dot{\epsilon}_i = \frac{\partial \beta(\eta_i, y_i)}{\partial \eta_i} l(\eta_i, y_i, u_i) + \left(\frac{\partial \beta(\eta_i, y_i)}{\partial y_i} C_1 - C_2 \right) \Big(f(x_i) + B u_i \Big). \tag{3.12}$$

It is assumed that the functions $l(\cdot)$ and $\beta(\cdot)$ are designed such that the estimation error dynamics (3.12) has the following structure

$$\dot{\epsilon}_i = \phi(\epsilon_i, x_i), \tag{3.13}$$

with sufficiently smooth function $\phi : \mathbb{R}^m \times \mathbb{R}^n \to \mathbb{R}^m$ and $\phi(0, x_j) = 0$ for all $x_i \in \mathbb{R}^n$. The estimated $\hat{z}_i$ uniformly asymptotically converges to z_i, if the origin of the estimation error dynamics (3.13) is uniformly asymptotically stable. In general, it is unknown under what conditions on (3.1) and (3.3) the (nonlinear) observer (3.10) can be designed. In this chapter, it is assumed that the observer exists and is given. Nevertheless, we forward the interested reader to [84] and [56] for existence conditions and interesting design methods of (nonlinear) observers.

3.3.2 Observer-based Diffusive Dynamic Couplings

Let the k systems (3.1),(3.2) be interconnected through diffusive dynamic couplings of the form

$$\begin{cases} \dot{\eta}_i = l(\eta_i, y_i, u_i), \\ \hat{z}_i = \beta(\eta_i, y_i), \\ u_i = \gamma \sum\limits_{j \in \mathcal{E}_i} a_{ij} \left(\hat{z}_j - \hat{z}_i \right), \end{cases} \tag{3.14}$$

where $\gamma \in \mathbb{R}_{>0}$ denotes the coupling strength and $a_{ij} \geq 0$ are the interconnection weights. Moreover, since the coupling strength is encompassed in the constant γ, it is assumed without loss of generality that $\max_{i \in \mathcal{I}} \sum_{j \in \mathcal{E}_i} a_{ij} = 1$. The dynamic coupling (3.14) is the combination of the nonlinear observer (3.10) and an estimated version of the diffusive static coupling (3.6).

3.3.3 Boundedness of the Interconnected Systems

Here, we derive sufficient conditions for boundedness of the solutions of the coupled systems (3.1),(3.2),(3.14).

Lemma 3.4. *Consider k coupled systems* (3.1),(3.2),(3.14) *on a simple strongly connected graph with coupling strength $\gamma \in \mathbb{R}_{\geq 0}$. Assume that:*

(H3.3) *There exists a nonlinear observer* (3.10) *such that the corresponding estimation error dynamics* (3.13) *is uniformly asymptotically stable with positive definite radially unbounded Lyapunov function $V_0 \in \mathcal{C}^1(\mathbb{R}^m, \mathbb{R}_{\geq 0})$ satisfying*

$$(\nabla V_0(\epsilon_i))^T \phi(\epsilon_i, x_i) \leq -\kappa \, |\epsilon_i|^2 \,, \tag{3.15}$$

uniformly in $x_i(t)$ for some constant $\kappa \in \mathbb{R}_{>0}$.

(H3.4) *Each system* (3.1),(3.3) *is strictly $\mathcal{C}^1$-semipassive with radially unbounded storage function, and the functions $H(x_i)$ are such that there exists $R \in \mathbb{R}_{>0}$ such that $|x_i| > R$ implies that $H(x_i) - \gamma d_i |z_i|^2 > 0$ with $d_i = \sum_{j \in \mathcal{E}_i} a_{ij}$.*

Let γ_{max} be the largest γ that satisfies (H3.4), *then the solutions of the coupled system* (3.1),(3.2),(3.14) *are ultimately bounded for $\gamma \in [0, \gamma_{max}]$.*

The proof of Lemma 3.4 can be found in Appendix A.

3.4 Synchronization of Semipassive Systems

In the following theorem, we give sufficient conditions for synchronization of the coupled systems (3.1),(3.2),(3.14).

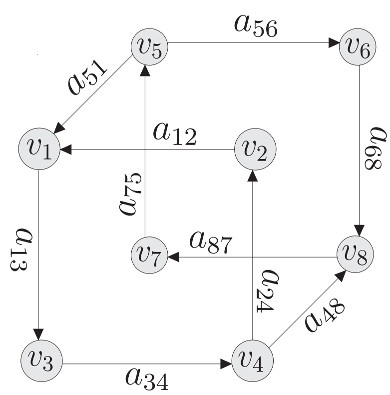

Figure 3.1 A network of eight identical systems. The graph is strongly connected.

Theorem 3.5. *Consider k coupled systems* (3.1),(3.2),(3.14) *on a simple strongly connected graph with coupling strength $\gamma \in \mathbb{R}_{\geq 0}$. Suppose that the conditions stated in Lemma 3.4 are satisfied. In addition, assume that*

(H3.5) *The internal dynamics* (3.4) *is an exponentially convergent system, i.e., there is a positive definite matrix $P \in \mathbb{R}^{(n-m)\times(n-m)}$ such that the eigenvalues of the symmetric matrix*

$$Q(\zeta_i, z_i) = \frac{1}{2}\left(P\left(\frac{\partial q}{\partial \zeta_i}(\zeta_i, z_i)\right) + \left(\frac{\partial q}{\partial \zeta_i}(\zeta_i, z_i)\right)^T P\right), \tag{3.16}$$

are uniformly negative and bounded away from zero for all $\zeta_i \in \mathbb{R}^{n-m}$ and $z_i \in \mathbb{R}^m$.

Then, the solutions of the closed-loop system (3.1),(3.2),(3.14) *are ultimately bounded and there exist positive constants γ' and κ' such that if $\gamma \in (\gamma', \gamma_{max}]$ (with γ_{max} being the largest coupling strength for which boundedness of solutions is guaranteed) and $\kappa > \kappa'$ (with κ from assumption* (H3.3)*), then there exists a globally asymptotically stable subset of the diagonal set $\mathcal{M}$.*

The proof of Theorem 3.5 can be found in Appendix A.

3.5 Example: FitzHugh-Nagumo Neural Oscillators

In this section, we present an illustrative example where we show step by step how to apply Theorem 3.5 to conclude synchronization of the coupled systems. It is assumed that each system in the network is a FitzHugh-Nagumo neural oscillator.

A. Network Topology. Consider a network of eight systems interconnected according to the graph depicted in Figure 3.1 with $a_{ij} = 1$ if $\{ij\} \in \mathcal{E}$ and $a_{ij} = 0$ otherwise. The network is strongly connected and simple. Moreover, the associated adjacent matrix is not symmetric, i.e., $A \neq A^T$. The Laplacian matrix is given by

$$L = \begin{pmatrix} 2 & -1 & 0 & 0 & -1 & 0 & 0 & 0 \\ 0 & 1 & 0 & -1 & 0 & 0 & 0 & 0 \\ -1 & 0 & 1 & 0 & 0 & 0 & 0 & 0 \\ 0 & 0 & -1 & 1 & 0 & 0 & 0 & 0 \\ 0 & 0 & 0 & 0 & 1 & 0 & -1 & 0 \\ 0 & 0 & 0 & 0 & -1 & 1 & 0 & 0 \\ 0 & 0 & 0 & 0 & 0 & 0 & 1 & -1 \\ 0 & 0 & 0 & -1 & 0 & -1 & 0 & 2 \end{pmatrix}. \tag{3.17}$$

B. Semipassivity and Convergence. Each system in the network is assumed to be a FitzHugh-Nagumo neural oscillator of the form

$$\begin{cases} \dot{x}_{1i} = x_{1i} - \frac{x_{1i}^3}{3} - x_{2i} + I + u_i, \\ \dot{x}_{2i} = \psi\left(x_{1i} + a - bx_{2i}\right), \\ y_i \;\; = x_{2i}, \end{cases} \tag{3.18}$$

with measurable output y_i, state $x_i = (x_{1i}, x_{2i})^T \in \mathbb{R}^2$, input $u_i \in \mathbb{R}$, positive constants $\psi, a, b \in \mathbb{R}_{>0}$, and $i \in \mathcal{I} = \{1, ..., 8\}$. Consider the following storage function

$$V(x_i) = \frac{1}{2}(x_{1i}^2 + \frac{1}{\psi}x_{2i}^2). \tag{3.19}$$

Straightforward computations show that

$$\dot{V}(x_i) \leq u_i x_{1i} - H(x_i),$$

where

$$H(x_i) = \frac{x_{1i}^4}{3} - x_{i1}^2 - Ix_{i1} + bx_{i2}^2 - ax_{i2}. \tag{3.20}$$

It is easy to verify that $H(x_i) > 0$ for sufficiently large $|x_i|$. It follows that system (3.18) is strictly $\mathcal{C}^1$-semipassive with input u_i, output $z_i = x_{1i}$, and storage function (3.19). Moreover, verifying the Demidovich's condition (3.9) along the internal dynamics of (3.18), it follows that for $P = 1$, the matrix $Q(x_i)$ is simply given by $Q(x_i) = -\psi b$. Since $b, \psi \in \mathbb{R}_{>0}$, then by Proposition 3.2, the internal dynamics is an exponentially convergent system. At this point, Theorem 3.1 could be applied to conclude that diffusively coupled FitzHugh-Nagumo neural oscillators possess bounded solutions and for sufficiently large coupling strength the systems synchronize. However, the variable z_i is not available for feedback. The coupling variable is the measurable output y_i and therefore Theorem 3.1 cannot be used. Nevertheless, if there exists a nonlinear observer which asymptotically estimates z_i from measurements of y_i, we could construct the dynamic coupling (3.14) and apply Theorem 3.5 to investigate synchronization.

C. Nonlinear Observer.

Proposition 3.6. *Consider the system*

$$\dot{\eta}_i = \left(\kappa\psi b - \kappa^2\psi + \kappa - 1\right) y_i + (1 - \kappa\psi)\,\eta_i - \kappa\psi a - \frac{(\kappa y_i + \eta_i)^3}{3} + I + u_i, \quad (3.21)$$

with state $\eta_i \in \mathbb{R}$ and some constant $\kappa \in \mathbb{R}$. Then, there exists a nonempty set $\mathcal{K} \subseteq \mathbb{R}$ such that for all initial conditions $\eta_i(0) \in \mathbb{R}$ and $\kappa \in \mathcal{K}$ it is satisfied that:

$$\lim_{t\to\infty} \left(z_i(t) - \kappa y_i(t) - \eta_i(t)\right) = 0.$$

Proof: Define the estimation error

$$\epsilon_i = \kappa y_i + \eta_i - z_i, \quad (3.22)$$

straightforward computations show that the estimation error satisfies the following differential equation

$$\dot{\epsilon}_i = -\left(\kappa\psi - 1 + \frac{(\kappa y_i + \eta_i)^2}{4} + \frac{(3\kappa y_i + 3\eta_i - 2\epsilon_i)^2}{12}\right)\epsilon_i. \quad (3.23)$$

Consider the positive definite Lyapunov function $V_0(\epsilon_i) = \frac{1}{2}\epsilon_i^2$, then

$$\begin{aligned} \dot{V}_0(\epsilon_i, y_i) &= -\left(\kappa\psi - 1 + \frac{(\kappa y_i + \eta_i)^2}{4} + \frac{(3\kappa y_i + 3\eta_i - 2\epsilon_i)^2}{12}\right)\epsilon_i^2 \\ &\leq -(\kappa\psi - 1)\epsilon_i^2, \end{aligned} \quad (3.24)$$

therefore for $\kappa > \frac{1}{\psi}$ the origin of (3.23) is globally uniformly asymptotically stable. $\square$

D. Diffusive Dynamic Coupling. Combining the observer (3.21) and an estimated version of (3.6) the dynamic coupling (3.14) takes the following form

$$\begin{cases} \dot{\eta}_i = \left(\kappa\psi b - \kappa^2\psi + \kappa\right) y_i + (1 - \kappa\psi)\,\eta_i - \kappa\psi a - \frac{(\kappa y_i + \eta_i)^3}{3} - y_i + I + u_i, \\ \hat{z}_i = \kappa y_i + \eta_i, \\ u_i = \gamma \sum\limits_{j\in\mathcal{E}_i} a_{ij}\left(\hat{z}_j - \hat{z}_i\right). \end{cases} \quad (3.25)$$

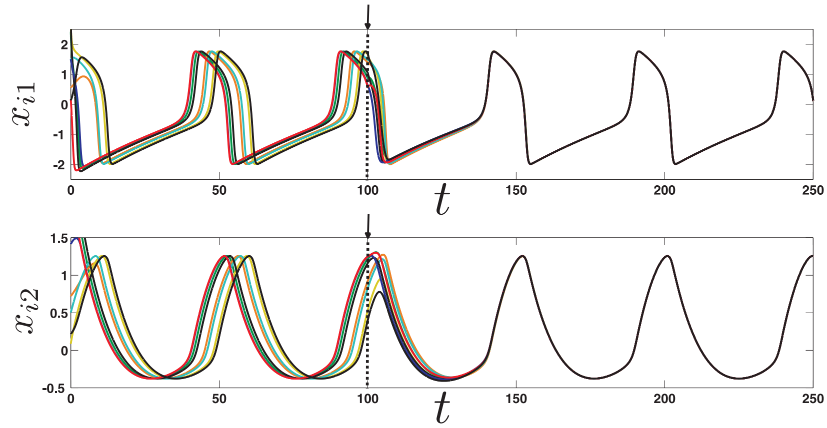

Figure 3.2 Synchronization of eight FitzHugh-Nagumo oscillators. The controller is turned on at t = 100.

It follows from Theorem 3.5 that for sufficiently large γ and κ the solutions of the closed-loop system (3.18),(3.25) are ultimately bounded and the goal of synchronization is achieved.

E. Numerical Results. Figure 3.2 depicts the simulation results for the network of eight FitzHugh-Nagumo neural oscillators coupled through (3.25) with coupling strength $\gamma = 0.5$, $\kappa = 13$, $\psi = 0.08$, $a = 0.7$, $b = 0.8$, and $I = 0.33$.

3.6 Conclusions

Sufficient conditions for network synchronization and boundedness of the solutions of coupled semipassive systems interconnected through observer based diffusive couplings have been derived. Such couplings are constructed by combining nonlinear observers and output interconnection terms. It has been shown that synchronization can be achieved if the coupling strength γ is sufficiently large, and the rate of convergency of the observer is sufficiently fast. In general, it is not easy to find a nonlinear observer such that assumption (H3.3) is satisfied. However, the aim of this chapter is not to give a design method for the observer dynamics but to provide sufficient conditions for network synchronization when the observer is given. Nevertheless, in the next chapter, we include an observer design method for the class of systems under study (semipassive systems with convergent internal dynamics). The performance of the scheme is verified by computer simulations of coupled FitzHugh-Nagumo neural oscillators.

Chapter 4

Synchronization via Invariant-Manifold-Based Couplings with Time-Delays

Abstract. We address the problem of controlled synchronization in networks of nonlinear systems interconnected through *diffusive time-delayed dynamic couplings*. These couplings can be realized as dynamic output feedback controllers constructed by combining nonlinear observers and time-delayed feedback interconnection terms. Using *Immersion and Invariance* techniques, we present a general tool for constructing the dynamics of the couplings. Sufficient conditions on the systems to be interconnected, the network topology, the couplings, and the time-delay that guarantee (global) state synchronization are derived. The asymptotic stability of the synchronization manifold is proved using Lyapunov-Razumikhin methods. Moreover, using Lyapunov-Krasovskii functionals and the notion of *semipassivity*, we prove that under some mild assumptions, the solutions of the interconnected systems are ultimately bounded. Simulation results using FitzHugh-Nagumo neural oscillators illustrate the performance of the control scheme.

4.1 Introduction

The results presented in this chapter follow the same research line as [104, 108] and [132], where sufficient conditions for synchronization of diffusively interconnected *semipassive systems* with and without time-delays are derived. Nevertheless, their results apply to systems which are *semipassive* and their internal dynamics are *convergent* [37] with respect to the coupling variable (the measurable output). In this chapter, we do not assume *semipassivity* plus

This chapter is based on [76].

convergence with respect to the measurable outputs y_i as in [104], but this is supposed to hold with respect to a state function z_i, which is not directly measured. However, if there exists a nonlinear observer which reconstructs z_i from measurements of y_i, then a *diffusive dynamic coupling* which only depends on the measurable outputs y_i could be constructed to interconnect the systems. There are some results in this direction already. For instance, in [119, 144], the synchronization problem for a class of linear systems with time-varying topologies interconnected through *observer-based diffusive dynamic couplings* is considered. In [116], the authors propose a *dynamic output feedback controller* that solves the synchronization problem of two robot manipulators in the case when position measurements are available only. Using *adaptive control methods*, the authors in [86, 87] construct diffusive dynamic couplings which solve the network synchronization problem for dynamical systems described by Euler-Lagrange equations and subject to time-delays. In [77], we have started the *analysis part* of these ideas. We have derived sufficient conditions on the *convergence rate* of the observer ensuring network synchronization. However, in our previous work, it is assumed that the observer exists, it is given, and the communication among the systems is instantaneous, i.e., there are no time-delays in the loop. In practical situations, time-delays caused by signal transmission affect the behavior of the interconnected systems. *Diffusive time-delayed couplings* arise naturally for interconnected systems since the transmission of signals can be expected to take some time. This chapter addresses and solves the *synthesis part* of a more general setting. We develop a general tool for constructing *diffusive time-delayed dynamic couplings* using the ideas of *immersion and invariance* that are introduced in [17]. Sufficient conditions are derived on the systems to be interconnected, the network topology, the coupling dynamics, and the time-delay that guarantee boundedness and (global) state synchronization of the solutions of the coupled system.

The remainder of the chapter is organized as follows. In Section 4.2, the system description and the motivation for this chapter are presented. Moreover, the definition of the *diffusive time-delayed coupling* and the result presented in [132] are also presented. The observer design is given in Section 4.3 before discussing the main results on network synchronization in Section 4.4. In Section 4.5, an illustrative example that shows step by step how to construct the proposed couplings is presented. Moreover, it is also shown how to apply the results of Section 4.3 and Section 4.4 to prove boundedness and synchronization of the solutions of the closed-loop system. Finally, conclusions are stated in Section 4.6.

4.2 System Description and Diffusive Time-Delayed Couplings

Consider k identical nonlinear systems of the form

$$\dot{x}_i = f(x_i) + Bu_i, \tag{4.1}$$
$$y_i = C_1 x_i, \tag{4.2}$$
$$z_i = C_2 x_i, \tag{4.3}$$

with $i \in \mathcal{I} := \{1, ..., k\}$, state $x_i \in \mathbb{R}^n$, input $u_i \in \mathbb{R}^m$, measurable output $y_i \in \mathbb{R}^s$, semipassive output $z_i \in \mathbb{R}^m$, sufficiently smooth function $f : \mathbb{R}^n \to \mathbb{R}^n$, matrices C_1, C_2, and B of appropriate dimensions, and the matrix $C_2 B \in \mathbb{R}^{m\times m}$ being similar to a positive definite matrix. The systems (4.1),(4.3) are assumed to be strictly semipassive and to have relative degree one. Then, there exists a globally defined coordinate transformation such that systems (4.1),(4.3) can be written in the following *normal form*, (this transformation is explicitly computed in [107]),

$$\dot{\zeta}_i = q(\zeta_i, z_i), \tag{4.4}$$
$$\dot{z}_i = a(\zeta_i, z_i) + C_2 B u_i, \tag{4.5}$$

with internal state $\zeta_i \in \mathbb{R}^{n-m}$ and sufficiently smooth vector fields $q : \mathbb{R}^{n-m} \times \mathbb{R}^m \to \mathbb{R}^{n-m}$ and $a : \mathbb{R}^{n-m} \times \mathbb{R}^m \to \mathbb{R}^m$. For the sake of simplicity, it is assumed that $C_2 B = I_n$ (results for the general case with $C_2 B$ being similar to a positive definite matrix can easily be derived). Define the linear manifold

$$\mathcal{M} := \{\mathrm{col}(z, \zeta) \in \mathbb{R}^{kn} | z_i = z_j \text{ and } \zeta_i = \zeta_j, \forall\, i, j \in \mathcal{I}\},$$

where $\zeta := \mathrm{col}(\zeta_1, \ldots, \zeta_k) \in \mathbb{R}^{k(n-m)}$ and $z := \mathrm{col}(z_1, \ldots, z_k) \in \mathbb{R}^{km}$. The manifold $\mathcal{M}$ is called the synchronization manifold or the diagonal set. The coupled systems are said to synchronize, if the synchronization manifold $\mathcal{M}$ contains an asymptotically stable subset.

4.2.1 Diffusive Time-Delayed Couplings

The main results of this chapter follow the same research line as [132], where synchronization of semipassive systems interconnected through *diffusive time-delayed couplings* is considered. The network is called *diffusively time-delayed coupled* if the systems interact through weighted differences of the form

$$u_i = \gamma \sum_{j \in \mathcal{E}_i} a_{ij}(z_j^\tau - z_i), \tag{4.6}$$

$$u_i = \gamma \sum_{j \in \mathcal{E}_i} a_{ij}(z_j^\tau - z_i^\tau), \; i \in \mathcal{I}, \tag{4.7}$$

where z_j are the outputs of systems j to which systems i are connected, $\gamma > 0$ denotes the coupling strength, $a_{ij} \geq 0$ are the weights of the interconnections, $\mathcal{E}_i$ is the set of neighbors of system i, $z_i(t)^\tau := z_i(t - \tau)$, and $\tau \in \mathbb{R}_{\geq 0}$ is the finite time-delay. Moreover, since the coupling strength is encompassed in the constant γ, then it is assumed without loss of generality that $\max_{i \in \mathcal{I}} \sum_{j \in \mathcal{E}_i} a_{ij} = 1$. In case of coupling (4.6), the transmitted signals (the outputs of nodes j) are delayed τ units of time and compared with the current output of node i. This type of coupling arises naturally for interconnected systems since the transmission of signals can be expected to take some time. In coupling (4.7), all signals are time-delayed. Such a coupling may arise, for instance, when the systems are interconnected by centralized control laws. Notice that the controllers (4.6) and (4.7) can be written in matrix form as follows

$$u = -\gamma\,(D \otimes I_m)\,z + \gamma\,(A \otimes I_m)\,z^\tau, \tag{4.8}$$

$$u = -\gamma\,(L \otimes I_m)\,z^\tau, \tag{4.9}$$

where $u := \mathrm{col}(u_1, \ldots, u_k)$, $z = \mathrm{col}(z_1, \ldots, z_k)$, Laplacian matrix $L \in \mathbb{R}^{k \times k}$, adjacency matrix $A \in \mathbb{R}^{k \times k}$, and diagonal degree matrix $D \in \mathbb{R}^{k \times k}$. The main results of [132] are summarized in the following lemma and theorem.

Lemma 4.1. [132]. *Consider the k nonlinear systems* (4.1),(4.3) *coupled through the diffusive time-delayed coupling* (4.6) *with coupling strength $\gamma \in \mathbb{R}_{\geq 0}$ and time-delay $\tau \in \mathbb{R}_{\geq 0}$ on a simple strongly connected graph. Suppose that each system* (4.1),(4.3) *is strictly $\mathcal{C}^1$-semipassive with radially unbounded storage function $V(x_i)$, then the solutions of the coupled systems* (4.1),(4.3),(4.6) *are ultimately bounded for any finite $\tau, \gamma \in \mathbb{R}_{\geq 0}$. If the systems* (4.1),(4.3) *are coupled through* (4.7), *assume that:*

(H4.1) *The functions $H(x_i)$ are such that there exists $R > 0$ such that $|x_i| > R$ implies that $H(x_i) - \gamma|z_i|^2 > 0$.*

Let γ_{max} be the largest γ that satisfies (H4.1), *then the solutions of the coupled systems* (4.1),(4.3),(4.7) *are ultimately bounded for any finite $\tau \in \mathbb{R}_{\geq 0}$ and $\gamma \in [0, \gamma_{max}]$.*

Theorem 4.2. [132]. *Consider the k nonlinear systems* (4.1),(4.3) *interconnected through either coupling* (4.6) *or* (4.7) *with coupling strength $\gamma \in \mathbb{R}_{\geq 0}$ and time-delay $\tau \in \mathbb{R}_{\geq 0}$ on a simple strongly connected graph. Assume that the conditions stated in Lemma 4.1 are satisfied and*

(H4.2) *The internal dynamics* (4.4) *is an exponentially convergent system, i.e., there is a positive definite matrix $P \in \mathbb{R}^{(n-m)\times(n-m)}$ such that the eigenvalues of the symmetric matrix*

$$Q = \frac{1}{2}\left(P\left(\frac{\partial q}{\partial \zeta_i}(\zeta_i, z_i)\right) + \left(\frac{\partial q}{\partial \zeta_i}(\zeta_i, z_i)\right)^T P\right), \tag{4.10}$$

are uniformly negative and bounded away from zero for all $\zeta_i \in \mathbb{R}^{n-m}$ and $z_i \in \mathbb{R}^m$.

Then, the solutions of the closed-loop systems (4.1),(4.3),(4.6) *and* (4.1),(4.3),(4.7) *are ultimately bounded and there exist positive constants $\gamma', \Xi' \in \mathbb{R}_{>0}$ such that if $\gamma \in (\gamma', \gamma_{max}]$ (with γ_{max} being the maximal coupling strength for which boundedness of solutions is guaranteed) and $\gamma\tau < \Xi'$, then there exists a (globally) asymptotically stable subset of the diagonal set $\mathcal{M}$.*

Remark 4.3. *In Theorem 4.2, it is assumed that the internal dynamics* (4.4) *is an exponentially convergent system. This assumption is employed to ensure that the internal states ζ_i asymptotically synchronize whenever the semipassive outputs z_i asymptotically synchronize. Indeed, there are some other methods to verify this, for instance, contraction theory* [68]*, Lyapunov function approach to incremental stability* [15]*, the quadratic (*QUAD*) inequality approach (a Lipschitz-like condition)* [36]*, and differential dissipativity* [43]*, which are all concepts that are closely related to notion of convergent systems* [94] *that we use here.*

We also refer the interested reader to [25, 36], where a fairly detailed comparison among some of these techniques can be found.

4.2.2 Problem Statement and Outline of the Results

In the result stated in Theorem 4.2, it is assumed that the variable z_i that render the internal dynamics convergent, and for which each system is strictly $\mathcal{C}^1$-semipassive is available for feedback. Therefore, if the measurable output is a different state function y_i, which does not have the desired properties, Theorem 4.2 cannot be applied. To overcome these obstacles, in this manuscript, two different types of observer-based *diffusive dynamic couplings* are proposed. The ideas of *immersion and invariance* [17] are used to construct nonlinear observers which reconstruct the desired outputs z_i from the measurable outputs y_i. Then, the systems are interconnected using these estimated variables $\hat{z}_i$. We prove that under some mild conditions network synchronization and boundedness of the solutions can also be achieved when the systems are coupled through these estimated outputs $\hat{z}_i$. The results are presented as follows: First, in Proposition 4.6, we give a general tool for constructing the observer dynamics before introducing the proposed observer-based *diffusive dynamic couplings* in Section 4.4. Next, in Lemma 4.8, we present a preliminary result which ensures boundedness of the solutions of the closed-loop system. Finally, the main result on network synchronization is stated in Theorem 4.11.

Remark 4.4. *The results presented in this chapter also hold when the systems* (4.1) *are of the form*

$$\dot{x}_i = f(x_i) + B\left(u_i + \omega(t)\right),$$

with an external known signal $\omega : \mathbb{R}_{\geq 0} \to \mathbb{R}^m$*, which is assumed to be piecewise continuous and uniformly bounded for all* $t \in (-\infty, \infty)$*, i.e.,* $|\omega(t)| \leq \delta$ *for some positive constant* δ*. The signal* $\omega(t)$ *acts as either an external force or a reference signal that is applied to all the systems. However, for simplicity of notation, we do not analyze this case.*

4.3 Invariant-Manifold-Based Observer

Consider the k identical nonlinear systems (4.1)-(4.3). Assume that for any initial condition $x_i(t_0) \in \mathbb{R}^n$ and every input signal u_i, the corresponding solution $x_i(t)$ is defined for all $t \geq t_0$, i.e., the systems are *forward complete*. Clearly, when measuring $y_i = C_1 x_i$, it appears that it is only needed to reconstruct the remaining part of the state $\rho_i = N_1 x_i$, where N_1 is chosen such that $(N_1^T, C_1^T)^T$ has full column rank. Generally, this allows for reduced order observers (especially when ρ_i and y_i have some shared components). Assume that C_1 has full row rank, then there exists $N_1 \in \mathbb{R}^{p \times n}$ with $p = n - s$, such that

$$\begin{pmatrix} \rho_i \\ y_i \end{pmatrix} = \begin{pmatrix} N_1 \\ C_1 \end{pmatrix} x_i, \;\; x_i = \begin{pmatrix} N_2 & N_3 \end{pmatrix} \begin{pmatrix} \rho_i \\ y_i \end{pmatrix}, \tag{4.11}$$

with

$$\begin{pmatrix} N_1 \\ C_1 \end{pmatrix}^{-1} = \begin{pmatrix} N_2 & N_3 \end{pmatrix}.$$

It follows that systems (4.1),(4.2) can be rewritten as

$$\dot{\rho}_i = N_1 f(x_i) + N_1 B u_i, \tag{4.12}$$
$$\dot{y}_i = C_1 f(x_i) + C_1 B u_i, \tag{4.13}$$

with $x_i = N_2\rho_i + N_3 y_i$.

Definition 4.5. *Consider the system*

$$\dot{\eta}_i = l(\eta_i, y_i) + s(\eta_i, y_i)u_i, \tag{4.14}$$
$$\hat{\rho}_i = \beta(\eta_i, y_i), \tag{4.15}$$

with $i \in \mathcal{I}$, state $\eta_i \in \mathbb{R}^r$, $r \geq p = n - s$, and sufficiently smooth functions $l : \mathbb{R}^r \times \mathbb{R}^s \to \mathbb{R}^r$, $s : \mathbb{R}^r \times \mathbb{R}^s \to \mathbb{R}^{r\times m}$, and $\beta : \mathbb{R}^r \times \mathbb{R}^s \to \mathbb{R}^p$. The system (4.14),(4.15) *is called an observer for system* (4.12),(4.13) *if there exists a mapping $\beta(\cdot)$ such that the manifold*

$$\mathcal{A} := \{(\rho_i, y_i, \eta_i) \in \mathbb{R}^p \times \mathbb{R}^s \times \mathbb{R}^r : \beta(\eta_i, y_i) = \rho_i\}, \tag{4.16}$$

has the following properties.

(P4.1) *All trajectories of the extended system* (4.12)-(4.15) *that start on the manifold $\mathcal{A}$ remain there for all future times, i.e., $\mathcal{A}$ is positively invariant.*

(P4.2) *All trajectories of the extended system* (4.12)-(4.15) *that start in a neighborhood of $\mathcal{A}$ asymptotically converge to $\mathcal{A}$.*

The above definition implies that an asymptotically converging estimate of the state ρ_i is given by (4.15). Note that the estimation error $\epsilon_i := \hat{\rho}_i - \rho_i$ is zero on the manifold $\mathcal{A}$. Moreover, if property (P4.2) holds for any initial state $\rho_i(t_0), y_i(t_0), \eta_i(t_0) \in \mathbb{R}^p \times \mathbb{R}^s \times \mathbb{R}^r$, then (4.14),(4.15) is a *global* observer for system (4.12),(4.13).

4.3.1 Observer Design

In this section, we present a general tool for constructing nonlinear (reduced order) observers of the form given in Definition 4.5 for the class of systems under study. The design is based on the work presented in [17, 56].

Proposition 4.6. *Consider the system* (4.12)-(4.15) *and suppose that there exist a* $\mathcal{C}^1$*-mapping* $\beta : \mathbb{R}^r \times \mathbb{R}^s \to \mathbb{R}^p$ *such that the following holds.*

(H4.3) *For all* y_i *and* η_i *the function* $\beta(\eta_i, y_i)$ *is left-invertible*[1] *with respect to* η_i *and*

$$\det\left(\frac{\partial\beta}{\partial\eta_i}\right) \neq 0.$$

(H4.4) *The system*

$$\dot{\epsilon}_i = \phi(\epsilon_i, x_i) := (N_1 - \frac{\partial\beta}{\partial y_i}C_1)\left(f(\hat{x}_i) - f(x_i)\right), \tag{4.17}$$

with $x_i = N_2\rho_i + N_3 y_i$ *and* $\hat{x}_i = N_2(\rho_i + \epsilon_i) + N_3 y_i$ *has a (globally) asymptotically stable equilibrium at* $\epsilon_i = 0$*, uniformly in* $\rho_i(t)$ *and* $y_i(t)$*. Then, the system* (4.14),(4.15) *with*

$$l(\eta_i, y_i) = \left(\frac{\partial\beta}{\partial\eta_i}\right)^{-1}\left(N_1 - \frac{\partial\beta}{\partial y_i}C_1\right) f(\hat{x}_i), \tag{4.18}$$

$$s(\eta_i, y_i) = \left(\frac{\partial\beta}{\partial\eta_i}\right)^{-1}\left(N_1 - \frac{\partial\beta}{\partial y_i}C_1\right) B, \tag{4.19}$$

and $\hat{x}_i = N_2\beta(\eta_i, y_i) + N_3 y_i$*, is a (global) observer for the system* (4.12),(4.13).

Proof: Consider the estimation error $\epsilon_i = \beta(\eta_i, y_i) - \rho_i$, where $\beta(\cdot)$ is a continuous differentiable function such that (H4.3) holds. Note that $|\epsilon_i|$ represents the distance of the system trajectories from the manifold $\mathcal{A}$ defined in (4.16). The dynamics of ϵ_i is then given by

$$\begin{aligned}\dot{\epsilon}_i = &\frac{\partial\beta}{\partial\eta_i}l(\eta_i, y_i) + \frac{\partial\beta}{\partial y_i}C_1 f(x_i) - N_1 f(x_i) \\ &+ \left(\frac{\partial\beta}{\partial\eta_i}s(\eta_i, y_i) + \frac{\partial\beta}{\partial y_i}C_1 B - N_1 B\right) u_i.\end{aligned} \tag{4.20}$$

By assumption (H4.3) the functions $l(\cdot)$ and $s(\cdot)$ in (4.18) and (4.19) are well defined. Then, substitution of (4.18) and (4.19) in (4.20) yields the dynamics (4.17). It follows from (H4.4) that the distance $|\epsilon_i|$ from the manifold $\mathcal{A}$ converges asymptotically to zero. Moreover, note that the manifold $\mathcal{A}$ is invariant, i.e., if $\epsilon_i(t) = 0$ for some t, then $\epsilon_i(\sigma) = 0$ for all $\sigma > t$. Hence, by Definition 4.5, the system (4.14),(4.15) with $l(\cdot)$ and $s(\cdot)$ as in (4.18) and (4.19) is a (global) observer for (4.12),(4.13). ■

[1] A mapping $\psi(x, y, t) : \mathbb{R}^l \times \mathbb{R}^m \times \mathbb{R} \to \mathbb{R}^r$ is left-invertible (with respect to x) if there exists a mapping $\psi^L : \mathbb{R}^r \times \mathbb{R}^m \times \mathbb{R} \to \mathbb{R}^l$ such that $\psi^L(\psi(x, y, t), y, t) = x$ for all x, y, and t.

Proposition 4.6 provides an implicit description of the observer dynamics (4.14), (4.15) in terms of the mapping $\beta(\cdot)$ which must be selected to satisfy (H4.4). As a result, the problem of constructing an observer for the system (4.12),(4.13) is reduced to the problem of rendering the system (4.17) asymptotically stable by assigning the function $\beta(\cdot)$. Associated with the observer (4.14),(4.15), we have the estimation error $\epsilon_i \in \mathbb{R}^p$ defined as $\epsilon_i = \hat{\rho}_i - \rho_i = \beta(\eta_i, y_i) - \rho_i$, and the estimation error dynamics $\dot{\epsilon}_i = \phi(\epsilon_i, x_i)$, with $\phi(\cdot)$ defined in (4.17) and $\phi(0, x_i) = 0$ for all x_i. Given a function $\beta(\cdot)$ such that the origin of (4.17) is uniformly asymptotically stable, it follows that $\hat{\rho}_i$ asymptotically converges to ρ_i.

4.4 Time-Delayed Output Dynamic Couplings

Let the k systems (4.1),(4.2) be interconnected through a *Diffusive Time-Delayed Dynamic Coupling* (DTDC) of the form

$$\begin{aligned} \dot{\eta}_i &= l(\eta_i, y_i) + s(\eta_i, y_i)u_i, \\ \hat{z}_i &= C_2 N_2 \beta(\eta_i, y_i) + C_2 N_3 y_i, \end{aligned} \tag{4.21}$$

$$u_i = \gamma \sum_{j \in \mathcal{E}_i} a_{ij} \left(\hat{z}_j^{\tau} - \hat{z}_i \right), \tag{4.22}$$

$$u_i = \gamma \sum_{j \in \mathcal{E}_i} a_{ij} \left(\hat{z}_j^{\tau} - \hat{z}_i^{\tau} \right), \tag{4.23}$$

with finite time-delay $\tau \in \mathbb{R}_{\geq 0}$, coupling strength $\gamma \in \mathbb{R}_{\geq 0}$, interconnection weights $a_{ij} \geq 0$, $\max_{i \in \mathcal{I}} \sum_{j \in \mathcal{E}_i} a_{ij} = 1$, N_2 and N_3 as in (4.11), and $l(\cdot)$ and $s(\cdot)$ as in (4.18) and (4.19), respectively. The DTDC (4.21)-(4.23) is the combination of the observer (4.14),(4.15) and estimations of (4.6) and (4.7).

Remark 4.7. *The observer dynamics* (4.14),(4.15) *is independent of the time-delay, i.e., it is assumed that the measurements of* y_i *are not subject to time-delay and the delay in the* DTDC (4.21)-(4.23) *is induced when the estimated outputs* $\hat{z}_i$ *are transmitted. Under this assumption, it is possible to maintain the same observer structure while analyzing the effect of transmission delays.*

4.4.1 Boundedness of the Interconnected Systems

Lemma 4.8. *Consider the k nonlinear systems* (4.1),(4.2) *interconnected through either the* DTDC (4.21),(4.22) *or* (4.21),(4.23) *with coupling strength $\gamma \in \mathbb{R}_{\geq 0}$ and time-delay $\tau \in \mathbb{R}_{\geq 0}$ on a simple strongly connected graph. Suppose that each system* (4.1),(4.3) *is strictly $\mathcal{C}^1$-semipassive with radially unbounded storage function $V(x_i)$. In addition assume that:*

(H4.5) *There exists a function $\beta(\cdot)$ such that* (H4.3) *is satisfied and the estimation error dynamics* (4.17) *is (globally) asymptotically stable with radially unbounded Lyapunov function $V_0 \in \mathcal{C}^1(\mathbb{R}^p, \mathbb{R}_{\geq 0})$ such that*

$$(\nabla V_0(\epsilon_i))^T \phi(\epsilon_i, x_i) \leq -\kappa \left|\epsilon_i\right|^2, \tag{4.24}$$

uniformly in $x_i(t)$ for some constant $\kappa \in \mathbb{R}_{>0}$.

(H4.6) *If the systems are coupled through* (4.21),(4.22)*, the functions $H(x_i)$ are such that there exists $R > 0$ such that $|x_i| > R$ implies that $H(x_i) - \gamma c|z_i|^2 > 0$, with $c = \|C_2\|\|N_2\|$.*

(H4.7) *If the systems are coupled through* (4.21),(4.23)*, the functions $H(x_i)$ are such that there exists $R > 0$ such that $|x_i| > R$ implies that $H(x_i) - \gamma\tilde{c}|z_i|^2 > 0$, with $\tilde{c} = \|C_2\|\|N_2\| + 2$.*

Let γ_{max} be the largest γ that satisfies (H4.6) *and* (H4.7)*, then the solutions of the coupled systems* (4.1),(4.2),(4.21),(4.22) *and* (4.1),(4.2), (4.21),(4.23) *are ultimately bounded for any finite $\tau \in \mathbb{R}_{\geq 0}$ and $\gamma \in [0, \gamma_{max}]$.*

The proof of Lemma 4.8 can be found in the Appendix A.

Remark 4.9. *If the conditions stated in Lemma 4.8 are satisfied, then existence and ultimate boundedness of the solutions of the closed-loop system are guaranteed. Before studying network synchronization (a relative stability notion), it is necessary to ensure that solutions exist and are bounded; otherwise, it would not make sense to talk about synchronization simply because solutions are not guaranteed to be well defined.*

4.4.2 Network Synchronization

First, we derive conditions that guarantee invariance of the synchronization manifold $\mathcal{M}$ under the closed-loop dynamics (4.1),(4.2),(4.21)-(4.23).

Proposition 4.10. *The synchronization manifold $\mathcal{M}$ is invariant under the closed-loop dynamics* (4.1),(4.2),(4.21),(4.22) *on a simple strongly connected graph if at least one of the following conditions is satisfied.*

1. *The estimated states are τ-periodic, i.e.,*

$$\hat{z}_i(t) = \hat{z}_i(t - \tau).$$

2. *$\sum_{j \in \mathcal{E}_i} a_{ij} = \bar{d}$ for some $\bar{d} \in \mathbb{R}_{>0}$ and for all $i \in \mathcal{I}$.*

Proof: For the existence of the synchronized state, it is required that the dynamics of the systems are identical on the synchronization manifold. Since all the systems (4.1),(4.2) are assumed to be identical, it follows that $\mathcal{M}$ is invariant under (4.1),(4.2),(4.21),(4.22) if $u_i = u_j$ on $\mathcal{M}$ for all $i, j \in \mathcal{I}$, i.e.,

$$0 = u_i - u_j = \gamma(d_i - d_j)\left(\hat{z}_* - \hat{z}_*^{\tau}\right),$$

for all $\hat{z}_* \in \hat{\mathcal{M}}_z := \{\hat{z} \in \mathbb{R}^{km} | \hat{z}_i = \hat{z}_j, \forall\, i, j \in \mathcal{I}\}$ with $\hat{z} := \mathrm{col}(\hat{z}_1, \ldots, \hat{z}_k)$. Then, $u_i = u_j$ only if $d_i = \sum_{j \in \mathcal{E}_i} a_{ij} = \bar{d} \in \mathbb{R}_{>0}$ for all $i \in \mathcal{I}$ or if $\hat{z} = \hat{z}^{\tau}$, i.e., the estimated states are τ-periodic. ■

Therefore, it is assumed that:

(H4.8) $\sum_{j \in \mathcal{E}_i} a_{ij} = \bar{d} \in \mathbb{R}_{>0}\ \forall\ i \in \mathcal{I}$, for systems interacting through the DTDC (4.21),(4.22).

Clearly, if the systems are interconnected through (4.21),(4.23), all the coupling functions vanish on the synchronization manifold. Hence, the synchronization manifold $\mathcal{M}$ is positively invariant under the dynamics (4.1),(4.2),(4.21),(4.23). In the following theorem, we give sufficient conditions for network synchronization of the interconnected systems.

Theorem 4.11. *Consider the k nonlinear systems* (4.1),(4.2) *interconnected through either the* DTDC (4.21),(4.22) *or* (4.21),(4.23) *with coupling strength $\gamma \in \mathbb{R}_{\geq 0}$ and time-delay $\tau \in \mathbb{R}_{\geq 0}$ on a simple strongly connected graph. Suppose that the conditions stated in Lemma 4.8 and assumption* (H4.2) *are satisfied and in the case of* (4.21),(4.22) *assumption* (H4.8) *holds. Then, the solutions of the coupled systems* (4.1),(4.2),(4.21), (4.22) *and* (4.1),(4.2),(4.21),(4.23) *are ultimately bounded and there exist positive constants γ', Ξ', and κ' such that if $\gamma \in (\gamma', \gamma_{max}]$ (with γ_{max} being the maximal coupling strength for which boundedness of solutions is guaranteed), $\gamma\tau < \Xi'$, and $\kappa > \kappa'$ (with κ from* (H4.5)*), then there exists a (globally) asymptotically stable subset of the diagonal set $\mathcal{M}$.*

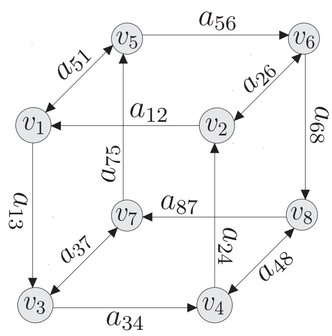

Figure 4.1 Network of eight identical systems. The graph is directed and strongly connected.

The proof of Theorem 4.11 can be found in the Appendix A. The result stated in Theorem 4.11 amounts to the following. The interconnected systems asymptotically synchronize provided that the coupling strength γ belongs to the set $(\gamma', \gamma_{max}]$, the time-delay τ is sufficiently small, and the estimation errors ϵ_i converge sufficiently fast to the origin.

4.5 Example: FitzHugh-Nagumo Neural Oscillators

It is well known that individual neurons in parts of the brain discharge their action potentials in synchrony. Synchronous oscillations of neurons have been reported in the olfactory bulb, the visual cortex, the hippocampus, and in the motor cortex [45, 124]. The presence or absence of synchrony in the brain is often linked to specific brain functions or critical physiological states (e.g., epilepsy). Hence, understanding conditions that lead to such a behavior, exploring the possibilities to manipulate these conditions, and describe them rigorously is vital for further progress in neuroscience and related branches of physics [136]. Thus, to show the performance of our control-scheme, we have selected networks of coupled FitzHugh-Nagumo neural oscillators. The FitzHugh Nagumo neuronal model is one of many neuronal models that fulfils the conditions stated in Theorem 4.11 at the level of the systems, namely, *semipassivity* and *convergence*, see [136].

A. Convergence and Semipassivity. Each system in the network is assumed to be a forced FitzHugh-Nagumo oscillator of the form

$$\begin{cases} \dot{z}_i = z_i - \frac{z_i^3}{3} - y_i + \delta\cos(t) + u_i, \\ \dot{y}_i = \psi\left(z_i + a - by_i\right), \end{cases} \tag{4.25}$$

with measurable output $y_i \in \mathbb{R}$, semipassive output $z_i \in \mathbb{R}$, input $u_i \in \mathbb{R}$, state $x_i = (z_i, y_i)^T \in \mathbb{R}^2$, positive constants $\psi, a, b, \delta \in \mathbb{R}_{>0}$, and $i \in \mathcal{I} = \{1, ..., 8\}$. The FitzHugh-Nagumo oscillator is strictly $\mathcal{C}^1$-semipassive with input u_i, output z_i, storage function $V(x_i) = \frac{1}{2}(z_i^2 + \frac{1}{\psi}y_i^2)$, and function $H(\cdot)$ as follows

$$H(x_i) = \frac{z_i^4}{3} - z_i^2 - \delta\left|z_i\right| + by_i^2 - ay_i, \tag{4.26}$$

which is strictly positive for sufficiently large $|x_i|$. Moreover, if we apply Demidovich's condition (4.10) to the internal dynamics of (4.25), it follows that for $P = 1$ the matrix $Q(x_i)$ is simply given by $Q(x_i) = -\psi b$. Since $b, \psi \in \mathbb{R}_{>0}$, it follows that $Q(x_i)$ is strictly negative and then the internal dynamics is an exponentially convergent system; therefore, assumption (H4.2) is satisfied. However, the variable z_i is not available for feedback, the coupling variable is the measurable output y_i and therefore Theorem 4.2 cannot be applied. Nevertheless, if there exists a function $\beta(\cdot)$ such that (H4.5) is satisfied, then the DTDC (4.21)-(4.23) could be constructed and therefore Theorem 4.11 may be applied to conclude synchronization of the closed-loop system.

B. Network Topology. Consider a network of eight systems coupled according to the graph depicted in Figure 4.1 with $a_{ij} = 1$ if $\{ij\} \in \mathcal{E}$ and $a_{ij} = 0$ otherwise. The network is strongly connected and simple. Moreover, the degree matrix is given by $D = diag\{2, ..., 2\}$, assumption (H4.8) is satisfied, and the associated adjacency matrix is not symmetric, i.e., $A \neq A^T$.

C. Nonlinear Observer. Next, using Proposition 4.6, an observer of the form given in Definition 4.5 is constructed. Associated with system (4.25), the estimation error dynamics (4.17) takes the following form

$$\begin{aligned} \dot{\epsilon}_i &= -\begin{pmatrix} 1 & -\frac{\partial\beta}{\partial y_i} \end{pmatrix} \begin{pmatrix} z_i^2\epsilon_i + z_i\epsilon_i^2 + \frac{\epsilon_i^3}{3} - \epsilon_i \\ -\psi\epsilon_i \end{pmatrix} \\ &= -\left(\frac{\epsilon_i^2}{12} + \left(z_i + \frac{\epsilon_i}{2}\right)^2 - 1 + \frac{\partial\beta}{\partial y_i}\psi\right)\epsilon_i. \end{aligned} \tag{4.27}$$

Consider the Lyapunov function $V_0(\epsilon_i) = \frac{1}{2}\epsilon_i^2$, then

$$\begin{aligned}\dot{V}_0(\epsilon_i, z_i) &= -\left(\frac{\epsilon_i^2}{12} + \left(z_i + \frac{\epsilon_i}{2}\right)^2 - 1 + \frac{\partial \beta}{\partial y_i}\psi\right)\epsilon_i^2 \\ &\leq -\left(\frac{\partial \beta}{\partial y_i}\psi - 1\right)\epsilon_i^2. \end{aligned} \tag{4.28}$$

Taking the function $\beta(\eta_i, y_i) = \eta_i + \kappa y_i$ with $\kappa \in \mathbb{R}_{>0}$, yields $\dot{V}_0 \leq -(\kappa\psi - 1)\epsilon_i^2$; therefore, for any $\kappa > \frac{1}{\psi}$ the origin of (4.27) is globally uniformly asymptotically stable. Notice that $\det\left(\frac{\partial \beta}{\partial \eta_i}\right) = 1 \neq 0$, i.e., assumption (H4.3) is satisfied. It follows that the functions $l(\cdot)$ and $s(\cdot)$ in (4.18) and (4.19) are well defined; hence, the nonlinear observer (4.14),(4.15) takes the following form

$$\begin{cases} \dot{\eta}_i = \left(\kappa\psi b - \kappa^2\psi + \kappa - 1\right) y_i + (1 - \kappa\psi)\,\eta_i \\ \quad - \kappa\psi a - \frac{(\kappa y_i + \eta_i)^3}{3} + \delta \cos(t) + u_i, \\ \hat{z}_i = \kappa y_i + \eta_i. \end{cases} \tag{4.29}$$

D. Diffusive Dynamic Coupling. Combining the observer (4.29) and estimated versions of (4.6) and (4.7), the dynamic couplings (4.21) and (4.23) are given by

$$u_i = \gamma \sum_{j \in \mathcal{E}_i} a_{ij}\left(\kappa y_j^\tau - \kappa y_i + \eta_j^\tau - \eta_i\right), \tag{4.30}$$

$$u_i = \gamma \sum_{j \in \mathcal{E}_i} a_{ij}\left(\kappa y_j^\tau - \kappa y_i^\tau + \eta_j^\tau - \eta_i^\tau\right). \tag{4.31}$$

Let the 8 systems (4.25) be interconnected according to the graph depicted in Figure 4.1 through the DTDC (4.29)-(4.31). Next, we check whether the assumptions of Lemma 4.8 and Theorem 4.11 are satisfied. It is already shown that (H4.5) of Lemma 4.8 is satisfied and that each system (4.25) is strictly $\mathcal{C}^1$-semipassive with $H(x_i)$ as in (4.26). The function $H(x_i)$ has to satisfy the conditions stated in (H4.6) and (H4.7). Since, the function $H(x_i)$ has a positive fourth-degree term in z_i and a positive quadratic term in y_i, which for large $|x_i|$ dominate all the other terms, it follows that the inequalities in (H4.6) and (H4.7) are always satisfied for sufficiently large $|x_i|$ and arbitrary large coupling strength γ. Therefore, by Theorem 4.11, the solutions of the coupled systems (4.25),(4.29)-(4.31) are ultimately bounded, and for sufficiently small time-delay τ and sufficiently large γ and κ, the systems synchronize.

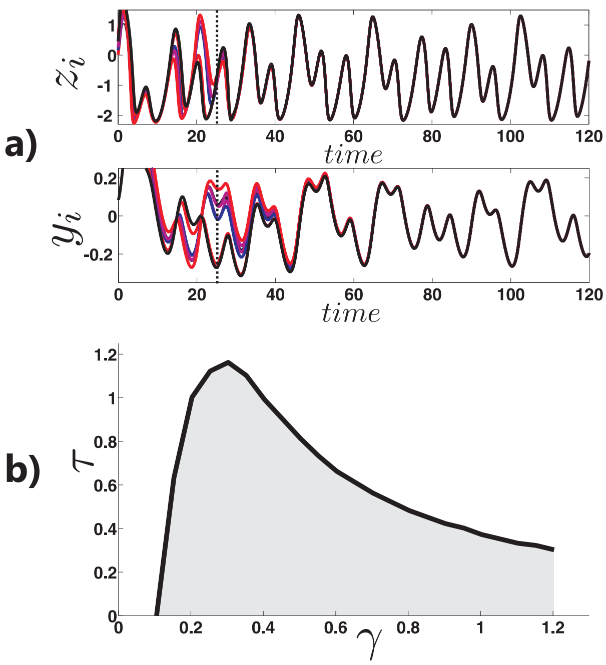

Figure 4.2 Synchronization of eight FitzHugh-Nagumo oscillators: (a) Time responses. (b) Values of γ and τ, obtained by extensive computer simulation, for which the systems synchronize (gray region).

E. Numerical Results. Consider the following parameters, $\psi = 0.08$, $a = 0.7$, $b = 0.8$, and $\delta = 1.325$. For these parameters, the solutions of the FitzHugh-Nagumo oscillator exhibit chaotic behavior. Figure 4.2 depicts the simulation results of the network of FitzHugh-Nagumo oscillators interconnected via (4.29), (4.31) on the graph depicted in Figure 4.1. Figure 4.2(a) shows the time responses for $\gamma = 0.75$, $\kappa = 13$, and $\tau = 0.5$. The top panel shows the eight z_i states and the eight y_i states are depicted in the bottom one. The controller is turned on at $t = 25$ [s]. In Figure 4.2(b), we show the values of γ and τ, obtained by extensive computer simulation, for which the systems synchronize (gray region).

4.6 Conclusions

In this chapter, we have addressed the problem of controlled network synchronization of general nonlinear underactuated systems. We have developed a general tool for constructing two different types of *time-delayed diffusive dynamic couplings* using the ideas of *immersion and invariance*. The coupling design problem is recast as a problem of rendering attractive and invariant a manifold defined in the extended *state-space* of the plant and the coupling. Sufficient conditions on the systems to be interconnected, the network topology, the coupling dynamics, and the time-delay that guarantee (global) state synchronization and boundedness have been derived. We have presented simulation results using chaotic FitzHugh-Nagumo neural oscillators that shows step by step how to construct the proposed time-delayed dynamic diffusive couplings and how to apply the results stated in Section 4.4 and Section 4.5 to prove boundedness and synchronization of the solutions of the closed-loop system.

Chapter 5

Partial Synchronization via Observer-Based Diffusive Dynamic Couplings

Abstract. Partial synchronization in networks of semipassive systems interconnected through a class of diffusive dynamic couplings is studied. The couplings are constructed by combining nonlinear observers and feedback interconnection terms. Sufficient conditions on the systems to be interconnected, the network topology, the observer dynamics, and the coupling strength that guarantee (global) partial synchronization are derived. The results are illustrated by computer simulations of coupled Hindmarsh-Rose neural oscillators.

5.1 Introduction

In this chapter, we study a phenomenon called *partial synchronization* or *clustering* in networks of coupled oscillators, i.e., some oscillators in the network do synchronize while others do not. The study of partial synchronization is relevant in many science and engineering applications. For instance in [141], the authors report the occurrence of partial synchronization in arrays of chaotic semiconductor lasers. In [117], experimental partial synchronization in networks of chaotic circuits with applications to communication systems is considered. The clustering problem of Josephson junction arrays with applications to high frequency electromagnetic generators is addressed in [111]. The occurrence of partial synchronization in networks of diffusively coupled nonlinear oscillators has been investigated in, for instance, [21, 105, 109, 148]. In particular, the au-

This chapter is based on [80].

thors in [105, 109] derive conditions for the existence and stability of partial synchronization modes in networks of nonlinear *semipassive* systems with *convergent* internal dynamics. Moreover, they show that if a network contains certain symmetries, then these symmetries identify modes of partial synchronization. In these results, it is assumed that the variable z_i that renders the internal dynamics *convergent*, and for which each system is *strictly semipassive* is used in the diffusive (feedback) coupling. Therefore, if the measurable output is a different state function y_i, which does not have the desired stability properties, then these results cannot be applied. Nevertheless, if there exists a (nonlinear) observer, which reconstructs z_i from measurements of y_i, then an *observer-based diffusive dynamic coupling*, which only depends on the measurable output y_i could be constructed to interconnect the systems. In [77], we have started with the analysis of these ideas for the study of *full network synchronization*. Following the same approach, in this chapter, we extend the ideas presented in [105] to the case of *observer-based diffusive dynamic couplings*. We derive sufficient conditions on the individual systems, the network topology, the observer dynamics, and the coupling strength that guarantee *partial network synchronization*.

5.2 System Description

Consider k identical nonlinear systems of the form

$$\dot{x}_i = f(x_i) + Bu_i, \tag{5.1}$$

$$y_i = C_1 x_i, \tag{5.2}$$

$$z_i = C_2 x_i, \tag{5.3}$$

with $i \in \mathcal{I} := \{1, ..., k\}$, state $x_i \in \mathbb{R}^n$, input $u_i \in \mathbb{R}^m$, measurable output $y_i \in \mathbb{R}^s$, semipassive output $z_i \in \mathbb{R}^m$, sufficiently smooth function $f : \mathbb{R}^n \to \mathbb{R}^n$, and matrices $C_1 \in \mathbb{R}^{s\times n}$, $C_2 \in \mathbb{R}^{m\times n}$, and $B \in \mathbb{R}^{n\times m}$ with the matrix $C_2B \in \mathbb{R}^{m\times m}$ being similar to a positive definite matrix. In addition, it is assumed that the systems (5.1),(5.3) are *strictly $\mathcal{C}^1$-semipassive*, they have relative degree one, and their corresponding internal dynamics are *exponentially convergent systems*. The network is called *diffusively coupled* if the systems interact via couplings of the form

$$u_i = \gamma \sum_{j\in\mathcal{E}_i} a_{ij}(z_j - z_i), \;\; i \in \mathcal{I}, \tag{5.4}$$

where z_j is the output of system j to which system i is connected, $\gamma \in \mathbb{R}_{>0}$ denotes the coupling strength, $a_{ij} \geq 0$ are the weights of the interconnections, and $\mathcal{E}_i$ is the set of neighbors of system i. Notice that the coupling (5.4) can be written in the following matrix form

$$u = -\gamma \left(L \otimes I_m \right) z, \tag{5.5}$$

where $L \in \mathbb{R}^{k \times k}$ denotes the Laplacian matrix, $z := \mathrm{col}(z_1, ..., z_k) \in \mathbb{R}^{km}$, and $u := \mathrm{col}(u_1, ..., u_k) \in \mathbb{R}^{km}$. Define $x := \mathrm{col}(x_1, ..., x_k) \in \mathbb{R}^{kn}$ and the linear manifold

$$\mathcal{M} := \{x \in \mathbb{R}^{kn} | x_i = x_j, \forall\, i, j \in \mathcal{I}\}.$$

The manifold $\mathcal{M}$ is called the synchronization manifold or the diagonal set. The systems (5.1),(5.3),(5.4) are said to fully synchronize, or simply synchronize, if the synchronization manifold $\mathcal{M}$ contains an asymptotically stable subset. In a similar manner, consider the linear manifold

$$\mathcal{M}_P := \{x \in \mathbb{R}^{kn} | x_i = x_j, \text{ for some } i, j \in \mathcal{I}\}.$$

The manifold $\mathcal{M}_P$ is called a partial synchronization manifold. The systems (5.1), (5.3),(5.4) are said to partially synchronize, if the partial synchronization manifold $\mathcal{M}_P$ is invariant under the closed-loop dynamics and contains an asymptotically stable subset. The result presented here is a direct extension of the results presented in [105, 106], where sufficient conditions for partial synchronization in networks of diffusively interconnected semipassive systems are derived. These papers show that if a network contains certain symmetries, then these symmetries identify modes of partial synchronization. Moreover, the authors prove that if the individual systems are *semipassive* and their corresponding internal dynamics are *exponentially convergent systems*, then the partial synchronization manifold may contain an asymptotically stable subset.

Remark 5.1. *In the results presented in [105, 106], it is assumed that the variable z_i that renders the internal dynamics convergent, and for which each system is strictly $\mathcal{C}^1$-semipassive is available for feedback. Therefore, if the measurable output is a different state function y_i, which does not have the desired stability properties, then these results cannot be applied.*

It is therefore interesting to extend these results to the case when the variable z_i is not measurable, but there exists a (nonlinear) observer which reconstructs z_i from the measurable output y_i. If such an observer exists, we can construct a *diffusive dynamic coupling* combining the observer and an estimated version of the *diffusive coupling* (5.4). Then, a natural question arises, "If the systems are interconnected through an estimated variable $\hat{z}_i$, is it still possible to achieve partial synchronization of the closed loop system?" In order to answer this question, we first need to make some stability assumptions on the observer dynamics.

5.3 Observer-based Diffusive Dynamic Couplings

In this section, the structure of the observers that we consider and the *diffusive dynamic coupling* that is used to interconnect the systems are introduced. Moreover, sufficient conditions for boundedness of the closed-loop system are also presented.

5.3.1 Nonlinear Observer

Consider the k identical systems (5.1)-(5.3). Assume that for any initial condition $x_i(t_0) \in \mathbb{R}^n$ and every input signal u_i, the corresponding solution $x(t)$ is well defined and ultimately bounded for all $t \geq t_0$, (in Section 5.3.3, we give sufficient conditions for ultimate boundedness of the closed-loop system for the class of inputs under study). Consider (nonlinear) observers of the form

$$\begin{cases} \dot{\eta}_i = l(\eta_i, y_i, u_i), \\ \hat{z}_i = \beta(\eta_i, y_i), \end{cases} \tag{5.6}$$

with $i \in \mathcal{I}$, state $\eta_i \in \mathbb{R}^p$, $p \geq n - s$, estimated semipassive output $\hat{z}_i \in \mathbb{R}^m$, and sufficiently smooth functions $l : \mathbb{R}^p \times \mathbb{R}^s \times \mathbb{R}^m \to \mathbb{R}^p$ and $\beta : \mathbb{R}^p \times \mathbb{R}^s \to \mathbb{R}^m$ designed such that $\hat{z}_i$ asymptotically converges to the actual value of z_i. Associated with the observer (5.6), we have the estimation error $\epsilon_i \in \mathbb{R}^m$ defined as

$$\epsilon_i := \hat{z}_i - z_i = \beta(\eta_i, y_i) - z_i. \tag{5.7}$$

Then, the estimation error dynamics is given by

$$\dot{\epsilon}_i = \frac{\partial \beta(\eta_i, y_i)}{\partial \eta_i} l(\eta_i, y_i, u_i) + \left(\frac{\partial \beta(\eta_i, y_i)}{\partial y_i} C_1 - C_2 \right) \Big(f(x_i) + B u_i \Big). \tag{5.8}$$

It is assumed that the functions $l(\cdot)$ and $\beta(\cdot)$ are designed such that the estimation error dynamics (5.8) has the following structure

$$\dot{\epsilon}_i = \phi(\epsilon_i, x_i), \tag{5.9}$$

with sufficiently smooth function $\phi : \mathbb{R}^m \times \mathbb{R}^n \to \mathbb{R}^m$ and $\phi(0, x_j) = 0$ for all $x_i \in \mathbb{R}^n$. The estimated $\hat{z}_i$ uniformly asymptotically converges to z_i, if the origin of the estimation error dynamics (5.9) (or 5.8) is uniformly asymptotically stable. In general, it is unknown under what conditions on (5.1),(5.2) the (nonlinear) observer (5.6) can be constructed. In this manuscript, it is assumed that the observer exists and it is given. Nevertheless, we forward the interested reader to [56, 84] for existence conditions and interesting design methods of (nonlinear) observers.

5.3.2 Diffusive Dynamic Couplings

Let the k systems (5.1),(5.2) be interconnected through dynamic diffusive couplings of the form

$$\begin{aligned} \dot{\eta}_i &= l(\eta_i, y_i, u_i), & (5.10)\\ \hat{z}_i &= \beta(\eta_i, y_i), & (5.11)\\ u_i &= \gamma \sum_{j\in\mathcal{E}_i} a_{ij}\left(\hat{z}_j - \hat{z}_i\right), & (5.12) \end{aligned}$$

where $\gamma \in \mathbb{R}_{\geq 0}$ denotes the coupling strength and $a_{ij} \geq 0$ are the interconnection weights. Moreover, since the coupling strength is encompassed in the constant γ, then it is assumed without loss of generality that $\max_{i\in\mathcal{I}} \sum_{j\in\mathcal{E}_i} a_{ij} = 1$. The dynamic coupling (5.10)-(5.12) is the combination of the nonlinear observer (5.6) and an estimated version of the diffusive coupling (5.4).

5.3.3 Boundedness of the Interconnected Systems

In this part, we derive sufficient conditions for boundedness of the solutions of the coupled systems (5.1),(5.2),(5.10)-(5.12).

Lemma 5.2. [77]. *Consider k coupled systems* (5.1),(5.2),(5.10)-(5.12) *on a simple strongly connected graph with coupling strength $\gamma \in \mathbb{R}_{\geq 0}$. Assume that:*

(H5.1) *There exists a nonlinear observer* (5.6) *such that the corresponding estimation error dynamics* (5.9) *is uniformly asymptotically stable with positive definite radially unbounded Lyapunov function $V_0 \in \mathcal{C}^1(\mathbb{R}^m, \mathbb{R}_{\geq 0})$ satisfying*

$$\left(\nabla V_0(\epsilon_i)\right)^T \phi(\epsilon_i, x_i) \leq -\kappa \left|\epsilon_i\right|^2, \tag{5.13}$$

uniformly in $x_i(t)$ for some constant $\kappa \in \mathbb{R}_{>0}$.

(H5.2) *Each system* (5.1),(5.3) *is strictly $\mathcal{C}^1$-semipassive with radially unbounded storage function, and the functions $H(x_i)$ are such that there exists $R \in \mathbb{R}_{>0}$ such that $|x_i| > R$ implies that $H(x_i) - \gamma d_i |z_i|^2 > 0$ with $d_i = \sum_{j\in\mathcal{E}_i} a_{ij}$.*

Let γ_{max} be the largest γ that satisfies (H5.2)*, then the solutions of the coupled system* (5.1),(5.2),(5.10)-(5.12) *are ultimately bounded for $\gamma \in [0, \gamma_{max}]$.*

5.4 Symmetries and Invariant Manifolds

In this section, we extend the ideas presented by [105] for the identification of partial synchronization modes to the case of *diffusive dynamic couplings*. If a given network possesses certain symmetry, this symmetry must be present in the adjacency matrix A (and thus also in the Laplacian matrix L). In particular, the network may contain some repeated patterns when considering the arrangements of the constants a_{ij} and hence the permutation of some elements would leave the network unchanged. That is, the structure of the network is preserved after simultaneous swapping of (some of) the nodes of the network. The matrix representation of a permutation of the set $\mathcal{I} = \{1, ..., k\}$ is a permutation matrix $\Pi \in \mathbb{R}^{k\times k}$. Consider the closed-loop system (5.1),(5.2),(5.10)-(5.12)

$$\begin{aligned}
\dot{\eta}_i &= l(\eta_i, y_i, u_i),\\
\hat{z}_i &= \beta(\eta_i, y_i),\\
\dot{x}_i &= f(x_i) + \gamma B \sum_{j\in\mathcal{E}_i} a_{ij}\left(\hat{z}_j - \hat{z}_i\right), \ \ i \in \mathcal{I}.
\end{aligned}$$

Given that $\epsilon_i = \hat{z}_i - z_i$, the closed-loop system can be written in terms of the estimation errors ϵ_i as follows

$$\begin{aligned}
\dot{\epsilon}_i &= \phi(\epsilon_i, x_i), && (5.14)\\
\dot{x}_i &= f(x_i) + \gamma B \sum_{j\in\mathcal{E}_i} a_{ij}\left(z_j - z_i + \epsilon_j - \epsilon_i\right), && (5.15)
\end{aligned}$$

with $\phi(\cdot)$ from (5.9). Introduce the new set of variables: $\epsilon := \mathrm{col}(\epsilon_1, \ldots, \epsilon_k)$, $x := \mathrm{col}(x_1, \ldots, x_k)$, $\Xi := \left(\Pi \otimes I_n\right)$, $F(x) := \mathrm{col}(f(x_1), \ldots, f(x_k))$, and $\Phi(\epsilon, x) := \mathrm{col}(\phi(\epsilon_1, x_1), \ldots, \phi(\epsilon_k, x_k))$. Then, the stacked closed-loop system (5.14), (5.15) can be written as

$$\begin{aligned}
\dot{\epsilon} &= \Phi(\epsilon, x), && (5.16)\\
\dot{x} &= F(x) - \gamma(L \otimes BC_2)x - \gamma(L \otimes B)\epsilon. && (5.17)
\end{aligned}$$

Using this new notation, in the following lemma, we show that a symmetry in the network defines a linear invariant manifold for the closed-loop dynamics.

Lemma 5.3. *Consider a network of k systems* (5.1),(5.2) *interconnected through the dynamic coupling* (5.10)-(5.12) *with coupling strength $\gamma \in \mathbb{R}_{>0}$ and Laplacian matrix $L \in \mathbb{R}^{k\times k}$. Let $\Pi \in \mathbb{R}^{k\times k}$ be a permutation matrix and $X \in \mathbb{R}^{k\times k}$ denote a solution to the matrix equation*

$$(I_k - \Pi)\, L = X\,(I_k - \Pi)\,, \tag{5.18}$$

then the set

$$\mathcal{N} := \left\{(\epsilon, x) \in \mathbb{R}^{km} \times \mathbb{R}^{kn} | \epsilon = \mathbf{0}_{km\times 1} \wedge\ (I_{kn} - \Pi \otimes I_n)\, x = \mathbf{0}_{kn\times 1}\right\}, \tag{5.19}$$

defines a linear invariant manifold for the coupled systems (5.14),(5.15).

Proof: Assume that at some time t^* it is satisfied that $(I_{kn} - \Xi)x(t^*) = \mathbf{0}$ and $\epsilon(t^*) = \mathbf{0}$. Then, the set $\mathcal{N}$ is invariant under the closed-loop dynamics if $(I_{kn} - \Xi)x(t^*) = \mathbf{0}$ and $\epsilon(t^*) = \mathbf{0}$ imply $(I_{kn} - \Xi)\dot{x}(t^*) = \mathbf{0}$ and $\dot{\epsilon}(t^*) = \mathbf{0}$. By construction $\epsilon = \mathbf{0}$ is an equilibrium point of (5.16), then $\epsilon(t^*) = \mathbf{0} \to \dot{\epsilon}(t^*) = \mathbf{0}$. Consider (5.17) and the solution X of the matrix equation (5.18). Since Π is a permutation matrix, it follows that $\Xi F(x(t^*)) = F(\Xi x(t^*))$, then

$$\begin{aligned}(I_{kn} - \Xi)\dot{x}(t^*) &= (I_{kn} - \Xi)F(x(t^*)) - \gamma(I_{kn} - \Xi)(L \otimes BC_2)x(t^*),\\ &- \gamma(I_{kn} - \Xi)(L \otimes B)\epsilon(t^*),\\ &= F(x(t^*)) - F(\Xi x(t^*)) - \gamma(X \otimes BC_2)(I_{kn} - \Xi)x(t^*)\\ &- \gamma(I_{kn} - \Xi)(L \otimes B)\epsilon(t^*) = \mathbf{0},\end{aligned}$$

because it is assumed that $(I_{kn} - \Xi)x(t^*) = \mathbf{0}$ and $\epsilon(t^*) = \mathbf{0}$. Then, $\epsilon(t) = \mathbf{0}$ and $(I_{kn} - \Xi)x(t) = \mathbf{0}$ for all $t \geq t^*$; therefore, the set $\mathcal{N}$ defines a linear invariant manifold for the interconnected systems (5.14),(5.15). ■

5.5 Partial Synchronization

In the previous section, conditions for the existence of linear invariant manifolds are presented. For partial synchronization to occur, we require these manifolds to contain an asymptotically stable subset. In this section, we present sufficient conditions for a linear invariant manifold to contain an asymptotically stable subset. Consider the k systems (5.1)-(5.3). Since it is assumed that the systems have relative degree one and the matrix C_2B is similar to a positive definite matrix, then there exists a globally defined coordinate transformation such that systems

(5.1),(5.3) can be written in the following *normal form*, (this transformation is explicitly computed in [107]),

$$\dot{\zeta}_i = q(\zeta_i, z_i), \tag{5.20}$$
$$\dot{z}_i = a(\zeta_i, z_i) + C_2 B u_i, \tag{5.21}$$

with internal state $\zeta_i \in \mathbb{R}^{n-m}$, and sufficiently smooth vector fields $q : \mathbb{R}^{n-m} \times \mathbb{R}^m \to \mathbb{R}^{n-m}$ and $a : \mathbb{R}^{n-m} \times \mathbb{R}^m \to \mathbb{R}^m$. For the sake of simplicity, it is assumed that $C_2 B = I_n$ (results for the general case with $C_2 B$ being similar to a positive definite matrix can easily be derived). In the following theorem, we give sufficient conditions for partial synchronization to occur.

Theorem 5.4. *Consider the k nonlinear systems* (5.1),(5.2) *interconnected through the diffusive dynamic coupling* (5.10)-(5.12) *on a simple strongly connected graph. Suppose the conditions of Lemma 5.2 and Lemma 5.3 are satisfied for some matrix X and permutation matrix Π. In addition assume that:*

(H5.3) *There is a constant $\lambda' \in \mathbb{R}_{>0}$ such that*

$$\frac{1}{2}\vartheta^T \left(I - \Pi\right)^T \left(X + X^T\right) \left(I - \Pi\right) \vartheta \geq \lambda' \left|\left(I - \Pi\right) \vartheta\right|^2 .$$

(H5.4) *The internal dynamics (5.20) is an exponentially convergent system, i.e., there is a positive definite matrix $P \in \mathbb{R}^{(n-m)\times(n-m)}$ such that the eigenvalues of the symmetric matrix*

$$Q(\zeta_i, z_i) = \frac{1}{2}\left(P\left(\frac{\partial q}{\partial \zeta_i}(\zeta_i, z_i)\right) + \left(\frac{\partial q}{\partial \zeta_i}(\zeta_i, z_i)\right)^T P\right), \tag{5.22}$$

are uniformly negative and bounded away from zero for all $\zeta_i \in \mathbb{R}^{n-m}$ and $z_i \in \mathbb{R}^m$.

Then, there exist positive constants γ' and κ' such that if $\gamma > \gamma'$ and $\kappa > \kappa'$ with κ from (5.13), *then the set $\mathcal{N}$ contains a globally asymptotically stable subset.*

The proof of Theorem 5.4 is presented in the Appendix A. Notice that if the matrices L and Π commute, then the matrix equation (5.18) admits a solution $X = L$. The problem of finding a $\lambda' \in \mathbb{R}_{>0}$ satisfying (H5.3) can be solved via singular value decomposition, see [106]. Moreover, if $X + X^T$ commutes with Π, then λ' is the minimal eigenvalue of $\frac{1}{2}(X + X^T)$ under the restriction that the eigenvectors of $\frac{1}{2}(X + X^T)$ are taken from the set range$(I_k - \Pi)$.

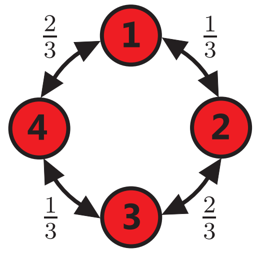

Figure 5.1 A network of four identical systems.

5.6 Example: Hindmarsh-Rose neural oscillators

In this section, we present an illustrative example where we show step by step how to apply Theorem 5.4 to conclude partial synchronization of the coupled systems. It is assumed that each system in the network is a Hindmarsh-Rose neural oscillator, see [51].

A. Convergence and Semipassivity. Consider four identical Hindmarsh-Rose oscillators of the form

$$\dot{\zeta}_{1i} = 0.005\,(4\,(z_i + 1.618) - \zeta_{1i})\,, \tag{5.23}$$

$$\dot{\zeta}_{2i} = -2z_i - z_i^2 - \zeta_{2i}, \tag{5.24}$$

$$\dot{z}_i = -z_i^3 + 3z_i - 4.75 + 5\zeta_{2i} - \zeta_{1i} + u_i, \tag{5.25}$$

$$y_i = \left(\zeta_{1i}, \zeta_{2i} \right)^T, \tag{5.26}$$

with $i \in \mathcal{I} = \{1, 2, 3, 4\}$, measurable output y_i, state $x_i = (\zeta_{1i}, \zeta_{2i}, z_i)^T \in \mathbb{R}^3$, and input $u_i \in \mathbb{R}$. It is shown in [82] that the system (5.23)-(5.25) is *strictly $\mathcal{C}^1$-semipassive* with input u_i, output z_i, and storage function

$$V(x_i) = \frac{1}{2}\left(\frac{1}{0.005 \cdot 4}\zeta_{1i}^2 + \mu\zeta_{2i}^2 + z_i^2\right),$$

for some $\mu \in \mathbb{R}_{>0}$. Moreover, the corresponding $H(x_i)$ satisfies (H5.2) for arbitrarily large γ. Assumption (H5.4) is satisfied with $P = I_2$, i.e., the internal dynamics (5.23),(5.24) is an *exponentially convergent system*. At this point, Theorem 1 in [105] could be applied to conclude that the network of coupled Hindmarsh-Rose systems may exhibit partial synchronization. However, the variable z_i is not available for feedback. The coupling variable is the measurable output y_i; therefore, the results in [105] cannot be used. Nevertheless, if there exists an observer which estimates z_i from measurements of y_i, then the dynamic coupling (5.10)-(5.12) could be constructed and therefore Theorem 5.4 may be used to study partial synchronization.

B. Nonlinear Observer.

Proposition 5.5. *Consider four systems of the form*

$$\begin{aligned} \dot{\eta}_i &= -0.005\kappa_1 \left(\frac{4}{\kappa_2}\beta + 4.472 - y_{1i} \right) \\ &\quad + \kappa_2 \left(-\frac{\beta^3}{\kappa_2^3} + \frac{3\beta}{\kappa_2} - 4.75 + 5y_{2i} - y_{1i} + u_i \right), \end{aligned} \tag{5.27}$$

$$\hat{z}_i = \frac{1}{\kappa_2}\beta(y_i, \eta_i), \tag{5.28}$$

with $i \in \mathcal{I}$, state $\eta_i \in \mathbb{R}$, function $\beta(y_i, \eta_i) = \kappa_1 y_{1i} + \eta_i$, and constants κ_1 and κ_2. Then, there exist $\kappa_1 \in \mathbb{R}_{>0}$ and $\kappa_2 \in \mathbb{R}_{>0}$ such that for all initial conditions $\eta_i(t_0) \in \mathbb{R}$, it is satisfied that: $\lim_{t\to\infty} (\kappa_1 y_{1i} + \eta_i - \kappa_2 z_i) = 0$.

Proof: Define the estimation error

$$\epsilon_i := \kappa_1 y_{1i} + \eta_i - \kappa_2 z_i. \tag{5.29}$$

Straightforward computations show that the estimation error satisfies the following differential equation

$$\dot{\epsilon}_i = -\left(\frac{\kappa_1}{5\kappa_2} - 3 + \frac{1}{\kappa_2}\left(\epsilon_i + \frac{3\kappa_2}{2} z_i \right)^2 + \frac{3\kappa_2}{4} z_i^2 \right) \epsilon_i. \tag{5.30}$$

Consider the positive definite Lyapunov function $V_0(\epsilon_i) = \frac{1}{2}\epsilon_i^2$, then along the solutions of (5.30), it is satisfied that

$$\dot{V}_0 \leq -\left(\frac{\kappa_1}{5\kappa_2} - 3 \right) \epsilon_i^2. \tag{5.31}$$

Therefore, for $\kappa_1 > 15\kappa_2 > 0$, the origin of (5.30) is globally uniformly asymptotically stable. ∎

C. Dynamic Diffusive Coupling. Combining the observer (5.27),(5.28) and an estimated version of (5.4), the dynamic coupling (5.12) takes the form

$$u_i = \frac{\gamma}{\kappa_2} \sum_{j\in\mathcal{E}_i} a_{ij} \left(\kappa_1 y_{1j} - \kappa_1 y_{1i} + \eta_j - \eta_i \right). \tag{5.32}$$

D. Network Topology. Consider a network of four systems coupled according to the graph depicted in Figure 5.1, (this topology is taken from [134]). The network is strongly connected and simple. The associated Laplacian matrix is given by

$$L = \frac{1}{3}\begin{pmatrix} 3 & -1 & 0 & -2 \\ -1 & 3 & -2 & 0 \\ 0 & -2 & 3 & -1 \\ -2 & 0 & -1 & 3 \end{pmatrix}. \tag{5.33}$$

Note that the above Laplacian commutes with the following permutation matrices

$$\Pi_1 = \begin{pmatrix} 0 & 1 & 0 & 0 \\ 1 & 0 & 0 & 0 \\ 0 & 0 & 0 & 1 \\ 0 & 0 & 1 & 0 \end{pmatrix}, \Pi_2 = \begin{pmatrix} 0 & 0 & 1 & 0 \\ 0 & 0 & 0 & 1 \\ 1 & 0 & 0 & 0 \\ 0 & 1 & 0 & 0 \end{pmatrix}, \Pi_3 = \begin{pmatrix} 0 & 0 & 0 & 1 \\ 0 & 0 & 1 & 0 \\ 0 & 1 & 0 & 0 \\ 1 & 0 & 0 & 0 \end{pmatrix},$$

i.e., $L\Pi_j = \Pi_j L$ for all $j \in \{1,2,3\}$, and hence $X = L$ is a solution of the matrix equations $(I_4 - \Pi_j)L = X(I_4 - \Pi_j)$. Let $x = \mathrm{col}(x_1, \ldots, x_4) \in \mathbb{R}^{12}$ and the stacked estimation error $\epsilon = \mathrm{col}(\epsilon_1, \ldots, \epsilon_4) \in \mathbb{R}^4$. Then, from Lemma 5.3, it follows that the sets $\mathcal{N}_j := \left\{(\epsilon, x) \in \mathbb{R}^4 \times \mathbb{R}^{12} | \epsilon = \mathbf{0} \wedge (I_{12} - \Pi_j \otimes I_3)\, x = \mathbf{0}\right\}$, define linear invariant manifolds for the closed-loop system. Moreover, since L is symmetric and commutes with Π_j, then λ' in (H5.3) can be estimated as the minimal eigenvalue of L under the restriction that the eigenvectors of L are taken from the set range$(I_k - \Pi_j)$, see [109] for details. Let λ_i be an eigenvalue of L and μ_i the corresponding eigenvector, then $\lambda_1 = 0, \lambda_2 = \frac{2}{3}, \lambda_3 = \frac{4}{3}, \lambda_4 = 2$, and

$$\mu_1 = \begin{pmatrix} 1 \\ 1 \\ 1 \\ 1 \end{pmatrix}, \mu_2 = \begin{pmatrix} 1 \\ -1 \\ -1 \\ 1 \end{pmatrix}, \mu_3 = \begin{pmatrix} 1 \\ 1 \\ -1 \\ -1 \end{pmatrix}, \mu_4 = \begin{pmatrix} -1 \\ 1 \\ -1 \\ 1 \end{pmatrix}.$$

Then, after some straightforward computations, it follows that $\lambda' = \lambda_2$ for both Π_1 and Π_2, and $\lambda' = \lambda_3$ for Π_3. Therefore, all the assumptions stated in Theorem 5.4 are satisfied, and it can be concluded that for sufficiently large γ, κ_1, and κ_2 the sets $\mathcal{N}_j$ contain globally asymptotically stable subsets. Note that the conditions for partial synchronization of Π_1 and Π_2 are the same. It may be that multiple partial synchronization manifolds coexist and also their conditions for being stable might coincide. The case in which all partial synchronization manifolds are stable coincides the fully synchronized state. It follows that to observe partial synchronization, it is necessary that the values of γ, κ_1, and κ_2 for which a partial manifold is stable do not coincide with those for which the full synchronization manifold is stable. Particularly, in this example, the only partial synchronization manifold that can be observed is the corresponding to the set $\mathcal{N}_3$, i.e., $x_1 = x_4 \neq x_2 = x_3$.

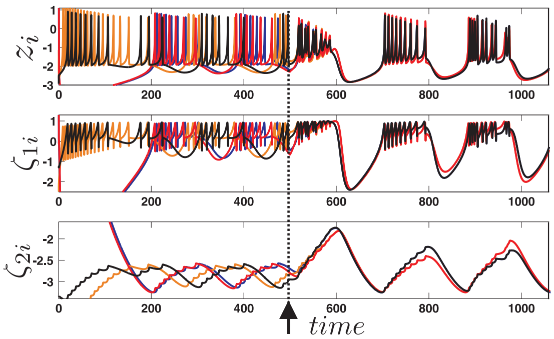

Figure 5.2 States responses. The controller is turned-on at $time = 500$[ms].

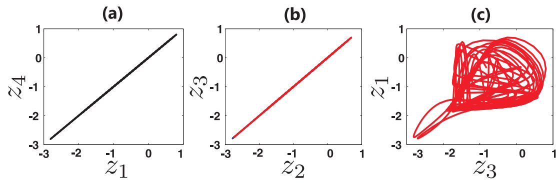

Figure 5.3 (a) Partial synchronization of neurons 1 and 4. (b) Partial synchronization of neurons 2 and 3. (c) No synchronization of neurons 1 and 3.

E. Numerical Results. Figure 5.2 and Figure 5.3 depict simulation results of the network of four Hindmarsh-Rose oscillators with coupling constants $\gamma = 1$, $\kappa_1 = 10$, and $\kappa_2 = 0.07$. In Figure 5.2, the top panel shows the z_i states of the four oscillators and the ζ_{1i} and ζ_{2i} states are depicted in the bottom ones. The controller is turned on at $time = 500$[ms].

5.7 Conclusion

We have presented a methodology for studying the emergence of partial network synchronization for a class of nonlinear oscillators interconnected through *observer-based diffusive dynamic couplings*. It has been shown that symmetries in the network define linear invariant manifolds, which, when being attracting, define modes of partial synchronization. Sufficient conditions on the systems to be interconnected, the network topology, the observer dynamics, and the coupling strength that guarantee (global) partial synchronization have been derived. The results have been illustrated by computer simulations of coupled Hindmarsh-Rose neural oscillators.

Chapter 6

Immersion and Invariance Observers with Time-Delayed Output Measurements

Abstract. We address the problem of constructing (globally) convergent, (reduced-order) observers for general nonlinear systems when the output measurements are subject to constant time-delays. *Immersion and invariance* (I&I) techniques are used to derive a general tool for constructing I&I observers in the presence of time-delays. We show that an asymptotic estimate of the unknown states can be obtained by rendering attractive an appropriately selected invariant manifold in the extended state space. In this manuscript, the observer may play two different roles. On the one hand, it may be used to reconstruct a delayed version of the unmeasured state from measurements of the available delayed outputs. We show that if the time-delay is known, standard I&I techniques can be directly applied to estimate the delayed unmeasured states. In this case, we refer to the observer as a *retarded immersion and invariance observer*. On the other hand, the observer may be used to reconstruct both the delay-free unmeasured states and the delay-free output from measurements of the delayed output. In this case, we refer to it as an *immersion and invariance predictor*. Two examples with chaotic oscillators are presented to show the performance of the observers.

6.1 Introduction

There has been considerable interest in the study of systems exhibiting complex behavior during the last decades. Particularly, the problem of estimating the state

This chapter is based on [75].

of dynamical systems has received a lot of attention due to its importance in practical applications, where part of the state may not be available for measuring. Frequently, it is necessary to estimate the unmeasured states, for instance, when they are used for synthesizing state controllers or for process monitoring purposes. To this end, a state observer is usually employed to reconstruct the complete state of the system from measurements of the available outputs. In the celebrated paper of Luenberger [69], the (reduced-order) observer design problem is completely addressed and solved for linear time-invariant systems. Luenberger derives an observer design technique based on the solution of a *Silvester-type matrix equation*. After this result, several research groups started developing observer design methods for specific classes of nonlinear systems. The classical approach to nonlinear observer design consists in finding a transformation that linearizes the plant up to an output injection term and then applying standard linear observer design techniques, see [60, 61]. We refer the reader to [84] and references therein for a fairly complete literature review of the existing observer design techniques for nonlinear systems. More recently, in [14, 58], the early ideas of Luenberger are extended to the nonlinear case. In these papers, sufficient conditions for the existence of *linear observers with nonlinear output injection terms* are derived in terms of the solution of a partial differential equation (PDE). In the same spirit, in [56], it is shown that an asymptotic estimate of the unknown states can be obtained by rendering attractive an appropriately selected (invariant) manifold in the extended state space (the union of the state spaces of the system and the observer). For a class of nonlinear time-varying systems, the authors propose a nonlinear observer in terms of two mappings which must be selected to render the origin of the estimation error dynamics asymptotically stable. As pointed out by the authors, in *Remark 2* in [56], this stabilization problem may be extremely difficult to solve, since it relies on the solution of a set of partial differential equations (or inequalities). However, in many cases of practical interest, these equations are solvable.

We remark that in all the aforementioned papers, it is assumed that the communication between the system and the observer is instantaneous, i.e., there are no time-delays in the loop. The estimation of the system state based on delayed output measurements is an important problem in many engineering applications. For instance, when the measurement process intrinsically causes non-negligible time-delays or when the system is controlled or monitored through a communication network which results in unavoidable time-delays. Then, it is important to study the effect of time-delays in the existing observer design techniques. There are some results in this direction already. For instance, the authors in [30] and [70] present state observers for drift observable nonlinear systems when the output measurements are affected by known time-delays. Again, these results consist in finding a transformation that linearizes part of the plant and then applying standard *linear or hight gain observer design techniques*. In [59], the ideas of their previous work [58] are extended to the case when the output measurements are subject to constant time-delays. The authors propose a nonlinear observer with state-dependent gain which is computed from the solution of a system of first-order singular PDEs. In this chapter, we study the *immersion and invariance* (I&I) techniques presented in [17, 56] for designing nonlinear observers. We show how these I&I ideas may be extended when the output measurements are corrupted by constant time-delays. Following the design method developed in [17], we derive a general tool for constructing I&I *observers* in the presence of time-delays. It is important to point out that, as it is the case in the delay-free setting considered in [17], the observer design relies on the existence of two mappings, $\beta(\cdot)$ and $\phi(\cdot)$, which must be selected to render the zero solution of the estimation error dynamics asymptotically stable. This stabilization problem may be difficult to solve, since, in general, it relies on the solution of a set of partial differential equations (or inequalities). However, as it is shown in the examples, for some systems these equations turn out to be solvable. Throughout this chapter, the observer may play two different roles. On the one hand, it may be used to reconstruct a delayed version of the unmeasured state $\rho(t)$ from measurements of the available delayed output $y(t-\tau)$, where τ denotes a constant time-delay which is assumed to be known. In other words, the observer is used to estimate $\rho(t-\tau)$ from $y(t-\tau)$. In this case, we refer to it as a *retarded immersion and invariance observer*. On the other hand, the observer may be used to reconstruct both the delay-free unmeasured state $\rho(t)$ and the delay-free output $y(t)$ from measurements of $y(t-\tau)$. In this case, we refer to it as an *immersion and invariance predictor*.

The remainder of the chapter is organized as follows. In Section 6.2, we formulate the I&I observer design problem in the presence of time-delays and propose a general tool for constructing asymptotically convergent *retarded* I&I *observers*. This is illustrated with an example using the *Lorenz system*. Next, in Section 6.3, we give a general tool for constructing I&I *predictors*. Its performance is illustrated with numerical simulations using the forced *Duffing system*. Finally, conclusions are stated in Section 6.4.

6.2 Retarded Immersion and Invariance Observer

Consider a nonlinear time-varying system of the form

$$\begin{cases} \dot{\rho} = f_1(\rho, y, t), \\ \dot{y} = f_2(\rho, y, t), \end{cases} \tag{6.1}$$

with unknown part of the state $\rho \in \mathbb{R}^n$, output $y \in \mathbb{R}^m$, stacked state $x := (\rho^T, y^T)^T \in \mathbb{R}^{n+m}$, and sufficiently smooth functions $f_1 : \mathbb{R}^n \times \mathbb{R}^m \times \mathbb{R} \to \mathbb{R}^n$ and $f_2 : \mathbb{R}^n \times \mathbb{R}^m \times \mathbb{R} \to \mathbb{R}^m$. It is assumed that the system (6.1) is *forward complete*, i.e., trajectories starting at time t_0 are defined for all $t \geq t_0$. A k-dimensional manifold in $\mathbb{R}^{n+m}$ $(1 \leq k \leq n+m)$ has a rigorous mathematical definition. We refer the interested reader to, for instance, [46, 127] for precise definitions.

6.2.1 I&I Observer Design

Consider the system

$$\begin{cases} \dot{\eta} = l(\eta, y_\tau, t-\tau), \\ \eta(\theta) = \varphi(\theta), \quad \theta \in [-\tau, 0], \end{cases} \tag{6.2}$$

with state $\eta \in \mathcal{C}([-\tau,0],\mathbb{R}^r)$, $\mathcal{C}([-\tau,0],\mathbb{R}^r)$ being the *Banach space* of continuous functions mapping the interval $[-\tau,0]$ into $\mathbb{R}^r$, $r \geq n$, delayed output $y_\tau(t) := y(t-\tau) \in \mathcal{C}([-\tau,0],\mathbb{R}^m)$ of system (6.1), sufficiently smooth function $l : \mathbb{R}^r \times \mathbb{R}^m \times \mathbb{R} \to \mathbb{R}^r$, and continuous function $\varphi : [-\tau,0] \to \mathbb{R}^r$ specifying the initial data of the system.

Definition 6.1. *System* (6.2) *is called a retarded* I&I *observer for system* (6.1) *if there exist mappings* $\beta : \mathbb{R}^r \times \mathbb{R}^m \times \mathbb{R} \to \mathbb{R}^r$, $(\eta, y_\tau, t) \mapsto \beta(\eta, y_\tau, t)$ *and* $\phi : \mathbb{R}^n \times \mathbb{R}^m \times \mathbb{R} \to \mathbb{R}^r$, $(\rho_\tau, y_\tau, t) \mapsto \phi(\rho_\tau, y_\tau, t)$, $\rho_\tau := \rho(t-\tau)$ *that are left invertible (with respect to their first arguments)*[1] *such that the manifold*

$$\mathcal{M} := \{(\rho, y, \eta, t) \in \mathbb{R}^n \times \mathbb{R}^m \times \mathbb{R}^r \times \mathbb{R} : \beta(\eta, y_\tau, t) = \phi(\rho_\tau, y_\tau, t)\}, \tag{6.3}$$

has the following properties:

(P6.1) *All trajectories of the extended system* (6.1),(6.2) *that start on* $\mathcal{M}$ *remain there for future time, i.e.,* $\mathcal{M}$ *is positively invariant.*

(P6.2) *All trajectories of the extended system* (6.1),(6.2) *that start in a neighborhood of* $\mathcal{M}$ *asymptotically converge to* $\mathcal{M}$.

[1] A mapping $\psi(x,y,t) : \mathbb{R}^l \times \mathbb{R}^m \times \mathbb{R} \to \mathbb{R}^r$ is left invertible (with respect to x) if there exists a mapping $\psi^L : \mathbb{R}^r \times \mathbb{R}^m \times \mathbb{R} \to \mathbb{R}^l$ such that $\psi^L(\psi(x,y,t),y,t) = x$ for all x, y, and t.

The above definition implies that an asymptotically converging estimate of the retarded unknown state ρ_τ is given by

$$\hat{\rho}_\tau = \phi^L(\beta(\eta, y_\tau, t), y_\tau, t),$$

where $\phi^L(\cdot)$ denotes a left inverse of $\phi(\cdot)$. Note that the estimation error $\epsilon := \hat{\rho}_\tau - \rho_\tau$ is zero on the manifold $\mathcal{M}$. Moreover, if (P6.2) holds for any initial state, then (6.2) is a *global retarded* I&I *observer* for the system (6.1). Following the procedure presented in [17], we derive a general tool for constructing nonlinear retarded observers of the form given in Definition 6.1.

Remark 6.2. *Note that left invertibility of $\beta(\cdot)$ and $\phi(\cdot)$ in (6.3) does not necessarily imply that $\mathcal{M}$ is a manifold. However, in this manuscript, it is assumed that $\mathcal{M}$ in (6.3) is a manifold in the sense of* [127].

Proposition 6.3. *Consider the extended system* (6.1),(6.2) *and suppose that there exist $\mathcal{C}^1$-mappings $\beta : \mathbb{R}^r \times \mathbb{R}^m \times \mathbb{R} \to \mathbb{R}^r$ and $\phi : \mathbb{R}^n \times \mathbb{R}^m \times \mathbb{R} \to \mathbb{R}^r$ with left inverse $\phi^L : \mathbb{R}^r \times \mathbb{R}^m \times \mathbb{R} \to \mathbb{R}^n$ such that the following holds.*

(H6.1) *For all y_τ, η, and t, $\beta(\eta, y_\tau, t)$ is left invertible with respect to η and*

$$\det\left(\frac{\partial \beta}{\partial \eta}\right) \neq 0. \tag{6.4}$$

(H6.2) *The system*

$$\begin{aligned}\dot{\epsilon} = {} & \frac{\partial \beta}{\partial y_\tau}\big(f_2(\rho_\tau, y_\tau, t-\tau) - f_2(\hat{\rho}_\tau, y_\tau, t-\tau)\big) - \frac{\partial \phi}{\partial t} + \left.\frac{\partial \phi}{\partial t}\right|_{\rho_\tau = \hat{\rho}_\tau} \\ & + \left.\frac{\partial \phi}{\partial \rho_\tau}\right|_{\rho_\tau = \hat{\rho}_\tau} f_1(\hat{\rho}_\tau, y_\tau, t-\tau) - \frac{\partial \phi}{\partial \rho_\tau} f_1(\rho_\tau, y_\tau, t-\tau) \\ & + \left.\frac{\partial \phi}{\partial y_\tau}\right|_{\rho_\tau = \hat{\rho}_\tau} f_2(\hat{\rho}_\tau, y_\tau, t-\tau) - \frac{\partial \phi}{\partial y_\tau} f_2(\rho_\tau, y_\tau, t-\tau)\end{aligned} \tag{6.5}$$

with $\hat{\rho}_\tau = \phi^L(\phi(\rho_\tau, y_\tau, t) + \epsilon)$, has a (global) asymptotically stable equilibrium at $\epsilon = 0$, uniformly in ρ_τ, y_τ, and t. Then, the system (6.2) *with*

$$\begin{aligned}l(\eta, y_\tau, t-\tau) = -\left(\frac{\partial \beta}{\partial \eta}\right)^{-1} \Bigg(& \frac{\partial \beta}{\partial y_\tau} f_2(\hat{\rho}_\tau, y_\tau, t-\tau) \\ & + \frac{\partial \beta}{\partial t} - \left.\frac{\partial \phi}{\partial \rho_\tau}\right|_{\rho_\tau = \hat{\rho}_\tau} f_1(\hat{\rho}_\tau, y_\tau, t-\tau) \\ & - \left.\frac{\partial \phi}{\partial y_\tau}\right|_{\rho_\tau = \hat{\rho}_\tau} f_2(\hat{\rho}_\tau, y_\tau, t-\tau) - \left.\frac{\partial \phi}{\partial t}\right|_{\rho_\tau = \hat{\rho}_\tau} \Bigg),\end{aligned} \tag{6.6}$$

and $\hat{\rho}_\tau = \phi^L(\beta(\eta, y_\tau, t), y_\tau, t)$, is a (global) retarded observer for the system (6.1).

Proof: Define the estimation error

$$\epsilon = \beta(\eta, y_\tau, t) - \phi(\rho_\tau, y_\tau, t), \tag{6.7}$$

where $\beta(\cdot)$ is a $\mathcal{C}^1$-function such that (H6.1) holds. Note that $|\epsilon|$ represents the distance of the system trajectories from the manifold $\mathcal{M}$ defined in (6.3). The dynamics of ϵ along the solutions of the systems is given by

$$\begin{aligned}\dot{\epsilon} = &\frac{\partial \beta}{\partial y_\tau} f_2(\rho_\tau, y_\tau, t-\tau) + \frac{\partial \beta}{\partial \eta} l(\eta, y_\tau, t-\tau) + \frac{\partial \beta}{\partial t} \\ &- \frac{\partial \phi}{\partial \rho_\tau} f_1(\rho_\tau, y_\tau, t-\tau) - \frac{\partial \phi}{\partial y_\tau} f_2(\rho_\tau, y_\tau, t-\tau) - \frac{\partial \phi}{\partial t}.\end{aligned} \tag{6.8}$$

By assumption (H6.1), the function $l(\cdot)$ in (6.6) is well defined. Then, substitution of (6.6) in (6.8) yields the dynamics (6.5). It follows from (H6.2) that the distance $|\epsilon|$ from the manifold $\mathcal{M}$ converges asymptotically to zero. Hence, by Definition 6.1 the system (6.2) with $l(\cdot)$ as in (6.6) is a *(global) retarded I&I observer* for system (6.1). ■

Proposition 6.3 provides an implicit description of the observer dynamics (6.2) in terms of the mappings $\beta(\cdot)$ and $\phi(\cdot)$ which must be selected to satisfy (H6.2). As a result, the problem of constructing a retarded observer for the system (6.1) is reduced to the problem of rendering the system (6.5) asymptotically stable by assigning the functions $\beta(\cdot)$ and $\phi(\cdot)$.

6.2.2 Example: Lorenz system

Consider the *Lorenz system*

$$\dot{y} = \sigma(\rho_1 - y), \tag{6.9}$$

$$\dot{\rho}_1 = ry - \rho_1 - y\rho_2, \tag{6.10}$$

$$\dot{\rho}_2 = -b\rho_2 + y\rho_1, \tag{6.11}$$

with output $y \in \mathbb{R}$, internal state $\rho = (\rho_1, \rho_2)^T \in \mathbb{R}^2$, and positive constants $\sigma, r, b \in \mathbb{R}_{>0}$. It is assumed that the output y is subject to constant time-delay, i.e., the available output is y_τ, where τ denotes a constant time-delay. Using Proposition 6.3, we derive a retarded reduced-order observer of the form given in Definition 6.1. Let $\phi(\rho_\tau, y_\tau, t) = \rho_\tau$ in (6.7), then

$$\epsilon = \beta(\eta, y_\tau) - \rho_\tau, \tag{6.12}$$

with $\epsilon = (\epsilon_1, \epsilon_2)^T \in \mathbb{R}^2$, $\eta = (\eta_1, \eta_2)^T \in \mathbb{R}^2$, and $\beta(\cdot) = (\beta_1(\cdot), \beta_2(\cdot))^T$. Associated with the system (6.9)-(6.11) and the estimation error (6.12), the estimation error dynamics (6.5) takes the following form

$$\begin{aligned}\dot{\epsilon} &= \frac{\partial \beta}{\partial y_\tau}\left(f_2(\rho_\tau, y_\tau, t-\tau) - f_2(\rho_\tau + \epsilon, y_\tau, t-\tau)\right) \qquad (6.13)\\ &- \frac{\partial \phi}{\partial \rho_\tau}\left(f_1(\rho_\tau, y_\tau, t-\tau) - f_1(\rho_\tau + \epsilon, y_\tau, t-\tau)\right)\\ &= \begin{pmatrix} \frac{\partial \beta_1}{\partial y_\tau} \\ \frac{\partial \beta_2}{\partial y_\tau}\end{pmatrix}(-\sigma\epsilon_1) - \begin{pmatrix} 1 & 0 \\ 0 & 1\end{pmatrix}\begin{pmatrix} \epsilon_1 + y_\tau \epsilon_2 \\ b\epsilon_2 - y_\tau\epsilon_1\end{pmatrix}\\ &= \begin{pmatrix} -\sigma\frac{\partial \beta_1}{\partial y_\tau}\epsilon_1 - \epsilon_1 - y_\tau\epsilon_2 \\ -\sigma\frac{\partial \beta_2}{\partial y_\tau}\epsilon_1 - b\epsilon_2 + y_\tau\epsilon_1\end{pmatrix}.\end{aligned}$$

Then, the problem of constructing a retarded observer for the system (6.9)-(6.11) is reduced to the problem of rendering the system (6.13) asymptotically stable by assigning the function $\beta(\cdot)$. Consider the positive definite function $V = \frac{1}{2}\epsilon^T\epsilon$, then

$$\begin{aligned}\dot{V} &= -\sigma\frac{\partial \beta_1}{\partial y_\tau}\epsilon_1^2 - \epsilon_1^2 - y_\tau\epsilon_2\epsilon_1 - \sigma\frac{\partial \beta_2}{\partial y_\tau}\epsilon_2\epsilon_1 - b\epsilon_2^2 + y_\tau\epsilon_2\epsilon_1\\ &= -\left(\sigma\frac{\partial \beta_1}{\partial y_\tau} + 1\right)\epsilon_1^2 - \sigma\frac{\partial \beta_2}{\partial y_\tau}\epsilon_2\epsilon_1 - b\epsilon_2^2, \qquad (6.14)\end{aligned}$$

by selecting $\beta_1 = \kappa y_\tau + \eta_1$, $\kappa > 0$, and $\beta_2 = \eta_2$ yields

$$\dot{V} = -\left(\sigma\kappa + 1\right)\epsilon_1^2 - b\epsilon_2^2 < 0, \qquad (6.15)$$

which is negative definite for any $\kappa > -\frac{1}{\sigma}$, and therefore the origin of the estimation error dynamics (6.13) with function $\beta(\cdot)$ as above is globally uniformly asymptotically stable. Then, the retarded observer (6.2) with $l(\cdot)$ as in (6.6) takes the following form

$$\begin{aligned}\dot{\eta} &= \begin{pmatrix} -\frac{\partial \beta_1}{\partial y_\tau} \\ -\frac{\partial \beta_2}{\partial y_\tau}\end{pmatrix}\Big(\sigma(\beta_1(\eta_1, y_\tau) - y_\tau)\Big) + \begin{pmatrix} r y_\tau - \beta_1(\eta_1, y_\tau) - y_\tau\beta_2(\eta_2, y_\tau) \\ -b\beta_2(\eta_2, y_\tau) + y_\tau\beta_1(\eta_1, y_\tau)\end{pmatrix}\\ &= \begin{pmatrix} -(\sigma\kappa + 1)\eta_1 - y_\tau\eta_2 + \left(\kappa\sigma - \kappa^2\sigma + r - \kappa\right)y_\tau \\ -b\eta_2 + y_\tau\eta_1 + \kappa y_\tau^2\end{pmatrix}. \qquad (6.16)\end{aligned}$$

Figure 6.1 depicts the simulation results for $\sigma = 10$, $r = 28$, $b = \frac{8}{3}$, time-delay $\tau = 0.25$ [s], and $\kappa = 0.25 > -\frac{1}{\sigma} = -0.1$. The top panel shows the state $\rho_1(t)$ and the estimated retarded state $\hat{\rho}_1(t-\tau)$ while $\rho_2(t)$ and $\hat{\rho}_2(t-\tau)$ are depicted in the bottom panel. In Figure 6.2, the norm of the estimation error $\epsilon = \rho_\tau - \hat{\rho}_\tau$ for different values of κ is shown.

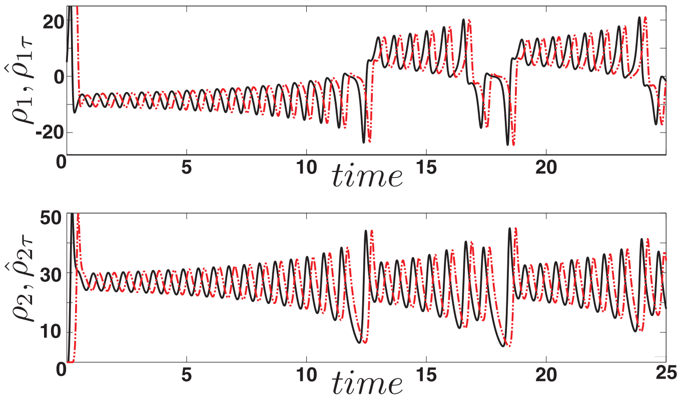

Figure 6.1 The continuous lines are the current internal states $\rho(t)$ and the dashed-dotted lines are the estimated retarded states $\hat{\rho}(t-\tau)$.

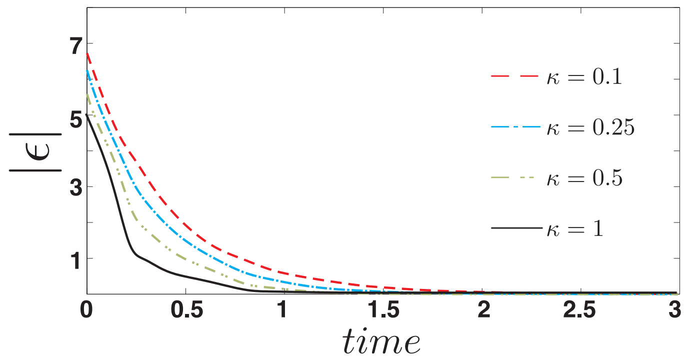

Figure 6.2 Norm of the estimation error for different values of the observer gain κ.

6.3 Immersion and Invariance Predictor

Consider the system (6.1) and the stacked state $x := (\rho^T, y^T)^T \in \mathbb{R}^{n+m}$. Then, system (6.1) can be rewritten in the following compact form

$$\dot{x} = f(x,t), \tag{6.17}$$

where

$$f(x,t) := \begin{pmatrix} f_1(\rho, y, t) \\ f_2(\rho, y, t) \end{pmatrix}. \tag{6.18}$$

Consider the system

$$\begin{cases} \dot{\eta} = l(\eta, y_\tau, t-\tau), \\ \eta(\theta) = \varphi(\theta), \quad \theta \in [-2\tau, 0], \end{cases} \tag{6.19}$$

with state $\eta \in \mathcal{C}([-\tau, 0], \mathbb{R}^r)$, $r \geq n+m$, sufficiently smooth function $l : \mathbb{R}^r \times \mathbb{R}^m \times \mathbb{R} \to \mathbb{R}^r$, and continuous function $\varphi : [-\tau, 0] \to \mathbb{R}^r$ specifying the initial data of the system.

Definition 6.4. *The system* (6.19) *is called an* I&I *predictor for system* (6.1) *if there exist mappings* $\beta : \mathbb{R}^r \times \mathbb{R}^m \times \mathbb{R} \to \mathbb{R}^r$, $(\eta, y_\tau, t) \mapsto \beta(\eta, y_\tau, t)$ *and* $\phi : \mathbb{R}^{n+m} \times \mathbb{R}^m \times \mathbb{R} \to \mathbb{R}^r$, $(x, y_\tau, t) \mapsto \phi(x, y_\tau, t)$ *that are left invertible (with respect to their first arguments) such that the manifold*

$$\mathcal{M} := \{(x, y, \eta, t) \in \mathbb{R}^{n+m} \times \mathbb{R}^m \times \mathbb{R}^r \times \mathbb{R} : \beta(\eta, y_\tau, t) = \phi(x, y_\tau, t)\}, \tag{6.20}$$

has the following properties:

(P6.3) *All trajectories of the extended system* (6.1),(6.19) *that start on* $\mathcal{M}$ *remain there for future time, i.e.,* $\mathcal{M}$ *is positively invariant.*

(P6.4) *All trajectories of the extended system* (6.1),(6.19) *that start in a neighborhood of* $\mathcal{M}$ *asymptotically converge to* $\mathcal{M}$.

The above definition implies that an asymptotically converging estimate of the state x is given by

$$\hat{x} = \phi^L(\beta(\eta, y_\tau, t), y_\tau, t),$$

where $\phi^L(\cdot)$ denotes a left inverse of $\phi(\cdot)$. Note that the prediction error $\epsilon = \hat{x} - x$ is zero on the manifold $\mathcal{M}$. Moreover, if property (P6.4) holds for any initial state, then (6.19) is a *global* I&I *predictor* for the system (6.1). Following the same procedure as in [17], we derive a general tool for constructing predictors of the form given in Definition 6.4.

Proposition 6.5. *Consider the system* (6.1),(6.19) *and suppose that there exist* $\mathcal{C}^1$ *mappings* $\beta : \mathbb{R}^r \times \mathbb{R}^m \times \mathbb{R} \to \mathbb{R}^r$ *and* $\phi : \mathbb{R}^{n+m} \times \mathbb{R}^m \times \mathbb{R} \to \mathbb{R}^r$ *with left inverse* $\phi^L : \mathbb{R}^r \times \mathbb{R}^m \times \mathbb{R} \to \mathbb{R}^{n+m}$ *such that the following holds.*

(H6.3) *For all* y_τ, η, *and* t, $\beta(\eta, y_\tau, t)$ *is left invertible with respect to* η *and*

$$\det\left(\frac{\partial \beta}{\partial \eta}\right) \neq 0. \tag{6.21}$$

(H6.4) *The system*

$$\begin{aligned}\dot{\epsilon} &= \frac{\partial \beta}{\partial y_\tau}\left(f_2(\rho_\tau, y_\tau, t-\tau) - f_2(\hat{\rho}_\tau, y_\tau, t-\tau)\right) \\ &+ \left.\frac{\partial \phi}{\partial x}\right|_{x=\hat{x}} f(\hat{x}, t) - \frac{\partial \phi}{\partial x} f(x,t) - \frac{\partial \phi}{\partial t} + \left.\frac{\partial \phi}{\partial t}\right|_{x=\hat{x}} \\ &+ \left.\frac{\partial \phi}{\partial y_\tau}\right|_{x=\hat{x}} f_2(\hat{\rho}_\tau, y_\tau, t-\tau) - \frac{\partial \phi}{\partial y_\tau} f_2(\rho_\tau, y_\tau, t-\tau),\end{aligned} \tag{6.22}$$

with $\hat{x} = \phi^L(\phi(x, y_\tau, t) + \epsilon)$*, has a (globally) asymptotically stable equilibrium at* $\epsilon = 0$*, uniformly in* x*,* x_τ*, and* t*. Then, the system* (6.19) *with*

$$\begin{aligned}l(\eta, y_\tau, t-\tau) = -\left(\frac{\partial \beta}{\partial \eta}\right)^{-1} &\left(\frac{\partial \beta}{\partial y_\tau} f_2(\hat{\rho}_\tau, y_\tau, t-\tau)\right. \\ &+ \frac{\partial \beta}{\partial t} - \left.\frac{\partial \phi}{\partial x}\right|_{x=\hat{x}} f(\hat{x}, t) \\ &\left. - \left.\frac{\partial \phi}{\partial y_\tau}\right|_{x=\hat{x}} f_2(\hat{\rho}_\tau, y_\tau, t-\tau) - \left.\frac{\partial \phi}{\partial t}\right|_{x=\hat{x}}\right),\end{aligned} \tag{6.23}$$

and $\hat{x} = \phi^L(\beta(\eta, y_\tau, t), y_\tau, t)$*, is a (global)* I&I *predictor for the system* (6.1).

Proof: Define the (off-the-manifold) error

$$\epsilon := \beta(\eta, y_\tau, t) - \phi(x, y_\tau, t), \tag{6.24}$$

where $\beta(\cdot)$ is a $\mathcal{C}^1$-function such that (H6.3) holds. Then, the error dynamics is given by

$$\begin{aligned}\dot{\epsilon} &= \frac{\partial \beta}{\partial \eta} l(\eta, y_\tau, t-\tau) + \frac{\partial \beta}{\partial y_\tau} f_2(\rho_\tau, y_\tau, t-\tau) + \frac{\partial \beta}{\partial t} \\ &- \frac{\partial \phi}{\partial x} f(x,t) - \frac{\partial \phi}{\partial y_\tau} f_2(\rho_\tau, y_\tau, t-\tau) - \frac{\partial \phi}{\partial t}.\end{aligned} \tag{6.25}$$

By assumption (H6.3), the function $l(\cdot)$ in (6.23) is well defined. Then, substitution of (6.23) in (6.25) yields the dynamics (6.22). It follows from (H6.4) that the distance $|\epsilon|$ from the manifold $\mathcal{M}$ converges asymptotically to zero. Hence, by Definition 6.4 the system (6.19) with $l(\cdot)$ as in (6.23) is a (global) I&I predictor for system (6.1). ■

6.3.1 Example: Duffing system

Consider the *forced-Duffing system*

$$\begin{aligned} \dot{\rho} &= -a\rho - by - cy^3 + q\cos(\omega t), && (6.26)\\ \dot{y} &= \rho, && (6.27) \end{aligned}$$

with output $y \in \mathbb{R}$, internal state $\rho \in \mathbb{R}$, stacked state $x = (\rho, y)^T \in \mathbb{R}^2$ and positive constants $a, b, c, q, \omega \in \mathbb{R}_{>0}$. It is assumed that the measurements of y are subject to constant time-delay, i.e., the measurable output is y_τ. Using Proposition 6.5, we derive a predictor of the form given in Definition 6.4 such that we reconstruct x from measurements of y_τ. Let $\phi(x, y_\tau, t) = x$ in (6.24), then $\epsilon = \beta(\eta, y_\tau) - x$, with $\epsilon = (\epsilon_1, \epsilon_2)^T \in \mathbb{R}^2$, $\eta = (\eta_1, \eta_2)^T \in \mathbb{R}^2$, and $\beta(\cdot) = (\beta_1(\cdot), \beta_2(\cdot))^T$. Thus, the estimation error dynamics (6.22) takes the following form

$$\begin{aligned} \dot{\epsilon} &= -\begin{pmatrix} \frac{\partial\beta_1}{\delta y_\tau} \\ \frac{\partial\beta_2}{\delta y_\tau} \end{pmatrix}\epsilon_{1\tau} + \begin{pmatrix} -a\epsilon_1 - b\epsilon_2 + cy^3 - c(y+\epsilon_2)^3 \\ \epsilon_1 \end{pmatrix} \\ &= \begin{pmatrix} -\frac{\partial\beta_1}{\delta y_\tau}\epsilon_{1\tau} - a\epsilon_1 - b\epsilon_2 - 3c\left(\frac{\epsilon_2}{2} + y\right)^2\epsilon_2 - \frac{c}{4}\epsilon_2^3 \\ -\frac{\partial\beta_2}{\delta y_\tau}\epsilon_{1\tau} + \epsilon_1 \end{pmatrix}. \qquad (6.28) \end{aligned}$$

$$(6.29)$$

Again, it follows that the problem of constructing a predictor for the system (6.26), (6.27) is reduced to the problem of rendering the origin of the system (6.29) uniformly asymptotically stable by assigning the function $\beta(\cdot)$. This stabilization problem is difficult to solve because the error dynamics (6.29) is a time-varying retarded nonlinear system. In order to simplify the problem, the function $\beta(\cdot)$ is selected as

$$\beta(\eta, y_\tau) = \begin{pmatrix} \eta_1 + \kappa y_\tau \\ \eta_2 \end{pmatrix}, \qquad (6.30)$$

with $\kappa \in \mathbb{R}_{>0}$. It follows that

$$\dot{\epsilon} = \begin{pmatrix} -\kappa\epsilon_{1\tau} - a\epsilon_1 - b\epsilon_2 - 3c\left(\frac{\epsilon_2}{2} + y\right)^2\epsilon_2 - \frac{c}{4}\epsilon_2^3 \\ \epsilon_1 \end{pmatrix}. \qquad (6.31)$$

Linearizing (6.31) around the origin yields

$$\begin{aligned} \dot{\tilde{\epsilon}}_1 &= -\kappa\tilde{\epsilon}_{1\tau} - a\tilde{\epsilon}_1 - b\tilde{\epsilon}_2 - 3cy^2\tilde{\epsilon}_2, && (6.32)\\ \dot{\tilde{\epsilon}}_2 &= \tilde{\epsilon}_1. && (6.33) \end{aligned}$$

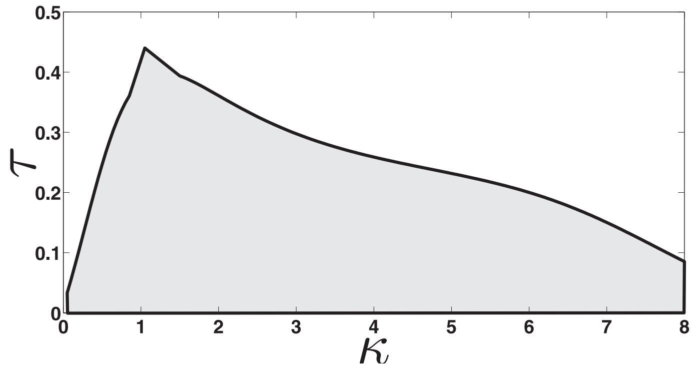

Figure 6.3 Stability region $\mathcal{S}$ in the parameter space.

Proposition 6.6. *There exist positive constants* $\bar{\kappa}$ *and* $\bar{\chi}$ *such that if* $\kappa > \bar{\kappa}$ *and* $\kappa\tau < \bar{\chi}$*, then the origin* $\tilde{\epsilon}_1 = \tilde{\epsilon}_2 = 0$ *of the linearized system* (6.32),(6.33) *is globally asymptotically stable.*

The proof of Proposition 6.6 can be found in the Appendix A. The result of Proposition 6.6 amounts to the following. If the gain κ is sufficiently large and the time-delay τ is sufficiently small, then the origin of the prediction error dynamics (6.31) is locally asymptotically stable. In other words, there exists a region $\mathcal{S} = \{\kappa, \tau \in \mathbb{R}_{\geq 0} | \kappa > \bar{\kappa} \text{ and } \kappa\tau < \bar{\chi}\}$, such that if $(\kappa, \tau) \in \mathcal{S}$, then (6.31) converges to the origin asymptotically. Taking $\beta(\cdot)$ as in (6.30) and $l(\cdot)$ as in (6.23), the predictor dynamics (6.19) takes the following form

$$\begin{aligned} \dot{\eta} &= \frac{\partial \phi}{\partial x} f(\beta(\eta, y_\tau), t) - \frac{\partial \beta}{\partial y_\tau} f_2(\beta_1(\eta_\tau, y_{(2\tau)}), y_\tau, t - \tau) \\ &= \begin{pmatrix} -\kappa(\eta_{1\tau} + \kappa y_{(2\tau)}) - a(\eta_1 + \kappa y_\tau) - b\eta_2 - c\eta_2^3 + q\cos\omega t \\ \eta_1 + \kappa y_\tau \end{pmatrix}. \end{aligned} \tag{6.34}$$

with $y_{(2\tau)} := y(t - 2\tau)$. Figure 6.3 depicts the region $\mathcal{S}$ obtained by extensive computer simulations with $a = 0.3$, $b = 1$, $c = 1$, $q = 20$, $\omega = 1.2$ and initial history $\eta_1(\theta) = \eta_2(\theta) = 0$, $\rho(\theta) = y(\theta) = 3$, $\theta \in [-2\tau, 0]$, (for these parameters the Duffing system possesses chaotic solutions). It follows that if $(\kappa, \tau) \in \mathcal{S}$, the gray region in Figure 6.3, the system (6.34) locally asymptotically predicts the value of $x(t)$ from measurements of $y(t - \tau)$. In other words, the system (6.34) is a *local* I&I *predictor* for the system (6.26),(6.27). Figure 6.4 depicts the states $x(t)$ and the predicted states $\hat{x}(\eta(t), y(t - \tau))$ for $\tau = 0.4$ and $\kappa = 1.2$.

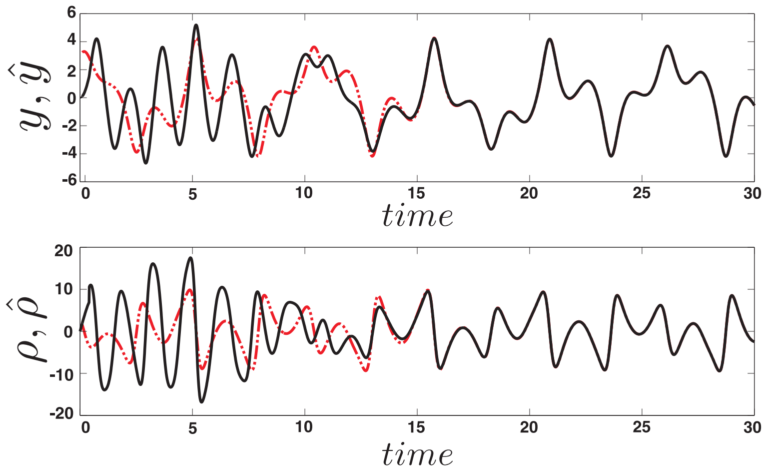

Figure 6.4 The dashed-dotted lines are the current states (ρ, y) and the continuous lines are the predicted states $(\hat{\rho}(\eta, y_\tau), \hat{y}(\eta, y_\tau))$.

6.4 Conclusions

We have derived an extension to the work presented in [56] for constructing nonlinear observers in the case the output measurements are corrupted with time-delays. Following the framework proposed in [56], a general methodology has been developed which relies on rendering attractive an appropriately selected invariant manifold in the extended state space (the union of the state spaces of the system and the observer). Proposition 6.3 and Proposition 6.5 provide an implicit description of the observer dynamics in terms of the mappings, $\beta(\cdot)$ and $\phi(\cdot)$, which must be selected to render the origin of the estimation error dynamics asymptotically stable. This stabilization problem can be difficult to solve, since in general, it relies on the solution of a set of PDEs. However, as shown in the examples, in many cases of practical interest these equations turn out to be solvable. In [57] and [18], for the delay-free case, the authors present methodologies for selecting the functions $\beta(\cdot)$ and $\phi(\cdot)$ for some classes of systems. These methods may be extended to the time-delayed case. However, we remark that the aim of this manuscript is not to extend the methods presented in [57] or [18], but to show how the general I&I ideas introduced in [56] for designing observers may be extended when the output measurements are corrupted with time-delays.

Chapter 7

Synchronization via Predictor-Based Diffusive Dynamic Couplings

Abstract. We study the problem of controlled network synchronization of coupled *semipassive systems* in the case when the outputs (the coupling variables) and the inputs are subject to constant time-delays (as it is often the case in a networked context). *Predictor-based dynamic output feedback controllers* are proposed to interconnect the systems on a given network. Using Lyapunov-Krasovskii functionals and the notion of semipassivity, we prove that under some mild assumptions, the solutions of the interconnected systems are globally ultimately bounded. Sufficient conditions on the systems to be interconnected, the network topology, the coupling dynamics, and the time-delays that guarantee global state synchronization are derived. A local analysis is provided, in which we compare the performance of our predictor-based control scheme against the existing *diffusive static couplings* available in the literature. We show (locally) that the time-delay that can be induced to the network may be increased by including the predictors in the loop. The results are illustrated by computer simulations of coupled Hindmarsh-Rose neurons.

7.1 Introduction

This chapter focuses on controlled synchronization of identical nonlinear systems interacting on networks with general topologies and interconnected through *predictor-based diffusive dynamic couplings*. An important element of our control

This chapter is based on [79].

scheme is the use of a communication network. Network communication is necessary in the study of synchronization to transmit and receive measurement and control data among the systems. Because of the time needed to transmit data over the network, the use of networked communication results in unavoidable time-delays. This networked-induced delays are undesirable because they may lead to the loss of synchrony. Hence, when studying synchronization among dynamical systems with networked communication, it is important to design control algorithms which are robust with respect to time-delays. The results presented here follow the same research line as [104, 132], where sufficient conditions for synchronization of diffusively interconnected nonlinear systems with and without time-delays are derived. In order to derive their results, the authors assume that the individual systems are *semipassive* [107] with respect to the coupling variable y_i, and their corresponding internal dynamics have some desired stability properties (*convergent* internal dynamics [94]). In particular, in [132], the authors study the problem of network synchronization of *diffusively time-delayed coupled* semipassive systems. They prove that under some mild assumptions, there always exists a region $\mathcal{S}$ in the parameter space (coupling strength γ versus time-delay τ), such that if $(\gamma, \tau) \in \mathcal{S}$, the systems synchronize. Nevertheless, it is important to note that for this class of systems, once the network topology is specified, the region $\mathcal{S}$ is fixed. In other words, the time-delay that may be induced to the network without compromising the synchronous behavior is limited by the network topology[82]. Here, we show that by including predictors in the couplings, we may increase the time-delay that can be induced to the network without compromising the synchronous behavior. We propose *predictor-based diffusive dynamic couplings* based on the concept of *anticipating synchronization* [89] that on the one hand estimate future values $y_i(t+\tau)$ of the outputs $y_i(t)$, and on the other hand interconnect the systems through these time-ahead estimated signals. By including the predictors in the loop, a new parameter κ comes into play. This κ plays the role of the *predictor gain*, i.e., it is a parameter of the predictors that can be tuned to make the *prediction error dynamics* converge to the origin. We derive sufficient conditions for global state synchronization of the interconnected systems. In particular, it is proved that under some assumptions, there always exists a region in the *extended parameter space* (coupling strength γ, time-delay τ, and *predictor gain* κ), such that if γ, τ, and the new parameter κ belong to this region, the systems synchronize. In [78], we have started studying these ideas for a class of passive LTI systems. Note that for LTI systems the *separation principle* holds, i.e., the predictor dynamics and the coupling structure can be designed independently. However, the analysis becomes more involved for nonlinear systems, since in general, the separation principle does not hold; in this case, there is a strong nonlinear relation between the predictor dynamics and the coupling structure. Finally, we provide a *local analysis*, in which the performance of our predictor-based control scheme is compared against the existing *diffusive static couplings* available in the literature. It is shown (locally) that the amount of time-delay that can be induced to the network may be increased by including the predictors in the loop.

The remainder of the chapter is organized as follows. The system description and the problem statement are introduced in Section 7.2. The predictor structure is given in Section 7.3 before introducing the proposed *predictor-based diffusive dynamic coupling* in Section 7.4. In Sections 7.5 and 7.6, we present the main results on global boundedness and network synchronization. Moreover, a local analysis, in which we explain the "mechanism of action" behind our predictor-based couplings is also presented. In Section 7.7, simulation results of coupled Hindmarsh-Rose neurons are presented. Finally, conclusions are stated in Section 7.8.

7.2 System Description

Consider k identical nonlinear systems of the form

$$\dot{\zeta}_i = q(\zeta_i, y_i), \tag{7.1}$$

$$\dot{y}_i = a(\zeta_i, y_i) + Bu_i, \tag{7.2}$$

with $i \in \mathcal{I} := \{1, ..., k\}$, state $x_i := \mathrm{col}(\zeta_i, y_i) \in \mathbb{R}^n$, internal state $\zeta_i \in \mathbb{R}^{n-m}$, output $y_i \in \mathbb{R}^m$, input $u_i \in \mathbb{R}^m$, sufficiently smooth functions $q : \mathbb{R}^{n-m} \times \mathbb{R}^m \to \mathbb{R}^{n-m}$, $a : \mathbb{R}^{n-m} \times \mathbb{R}^m \to \mathbb{R}^m$, and matrix $B \in \mathbb{R}^{m\times m}$ being similar to a positive definite matrix. For the sake of simplicity it is assumed that $B = I_m$ (results for the general case with B being similar to a positive definite matrix can be easily derived). The systems (7.1),(7.2) are assumed to be *strictly $\mathcal{C}^1$-semipassive* and the internal dynamics (7.1) are supposed to be *convergent*. In [132], the authors derive sufficient conditions for network synchronization of *diffusively time-delayed coupled* semipassive systems, i.e., the systems (7.1),(7.2) interconnected through weighted differences of the form

$$u_i(t) = \gamma \sum_{j\in\mathcal{E}_i} a_{ij} \left(y_j(t-\tau) - y_i(t-\tau) \right), \tag{7.3}$$

where $\tau \in \mathbb{R}_{>0}$ denotes the time-delay, $y_j(t-\tau)$ and $y_i(t-\tau)$ are the time-delayed outputs of the jth and ith systems, $\gamma \in \mathbb{R}_{>0}$ denotes the coupling strength, $a_{ij} \geq 0$ are the weights of the interconnections, and $\mathcal{E}_i$ is the set of neighbors of system i. Moreover, since the coupling strength is encompassed in the constant γ, then it is assumed without loss of generality that $\max_{i\in\mathcal{I}} \sum_{j\in\mathcal{E}_i} a_{ij} = 1$. The authors in [132] prove that the systems (7.1)-(7.3) asymptotically synchronize provided that γ is sufficiently large and the product of the coupling strength and the time-delay

$\gamma\tau$ is sufficiently small. Then, there exists a region $\mathcal{S}$ in the parameter space, such that if $(\gamma, \tau) \in \mathcal{S}$, the systems synchronize. Nevertheless, it is important to notice that in the closed loop system (7.1)-(7.3), once the interconnections a_{ij} are specified, the region $\mathcal{S}$ is fixed. Hence, the amount of time-delay that may be induced to the network is limited by the network topology [82]. In this manuscript, we propose *predictor-based diffusive dynamic couplings* in order to enhance robustness against time-delays in the network, i.e., by including some dynamics in the coupling, we may expand the synchronization region $\mathcal{S}$. The time-delay τ that is being induced in coupling (7.3) could be realized as the sum of measurement and transmission time-delays. In this chapter, it is necessary to make a clear distinction among these delays. The measurement time-delay $\tau_1 \in \mathbb{R}_{>0}$ affects the outputs of the systems $y_i(t)$, resulting in time-delayed outputs $y_i(t - \tau_1)$ being available for control purposes. The transmission time-delays are encompassed in $\tau_2 \in \mathbb{R}_{>0}$. It affects the control inputs $u_i(t)$, resulting in the time-delayed control signals $u_i(t - \tau_2)$ being applied to the systems, see Figure 7.1. Notice that the total time-delay τ in (7.3) is simply given by the sum of the individual delays, i.e., $\tau := \tau_1 + \tau_2$. Therefore, the interconnected systems (7.1)-(7.3) could be realized as individual systems with input time-delay τ_2 as follows

$$\dot{\zeta}_i = q(\zeta_i, y_i), \tag{7.4}$$
$$\dot{y}_i = a(\zeta_i, y_i) + u_i(t - \tau_2), \tag{7.5}$$
$$x_i = \phi(t),\ t \in [-\tau_2, 0], \tag{7.6}$$

with time-delayed input $u_i^{\tau_2} \in \mathbb{R}^m$ and continuous function $\phi : [-\tau_2, 0] \to \mathbb{R}^n$ specifying the initial history, in closed-loop with the following diffusive time-delayed coupling

$$u_i(t) = \gamma \sum_{j\in\mathcal{E}_i} a_{ij} \left(y_j(t - \tau_1) - y_i(t - \tau_1)\right). \tag{7.7}$$

However, if the future value $y_i(t+\tau_2)$ of $y_i(t)$ could be obtained, then by applying the controller

$$u_i(t) = \gamma \sum_{j\in\mathcal{E}_i} a_{ij} \left(y_j(t + \tau_2) - y_i(t + \tau_2)\right), \tag{7.8}$$

the interconnected systems (7.4)-(7.6),(7.8) would be given by

$$\dot{\zeta}_i = q(\zeta_i, y_i), \tag{7.9}$$
$$\dot{y}_i = a(\zeta_i, y_i) + \gamma \sum_{j\in\mathcal{E}_i} a_{ij} \left(y_j(t) - y_i(t)\right), \tag{7.10}$$

which is the delayed-free closed-loop system. From this point of view, we propose a control scheme, in which a predictor is used to estimate the future values $y_i(t+\tau_2)$ from measurements of the available time-delayed output $y_i(t-\tau_1)$. Then, the output of the predictor is used to interconnect the systems, see Figure 7.3.

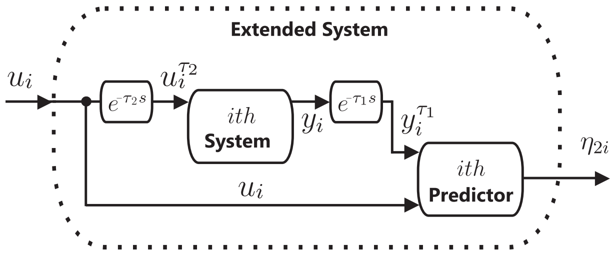

Figure 7.1 Configuration of the prediction scheme.

7.3 Synchronization-based Predictor

In this section, we introduce the state predictor based on synchronization that is used to estimate $y_i(t+\tau_2)$ from measurements of $y_i(t-\tau_1)$. In the first contribution concerning synchronization-based predictors [143], the author studies the following coupled Ikeda equations

$$\begin{aligned} \dot{\rho} &= -\alpha\rho - \beta\sin(\rho^\tau), &(7.11)\\ \dot{z} &= -\alpha z - \beta\sin(\rho), &(7.12) \end{aligned}$$

with states $\rho, z \in \mathbb{R}$, $\rho^\tau(t) = \rho(t-\tau)$, and constants $\alpha, \beta, \tau \in \mathbb{R}_{>0}$. Notice that the dynamics of the prediction error $e(t) := z(t-\tau) - \rho(t)$ is simply given by $\dot{e}(t) = -\alpha e(t)$; therefore, a necessary and sufficient condition for $e(t)$ to converge to the origin is that $\alpha > 0$. Thus, the solution of (7.12) asymptotically synchronizes with the future solution of (7.11) at time instant $t+\tau$; hence, (7.12) anticipates the dynamics of (7.11). This idea has been generalized into general multidimensional systems, in for instance, [88, 89]. Following these ideas, we propose a predictor based on synchronization for the class of systems under study. Consider k identical systems of the form

$$\dot{\eta}_{1i} = q(\eta_{1i}, \eta_{2i}), \tag{7.13}$$
$$\dot{\eta}_{2i} = a(\eta_{1i}, \eta_{2i}) + u_i + \kappa\left(y_i(t-\tau_1) - \eta_{2i}(t-\tau)\right), \tag{7.14}$$
$$\eta_i = \eta_{0i} \in R^n, \quad t \in [-\tau, 0], \tag{7.15}$$

with measurement time-delay $\tau_1 \in \mathbb{R}_{\geq 0}$, total time-delay $\tau = \tau_1 + \tau_2 \in \mathbb{R}_{\geq 0}$, transmission time-delay $\tau_2 \in \mathbb{R}_{\geq 0}$, $i \in \mathcal{I} = \{1, ..., k\}$, state $\eta_i := \operatorname{col}(\eta_{1i}, \eta_{2i}) \in \mathbb{R}^n$, internal state $\eta_{1i} \in \mathbb{R}^{n-m}$, actuated state $\eta_{2i} \in \mathbb{R}^m$, input $u_i \in \mathbb{R}^m$, smooth vectorfields $q(\cdot)$ and $a(\cdot)$ as in (7.1),(7.2), initial history η_{0i}, and gain $\kappa \in \mathbb{R}_{>0}$. The system (7.13)-(7.15) is called a predictor for system (7.4)-(7.6) if and only if

$$\lim_{t\to\infty} \big(x_i(t-\tau_1) - \eta_i(t-\tau)\big) \equiv \lim_{t\to\infty} \big(x_i(t+\tau_2) - \eta_i(t)\big) = \mathbf{0}.$$

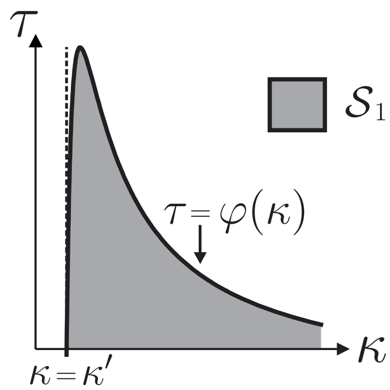

Figure 7.2 Prediction region $\mathcal{S}_1$.

Notice that if $\kappa = 0$ and $u_i(t) = \mathbf{0}$, the predictor dynamics (7.13),(7.14) is the same as the individual subsystems dynamics (7.4),(7.5) with $u^{\tau_2} = \mathbf{0}$. We construct the predictor in this way in order to take advantage of the stability properties of (7.4),(7.5), namely, *semipassivity* and *convergence*. Moreover, each system (7.4)-(7.6) together with the predictor (7.13)-(7.15) could be interpreted as an extended new system with input u_i, new output η_{2i}, and internal delays τ_1 and τ_2, see Figure 7.1. Define the prediction error $\epsilon_i = \mathrm{col}(\epsilon_{1i}, \epsilon_{2i}) := x_i - \eta_i^{\tau_2}$. Then, the prediction error dynamics is given by

$$\dot{\epsilon}_{1i} = q(\zeta_i, y_i) - q(\zeta_i - \epsilon_{1i}, y_i - \epsilon_{2i}) \tag{7.16}$$

$$\dot{\epsilon}_{2i} = a(\zeta_i, y_i) - a(\zeta_i - \epsilon_{1i}, y_i - \epsilon_{2i}) - \kappa\epsilon_{2i}^{\tau}. \tag{7.17}$$

It follows that the system (7.13)-(7.15) is a predictor for system (7.4)-(7.6) if the zero solution of (7.16),(7.17) is asymptotically stable. In the following lemma, we give sufficient conditions for asymptotic stability of the origin of (7.16),(7.17). In particular, we prove that under some mild assumptions, there always exists a region $\mathcal{S}_1$ in the parameter space (predictor gain κ and total time-delay τ), such that if $(\kappa, \tau) \in \mathcal{S}_1$, then the system (7.13)-(7.15) anticipates the dynamics (7.4)-(7.6). Moreover, it is also proved that the region $\mathcal{S}_1$ is bounded by a *unimodal function* $\varphi(\kappa)$ defined on some set $\mathcal{J} \subset \mathbb{R}$.

Definition 7.1. *The function $\varphi : \mathcal{J} \to \mathbb{R}_{\geq 0}$, $\kappa \mapsto \varphi(\kappa)$ is called unimodal if for some value $\kappa^* \in \mathcal{J}$, it is monotonically increasing for $\kappa \leq \kappa^*$ and monotonically decreasing for $\kappa \geq \kappa^*$. Hence, the maximum value of $\varphi(\kappa)$ is given by $\varphi(\kappa^*)$ and there are no other maxima.*

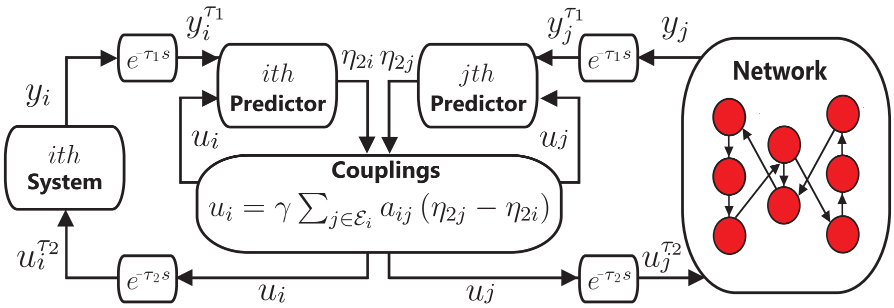

Figure 7.3 Configuration of the proposed control scheme.

Lemma 7.2. *Consider the k nonlinear systems* (7.4)-(7.6), (7.13)-(7.15) *and suppose that for every input signal u_i, any finite time-delay τ, and predictor gain κ, the solutions of the systems are ultimately bounded (in Section 7.5, Lemma 7.4, we give sufficient conditions for ultimate boundedness of the closed-loop system for the class of inputs under study). In addition assume that:*

(H7.1) *The internal dynamics* (7.4) *is an exponentially convergent system, i.e., there is a positive definite matrix $P = P^T \in \mathbb{R}^{(n-m)\times(n-m)}$ such that the eigenvalues of the symmetric matrix*

$$\frac{1}{2}\left(P\left(\frac{\partial q}{\partial \zeta_i}(\zeta_i, y_i)\right) + \left(\frac{\partial q}{\partial \zeta_i}(\zeta_i, y_i)\right)^T P\right), \tag{7.18}$$

are uniformly negative and bounded away from zero for all $\zeta_i \in \mathbb{R}^{n-m}$ and $y_i \in \mathbb{R}^m$.

Then, there exist a positive constant $\kappa' \in \mathbb{R}_{>0}$ and a unimodal function $\varphi : \mathcal{J} := [\kappa', \infty) \to \mathbb{R}_{\geq 0}$, $\kappa \mapsto \varphi(\kappa)$ with $\varphi(\kappa') = \lim_{\kappa\to\infty} \varphi(\kappa) = 0$, such that if $(\kappa, \tau) \in \mathcal{S}_1$ with $\mathcal{S}_1 := \{\kappa, \tau \in \mathbb{R}_{\geq 0} | \kappa > \kappa', \tau < \varphi(\kappa)\}$, then the system (7.13)-(7.15) *is a global predictor for system* (7.4)-(7.6)*; and therefore, $\lim_{t\to\infty} x_i(t + \tau_2) - \eta_i(t) = 0$.*

The proof of Lemma 7.2 can be found in the Appendix A. The result stated in Lemma 7.2 amounts to the following. If the solutions of (7.4)-(7.6),(7.13)-(7.15) exist and are ultimately bounded, the zero solution of the prediction error dynamics (7.16), (7.17) is asymptotically stable provided that the predictor gain κ is sufficiently large and the total time delay τ is smaller than some unimodal function $\varphi(\kappa)$, see Figure 7.2. Hence, there exists a region $\mathcal{S}_1$ (gray area in Figure 7.2) such that if $(\kappa, \tau) \in \mathcal{S}_1$, the system (7.13)-(7.15) asymptotically anticipates the dynamics (7.4)-(7.6).

7.4 Predictor-based Diffusive Dynamic Couplings

Let the k systems (7.4)-(7.6) be interconnected through a *Diffusive Dynamic Coupling* (DDC) of the form

$$\dot{\eta}_{1i} = q(\eta_{1i}, \eta_{2i}), \tag{7.19}$$

$$\dot{\eta}_{2i} = a(\eta_{1i}, \eta_{2i}) + u_i + \kappa\left(y_i(t-\tau_1) - \eta_{2i}(t-\tau)\right), \tag{7.20}$$

$$u_i = \gamma \sum_{j \in \mathcal{E}_i} a_{ij}\left(\eta_{2j} - \eta_{2i}\right), \tag{7.21}$$

$$\eta_i = \eta_{0i} \in \mathbb{R}^n, \quad t \in [-\tau, 0], \quad i \in \mathcal{I}, \tag{7.22}$$

with coupling strength $\gamma \in \mathbb{R}_{\geq 0}$, predictor gain $\kappa \in \mathbb{R}_{\geq 0}$, and interconnection weights $a_{ij} = a_{ji} \geq 0$. Since the coupling strength is encompassed in the constant γ, then it can be assumed without loss of generality that $\max_{i \in \mathcal{I}} \sum_{j \in \mathcal{E}_i} a_{ij} = 1$. The dynamic coupling (7.19)-(7.22) is the combination of the nonlinear predictor (7.13)-(7.15) and an estimated version of the time-ahead output controller (7.8), see Figure 7.3. Then, the closed-loop system is given by

$$\begin{aligned}
\dot{\zeta}_i &= q(\zeta_i, y_i), \\
\dot{y}_i &= a(\zeta_i, y_i) + \gamma \sum_{j \in \mathcal{E}_i} a_{ij}\left(\eta_{2j}^{\tau_2} - \eta_{2i}^{\tau_2}\right), \\
\dot{\eta}_{1i} &= q(\eta_{1i}, \eta_{2i}), \\
\dot{\eta}_{2i} &= a(\eta_{1i}, \eta_{2i}) + \gamma \sum_{j \in \mathcal{E}_i} a_{ij}\left(\eta_{2j} - \eta_{2i}\right) + \kappa\left(y_i^{\tau_1} - \eta_{2i}^{\tau}\right), \quad i \in \mathcal{I},
\end{aligned}$$

with initial history (7.6),(7.22). Alternatively, since $\epsilon_i = x_i - \eta_i^{\tau_2}$, the closed-loop system can be written in terms of the prediction errors as follows

$$\dot{\zeta}_i = q(\zeta_i, y_i), \tag{7.23}$$

$$\dot{y}_i = a(\zeta_i, y_i) + \gamma \sum_{j \in \mathcal{E}_i} a_{ij}\left(y_j - y_i + \epsilon_{2i} - \epsilon_{2j}\right), \tag{7.24}$$

$$\dot{\epsilon}_{1i} = q(\zeta_i, y_i) - q(\zeta_i - \epsilon_{1i}, y_i - \epsilon_{2i}) \tag{7.25}$$

$$\dot{\epsilon}_{2i} = a(\zeta_i, y_i) - a(\zeta_i - \epsilon_{1i}, y_i - \epsilon_{2i}) - \kappa\epsilon_{2i}^{\tau}, \quad i \in \mathcal{I}, \tag{7.26}$$

which is the delay-free closed-loop system (7.9)-(7.10) perturbed by the prediction errors ϵ_{2i}. Then, given the result in [104], it is intuitive to think that the systems may synchronize provided that γ is sufficiently large and the prediction errors converge sufficiently fast to the origin. However, before we start thinking about network synchronization, it is necessary to ensure that the solutions of the closed-loop system (7.4)-(7.6),(7.19)-(7.22) are well defined, i.e., the solutions exist and are bounded.

Remark 7.3. *In the following sections, we present results about boundedness and synchronization of the solutions of the interconnected systems* (7.4)-(7.6),(7.19)-(7.22). *These results are given in terms of the coupling strength γ, the predictor gain κ, and the total time-delay τ. By definition, the total time delay is given by the sum of the measurement time-delay τ_1 and transmission time-delay τ_2, i.e., $\tau := \tau_1 + \tau_2$. It follows that if boundedness and synchronization of the solutions is guaranteed for $\tau \leq \bar{\tau} \in \mathbb{R}_{>0}$, then boundedness and synchronization is guaranteed for all $\tau_1, \tau_2 \in \mathbb{R}_{\geq 0}$ such that $\tau_1 + \tau_2 \leq \bar{\tau}$.*

7.5 Boundedness of the Coupled Systems

In this section, we give sufficient conditions for ultimate boundedness of the solutions of closed-loop system (7.4)-(7.6),(7.19)-(7.22) interacting on *simple strongly connected graphs*.

Lemma 7.4. *Consider k nonlinear systems* (7.4)-(7.6) *interconnected through the predictor-based* DDC (7.19)-(7.22) *with coupling strength $\gamma \in \mathbb{R}_{\geq 0}$, predictor gain $\kappa \in \mathbb{R}_{\geq 0}$, and total time-delay $\tau \in \mathbb{R}_{\geq 0}$ on a simple strongly connected graph. Assume that:*

(H7.2) *Each system* (7.4),(7.5) *is strictly C^1-semipassive with input $u_i^{\tau_2}$, output y_i, radially unbounded storage function $V(x_i)$, and the functions $H(x_i)$ are such that there exist constants $R, \delta \in \mathbb{R}_{>0}$ such that $|x_i| > R$ implies that $H(x_i) - \delta |y_i|^2 > 0$.*

Let $\bar{\delta}$ be the largest δ that satisfies (H7.2)*, then the solutions of the coupled systems* (7.4)-(7.6),(7.19)-(7.22) *are ultimately bounded for any finite $\tau \in \mathbb{R}_{\geq 0}$ and $(\gamma, \kappa) \in \mathcal{N}$ with $\mathcal{N} := \{\gamma, \kappa \in \mathbb{R}_{\geq 0} | \frac{3\kappa}{2} + \gamma \leq \bar{\delta}\}$.*

The proof of Lemma 7.4 can be found in the Appendix A.

Remark 7.5. *The result stated in Lemma 7.4 is independent of the time-delay. Therefore, if the conditions stated in Lemma 7.4 are satisfied, the solutions of the closed-loop system* (7.4)-(7.6),(7.19)-(7.22) *are ultimately bounded for arbitrary large time-delays.*

7.6 Network Synchronization

In this section, we give sufficient conditions for network synchronization of the interconnected systems. Define $x := \mathrm{col}(x_1, \ldots, x_k)$ and the *synchronization manifold* $\mathcal{M} := \{x \in \mathbb{R}^{kn} \mid x_i = x_j, \ \forall \ i, j \in \mathcal{I}\}$. The systems (7.4)-(7.6),(7.19)-(7.22) are said to fully synchronize, or simply synchronize, if the synchronization manifold $\mathcal{M}$ contains an asymptotically stable subset.

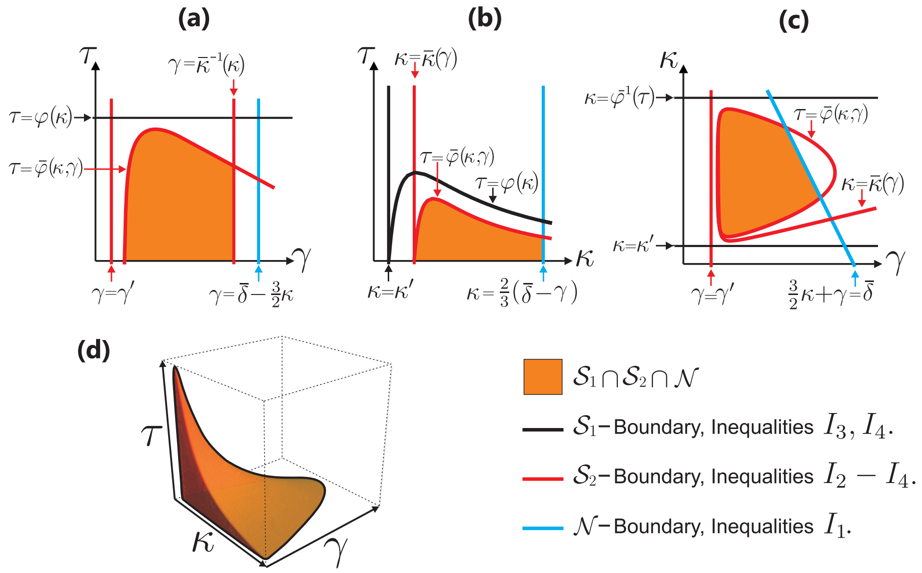

Figure 7.4 Projections and a three dimensional sketch of the synchronization region $\mathcal{S}_1 \cap \mathcal{S}_2 \cap \mathcal{N}$.

7.6.1 Global Result

Next, we give sufficient conditions for the existence of an asymptotically stable subset of the synchronization manifold. Particularly, we prove that under some mild assumptions, there always exists a region in the parameter space (coupling strength γ, predictor gain κ, and total time-delay τ), such that if γ, κ, and τ belong to this region, the systems synchronize. Moreover, it is also proved that this region is bounded by a concave function $\bar{\varphi} : \mathcal{K} \subseteq \mathbb{R}^2 \to \mathbb{R}_{\geq 0}$, $(\kappa, \gamma) \mapsto \bar{\varphi}(\kappa, \gamma)$. The function $\bar{\varphi}(\kappa, \gamma)$ has a unique maximum on $\mathcal{K}$ and it has no other extrema.

Theorem 7.6. *Consider k nonlinear systems* (7.4)-(7.6) *coupled through the predictor based* DDC (7.19)-(7.22) *with coupling strength $\gamma \in \mathbb{R}_{\geq 0}$, predictor gain $\kappa \in \mathbb{R}_{\geq 0}$, and total time-delay $\tau \in \mathbb{R}_{\geq 0}$ on a simple strongly connected graph. Assume that the conditions of Lemma 7.2 and Lemma 7.4 are satisfied. Then, there exist constants $\gamma', \sigma', \kappa' \in \mathbb{R}_{>0}$, a function $\bar{\kappa}(\gamma) := \kappa' + \frac{\sigma'\gamma^2}{\gamma-\gamma'}$, and a concave function $\bar{\varphi} : \mathcal{K} \to \mathbb{R}_{\geq 0}$, $(\kappa, \gamma) \mapsto \bar{\varphi}(\kappa, \gamma)$ with $\bar{\varphi}(\bar{\kappa}(\gamma), \gamma) = \lim_{\kappa\to\infty} \bar{\varphi}(\kappa, \gamma) = 0$, such that if $(\gamma, \kappa, \tau) \in \mathcal{S}_1 \cap \mathcal{S}_2 \cap \mathcal{N}$ with $\mathcal{S}_2 := \{\gamma, \kappa, \tau \in \mathbb{R}_{\geq 0} | \gamma > \gamma', \kappa > \bar{\kappa}(\gamma), \tau < \varphi(\kappa, \gamma)\}$, $\mathcal{S}_1$ the prediction set defined in Lemma 7.2, and $\mathcal{N}$ the boundedness set defined in Lemma 7.4, then the solutions of the closed-loop system* (7.4)-(7.6),(7.19)-(7.22) *are ultimately bounded and there exists a globally asymptotically stable subset of the synchronization manifold $\mathcal{M}$.*

The proof of Theorem 7.6 is presented in the Appendix A. The result stated in Theorem 7.6 amounts to the following. The interconnected systems asymptotically synchronize provided that the following inequalities are simultaneously satisfied

$$\frac{3\kappa}{2} + \gamma \leq \bar{\delta}, \tag{I$_1$}$$

$$\gamma > \gamma' = \frac{\kappa'}{\lambda_2}, \tag{I$_2$}$$

$$\kappa > \bar{\kappa}(\gamma) = \kappa' + \frac{\sigma'\gamma^2}{\gamma - \gamma'}, \tag{I$_3$}$$

$$\tau < \bar{\varphi}(\kappa, \gamma) < \varphi(\kappa), \tag{I$_4$}$$

with $\bar{\delta}$ the largest δ that satisfies (H7.2). The constants γ', σ', κ', and the *unimodal functions* $\varphi(\kappa)$ and $\bar{\varphi}(\kappa, \gamma)$ are derived in the proofs of Lemma 7.2 and Theorem 7.6, see (A.118),(A.121),(A.146),(A.148), and (A.149). Geometrically, the intersection of the inequalities (I_1)-(I_4) could be realized as a three-dimensional region in the parameter space. Hereafter, we refer to this region as the *synchronization region* and it is denoted as $\mathcal{S}_1 \cap \mathcal{S}_2 \cap \mathcal{N}$ as stated in Theorem 7.6. Indeed, it is not easy to visualize how the *synchronization region* looks like in the parameter space. Using inequalities (I_1)-(I_4), in Figure 4, we present sketches of the projections of $\mathcal{S}_1 \cap \mathcal{S}_2 \cap \mathcal{N}$ on the three planes and a three-dimensional sketch of the *synchronization region*.

7.6.2 Discussion

So far, we have proved that the k systems (7.4)-(7.6) interconnected through the *predictor-based diffusive dynamic coupling* (7.19)-(7.22) asymptotically synchronize provided that the conditions stated in Theorem 7.6 are satisfied. However, we have not shown in what sense the *synchronization region* $\mathcal{S}_1 \cap \mathcal{S}_2 \cap \mathcal{N}$ may be greater than the *synchronization region* $\mathcal{S}$ that would be obtained when the systems are coupled through the *diffusive static coupling* (7.7). The results presented in Theorem 7.6 are meant to prove *existence* of the *synchronization region*; therefore, the estimate of $\mathcal{S}_1 \cap \mathcal{S}_2 \cap \mathcal{N}$ given by the intersection of (I_1)-(I_4) may be conservative. This is because the approach taken in this manuscript is Lyapunov-based, i.e., we use Lyapunov-Razumikhin functions and Lyapunov-Krasovskii functionals to derive the results. It follows that the conditions stated in Lemma 7.2, Lemma 7.4, and Theorem 7.6 are sufficient but certainly not necessary. Hence, if both regions $\mathcal{S}_1 \cap \mathcal{S}_2 \cap \mathcal{N}$ and $\mathcal{S}$ are obtained using these Lyapunov methods, it may be hard to extract quantitative insights out of them. Thus, a direct comparison between these conservative regions to evaluate the performance of the couplings would be meaningless. In the following section, we provide a local analysis to illustrate the "mechanism of action" behind our predictor-based couplings. We compare (locally) the *synchronization regions* obtained with both controllers without using the mentioned Lyapunov methods. In particular, the provided analysis is related to the *Master Stability Function* (MSF) approach [99], in the sense that the conditions for local synchronization follow from the stability properties of linear variational systems.

7.6.3 Local Analysis

The k systems (7.4)-(7.6) can be written in the following compact form

$$\begin{aligned} \dot{x}_i &= f(x_i) + \mathcal{B}u_i(t-\tau_2), && (7.27)\\ y_i &= \mathcal{C}x_i, && (7.28)\\ x_i &= \phi(t),\ t \in [-\tau_2, 0], && (7.29) \end{aligned}$$

with $i \in \mathcal{I} = \{1, \ldots, k\}$, and

$$x_i = \mathrm{col}(\zeta_i, y_i),\ f(x_i) := \mathrm{col}\left(q(\zeta_i, y_i), a(\zeta_i, y_i)\right),$$
$$\mathcal{C} := \begin{pmatrix} \mathbf{0}_{m\times(n-m)} & I_m \end{pmatrix},\ \mathcal{B} := \mathcal{C}^T.$$

Then, the closed-loop stacked system (7.4)-(7.7) can be written as

$$\dot{x} = F(x) - \gamma\,(L \otimes \mathcal{B}\mathcal{C})\,x(t-\tau), \tag{7.30}$$

with $x := \mathrm{col}(x_1, \ldots, x_k)$, $F(x) := \mathrm{col}(f(x_1), \ldots, f(x_k))$, and Laplacian matrix $L \in \mathbb{R}^{k\times k}$. Assume that:

(H7.3) The solutions of the coupled systems (7.4)-(7.7) are ultimately bounded, i.e., there exists a constant $M \in \mathbb{R}_{>0}$ such that $|x_i(t)| < M$ for all $t \in [-\tau, \infty)$ and $i \in \mathcal{I}$.

We refer the reader to [130], Section 2, where sufficient conditions for boundedness of the solutions of the interconnected systems (7.4)-(7.7) are derived. The communication graph is *strongly connected* and $a_{ij} = a_{ji}$ by assumption. Then, the Laplacian matrix is symmetric and its eigenvalues are real. Moreover, the matrix L has an algebraically simple eigenvalue $\lambda_1 = 0$ and $\mathbf{1} = \mathrm{col}(1, \ldots, 1) \in \mathbb{R}^k$ is the corresponding eigenvector [29]. Applying Gerschgorin's disc theorem [138], it can be concluded that the eigenvalues of L are nonnegative, i.e., the matrix L is positive semidefinite. It follows that L has eigenvalues $\lambda_1, ..., \lambda_k \in \mathbb{R}_{\geq 0}$ ordered by increasing parts: $0 = \lambda_1 < \lambda_2 \leq \cdots \leq \lambda_k$. Since L is symmetric, then there exists a nonsingular matrix $T \in \mathbb{R}^{k\times k}$ so that $\Lambda := T^{-1}LT$, where Λ denotes an upper block-triangular matrix with the eigenvalues of L on its diagonal. It can be proved that the matrix T can be chosen to satisfy

$$T\begin{pmatrix}1\\0\\\vdots\\0\end{pmatrix} = \mathbf{1}_{k\times 1},\ \left(T^{-1}\right)^T\begin{pmatrix}1\\0\\\vdots\\0\end{pmatrix} = \nu, \tag{7.31}$$

for some vector $\nu \in \mathbb{R}^{k\times 1}$ satisfying $\nu^T \mathbf{1}_{k\times 1} = 1$ and $\nu^T L = 0$. It follows that the first column of T is $\mathbf{1}_{k\times 1}$ and the first row of T^{-1} equals ν^T. Introduce the change of coordinates $x := (T\otimes I_n)\bar{x}$, then the closed-loop system in the new coordinates is given by

$$\dot{\bar{x}} = (T^{-1}\otimes I_n)F((T\otimes I_n)\bar{x}) - \gamma\,(\Lambda\otimes\mathcal{BC})\,\bar{x}(t-\tau). \tag{7.32}$$

Notice that $\bar{x}_1 = \sum_{i=1}^k \nu_i x_i =: \xi$ with $\nu^T\mathbf{1}_{k\times 1} = 1$. Moreover, $\bar{x}_j = \mathbf{0}_{n\times 1}$, $j = 2,\dots,k$ implies that $x_i = \bar{x}_1 = \xi$ for all $i \in \mathcal{I}$, i.e., the coupled systems are synchronized. Linearizing (7.32) around $\bar{x} = \mathrm{col}(\xi, \mathbf{0}_{n\times 1},\dots,\mathbf{0}_{n\times 1})$ yields

$$\dot{\bar{x}} = (I_k\otimes J_f(\xi))\,\bar{x} - \gamma\,(\Lambda\otimes\mathcal{BC})\,\bar{x}(t-\tau), \tag{7.33}$$

with $J_f(\xi)$ denoting the Jacobian matrix of the function $f:\mathbb{R}^n\to\mathbb{R}^n$ evaluated along $\xi = \sum_{i=1}^k \nu_i x_i \in \mathbb{R}^n$. Smoothness of the vectorfield $f(\cdot)$ and boundedness of the solutions imply that the Jacobian matrix $J_f(\xi)$ is well defined and uniformly bounded. Moreover, since the system (7.33) is linear, then asymptotic stability of its zero solution $\bar{x}_j = \mathbf{0}_{n\times 1}$, $j = 2,\dots,k$ amounts to asymptotic stability of the following equations

$$\dot{z}_i = J_f(\xi)z_i - \gamma\lambda_i\mathcal{BC}z_i(t-\tau),\ \ i = 2,3,\dots,k. \tag{7.34}$$

Therefore, the k diffusively time-delayed coupled systems (7.4)-(7.7) locally synchronize provided that the coupling strength γ and the total time-delay τ are such that the zero solution of the $(k-1)$ linear equations (7.34) are asymptotically stable uniformly in $\xi(t)$. Next, consider the closed-loop system (7.4)-(7.6),(7.19)-(7.22). Using the same compact form (7.30), the interconnected systems can be written as

$$\begin{aligned}\dot{x} &= F(x) - \gamma\,(L\otimes\mathcal{BC})\,(x-\epsilon)\,, &(7.35)\\ \dot{\epsilon} &= F(x) - F(x-\epsilon) - \kappa\,(I_k\otimes\mathcal{BC})\,\epsilon(t-\tau), &(7.36)\end{aligned}$$

with prediction error $\epsilon_i := \mathrm{col}(\epsilon_{1i},\epsilon_{2i})$ and stacked error $\epsilon := \mathrm{col}(\epsilon_1,\dots,\epsilon_k)$. Assume that:

(H7.4) The conditions stated in Lemma 7.4 are satisfied.

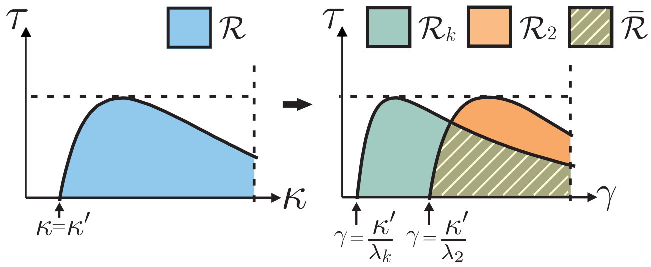

Figure 7.5 Synchronization regions $\mathcal{R}$, $\mathcal{R}_2$, $\mathcal{R}_k$, and $\bar{\mathcal{R}}$.

Therefore, the solutions of the interconnected systems (7.4)-(7.6),(7.19)-(7.22) are uniformly ultimately bounded for all $t \in [-\tau, \infty)$. Inducing again the change of coordinates $x = (T \otimes I_n)\bar{x}$ and $\epsilon := (T \otimes I_n)\bar{\epsilon}$ with T as in (7.31), the closed-loop system is written as

$$\dot{\bar{x}} = (T^{-1} \otimes I_n)F((T \otimes I_n)\bar{x}) - \gamma\,(\Lambda \otimes \mathcal{BC})\,\bar{x} + \gamma\,(\Lambda \otimes \mathcal{BC})\,\bar{\epsilon}, \tag{7.37}$$

$$\begin{aligned}\dot{\bar{\epsilon}} &= (T^{-1} \otimes I_n)F((T \otimes I_n)\bar{x}) - \kappa\,(I_k \otimes \mathcal{BC})\,\bar{\epsilon}^{\tau} \\ &\quad - (T^{-1} \otimes I_n)F((T \otimes I_n)\,(\bar{x} - \bar{\epsilon})).\end{aligned} \tag{7.38}$$

Linearizing the stacked systems (7.37),(7.38) around $\bar{x} = \mathrm{col}(\xi, \mathbf{0}_{n\times 1}, \ldots, \mathbf{0}_{n\times 1})$ and $\bar{\epsilon} = \mathrm{col}(\mathbf{0}_{n\times 1}, \ldots, \mathbf{0}_{n\times 1})$ yields

$$\dot{\bar{x}} = (I_k \otimes J_f(\xi))\,\bar{x} - \gamma\,(\Lambda \otimes \mathcal{BC})\,\bar{x} + \gamma\,(\Lambda \otimes \mathcal{BC})\,\bar{\epsilon}, \tag{7.39}$$

$$\dot{\bar{\epsilon}} = (I_k \otimes J_f(\xi))\,\bar{\epsilon} - \kappa\,(I_k \otimes \mathcal{BC})\,\bar{\epsilon}(t-\tau), \tag{7.40}$$

with $J_f(\xi)$ the Jacobian matrix of $f : \mathbb{R}^n \to \mathbb{R}^n$ evaluated along $\xi = \sum_{i=1}^{k} \nu_i x_i$. System (7.39),(7.40) is linear, then asymptotic stability of its zero solution $\bar{x}_j = \mathbf{0}_{n\times 1}$, $j = 2, \ldots, k$, and $\bar{\epsilon}_i = \mathbf{0}_{n\times 1}$, $i = 1, \ldots, k$ implies asymptotic stability of the following equations

$$\dot{z}_j \;=\; (J_f(\xi) - \gamma\lambda_j \mathcal{BC})\,z_j, \;\; j = 2, 3, \ldots, k, \tag{7.41}$$

$$\dot{\bar{\epsilon}}_i \;=\; J_f(\xi)\bar{\epsilon}_i - \kappa\mathcal{BC}\bar{\epsilon}_i(t-\tau), \;\; i = 1, 2, \ldots, k. \tag{7.42}$$

Hence, the k systems (7.4)-(7.6) interconnected through the predictor-based coupling (7.19)-(7.22) locally synchronize provided that the coupling strength γ, the predictor gain κ, and the total time-delay τ are such that the zero solution of the $(2k-1)$ linear equations (7.41),(7.42) are asymptotically stable uniformly in $\xi(t)$. Summarizing, local synchronization of the coupled systems (7.4)-(7.7) and (7.4)-(7.6),(7.19)-(7.22) amounts to asymptotic stability of the origin of the systems (7.34) and (7.41),(7.42), respectively.

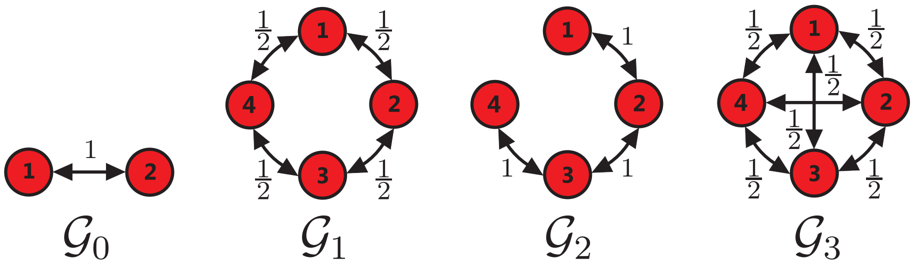

Figure 7.6 Network Topologies

Assume that:

(H7.5) The conditions stated in Lemma 7.2 are satisfied.

The k systems (7.42) are the linearization of the prediction error dynamics (7.16), (7.17) in the coordinates $\bar{\epsilon} = (T \otimes I_n)\epsilon$. Therefore, from Lemma 7.2, it follows that there exist a positive constant κ' and a unimodal function $\varphi : [\kappa', \infty) \to \mathbb{R}_{\geq 0}$ with $\varphi(\kappa') = \lim_{\kappa \to \infty} \varphi(\kappa) = 0$, such that the zero solution of system (7.42) is asymptotically stable if $(\kappa, \tau) \in \mathcal{R} := \{\kappa, \tau \in \mathbb{R}_{\geq 0} | \kappa > \kappa', \tau < \varphi(\kappa)\}$, see Figure 7.4. Notice that the dynamics (7.34), (7.41), and (7.42) share a similar structure. System (7.42) has the same dynamics as system (7.41) if $\kappa = \gamma\lambda_j$, $j = 2, \ldots, k$, and $\tau = 0$. Similarly, system (7.34) has the same dynamics as system (7.42) if $\gamma\lambda_j = \kappa$, $j = 2, \ldots, k$. Therefore, the existence of the region $\mathcal{R}$ implies that:

(P7.1) The zero solution of the $(k-1)$ systems (7.41) are asymptotically stable if

$$\gamma > \frac{\kappa'}{\lambda_2}. \tag{7.43}$$

(P7.2) The zero solution of the $(k-1)$ systems (7.34) are asymptotically stable if

$$(\gamma, \tau) \in \bar{\mathcal{R}} := \bigcap_{j=2}^{k} \mathcal{R}_j, \tag{7.44}$$

with $\mathcal{R}_j := \{(\gamma, \tau) | (\kappa = \gamma\lambda_j, \tau) \in \mathcal{R}\}$. Moreover, it can be proved that given unimodality of the function $\varphi(\cdot)$, the region $\bar{\mathcal{R}}$ is simply given by $\bar{\mathcal{R}} = \mathcal{R}_2 \cap \mathcal{R}_k$, see Section 5.3 in [129] for further details. In Figure 7.5, we provide a graphical interpretation of the statements given in Propositions (P7.1) and (P7.2). From (P7.1) and (P7.2), it follows that the coupled systems (7.4)-(7.7) locally synchronize if $(\gamma, \tau) \in \bar{\mathcal{R}}$ and the coupled systems (7.4)-(7.6),(7.19)-(7.22) locally synchronize if $(\kappa, \tau) \in \mathcal{R}$ and $\gamma > \frac{\kappa'}{\lambda_2}$. Notice that by introducing the predictor-based coupling, we have shifted the effect of the time-delay from the synchronization error dynamics to the prediction error dynamics. That is, if the k systems are coupled through the *diffusive static coupling* (7.7), the time-delay appears explicitly in the synchronization error dynamics (7.34) and it is directly linked to the network topology through the nonzero eigenvalues of the Laplacian matrix. On the other hand, if they interact through the *predictor-based coupling*, the time-delay appears in the prediction error dynamics (7.42), but not in the synchronization error dynamics (7.41); and therefore, in this case, the effect of the time-delay is not influenced by the network topology. Finally, from (P7.1) and (P7.2), we can immediately conclude the following:

(a) If $\lambda_2 < \lambda_k$, then area$(\mathcal{R}) >$ area$(\bar{\mathcal{R}})$.

(b) If $\lambda_2 = \lambda_k > 1$, then area$(\mathcal{R}) >$ area$(\bar{\mathcal{R}})$.

(c) If $\lambda_2 = \lambda_k = 1$, then area$(\mathcal{R}) =$ area$(\bar{\mathcal{R}})$.

(d) If $\lambda_2 = \lambda_k < 1$, then area$(\mathcal{R}) <$ area$(\bar{\mathcal{R}})$,

with λ_2 and λ_k being the smallest nonzero and the largest eigenvalues of the Laplacian matrix, and area$(\mathcal{R})$ and area$(\bar{\mathcal{R}})$ denoting the area of the regions $\mathcal{R}$ and $\bar{\mathcal{R}}$, respectively. Therefore, locally, the predictor-based coupling would lead to greater or equal synchronization regions in cases (a)-(c). It is worth noting that for a given strongly connected graph, $\lambda_2 = \lambda_k$, if the network topology is *all-to-all*, i.e., each system in the network receives information from all the remaining systems. □

7.6.4 On Robustness of the Control-Scheme

The results presented in the previous sections are derived for networks of coupled *identical systems*. However, in practical situations, the dynamics of the systems cannot be expected to be perfectly identical. Moreover, the vectorfields $q(\cdot)$ and $a(\cdot)$ of the dynamics (7.4)-(7.6) must be exactly *known* to be able to construct the predictor-based coupling (7.19)-(7.22). This is unrealistic in practical situations, where there may be parametric uncertainties and/or unmodeled dynamics in the available models. In this situation, the best that can be done is to construct the couplings with the *known* part of the dynamics, which, hereafter, is referred to as *the nominal dynamics*.

Hence, because of all these practical issues, we can not expect that the systems perfectly synchronize under the proposed control scheme. In the best case, if the uncertainties are sufficiently small (in some appropriate sense), it can be expected that the synchronization errors are bounded by a small constant $\mu \in \mathbb{R}_{>0}$, which, of course, needs to be small enough in order to consider that the systems are *"practically synchronized"*. Let the k systems (7.4)-(7.6) be the *nominal dynamics* of the following *perturbed* systems

$$\dot{\zeta}_i = q(\zeta_i, y_i) + \Delta q_i(\zeta_i, y_i), \quad (7.45)$$
$$\dot{y}_i = a(\zeta_i, y_i) + u_i(t - \tau_2) + \Delta a_i(\zeta_i, y_i), \quad (7.46)$$
$$x_i = \phi(t),\ t \in [-\tau_2, 0], \quad (7.47)$$

with $i = 1, ..., k$, state $x_i := \mathrm{col}(\zeta_i, y_i) \in \mathbb{R}^n$, internal state $\zeta_i \in \mathbb{R}^{n-m}$, output $y_i \in \mathbb{R}^m$, input $u_i \in \mathbb{R}^m$, sufficiently smooth *known* functions $q : \mathbb{R}^{n-m} \times \mathbb{R}^m \to \mathbb{R}^{n-m}$ and $a : \mathbb{R}^{n-m} \times \mathbb{R}^m \to \mathbb{R}^m$, and sufficiently smooth *unknown* functions $\Delta q_i : \mathbb{R}^{n-m} \times \mathbb{R}^m \to \mathbb{R}^{n-m}$ and $\Delta a_i : \mathbb{R}^{n-m} \times \mathbb{R}^m \to \mathbb{R}^m$. The vectorfields $q(\cdot)$ and $a(\cdot)$ are the *known* part of the dynamics while the terms $\Delta q_i(\zeta_i, y_i)$ and $\Delta a_i(\zeta_i, y_i)$ represent parametric uncertainties and/or unmodeled dynamics. In this setting, the predictor based coupling (7.19)-(7.22) is constructed using the *known* vectorfields $q(\cdot)$ and $a(\cdot)$ of the nominal dynamics. Then, at this point, one may wonder under what conditions the solutions of the coupled perturbed systems (7.45)-(7.47),(7.19)-(7.22) are ultimately bounded and practically synchronize. Firstly, we address the boundedness part in the following lemma, which is a slight modification of Lemma 7.4.

Lemma 7.7. *Consider k perturbed systems* (7.45)-(7.47) *interconnected through the predictor-based coupling* (7.19)-(7.22) *with coupling strength $\gamma \in \mathbb{R}_{\geq 0}$, predictor gain $\kappa \in \mathbb{R}_{\geq 0}$, and total time-delay $\tau \in \mathbb{R}_{\geq 0}$ on a simple strongly connected graph. Assume that:*

(H7.6) *Each system* (7.45),(7.46) *is strictly $\mathcal{C}^1$-semipassive with input $u_i^{\tau_2}$, output y_i, radially unbounded storage function $V_i(x_i)$, and the functions $H_i(x_i)$ are such that there exist constants $R_i, \delta_i \in \mathbb{R}_{>0}$ such that $|x_i| > R_i$ implies that $H_i(x_i) - \delta_i |y_i|^2 > 0$.*

Let $\bar{\delta}_i$ be the largest δ_i that satisfies (H7.6) *and define $\bar{\delta}_{\min} := \min(\bar{\delta}_1, \ldots, \bar{\delta}_k)$, then the solutions of the coupled systems* (7.45)-(7.47),(7.19)-(7.22) *exist and are ultimately bounded for any finite $\tau \in \mathbb{R}_{\geq 0}$ and $(\gamma, \kappa) \in \tilde{\mathcal{N}}$ with $\tilde{\mathcal{N}} := \{\gamma, \kappa \in \mathbb{R}_{\geq 0} | \frac{3\kappa}{2} + \gamma \leq \bar{\delta}_{\min}\}$.*

The proof of Lemma 7.7 follows the same lines as the proof of Lemma 7.4 and it is omitted here. The result stated in Lemma 7.7 implies that ultimate boundedness of the solutions of the coupled perturbed systems can still be guaranteed as long as each perturbed system (7.45),(7.46) is strictly $\mathcal{C}^1$-semipassive in the presence of the perturbation terms $\Delta q_i(\zeta_i, y_i)$ and $\Delta a_i(\zeta_i, y_i)$. This is not hard to satisfy when the perturbations are due to parametric uncertainties; then, semipassivity of the nominal system may imply semipassivity of the perturbed one if the uncertainties are sufficiently small.

The next step would be to show that under some conditions the coupled perturbed systems *"practically synchronize"*. *Practical synchronization* means that the differences between the states of the systems converge to some compact invariant set in finite time, and this set is bounded by a constant $\mu \in \mathbb{R}_{>0}$ which has to be small enough to consider that the systems are still synchronized. However, the formal study of practical synchronization goes beyond the scope of this chapter. The general purpose of this manuscript is to gain insights of the synchronization mechanisms for the class of systems and couplings under study. Particularly, we focus on the stability analysis of the synchronization manifold $\mathcal{M}$ with respect to the *coupled unperturbed systems*. The practical implications of the control-scheme are not considered here and are left for future research.

7.7 Example: Hindmarsh-Rose Neural Oscillators

A. Network Topology, Convergence, and Semipassivity. Consider a network of k systems coupled according to the graphs depicted in Figure 7.6. The networks are strongly connected and undirected. Each system in the network is assumed to be a Hindmarsh-Rose neuron [51] of the form

$$\begin{cases} \dot{z}_{1i} = 1 - 5y_i^2 - z_{1i}, \\ \dot{z}_{2i} = 0.005(4y_i + 6.472 - z_{2i}), \\ \dot{y}_i \ \ = -y_i^3 + 3y_i^2 + z_{1i} - z_{2i} + 3.25 + u_i^{\tau_2}, \end{cases} \tag{7.48}$$

with output $y_i \in \mathbb{R}$, internal states $z_{i1}, z_{i2} \in \mathbb{R}$, state $x_i = \mathrm{col}(z_{i1}, z_{i2}, y_i) \in \mathbb{R}^3$, delayed input $u_i^{\tau_2} \in \mathbb{R}$, transmission time-delay $\tau_2 \in \mathbb{R}_{\geq 0}$, and $i \in \mathcal{I} = \{1, \ldots, k\}$. It is well known that the Hindmarsh-Rose neuron (7.48) has a chaotic attractor [51] for $u_i = 0$. Furthermore, in [136], it is proved that the Hindmarsh-Rose neuron is strictly $\mathcal{C}^1$-semipassive with quadratic storage function $V(z_{1i}, z_{2i}, y_i) := \frac{1}{2}y_i^2 + \sigma z_{1i}^2 + 25z_{2i}^2$, constants $\varsigma_1, \varsigma_2 \in (0, 1)$, $0 < \sigma < \frac{4\varsigma_1(1-\varsigma_2)}{25}$, and

$$\begin{aligned} H(z_{1i}, z_{2i}, y_i) &= \varsigma_1 y_i^4 - 3y_i^3 - \frac{1}{4\sigma(1-\varsigma_2)} y_i^2 \\ &+ \left(\sigma\varsigma_2 - \frac{25\sigma^2}{4(1-\varsigma_1)}\right) z_{1i}^2 + \frac{1}{4} z_{2i}^2 - 1.618 z_{2i} \\ &+ \sigma(1-\varsigma_2)\left(z_{1i} - \frac{1}{2\sigma(1-\varsigma_2)} y_i\right)^2 - \sigma z_{1i} \\ &+ (1-\varsigma_1)\left(y_i^2 + \frac{5\sigma}{2(1-\varsigma_1)} z_{1i}\right)^2 - 3.25 y_i. \end{aligned} \tag{7.49}$$

Moreover, the (z_{1i}, z_{2i})-dynamics (the internal dynamics) is an *exponentially convergent system* (in the sense of Definition 1.4), i.e., it satisfies the Demidovich condition (7.18) with $P = I_2$; hence, assumption (H7.1) is satisfied.

B. Predictor-based Diffusive Dynamic Coupling. Associated with systems (7.48), the dynamic couplings (7.19)-(7.22) take the following form

$$\begin{cases} \dot{\eta}_{1i} = 1 - 5\eta_{3i}^2 - \eta_{1i}, \\ \dot{\eta}_{2i} = 0.005(4\eta_{3i} + 6.472 - \eta_{2i}), \\ \dot{\eta}_{3i} = -\eta_{3i}^3 + 3\eta_{3i}^2 + \eta_{1i} - \eta_{2i} + 3.25 + u_i + \kappa(y_i^{\tau_1} - \eta_{3i}^{\tau}), \\ u_i = \gamma \sum_{j \in \mathcal{E}_i} a_{ij}(\eta_{3j} - \eta_{3i}), \end{cases} \tag{7.50}$$

with predictor state $\eta_i = \mathrm{col}(\eta_{1i}, \eta_{2i}, \eta_{3i}) \in \mathbb{R}^3$, measurement time-delay $\tau_1 \in \mathbb{R}_{\geq 0}$, total time-delay $\tau \in \mathbb{R}_{\geq 0}$, coupling strength $\gamma \in \mathbb{R}_{\geq 0}$, and predictor gain $\kappa \in \mathbb{R}_{\geq 0}$. As previously mentioned, each system (7.48) is strictly $\mathcal{C}^1$-semipassive with $H(x_i)$ as in (7.49). It can be shown that the function $H(x_i)$ satisfies the boundedness assumption (H7.2) stated in Lemma 7.4 for arbitrary large coupling strength γ and predictor gain κ, i.e., $\mathcal{N} = \mathbb{R}_{\geq 0} \times \mathbb{R}_{\geq 0}$. Therefore, by Lemma 7.4, the solutions of the closed-loop system (7.48),(7.50) always exist and are ultimately bounded. Moreover, since the internal dynamics is *convergent*, (H7.1) is satisfied; hence, by Lemma 7.2, there exists a region $\mathcal{S}_1 \subset \mathbb{R}_{\geq 0} \times \mathbb{R}_{\geq 0}$ (as depicted in Figure 7.2), such that if $(\kappa, \tau) \in \mathcal{S}_1$, the predictor state η_i asymptotically anticipates the dynamics (7.48), i.e., $\lim_{t \to \infty} x_i(t + \tau_2) - \eta_i(t) = 0$. Finally, by Theorem 7.6, there exists a nonempty set $S_2 \subset \mathbb{R}_{\geq 0} \times \mathbb{R}_{\geq 0} \times \mathbb{R}_{\geq 0}$ (as depicted in Figure 7.4), such that if $(\gamma, \kappa, \tau) \in \mathcal{S}_1 \cap \mathcal{S}_2 \cap \mathcal{N}$, the systems synchronize.

C. Simulation Results. In Figures 7.7-7.10, we show the results obtained through extensive computer simulations for $\tau_1 = \tau_2 = \frac{\tau}{2}$. Figure 7.7 depicts the prediction region $\mathcal{S}_1$ introduced in Lemma 7.2. This region is clearly bounded by a unimodal function; hence, there is an optimal predictor gain $\kappa = \kappa^* := 2.05$ that leads to the maximum time-delay $\tau = \tau^* = 3.82$ that can be induced to the predictor. This maximum time-delay depends directly on the dynamics of the systems, but not on the network topology, (see the proof of Lemma 7.2). In Figure 7.8, for $\mathcal{G}_0$, we show the *synchronization region* $\mathcal{S}$ obtained when the two neurons are coupled via the *diffusive static coupling* (7.7) and a projection of the *synchronization region* $\mathcal{S}_1 \cap \mathcal{S}_2 \cap \mathcal{N}$ on the (γ, τ)-plane obtained through the predictor-based coupling (7.50) for $\kappa = \kappa^*$. For this particular topology and κ, both couplings lead to approximately the same maximum time-delay τ^*. This can be explained (locally) by the statement (b) of the local analysis since $\lambda_2(\mathcal{G}_0) = \lambda_k(\mathcal{G}_0) = 2$. However, the asymptotic behavior is quite different. The upper bound of $\mathcal{S}$ decreases asymptotically to zero as the coupling strength increases. On the other hand, the projection of the *synchronization region* $\mathcal{S}_1 \cap \mathcal{S}_2 \cap \mathcal{N}$ has an upper bound that converges

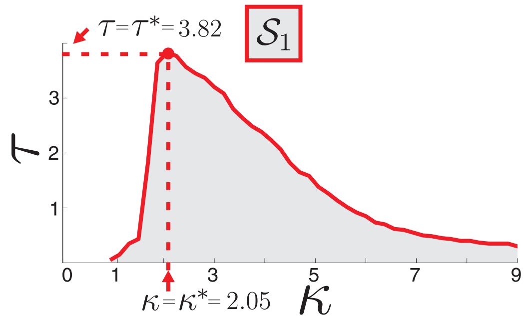

Figure 7.7 Prediction region $\mathcal{S}_1$.

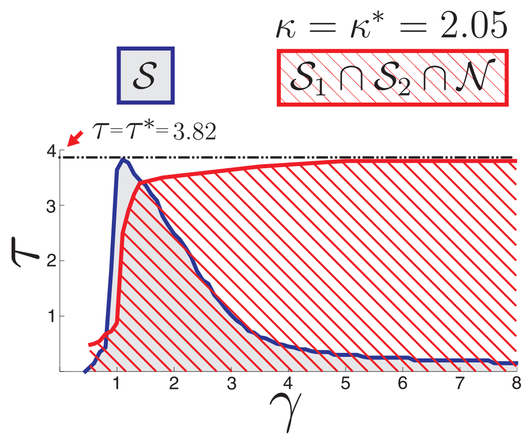

Figure 7.8 Synchronization regions $\mathcal{S}$ and $\mathcal{S}_1 \cap \mathcal{S}_2 \cap \mathcal{N}$ for $\kappa = \kappa^*$ and $\mathcal{G}_0$, i.e., two coupled systems.

to τ^* asymptotically as γ is increased. Hence, in the latter case (for large γ), the maximum time-delay is determined by the predictor gain κ, see Figure 7.7. Finally, in Figure 7.9 and Figure 7.10, we show the regions $\mathcal{S}$ and the projections of $\mathcal{S}_1 \cap \mathcal{S}_2 \cap \mathcal{N}$ for all the topologies depicted in Figure 7.6. It is clear that the regions $\mathcal{S}$ in Figure 7.10 are strongly influenced by the network topology [130]. Conversely, the regions $\mathcal{S}_1 \cap \mathcal{S}_2 \cap \mathcal{N}$ in Figure 7.9 are influenced by the network topology only for small coupling strength. The upper bounds of the synchronization regions converge asymptotically to τ^* independently of the network topology as γ is increased.

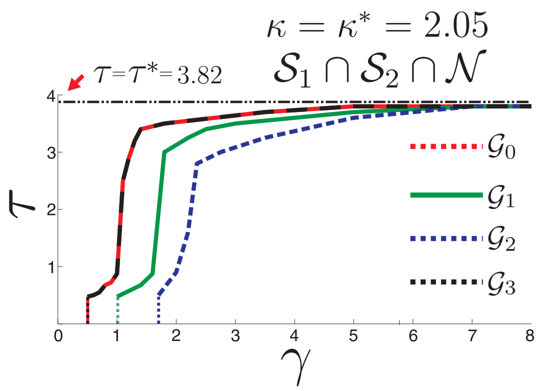

Figure 7.9 Synchronization region $\mathcal{S}_1 \cap \mathcal{S}_2 \cap \mathcal{N}$ for different topologies $\mathcal{G}_j$, $j = 1, 2, 3, 4$, and $\kappa = \kappa^*$.

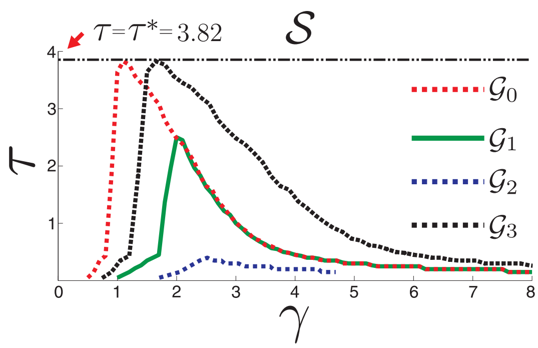

Figure 7.10 Synchronization region $\mathcal{S}$ for different topologies $\mathcal{G}_j$, $j = 1, 2, 3, 4$.

7.8 Conclusions

We have presented a result on network synchronization in the case when the measurements of the available outputs and the transmission of the controllers are subject to different constant time-delays. We have shown that the time-delay that can be induced to the network may be increased by the proposed predictor-based diffusive dynamic couplings. Using the notion of semipassivity, we have provided sufficient conditions which guarantee existence and ultimate boundedness of the solutions of the closed-loop system. Sufficient conditions that guarantee (global) state synchronization have also been derived. We have provided a local analysis to illustrate the "mechanism of action" behind our predictor-based couplings. Finally, we have presented an illustrative example that shows that indeed it is possible to extend the synchronization regions with the proposed control scheme. While the regions $\mathcal{S}$ obtained through the *diffusive static coupling* (7.7) are strongly influenced by the network topology, the regions $\mathcal{S}_1 \cap \mathcal{S}_2 \cap \mathcal{N}$ obtained with the predictor-based coupling are influenced by the network topology only for small coupling strength. As γ is increased, the upper bounds of $\mathcal{S}_1 \cap \mathcal{S}_2 \cap \mathcal{N}$ are determined by the prediction set $\mathcal{S}_1$, i.e., for a fixed κ and its corresponding maximum time-delay τ^*, see Figure 7.7, the upper bounds of $\mathcal{S}_1 \cap \mathcal{S}_2 \cap \mathcal{N}$ converge asymptotically to τ^* independently of the network topology.

Chapter 8

Synchronization in Networks of Hindmarsh-Rose Neurons: Experimental Results

Abstract. Experimental results about synchronization and partial synchronization in networks of Hindmarsh-Rose neurons that interact through diffusive time-delayed couplings are presented. In particular, we test the predictive value of our theoretical results using an experimental setup with electronic circuit realizations of the Hindmarsh-Rose neuron model.

8.1 Introduction

In this chapter, we present a set of experimental results on synchronization in networks of coupled dynamical systems with time-delays. Particularly, we test some theoretical results about *full synchronization* [132], *partial synchronization* [133], and *synchronization in relation to the network topology* [130] in networks of coupled semipassive systems. We employ an experimental setup with electronic circuit realizations of the Hindmarsh-Rose neuron model [51]. It is important to notice that in practical situations, the dynamics of the systems in the network cannot be expected to be perfectly identical. For instance, because the signals exchanged among the systems are contaminated with noise and/or there are small mismatches in the systems' parameters. Because of these inherent imperfections, we can not expect that the systems perfectly synchronize. It is necessary to allow for a mismatch between them, which, of course, needs to be small enough in order to consider that the systems are "*practically synchronized*". To this end, we

This chapter is based on [131].

introduce the notions of *practical synchronization* and *practical partial synchronization*, which states that circuits may be called (partially) synchronized if, after some transient, the differences between their outputs are sufficiently small on a long finite time interval. The experiments with networks of coupled Hindmarsh-Rose circuits shall indicate when the aforementioned theoretical results, derived for identical systems and without any noise, (fail to) have sufficient predictive value in reality.

We present experimental results on network synchronization of systems interconnected through diffusive time-delayed couplings. These coupling functions are of the form

$$u_i(t) = \gamma \sum_j a_{ij}\big(y_j(t-\tau) - y_i(t)\big),$$

which we refer to as *transmission delay couplings*, and

$$u_i(t) = \gamma \sum_j a_{ij}\big(y_j(t-\tau) - y_i(t-\tau)\big),$$

which is called *full delay couplings*. The function u_i denotes the input of system i, which has output y_i, y_j is the output of a neighboring system j, $\tau \in \mathbb{R}_{>0}$ denotes the networked-induced time-delay, the constants $a_{ij} \in \mathbb{R}_{\geq 0}$ are the interconnection weights, and $\gamma \in \mathbb{R}_{>0}$ is the coupling strength. In case of *transmission delay couplings*, the transmitted signals (the outputs of neighbors of system i) are delayed by τ units of time and compared with the current output of system i. These kind of couplings arise naturally in networked systems due to finite speed of propagation of signals. It takes some amount of time before system i receives information about the state of its neighbors (via the outputs y_j). *Full delay couplings*, where all signals are time-delayed by an amount τ, may arise, for instance, when the systems are interconnected by a centralized control law. In that case the central controller first has to sample the outputs of all the systems, then it has to compute the coupling inputs u_i and, finally, the controller needs to communicate these inputs to the systems. Full delay coupling functions also appear in traffic flows, where the time-delay corresponds to the human reaction time [125].

There are several results studying synchronization in networks of linearly coupled systems from a theoretical point of view, see , for instance, [47, 78, 90, 99, 104, 147]. Conditions are established to predict *synchronization* and *partial synchronization* in such networks. In addition the problem of how synchronization relates to the structure of the network has been investigated intensively, at least in the delay-free case, see [20, 22, 105, 142]. However, obtained results are usually tested using computer simulations. Much less attention is devoted to the verification of theoretical synchronization results in real experimental setups. The focus of this chapter is to test the validity of theory using an experimental setup that consists of electronic circuit board realizations of the (mathematical) Hindmarsh-Rose neuron model [51]. Particularly, this chapter presents results of a series of experiments that are conducted to verify the theoretical results about *full synchronization* [132], *partial synchronization* [134], and *synchronization in relation to the network topology* [130].

8.2 System Description and a Review of Theoretical Results

We consider networks of identical nonlinear systems, where the networks are described by graphs $\mathcal{G} = (\mathcal{V}, \mathcal{E}, A)$ and the systems are of the form

$$\dot{z}_i = q(z_i, y_i), \tag{8.1a}$$

$$\dot{y}_i = a(z_i, y_i) + u_i, \tag{8.1b}$$

with $i \in \mathcal{V} := \{1, ..., k\}$, internal state $z_i \in \mathbb{R}^{n-m}$, output $y_i \in \mathbb{R}^m$, state $x_i := \mathrm{col}(z_i, y_i)$, input $u_i \in \mathbb{R}^m$, and sufficiently smooth functions $q : \mathbb{R}^{n-m} \times \mathbb{R}^m \to \mathbb{R}^{n-m}$ and $a : \mathbb{R}^{n-m} \times \mathbb{R}^m \to \mathbb{R}^m$. We consider two types of time-delayed couplings, namely *transmission delay couplings*

$$u_i = \gamma \sum_{j \in \mathcal{N}_i} a_{ij} \big(y_j(t - \tau) - y_i(t) \big), \tag{8.2}$$

and *full delay couplings*

$$u_i = \gamma \sum_{j \in \mathcal{N}_i} a_{ij} \big(y_j(t - \tau) - y_i(t - \tau) \big). \tag{8.3}$$

The positive constant γ denotes the *coupling strength* and the non-negative constant τ is the time-delay. The constants $a_{ij} \geq 0$ are the entries of the weighted adjacency matrix A of the graph $\mathcal{G}$. Since the coupling strength is encompassed in the constant γ, it is assumed without loss of generality that $\max_{i \in \mathcal{V}} \sum_{j \in \mathcal{N}_i} a_{ij} = 1$. Note that in case of the transmission delay coupling (8.2) only the *transmitted signals* contain delays and in the full-delay coupling (8.3) *all signals* contain delay. It is important to point out that if all the systems in the network asymptotically synchronize, i.e., if the solutions of the systems asymptotically match

$$x_i(t) \to x_j(t) \text{ as } t \to \infty \text{ for all } i, j \in \mathcal{V},$$

then the full delay coupling (8.3) vanishes and the transmission delay coupling (8.2) generally does *not* vanish. So, we say that transmission delay coupling is *invasive* and full delay coupling is *non-invasive*. Define the staked state $x := \mathrm{col}(x_1, \ldots, x_k)$. A necessary condition for a network of k systems (8.1a),(8.1b) to synchronize is that the synchronization manifold

$$\mathcal{M} := \{x \in \mathbb{R}^{kn} | x_1 = x_2 = \ldots = x_k\},$$

is forward invariant with respect to the dynamics of the coupled systems. We observe that, because the systems (8.1) are identical and the full delay coupling (8.3) is non-invasive, the synchronization manifold $\mathcal{M}$ is forward invariant under the dynamics (8.1),(8.3). However, for the invasive transmission delay coupling (8.3), we need an additional assumption that ensures $\mathcal{M}$ to be forward invariant under the time-delayed coupled systems (8.1),(8.2). The least restrictive assumption for $\mathcal{M}$ being forward invariant under (8.1),(8.2) is that

$$\sum_{j \in \mathcal{N}_i} a_{ij} = 1 \text{ for all } i \in \mathcal{V}.$$

See Proposition 1 in Ref. [132] for further details. From now on, it is supposed that the above assumption is always satisfied for systems interacting through the transmission delay coupling (8.2).

8.2.1 Synchronization

So far, we have given conditions which ensure that the synchronization manifold $\mathcal{M}$ is forward invariant under the dynamics of the closed-loop dynamics (8.1),(8.2) and (8.1),(8.3). Next, we present conditions for the synchronization manifold $\mathcal{M}$ to contain an asymptotically stable subset. Clearly, asymptotic stability of (a subset) of $\mathcal{M}$ implies that the network of time-delayed coupled systems synchronizes.

Theorem 8.1. [132]. *Consider a network of k coupled systems* (8.1),(8.2) *or* (8.1),(8.3) *on a simple and strongly connected graph $\mathcal{G} = (\mathcal{V}, \mathcal{E}, A)$. Assume that:*

(H8.1) *The solutions of the coupled systems are uniformly ultimately bounded.*

(H8.2) *There exists a positive definite matrix $P \in \mathbb{R}^{(n-m)\times(n-m)}$ such that the eigenvalues of the symmetric matrix*

$$P\left(\frac{\partial q}{\partial z_i}(z_i, y_i)\right) + \left(\frac{\partial q}{\partial z_i}(z_i, y_i)\right)^T P,$$

are uniformly negative and bounded away from zero for all $z_i \in \mathbb{R}^{n-m}$ and $y_i \in \mathbb{R}^m$.

Then, there exist positive constants $\bar{\gamma}$ and $\bar{\chi}$ such that, if $\gamma \geq \bar{\gamma}$ and $\gamma\tau \leq \bar{\chi}$, then (a subset of) the synchronization manifold $\mathcal{M}$ is globally asymptotically stable for (8.1),(8.2) *or* (8.1),(8.3).

Remark 8.2. *The values of $\bar{\gamma}$ and $\bar{\chi}$ depend on the dynamics of the systems, the type of coupling* (*either* (8.2) *or* (8.3)), *and the network topology.*

In Theorem 8.1, it is assumed that the coupled systems have uniformly ultimately bounded solutions. Conditions (at the level of the systems) for this uniform ultimate boundedness are provided in Appendix B. Condition (H8.2) implies that the subsystem (8.1a) is an *exponentially convergent* system with input y_i. Such an exponentially convergent system has a unique exponentially stable steady state solution that depends on the driving input y_i, but not on the initial data $z_i(t_0)$. Roughly speaking, *an exponentially convergent system "forgets" its initial conditions exponentially fast*. It follows that given two exponentially convergent systems defined by the same function $q(\cdot)$, but driven by different inputs y_i and y_j, if $|y_i(t) - y_j(t)| \to 0$ as $t \to \infty$, then $|z_i(t) - z_j(t)| \to 0$ as $t \to \infty$. This implies that if all outputs y_i of the systems (8.1) synchronize, then all "internal states" z_i synchronize. For a precise definition of *convergent systems* see Section 1.4.3.

We remark that our results on uniform ultimate boundedness of solutions of networks with full delay coupling (8.3) involve an upper bound $\gamma_{\max}$ on the coupling strength γ, see Appendix B. Then, if the results presented in the appendix are used to ensure uniform ultimate boundedness of (8.1),(8.3), we have to impose the additional constraint $\gamma < \gamma_{\max}$ in Theorem 8.1.

8.2.2 Partial Synchronization

Partial synchronization is a form of incomplete network synchronization characterized by synchronized activity in clusters of systems. In other words, we say that a network shows partial synchronization if the states of at least two systems, but not all of them, asymptotically match, i.e., $x_i(t) \to x_j(t)$ as $t \to \infty$, for at least two systems i and j, $i, j \in \mathcal{V}$, but not all of them. Synchronization in networks of time-delayed coupled systems is associated with the asymptotic stability of the forward invariant synchronization manifold $\mathcal{M}$. Similarly, for partial synchronization, we need a forward invariant *partial synchronization manifold* $\mathcal{P}$ to be asymptotically stable. It turns out to be convenient to parametrize such a partial synchronization manifold in terms of a $k \times k$ permutation matrix Π. Particularly, for a given permutation matrix $\Pi \in \mathbb{R}^{k \times k}$, we define

$$\mathcal{P}(\Pi) := \{x \in \mathbb{R}^{kn} | x \in \ker(I_{kn} - \Pi \otimes I_n)\}.$$

We always assume that $\Pi \neq I_k$ and

$$\Pi \neq \begin{pmatrix} 0 & 1 & 0 & \cdots & 0 \\ 0 & 0 & 1 & \ddots & \vdots \\ \vdots & \vdots & \ddots & \ddots & 0 \\ 0 & 0 & \cdots & 0 & 1 \\ 1 & 0 & \cdots & 0 & 0 \end{pmatrix},$$

that is, we omit permutation matrices that define manifolds corresponding to synchronization of none of the systems and full synchronization.

Lemma 8.3. [137]. *Consider k systems* (8.1) *on a simple and strongly connected graph $\mathcal{G} = (\mathcal{V}, \mathcal{E}, A)$. Then, for a given permutation matrix $\Pi \in \mathbb{R}^{k \times k}$, the manifold $\mathcal{P}(\Pi)$ is forward invariant with respect to the dynamics of transmission delay coupled systems* (8.1),(8.2*) if and only if one of the following conditions is satisfied:*

i. $\ker(I - \Pi)$ *is a right invariant subspace of A.*

ii. There exists a matrix $X_A \in \mathbb{R}^{k \times k}$ that solves

$$(I - \Pi)A = X_A(I - \Pi).$$

The manifold $\mathcal{P}(\Pi)$ is forward invariant with respect to the dynamics of full delay coupled systems (8.1),(8.3) *if and only if one of the following conditions is satisfied:*

iii. $\ker(I - \Pi)$ *is a right invariant subspace of L.*

iv. There exists a matrix $X_L \in \mathbb{R}^{k \times k}$ that solves

$$(I - \Pi)L = X_L(I - \Pi).$$

In case the matrices Π and A (Π and L) commute, i.e., $\Pi A = A\Pi$ ($\Pi L = L\Pi$), then $X_A = A$ ($X_L = L$) solves the matrix equation of condition *ii* (condition *iv*). In this case, the matrix Π can be thought of as a re-labeling of the nodes, in such a way that the network before and after the re-labeling is identical. Condition *i* (condition *iii*) can be used to construct a permutation matrix Π that defines a partial synchronization manifold from repeated patterns in the right eigenvectors of the matrix A (L). Condition *ii* (condition *iv*) is particularly useful for the assessment of asymptotic stability of the forward invariant partial synchronization manifold $\mathcal{P}(\Pi)$.

Theorem 8.4. [135]. *Consider a network of k systems* (8.1) *on a simple and strongly connected graph $\mathcal{G} = (\mathcal{V}, \mathcal{E}, A)$. Assume that* (H8.1) *and* (H8.2) *of Theorem 8.1 are satisfied.*

(H8.3) *Let $\Pi \in \mathbb{R}^{k\times k}$ be a permutation matrix that satisfies condition* i *(hence condition* ii*) of Lemma 8.3 and suppose that there exists a positive constant c^* such that*

$$(I-\Pi)^T\big(I - \tfrac{1}{2}(X_A^T + X_A)\big)(I-\Pi) \geq c^*(I-\Pi)^T(I-\Pi).$$

(H8.4) *Let $\Pi \in \mathbb{R}^{k\times k}$ be a permutation matrix that satisfies condition* iii *(hence condition* iv*) of Lemma 8.3 and suppose that there exists a positive constant c' such that*

$$(I-\Pi)^T\big(\tfrac{1}{2}(X_L^T + X_L)\big)(I-\Pi) \geq c'(I-\Pi)^T(I-\Pi).$$

If (H8.3) *holds, then there exist positive constants γ^* and χ^* such that if $\gamma \geq \gamma^*$ and $\gamma\tau \leq \chi^*$, then (a subset of) the partial synchronization manifold $\mathcal{P}(\Pi)$ is globally asymptotically stable for* (8.1),(8.2).

If (H8.4) *holds, then there exist positive constants γ' and χ' such that if $\gamma \geq \gamma'$ and $\gamma\tau \leq \chi'$, then (a subset of) the partial synchronization manifold $\mathcal{P}(\Pi)$ is globally asymptotically stable for* (8.1),(8.3).

Remark 8.5. *The threshold values γ^* and χ^* (γ' and χ') depend on the dynamics of the systems, the type of coupling (either* (8.2) *or* (8.3)*), and the network topology. See the proofs of Theorem 5 and Theorem 6 in Ref. [135] for further details.*

The problem of finding the constant c^* (or constant c') specified in Theorem 8.4 can be solved using singular value decomposition, see Ref. [106]. We remark that the conditions for the occurrence of *synchronization* and *partial synchronization* at the level of the dynamics of the individual systems coincide. Whether systems in a network partially synchronize or fully synchronize depends in large extend on the network topology and the values of coupling strength and time-delay. It may happen that two partial synchronization manifolds are asymptotically stable for the same values of coupling strength and time-delay. In fact, it may happen that the conditions for all possible partial synchronization manifolds to be stable coincide with the conditions for the synchronization manifold $\mathcal{M}$ to be stable. Thus to have partial synchronization in a network of systems (8.1),(8.2) (or (8.1),(8.3)), we require at least that one of the following two conditions is satisfied:

- $\gamma^* < \bar{\gamma}$ ($\gamma' < \bar{\gamma}$);
- $\chi^* > \bar{\chi}$ ($\chi' > \bar{\chi}$).

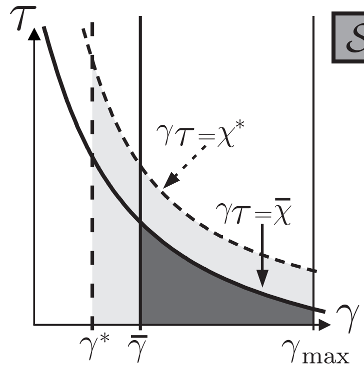

Figure 8.1 The dark gray area represents the full synchronization region. The lighter gray area represents the partial synchronization region.

An example where partial synchronization can be observed is schematically depicted in Figure 8.1. For network structures defined by undirected graphs $\mathcal{G} = (\mathcal{V}, \mathcal{E}, A)$ with symmetric adjacency matrix A, it is possible to derive necessary conditions for the above inequalities to be satisfied. These conditions can be found in Appendix B.

8.2.3 Condition for synchronization in relation to the network topology

Let $L = L^\top$ be the Laplacian matrix of a simple and strongly connected undirected graph $\mathcal{G}$, and order the eigenvalues of L as

$$0 = \lambda_1 < \lambda_2 \leq \ldots \leq \lambda_k.$$

It is shown in Ref. [130] that for any network with a symmetric Laplacian matrix L, the values of coupling strength γ and time-delay τ for which full delay coupled systems (8.1),(8.3) synchronize can be determined from the non-zero eigenvalues of L and the values of coupling strength and time-delay for which two coupled systems (8.1),(8.3) synchronize. In particular, given *two* symmetrically coupled systems (8.1),(8.3), if the conditions (H8.1) and (H8.2) of Theorem 8.1 are satisfied, there exists a non-empty set

$$\mathcal{S}^* := \{(\gamma, \tau) \in \mathbb{R}_{>0} \times \mathbb{R}_{\geq 0} | \bar{\gamma} \leq \gamma < \gamma_{\max} \text{ and } \gamma\tau \leq \bar{\chi}\},$$

such that for any $(\gamma, \tau) \in \mathcal{S}^*$ the two coupled systems synchronize. We refer to this set $\mathcal{S}^*$ as the *synchronization region* of two full delay coupled systems.

Theorem 8.6. [130]. *Consider a network of $k > 2$ coupled systems* (8.1),(8.3) *on an undirected graph $\mathcal{G} = (\mathcal{V}, \mathcal{E}, A)$ with symmetric adjacency matrix A. Suppose that the conditions* (H8.1) *and* (H8.2) *of Theorem 8.1 are satisfied and let $\mathcal{S}^*$ be the synchronization region of two full delay coupled systems* (8.1). *Then, the network of $k > 2$ systems* (8.1),(8.3) *synchronizes if $(\gamma, \tau) \in \mathcal{S}_2 \cap \mathcal{S}_k$, where*

$$\mathcal{S}_j := \left\{ \left(\tfrac{\lambda_j}{2}\gamma, \tau \right) \in \mathcal{S}^* \right\},$$

with λ_2 and λ_k the smallest non-zero and the largest eigenvalues of the symmetric Laplacian matrix L, respectively.

In other words, Theorem 8.6 states that for any undirected network of full delay coupled semipassive systems, the values of coupling strength and time-delay for which the network synchronizes can be found by taking the intersection of $\mathcal{S}_2$ and $\mathcal{S}_k$, where, for $j = 2, k$, $\mathcal{S}_j$ is a copy of $\mathcal{S}^*$ that is scaled by a factor $\frac{2}{\lambda_j}$ over the γ-axis.

8.3 The Experimental Setup

We test the theoretical results presented in the previous section in an experimental setup of time-delayed coupled Hindmarsh-Rose neurons. The Hindmarsh-Rose model [51] is given by the following set of ordinary differential equations:

$$\begin{cases} \dot{z}_{i,1} = 1 - 5y_i^2 - z_{i,1}, \\ \dot{z}_{i,2} = 0.005(4(y_i + 1.6180) - z_{i,2}), \\ \dot{y}_i = -y_i^3 + 3y_i^2 + z_{i,1} - z_{i,2} + E + u_i, \end{cases} \tag{8.4}$$

where $y_i \in \mathbb{R}$ is the output of the ith neuron, which represents its membrane potential, $z_i := \mathrm{col}(z_{i,1}, z_{i,2}) \in \mathbb{R}^2$ are the internal states, $u_i \in \mathbb{R}$ is an external input channel, which can be used to communicate with other neurons, and $E \in \mathbb{R}$ is a constant parameter. For zero external input, $u_i \equiv 0$, depending on the value of parameter E the membrane potential of the Hindmarsh-Rose neuron is either constant or spiking, i.e., a rapid rise and fall of the membrane potential, or bursting, where the neuron produces a number of spikes followed by a period of quiescence. We set $E = 3.3$, for which the Hindmarsh-Rose neuron operates in a *chaotic bursting mode*. As it is proved in [130, 136], independently of the value of E, the Hindmarsh-Rose neuron is strictly $\mathcal{C}^1$-semipassive with a quadratic storage function $V(z_i, y_i)$ and the function $H(z_i, y_i)$ being fourth-degree in y_i and quadratic in z_i. Using Theorem B.4 and Theorem B.5 in Appendix B, it can be shown that for every finite coupling strength γ, the solutions of the coupled Hindmarsh-Rose neurons are uniformly ultimately bounded. Moreover, as proved in [130, 136], the internal dynamics of the Hindmarsh-Rose neuron satisfies condition (H8.2) with matrix $P = I_2$, which implies that its internal dynamics is an exponentially convergent system with input y_i. Thus, the Hindmarsh-Rose neuron satisfies all assumptions at the level of the systems, and we conclude that synchronization and partial synchronization in networks of time-delayed coupled Hindmarsh-Rose neurons should happen when the coupling strength γ and time-delay τ are chosen appropriately.

8.3.1 A circuit realization of the Hindmarsh-Rose neuron model

An electronic circuit board with off-the-shelf components (resistors, capacitors, operational amplifiers, and analog voltage multipliers) is designed to mimic the dynamics of the Hindmarsh-Rose neuron (8.4). To ensure that the signals $z_{i,1}$, $z_{i,2}$, and y_i are in the (linear) operating range of the components of the circuit board, we redefine the variables t, $z_{i,1}$, $z_{i,2}$, and y_i:

$$
\begin{aligned}
t &\mapsto 100t, \\
z_{i,1} &\mapsto \tfrac{1}{5}(z_{i,1} + 4), \\
z_{i,2} &\mapsto z_{i,2} - 6, \\
y_i &\mapsto y_i - 1,
\end{aligned}
$$

and obtain

$$
\begin{cases}
\dot{z}_{i,1} = 100(-y_i^2 - 2y_i - z_{i,1}), \\
\dot{z}_{i,2} = 0.5(4y_i + 4.472 - z_{i,2}), \\
\dot{y}_i = 100\big(-y_i^3 + 3y_i - 8 + 5z_{i,1} - z_{i,2} + E + u_i\big).
\end{cases}
\tag{8.5}
$$

Because the change of variables is linear and invertible, we conclude that (8.5) is strictly $\mathcal{C}^1$-semi-passivity and its internal dynamics is exponentially convergent. Figure 8.2(a) shows the electronic circuit board that implements the equations (8.5). A detailed description of the circuit diagram can be found in [82]. Each state, $z_{i,1}$, $z_{i,2}$, and y_i can be measured as a voltage on one of the five coaxial connectors shown in Figure 8.2(a) at the right-side of the circuit board. The remaining two coaxial connectors are there to set the value of parameter E and provide the circuit its input signal u_i. Figure 8.3(a) shows the states $z_{i,1}$, $z_{i,2}$, and y_i of (8.5) obtained by numerical integration of the equations in Matlab®, and Figure 8.3(b) shows recorded states $z_{i,1}$, $z_{i,2}$, and y_i of an electrical circuit realization of equations (8.5). There is a good qualitative match of measured signals and those obtained though numerical integration. Both the circuits and the mathematical model show irregular bursting behavior and the time-scales and

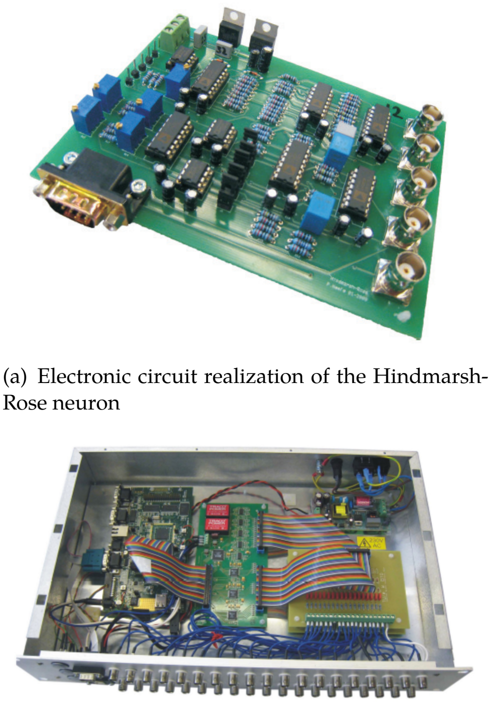

(a) Electronic circuit realization of the Hindmarsh-Rose neuron

(b) Coupling interface

Figure 8.2 The hardware.

amplitudes of the signals are nearly in the same range. In the remaining part of this chapter, we only show the outputs y_i of the Hindmarsh-Rose neurons. Recall that because the internal dynamics are exponentially convergent, synchronized outputs imply synchronized internal dynamics, and hence, synchronized states $x_i := \mathrm{col}(z_{i,1}, z_{i,2}, y_i)$.

8.3.2 The coupling interface and data acquisition

The network topology and coupling functions (8.2) or (8.3) are specified in the *coupling interface* depicted in Figure 8.2(b). This coupling interface allows us to construct networks with up to sixteen Hindmarsh-Rose neurons. The input and output channels of the Hindmarsh-Rose circuit boards are connected (via coaxial cables) to the coupling interface, which samples the outputs y_i of the connected circuits (with 16 bit resolution over a range of -10 [V] to 10 [V]) and returns the

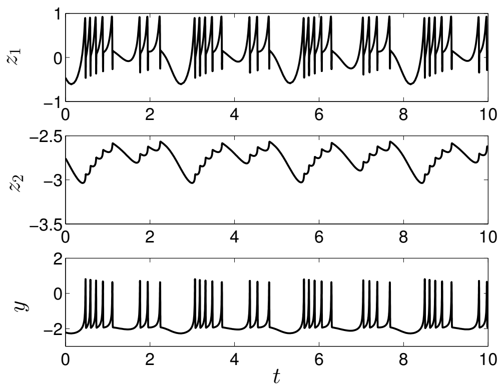

(a) Simulated solutions.

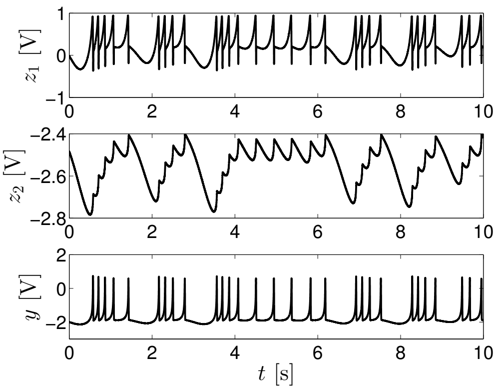

(b) Recorded data.

Figure 8.3 Simulated solutions of (8.4) and recorded data of an electronic Hindmarsh-Rose circuit.

inputs u_i (with 14 bit resolution over a range of -10 [V] to 10 [V]) according to the network topology and coupling functions, which are specified in software loaded to the heart of the coupling interface, a 210 [MHz] Atmel ARM© Thumb©–based AT91SAM9260 microcontroller. The coupling interface operates at a sampling rate of approximately 40 [kHz]. The sampling and updating of the signals happens simultaneously and the maximal throughput delay, which is equal for all connected circuits and less than 80 [μs]. The data (time-traces) from the electronic HR circuits is obtained using a National Instruments PCIe-6363 multifunction data acquisition device with two BNC-2090A connector blocks. This data acquision setup can measure up to thirty-two analog inputs (voltage range -10 [V] to 10 [V], 1 MS/s, 16 bit resolution) and has four analog output channels (voltage range -10 [V] to 10 [V], 2.86 MS/s, 16 bit resolution). We only use one analog output channel to specify E. The software that is used to acquire the data is National Instruments LabVIEW™ 2009 running on a HP wx4600 workstation with a 3.00 GHz Intel® Core™2 Duo CPU and 4 GB ram with Microsoft® Windows® XP Professional operating system. All data is plotted with Matlab® from The MathWorks, Inc.

8.4 Practical Synchronization of Coupled Hindmarsh-Rose Circuits

Because of the inherent imperfections of the experimental setup, we can not expect that differences between the outputs (and states) of circuits converge asymptotically to zero. It is necessary to allow for a mismatch between them, which, of course, needs to be small enough in order to consider that the systems are "*practically synchronized*".

Definition 8.7 (Practical synchronization)**.** *Consider k dynamical systems with outputs $y_i \in \mathbb{R}^m$, $i \in \mathcal{V} = \{1, 2, \ldots, k\}$, defined on an interval $[t_0, t_2)$. The k systems are said to be practically synchronized with bound ϵ, if there is a $t_1(\epsilon)$, $t_0 \leq t_1(\epsilon) < t_2$, such that $|y_i(t) - y_j(t)| < \epsilon$ for all $i, j \in \mathcal{V}$ and $t \in [t_1, t_2)$.*

For notational convenience, we fix the value of ϵ and refer to *practical synchronization with bound ϵ* simply as *practical synchronization*. In all the following experiments, we say that the circuits practically synchronize if the eventual difference between the outputs does not exceed $\epsilon = 0.25$ [V]. Although this value of ϵ looks rather large, one has to realize that a small mismatch in the shapes or timing of the spikes results in a relatively large synchronization error. Figure 8.4(a) shows practical synchronization of two circuits using the full delay coupling with $\gamma = 0.55[-]$ and $\tau = 80$ [μs] (the throughput delay). The outputs of the two systems are almost indistinguishable with $\epsilon = 0.25$ [V]. Figure 8.4(b) shows that the synchronization error $y_1 - y_2$ is within the bound $\epsilon = 0.25$ [V] and the errors are the largest when the practically synchronized circuits produce their spikes. Figure 8.5 depicts the practical synchronization regions of the two coupled systems for transmission delay coupling (Figure 8.5(a)) and full delay coupling (Figure 8.5(b)), where we define the practical synchronization region to be the set of all (γ, τ) for which the coupled circuits practically synchronize with bound $\epsilon = 0.25$ [V]. These practical synchronization regions are constructed by, for a fixed value of the time-delay τ, increasing the coupling strength from 0 [-] to 10 [-] and recording the values of γ for which the two coupled systems begin to practically synchronize and for

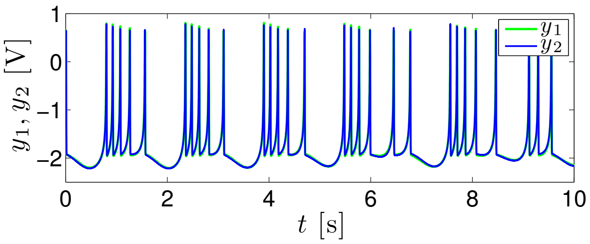

(a)

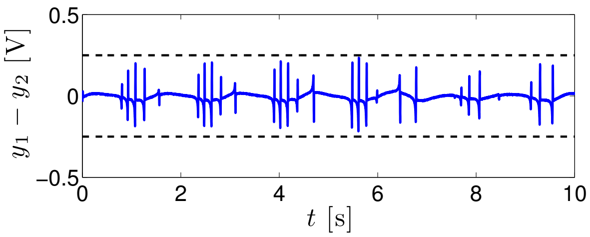

(b)

Figure 8.4 Practical synchronization of two electronic HR circuits for $\gamma = 0.55[-]$ and $\tau = 80$ [μs]. (a) Recorded time-traces of the outputs of the two circuits. (b) Time-trace of the difference in output signals. The dashes horizontal lines correspond to the bounds $\pm\epsilon = \pm 0.25$[V].

which practical synchronization is lost. These points are indicated by the stars in Figures 8.5. The practical synchronization regions, the shaded area in Figure 8.5, are obtained through simple linear interpolation of the measured boundary points (the stars). Results for $\gamma > 10$ [-] can not be presented because of hardware limitations. For values of the coupling strength $\gamma > 10$, we have observed that the coupling signals u_1, u_2 become saturated. The shape of the experimentally determined synchronization regions is a reasonable but not perfect match with the theoretical predictions of Theorem 8.1, which are schematically presented in Figure 8.1. However, we see that the two circuits practically synchronize if the coupling exceeds a certain threshold value. Moreover, for a fixed delay τ, an increase of coupling strength results in loss of practical synchronization but practical synchronization is regained by lowering the value of the delay. There are many reasons why the match between experiments and theory is not perfect. First of all, our theoretical results are sufficient results, which may be too conservative. On the other hand, in the experimental setting, the systems are not perfectly identical, signals are corrupted with noise and some additional errors are introduced because of the sampling of the coupling interface. All these imperfections are not taken into account in the theoretical framework. We emphasize once more that

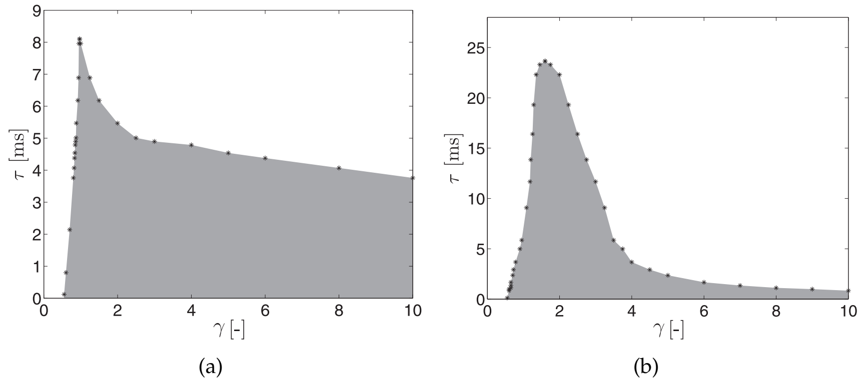

Figure 8.5 Approximated practical synchronization regions (shaded area) for two coupled HR circuits. The stars indicate the measured boundary points. (a) Transmission delay coupling. (b) Full delay coupling.

transmission delay coupling is *invasive*, contrary to the full delay coupling, which is *non-invasive*. Thus, the practically synchronized outputs of two full delay coupled electronic Hindmarsh-Rose circuits look just like the ones depicted in Figure 8.4(a). For transmission delay coupled circuits the shape of the synchronized outputs changes when the values of γ and τ are changed. This is depicted in Figure 8.6, which shows experimental results of practically synchronized outputs of two transmission delay coupled Hindmarsh-Rose circuits for $\gamma = 2$ [-] and $\tau = 2$ [ms], $\gamma = 4$ [-] and $\tau = 2$ [ms], and $\gamma = 2$ [-] and $\tau = 4$ [ms].

8.5 Practical Partial and Full Synchronization of Coupled Hindmarsh-Rose Circuits

We continue with experiments in networks of Hindmarsh-Rose neurons that interact through either transmission delay coupling or full delay coupling. In networks with more than two circuits, we may encounter, at least in theory, the partial synchronization phenomenon. Analogous to the definition of *practical synchronization* we define *practical partial synchronization*:

Definition 8.8 (Practical partial synchronization)**.** *Consider a network of k dynamical systems with outputs $y_i \in \mathbb{R}^m$, $i \in \mathcal{V}$, defined on an interval $[t_0, t_2)$. The network of systems is said to practically partially synchronize with bound ϵ if there is a $t_1 = t_1(\epsilon)$, $t_0 \leq t_1(\epsilon) < t_2$, such that $|y_i(t) - y_j(t)| < \epsilon$ holds for all $t \in [t_1, t_2)$ and at least two but not all $i, j \in \mathcal{V}$, $i \neq j$.*

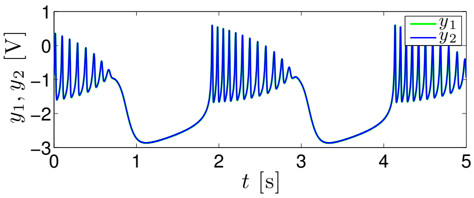

(a) $\gamma = 2$ [-], $\tau = 2$ [ms].

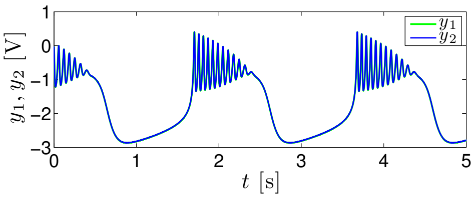

(b) $\gamma = 4$ [-], $\tau = 2$ [ms].

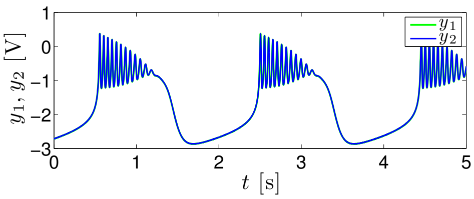

(c) $\gamma = 2$ [-], $\tau = 4$ [ms].

Figure 8.6 Trajectories of two practically synchronized transmission delay coupled Hindmarsh-Rose circuits for different values of γ and τ.

As before, we fix $\epsilon = 0.25$ [V] and refer to *practical partial synchronization with bound* ϵ as *practical partial synchronization*. We present three experimental studies on practical (partial) synchronization for:

1. The network shown in Figure 8.7 with four transmission delay coupled Hindmarsh-Rose neurons.

2. The network shown in Figure 8.10 with four transmission delay coupled Hindmarsh-Rose neurons.

3. The network shown in Figure 8.13 with ten full delay coupled Hindmarsh-Rose neurons.

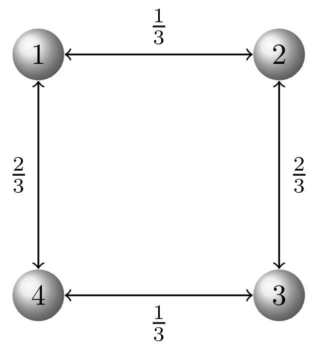

Figure 8.7 The network topology for practical (partial) synchronization of experiment 1.

8.5.1 Experiment 1

Consider four transmission delay coupled HR circuits with the network topology depicted in Figure 8.7. This network topology is taken from [134], where it is shown, theoretically and using numerical simulations, that this network exhibits partial synchronization. It is easy to verify that each permutation matrix

$$\Pi_1 = \begin{pmatrix} \mathcal{J} & \mathbf{0} \\ \mathbf{0} & \mathcal{J} \end{pmatrix}, \quad \Pi_2 = \begin{pmatrix} \mathbf{0} & I_2 \\ I_2 & \mathbf{0} \end{pmatrix}, \quad \Pi_3 = \begin{pmatrix} \mathbf{0} & \mathcal{J} \\ \mathcal{J} & \mathbf{0} \end{pmatrix},$$

where $\mathbf{0} = \mathbf{0}_{2\times 2}$ and

$$\mathcal{J} = \begin{pmatrix} 0 & 1 \\ 1 & 0 \end{pmatrix},$$

commutes with the weighted adjacency matrix

$$A = \frac{1}{3}\begin{pmatrix} 0 & 1 & 0 & 2 \\ 1 & 0 & 2 & 0 \\ 0 & 2 & 0 & 1 \\ 2 & 0 & 1 & 0 \end{pmatrix}.$$

By Lemma 8.3, $\mathcal{P}(\Pi_1)$, $\mathcal{P}(\Pi_2)$, and $\mathcal{P}(\Pi_3)$ are partial synchronization manifolds. The manifold $\mathcal{P}(\Pi_1)$ is associated with partial synchronization of neurons 1 and 2, respectively, neurons 3 and 4, manifold $\mathcal{P}(\Pi_2)$ corresponds to partial synchronization of neurons 1 and 3, respectively, neurons 2 and 4. Finally, manifold $\mathcal{P}(\Pi_3)$ defines partial synchronization of neurons 1 and 4, respectively, neurons 2 and 3. It is shown in [134], Section 7A, that the conditions for a (subset of) $\mathcal{P}(\Pi_1)$ to be stable coincide with the conditions for full synchronization. One can verify this using Proposition B.6 in the Appendix B. It can be shown, using numerical

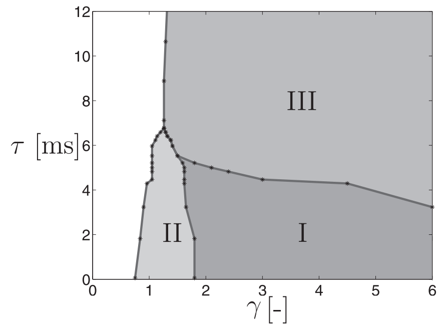

Figure 8.8 Practical partial synchronization region for four transmission delay coupled HR circuits with network structure shown in Figure 8.7. Crosses ($*$) indicate measured boundary points of a practical (partial) synchronization regimes. I. Practical synchronization, II. Practical partial synchronization of circuits 1 and 4, respectively, circuits 2 and 3, III. Practical partial synchronization of circuits 1 and 3, respectively, circuits 2 and 4.

simulations, that there exist values for the coupling strength γ and time-delay τ for which $\mathcal{P}(\Pi_2)$ and $\mathcal{P}(\Pi_3)$ are stable without having full synchronization. As it is shown below, our experiments confirm the theoretical and numerical findings presented in [134]. We have explored the (γ, τ)-parameter space to identify the regions of practical synchronization and practical partial synchronization. Figure 8.8 depicts the results of these experiments. It is worth mentioning that our theoretical results imply the existence of a constant $\chi^* > 0$ such that circuits 1 and 3, respectively, circuits 2 and 4 partially synchronize for $\gamma\tau \leq \chi^*$ (provided $\gamma \geq \gamma^*$), but, as we did not encounter a loss of practical partial synchronization when τ was increased, our experiments seem to imply that this bound is not sharp. Figure 8.9 shows outputs of the practically partially synchronized Hindmarsh-Rose circuits for different values of γ and τ. The top panel of Figure 8.9(a) shows practically partially synchronized outputs of the Hindmarsh-Rose circuits for $\gamma = 1.2$ [-], $\tau = 2$ [ms] (parameters in region II in Figure 8.8). The four smaller plots provide an alternative graphical representation of practical partial synchronization. In these a plots, we see that two circuits i and j are practically synchronized if their outputs y_i [V] and y_j [V] are within an 2ϵ-band centered around the diagonal in the (y_i, y_j)-plane. The diagonal and the bounds for practical synchronization are indicated by the dotted and dashed lines, respectively. These four plots show clearly the practical partial synchronization of circuits 1 and 4, respectively, circuits 2 and 3. Figure 8.9(b) shows the outputs of the four transmission delay coupled Hindmarsh-Rose circuits for $\gamma = 4$ [-] and $\tau = 8$ [ms] (parameters in region III in Figure 8.8), for which circuits 1 and 3, respectively, circuits 2 and 4 practically partially synchronize.

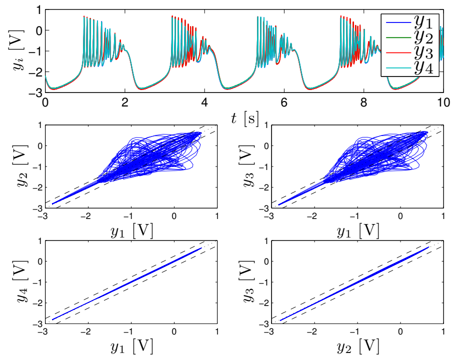

(a)

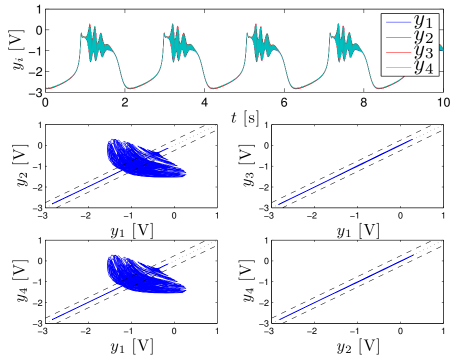

(b)

Figure 8.9 Outputs of practically partially synchronized Hindmarsh-Rose circuits. (a) Practical partial synchronization of circuits 1 and 4, respectively, 2 and 3 for $\gamma = 1.2$ [-] and $\tau = 2$ [ms]. (b) Practical partial synchronization of circuits 1 and 3, respectively, 2 and 4 for $\gamma = 4$ [-] and $\tau = 8$ [ms].

8.5.2 Experiment 2

Consider four Hindmarsh-Rose circuits with full delay coupling on the network depicted in Figure 8.10. The Laplacian matrix is given by

$$L = \frac{1}{3}\begin{pmatrix} 3 & -1 & -1 & -1 \\ -1 & 2 & -1 & 0 \\ -1 & -1 & 2 & 0 \\ -1 & 0 & 0 & 1 \end{pmatrix}.$$

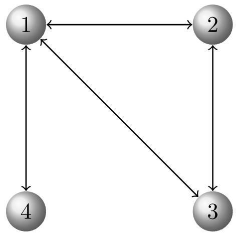

Figure 8.10 The network topology for practical (partial) synchronization experiment 2. All edges have weight $\frac{1}{3}$.

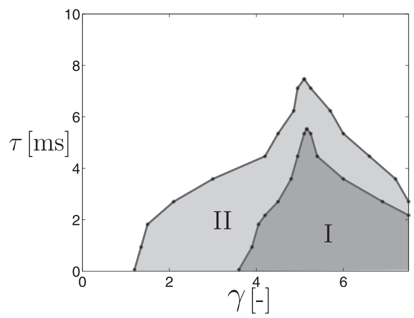

Figure 8.11 Practical partial synchronization region for four full delay coupled Hindmarsh-Rose circuits with network structure shown in Figure 8.10. Crosses ($*$) indicate measured boundary points of the practical (partial) synchronization regimes. (I) Practical full synchronization, (II) Practical partial synchronization of circuits 2 and 3.

The permutation matrix

$$\Pi = \begin{pmatrix} 1 & 0 & 0 & 0 \\ 0 & 0 & 1 & 0 \\ 0 & 1 & 0 & 0 \\ 0 & 0 & 0 & 1 \end{pmatrix},$$

commutes with L; hence, by Lemma 8.3, $\mathcal{P}(\Pi)$ is a partial synchronization manifold that corresponds to partial synchronization of circuits 2 and 3. In Section 6 of [134], Example 3 shows that this partial synchronization manifold can be asymptotically stable for values of the coupling strength and time-delay that do not coincide with those for which we find full synchronization. One can verify this using Proposition B.7 in Appendix B. The experimentally determined practical (partial) synchronization region for the four full delay coupled Hindmarsh-Rose circuits is shown in Figure 8.11. Figure 8.12 shows output trajectories of the partially practically synchronized Hindmarsh-Rose circuits for $\gamma = 3$ [-] and $\tau = 1.5$ [ms]. Note that the parameter region that corresponds to practical full synchronization of the network is enclosed in the parameter region for partial practical

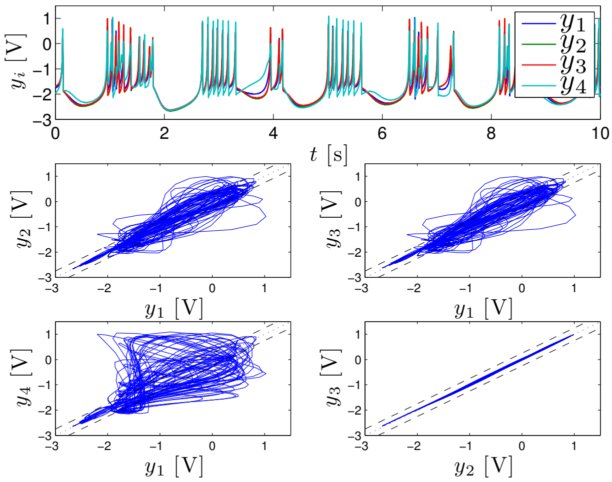

Figure 8.12 Outputs of partially practically synchronized full delay coupled Hindmarsh-Rose circuits 2 and 3 for $\gamma = 3$ [-] and $\tau = 1.5$ [ms] (region II in Figure 8.11).

synchronization of circuits 2 and 3, which is theoretically predicted in [134].

8.5.3 Experiment 3

Consider ten full delay coupled Hindmarsh-Rose circuits on the network topology shown in Figure 8.13. This network topology, which we refer to as the "sandglass network", is introduced in [82] to study partial synchronization of delay-free coupled Hindmarsh-Rose neurons. The Laplacian matrix of the sandglass network is

$$L = \frac{1}{2}\begin{pmatrix} 2 & -1 & 0 & -1 & 0 & 0 & 0 & 0 & 0 & 0 \\ -1 & 4 & -1 & -1 & -1 & 0 & 0 & 0 & 0 & 0 \\ 0 & -1 & 2 & 0 & -1 & 0 & 0 & 0 & 0 & 0 \\ 0 & -1 & 0 & 5 & -1 & -1 & -1 & 0 & 0 & 0 \\ 0 & -1 & -1 & -1 & 5 & -1 & -1 & 0 & 0 & 0 \\ 0 & 0 & 0 & -1 & -1 & 5 & -1 & -1 & -1 & 0 \\ 0 & 0 & 0 & -1 & -1 & -1 & 5 & 0 & -1 & -1 \\ 0 & 0 & 0 & 0 & 0 & -1 & 0 & 2 & -1 & 0 \\ 0 & 0 & 0 & 0 & 0 & -1 & -1 & -1 & 4 & -1 \\ 0 & 0 & 0 & 0 & 0 & 0 & -1 & 0 & -1 & 2 \end{pmatrix}.$$

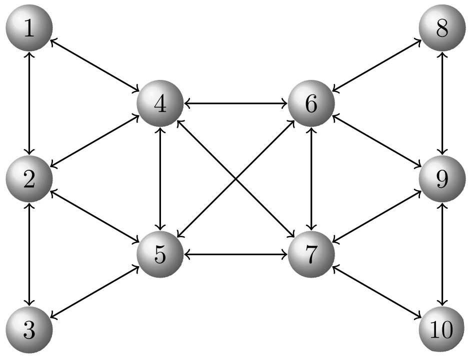

Figure 8.13 The sandglass network topology for (partial) practical synchronization experiment 3. All edges have weight $\frac{1}{2}$.

We remark that $\max_i \sum_{j \in \mathcal{N}_i} a_{ij} = \frac{5}{2}$, which violates our assumption $\max_i \sum_{j \in \mathcal{N}_i} a_{ij} = 1$. This violation is done for practical purposes; when $\max_i \sum_{j \in \mathcal{N}_i} a_{ij} = 1$, the coupling strength that is required for practical synchronization of all circuits would already be close to the maximal coupling strength in the experimental setup ($\gamma = 10$ [-]). Moreover, from a theoretical point of view, the factor $\frac{5}{2}$ could be absorbed in the coupling strength γ (by re-defining γ); hence, violating the assumption of $\max_i \sum_{j \in \mathcal{N}_i} a_{ij} = 1$ has no consequences for our theoretical results. Of course, we have to redefine $\gamma_{\max}$, $\bar{\gamma}$, $\bar{\chi}$, γ' and χ' accordingly. The sandglass network contains a lot of partial synchronization manifolds. The permutation matrices that correspond to

- swapping of 1 and 8, 2 and 9, 3 and 10, 4 and 6, 5 and 7;
- swapping of 1 and 10, 2 and 9, 3 and 8, 4 and 7, 5 and 6;
- swapping 1 and 3 while keeping the others fixed;
- swapping 4 and 5 while keeping the others fixed;
- swapping 6 and 7 while keeping the others fixed;
- swapping 8 and 10 while keeping the others fixed;

and any combination of the latter four, e.g., simultaneous swapping of 1 and 3, and 4 and 5, define partial synchronization manifolds, which can be verified using Lemma 8.3. The Laplacian matrix of the sandglass network has eigenvalues

$$\begin{array}{llll} \lambda_1 = 0, & \lambda_2 = 0.39, & \lambda_3 = \lambda_4 = 0.88, & \lambda_5 = 1.5, \\ \lambda_6 = 2.22, & \lambda_7 = 2.5, & \lambda_8 = \lambda_9 = 3.11, & \lambda_{10} = 3.37, \end{array}$$

with corresponding eigenvectors

$$
\begin{aligned}
\mu_1 &= \mathbf{1}_{10\times 1}, \\
\mu_2 &= \begin{pmatrix} a_2 & b_2 & a_2 & c_2 & c_2 & -c_2 & -c_2 & -a_2 & -b_2 & -a_2 \end{pmatrix}^T, \\
\mu_3 &= \begin{pmatrix} a_3 & 0 & -a_3 & b_3 & -b_3 & c_3 & -c_3 & d_3 & 0 & -d_3 \end{pmatrix}^T, \\
\mu_4 &= \begin{pmatrix} a_4 & 0 & -a_4 & b_4 & -b_4 & c_4 & -c_4 & d_4 & 0 & -d_4 \end{pmatrix}^T, \\
\mu_5 &= \begin{pmatrix} a_5 & 0 & a_5 & -a_5 & -a_5 & -a_5 & -a_5 & a_5 & 0 & a_5 \end{pmatrix}^T, \\
\mu_6 &= \begin{pmatrix} a_6 & b_6 & a_6 & c_6 & c_6 & -c_6 & -c_6 & -a_6 & -b_6 & -a_6 \end{pmatrix}^T, \\
\mu_7 &= \begin{pmatrix} a_7 & b_7 & a_7 & a_7 & a_7 & a_7 & a_7 & a_7 & b_7 & a_7 \end{pmatrix}^T, \\
\mu_8 &= \begin{pmatrix} a_8 & 0 & -a_8 & b_8 & -b_8 & c_8 & -c_8 & d_8 & 0 & -d_8 \end{pmatrix}^T, \\
\mu_9 &= \begin{pmatrix} a_9 & 0 & -a_9 & b_9 & -b_9 & c_9 & -c_9 & d_9 & 0 & -d_9 \end{pmatrix}^T, \\
\mu_{10} &= \begin{pmatrix} a_{10} & b_{10} & a_{10} & c_{10} & c_{10} & -c_{10} & -c_{10} & -a_{10} & -b_{10} & -a_{10} \end{pmatrix}^T,
\end{aligned}
$$

with $a_2, a_3, \ldots, b_2, b_3, \ldots, c_2, c_3 \ldots, d_2, \ldots, d_{10}$, being non-zero constants. The values of these constants are, of course, not arbitrary, but for our purpose there is no need to specify them. We only need to look at the repeating patterns in the eigenvectors. One observes that the linear span of eigenvectors μ_1, μ_2, μ_5, μ_6, μ_7 and μ_{10} is the set $\ker(I - \Pi)$ with permutation matrix

$$
\Pi = \begin{pmatrix}
0 & 0 & 1 & 0 & 0 & 0 & 0 & 0 & 0 & 0 \\
0 & 1 & 0 & 0 & 0 & 0 & 0 & 0 & 0 & 0 \\
1 & 0 & 0 & 0 & 0 & 0 & 0 & 0 & 0 & 0 \\
0 & 0 & 0 & 0 & 1 & 0 & 0 & 0 & 0 & 0 \\
0 & 0 & 0 & 1 & 0 & 0 & 0 & 0 & 0 & 0 \\
0 & 0 & 0 & 0 & 0 & 0 & 1 & 0 & 0 & 0 \\
0 & 0 & 0 & 0 & 0 & 1 & 0 & 0 & 0 & 0 \\
0 & 0 & 0 & 0 & 0 & 0 & 0 & 0 & 0 & 1 \\
0 & 0 & 0 & 0 & 0 & 0 & 0 & 0 & 1 & 0 \\
0 & 0 & 0 & 0 & 0 & 0 & 0 & 1 & 0 & 0
\end{pmatrix}.
$$

Thus, $\ker(I - \Pi)$ is an invariant subspace of L such that, by Lemma 8.3, $\mathcal{P}(\Pi)$ is a partial synchronization manifold. Moreover, Π and L commute and the eigenvectors $\mu_3, \mu_4, \mu_8, \mu_9 \in \text{range}(I - \Pi)$ such that, by Proposition B.7 in Appendix B, we may find partial synchronization of neurons 1 and 3, 4 and 5, 6 and 7, and 8 and 10. A repetition of this procedure shows that this is the only mode of partial synchronization that may be observed in this network. Figure 8.14 shows the experimentally determined practical (partial) synchronization region for the sandglass network. We see that circuits 1 and 3, respectively, 4 and 5, respectively, 6 and 7, respectively, 8 and 10 practically partially synchronize when the

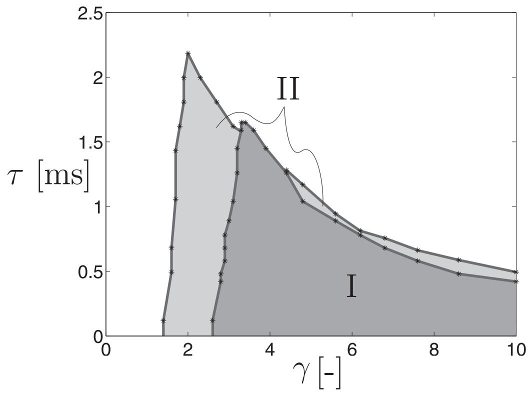

Figure 8.14 Practical partial synchronization region for ten full delay coupled Hindmarsh-Rose circuits on the sandglass network. Crosses ($*$) indicate measured boundary points of the practical (partial) synchronization regimes. (I) practical full synchronization; (II) practical partial synchronization of circuits 1 and 3, respectively, 4 and 5, respectively, 6 and 7, respectively, 8 and 10.

coupling is not strong enough to achieve practical full synchronization and in case the coupling is strong enough for practical full synchronization but the time-delay is too large. The shape of this practical partial synchronization region could have been expected because the smallest (largest) eigenvalue of L with eigenvector in range$(I - \Pi)$ is larger (smaller) than the smallest (largest) eigenvalue of L. Output trajectories of the ten full delay coupled Hindmarsh-Rose circuits with $\gamma = 2$ [-] and $\tau = 1$ [ms] are depicted in Figure 8.15. In particular, Figure 8.15(a) shows clearly that circuits 1 and 3, respectively, 4 and 5, respectively, 6 and 7, respectively, 8 and 10 practically synchronize. Figure 8.15(b) confirms that only these circuits practically partially synchronize. Since the Laplacian matrix L of the sandglass network is symmetric, the practical full synchronization region of full delay coupled Hindmarsh-Rose circuits could have been predicted with the help of Theorem 8.6, from the practical synchronization region $\mathcal{S}^*$ shown in Figure 8.5(b) for two coupled neurons. Indeed, as shown in Figure 8.16, the intersection of two scaled copies $\mathcal{S}_2$ and $\mathcal{S}_{10}$ of that practical synchronization region, i.e. $\mathcal{S}_2$ is a copy of $\mathcal{S}^*$ scaled by a factor $\frac{2}{\lambda_2} = \frac{2}{0.39}$ over the γ-axis and $\mathcal{S}_{10}$ is an other copy of $\mathcal{S}^*$ scaled by the factor $\frac{2}{\lambda_{10}} = \frac{2}{3.3733}$ over the γ-axis, gives a reasonable accurate prediction of the practical full synchronization region for full delay coupled Hindmarsh-Rose circuits on the sandglass network.

8.6 Conclusions

We have reviewed a number of theoretical results on synchronization and partial synchronization in networks of systems that interact via diffusive time-delayed couplings [130, 132, 133]. The predictive value of these theoretical results in practical situations is tested using an experimental setup built around electronic circuit board realizations of networks of Hindmarsh-Rose neurons. To account for the inevitable dissimilarities in the electronic Hindmarsh-Rose circuits, we have introduced the notions of *practical synchronization* and *practical partial synchronization*, which state that the circuits may be called (partially) synchronized if, after some transient time, the differences between their outputs are sufficiently small on a long finite time interval. In a first set of experiments, we have determined the practical synchronization regions for two Hindmarsh-Rose circuits with transmission delay coupling and full delay coupling. In a next set of experiments, we investigated full practical synchronization and partial practical synchronization in networks of Hindmarsh-Rose circuits with transmission delay coupling or full delay coupling. The first two experiments, in this set, used the settings of the numerical studies presented in [134]. The sandglass network topology of the third experiment was introduced in [82]. Lastly, we successfully applied the theory presented in [130] to construct the full practical synchronization region in the sandglass network of full delay coupled Hindmarsh-Rose circuits from the practical synchronization region of two full delay coupled Hindmarsh-Rose circuits. These experimental results indicate that the theoretical results presented in [130, 132, 133], which are derived for networks of noise-free identical systems, can be successfully applied to real-world applications. However, we have also found that these results are not always sharp (see Experiment 1 in Section 8.5). We conclude that our theoretical results can predict network synchronization reasonably well in a *qualitative* sense, but its predictive power at a *quantitative* level may be rather poor. This is because the theory is essentially about the existence of (partial) synchronization in time-delayed coupled networks. Practical applications often require constructive methods that allow for precise computations of the network parameters (coupling strength γ and time-delay τ) for given dynamical systems. The estimates that are computed from the proofs of the results are often conservative. Moreover, although the theory predicts the experimental observations in most cases quite well, a theory that would give us formal predictions for (practical) synchronization in networks of systems that have mismatches and operate under noisy conditions is yet to be developed.

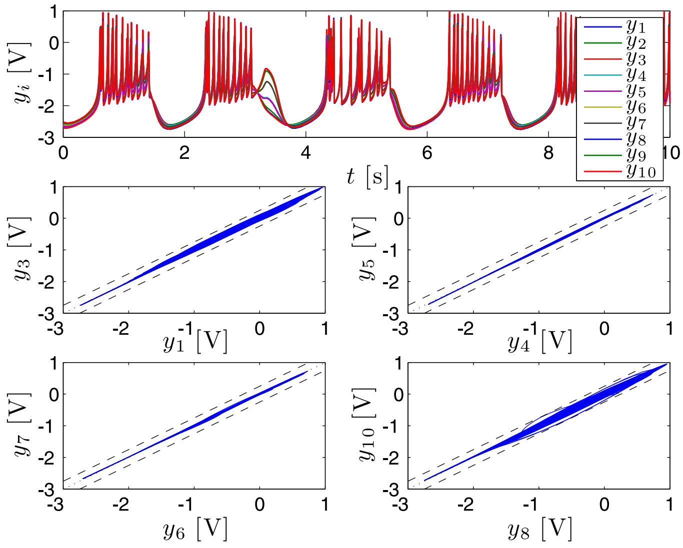

(a)

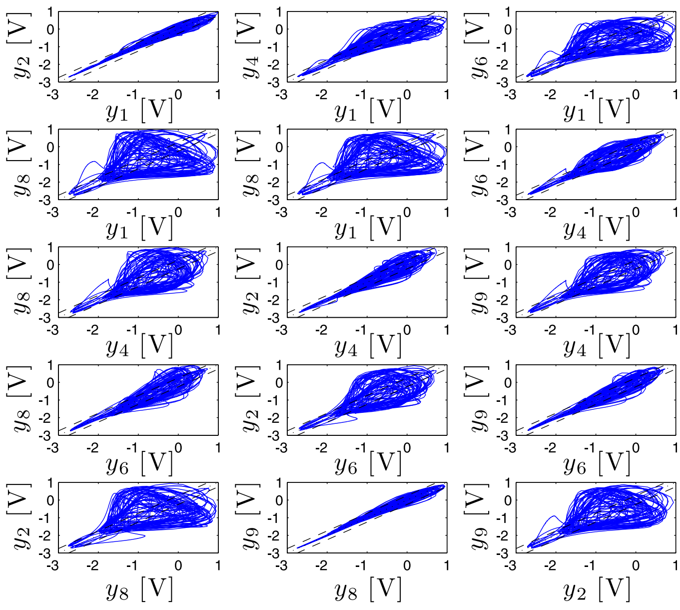

(b)

Figure 8.15 Outputs of practically partially synchronized full delay coupled Hindmarsh-Rose circuits for $\gamma = 2$ [-] and $\tau = 1$ [ms] (region II in Figure 8.14).

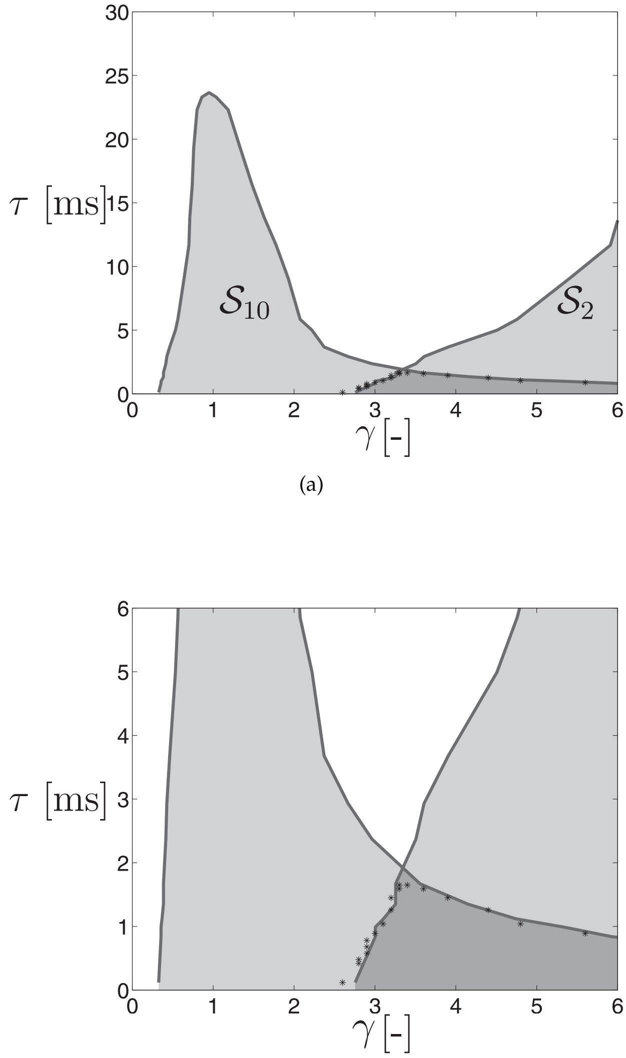

(a)

(b)

Figure 8.16 Construction of the practical full synchronization region for the sandglass network. (a) The scaled copies $\mathcal{S}_2$ and $\mathcal{S}_{10}$ of the practical synchronization region $\mathcal{S}^*$ shown in Figure 8.5(b) (light shade), their intersection $\mathcal{S}_2 \cap \mathcal{S}_{10}$ (dark shade), and the (boundary of the) practical full synchronization region for the sandglass network ($*$). (b) Zoomed version of (a).

Chapter 9

Conclusions and Recommendations

Abstract. The main contributions and results of this thesis are summarized in this chapter. Furthermore, some recommendations for future research directions are provided in the last section.

9.1 Conclusions

In [104, 108], the authors derive sufficient conditions for synchronization in networks of diffusively coupled semipassive systems. In this thesis, using the semipassivity-based framework introduced in [104], we have studied cases where the theory presented in [104, 108] cannot be used to conclude synchronization of the coupled systems. We have proposed different classes of couplings (both static and dynamic) to solve some particular problems of controlled synchronization. Particularly, we have addressed two cases. Firstly, the case when the semipassive (passive) outputs are not available for feedback has been studied. If the measurable outputs are different state functions which do not have the desired properties, namely, semipassivity (passivity) and exponentially convergent internal dynamics (detectability), then the results presented in [104] cannot be applied. We have proposed observer-based couplings to solve this issue. The observer must reconstruct the semipassive (passive) outputs from measurements of the available outputs. Then, using these estimated semipassive (passive) outputs, we interconnect the systems. Secondly, we have studied the possibility of increasing robustness against network-induced delays of the coupled systems by including some dynamics in the couplings. We have proposed predictor-based couplings that, on the one hand, *predict* the future values of the semipassive outputs to compensate for the network-induced delays and, on the other hand, interconnect the systems through these time-ahead estimated signals.

In Chapter 2, using the *passivity* and *detectability* properties of the studied *linear time-invariant systems*, sufficient conditions for synchronization and boundedness of the solutions of the coupled systems interconnected through observer-based diffusive time-delayed couplings have been derived. It has been shown that synchronization can be achieved if the coupling strength γ is sufficiently large, the product $\tau\gamma$ of the time-delay and the coupling strength is sufficiently small, and the origin of the estimation error dynamics is asymptotically stable. We have also derived synchronization conditions in the case when the systems are coupled through *diffusive static time-delayed couplings*.

In Chapter 3, we extend some of the results of Chapter 2 to the nonlinear case. Sufficient conditions for network synchronization and boundedness of the solutions of coupled *semipassive systems* interconnected through *observer-based diffusive couplings* have been derived. Such couplings are constructed by combining nonlinear observers and output interconnection terms. It has been shown that synchronization can be achieved if the coupling strength γ is sufficiently large and the rate of convergence of the observer is sufficiently fast. In general, it is not easy to find a nonlinear observer such that the assumptions of Chapter 3 are satisfied. However, the aim of Chapter 3 is not to give a design method for the observer dynamics but to provide sufficient conditions for network synchronization when the observer is given.

In Chapter 4, an observer design method for the class of systems under study (semipassive systems with exponentially convergent internal dynamics) is provided. We have developed a general tool for constructing two different types of *diffusive dynamic time-delayed couplings* using ideas of *immersion and invariance* (I&I). Sufficient conditions on the systems to be interconnected, the network topology, the observer dynamics, and the time-delay that guarantee (global) state synchronization and boundedness of the solutions of the coupled systems have been derived. We remark that the observer dynamics is assumed to be independent of the time-delay, i.e., the measurable outputs are not subject to time-delay and the delay in the observer-based couplings is only induced when the estimated semipassive outputs are transmitted. Under this assumption, it is possible to maintain a delay-free observer structure while analyzing the effect of transmission delays in the synchronous behavior.

In Chapter 5, we have presented a methodology for studying the possible emergence of partial synchronization in networks of semipassive systems interconnected through *observer-based diffusive dynamic couplings*. It has been shown that symmetries in the network define linear invariant manifolds, which, when being attracting, define modes of partial synchronization. Sufficient conditions that guarantee (global) partial synchronization have been derived.

In Chapter 6, we have derived an extension to the work presented in [56] for constructing nonlinear observers in the case when the output measurements are corrupted with time-delays. Following the framework proposed in [56], we have developed a general methodology which relies on rendering attractive an appropriately selected invariant manifold in the extended state space (the union of the state spaces of the system and the observer). An implicit description of the observer dynamics has been provided in terms of two mappings which must be selected to render the origin of the estimation error dynamics asymptotically stable. This stabilization problem may be difficult to solve, since in general, it relies on the solution of a set of PDEs. However, as shown in the examples, in some cases of practical interest these equations turn out to be solvable. The tools given in Chapter 6 may be directly used to construct more general versions of the observer-based couplings proposed in Chapter 4, i.e., with these techniques, we may also consider time-delays at the level of the observer and not only when transmitting the estimated semipassive outputs. However, this case is not analyzed here and is left for future research.

In Chapter 7 (and in Chapter 2 for the linear case), we have proposed predictor-based dynamic couplings which may enhance robustness against time-delays of the interconnected systems, i.e., these couplings may be capable of increasing the amount of time-delay that can be induced to the systems without compromising the synchronous behavior. Using the notion of semipassivity (passivity), we have provided sufficient conditions which guarantee existence and boundedness of the solutions of the coupled system. Sufficient conditions that guarantee (global) state synchronization have also been derived. Additionally, we have provided a local analysis to illustrate the "mechanism of action" behind our predictor-based couplings. An illustrative simulation example that shows that indeed it is possible to extend the synchronization regions with the proposed control scheme has been presented. While the synchronization regions obtained through *diffusive static couplings* are strongly influenced by the network topology, the synchronization regions obtained with the *predictor-based couplings* are influenced by the topology only for small coupling strength γ. As γ is increased the upper bounds of the synchronization regions are completely determined by the predictor dynamics.

Finally, in Chapter 8, we have reviewed a number of theoretical results on synchronization and partial synchronization in networks of systems that interact through diffusive static time-delayed couplings [130, 132, 133]. The predictive value of these theoretical results is tested in practical situations using an experimental setup built around electronic circuit board realizations of networks of Hindmarsh-Rose neurons. To account for the inevitable dissimilarities of the circuits, we have introduced the notions of *practical synchronization* and *practical partial synchronization*, which state that the circuits may be called practically (partially) synchronized if, after some transient time, the differences between their outputs is sufficiently small on a long finite time interval. In a first set of experiments, we have determined the practical synchronization regions for two Hindmarsh-Rose circuits with transmission delay coupling and full delay coupling. In a next set of experiments, we investigated full practical synchronization and partial practical synchronization in networks of more than two Hindmarsh-Rose circuits with transmission delay coupling or full delay coupling. Lastly, we have successfully applied the theory presented in [130] to construct the full practical synchronization region in the sandglass network of full delay coupled Hindmarsh-Rose circuits from the practical synchronization region of two full delay coupled Hindmarsh-Rose circuits. These experimental results indicate that the theoretical results presented in [130, 132, 133], which are derived for networks of noise-free identical systems, can be successfully applied to real-world applications.

9.2 Recommendations

Throughout this thesis, it has been assumed that the systems are identical, the time-delays are constant, and the topology of the network is fixed. However, as shown in Chapter 8, this setting is unrealistic in practical situations where the systems cannot be expected to be perfectly identical. There may be mismatches in the systems' parameters and/or the signals exchanged among the systems could be contaminated with noise. Moreover, communication losses may lead to time-varying network topologies and the network-induced delays may be time-varying, e.g., due to shared communication networks. Therefore, a natural extension would be to derive conditions for *practical (partial) synchronization* of diffusively time-delayed coupled semipassive systems under the aforemention practical issues. That is, sufficient conditions may be given on the systems with noise and parametric uncertainties, the upper bounds of the time-varying delays, and the time-varying topologies such that the differences between the states of the systems converge to some compact invariant set in finite time. This set must be bounded by a constant $\epsilon \in \mathbb{R}_{>0}$ which has to be small enough to consider that the systems are still synchronized. This kind of complete formal analysis of practical synchronization is missing in the existing literature. Usually, only individual aspects of of these practical issues are considered.

Another recommendation for future work would be to study network synchronization with *prescribed performance*. This means that the synchronization errors should converge to a prespecified arbitrarily small compact set with predefined convergence rate and exhibiting maximum overshoots less than a sufficiently small preassigned constant. The results presented in this thesis focus on asymptotic synchronization of coupled semipassive systems. However, the transient behavior of the synchronization errors is not taken into account. In some applications, it may be required that the coupled systems fulfilled the aforementioned performance specifications; then, designing coupling functions which are capable of inducing synchronization with prescribed performance is certainly an interesting line of research.

In Chapter 7, we have proposed predictor-based couplings to enhance robustness against time-delays of the interconnected systems. In order to be capable of constructing the proposed predictors, the time-delays must be constant and known. Then, a direct extension would be to consider time-varying delays and propose predictors which could be constructed using partial information about these delays, e.g., the upper and lower bounds on both the delays and their time-derivatives. Moreover, the proposed predictor dynamics is a copy of an individual system dynamics driven by some correction term. We construct the predictor in this way in order to take advantage of the stability properties of the systems, namely, *semipassivity* and *convergence*. However, we are certainly not restricted to this class of predictors. For instance, using the immersion and invariance techniques presented in Chapter 6, we may be able to construct predictors with more general structures. Then, if these I&I predictors are designed appropriately, it may be possible to further extend the synchronization regions presented in Chapter 7.

Throughout the thesis, we have proposed observer-based and predictor-based couplings to solve some particular problems of controlled synchronization. Nevertheless, to be able to construct such couplings, the dynamics of the systems must be exactly known. This is unrealistic in practical situations, where there may be parametric uncertainties and/or unmodeled dynamics in the available models. In this situation, the best that can be done is to construct the couplings with the *known* part of the dynamics. However, in this situation, we cannot expect that the systems perfectly synchronize under the proposed control schemes. In the best case, if the uncertainties are sufficiently small (in some appropriate sense), it can be expected that the synchronization errors converge to some compact invariant set. Then, an interesting extension would be to derive adaptive dynamic couplings which compensate for the unmodeled dynamics in the systems and drive the synchronization errors to the origin.

Indeed, there are many more open problems and interesting applications related to synchronization in networks of dynamical systems. Further research of this exciting phenomenon is required to develop advanced techniques that allow us to induce controlled synchronization in the most challenging scenarios.

Appendix A

Proofs

A.1 Proof of Lemma 2.2

First consider the nodes $\{v_1, ..., v_{k_1}\}$, i.e., the iSCC of the connected graph. Consider the storage function

$$W_1(x) = \frac{1}{2}\sum_{i=1}^{k_1} \nu_i x_i^T P x_i, \tag{A.1}$$

where ν_i are the entries of the left eigenvector corresponding to the zero eigenvalue of the Laplacian matrix L_s, i.e. $\nu = (\nu_1, ..., \nu_{k_1})^T$, $\nu^T L_s = \nu^T (\mathcal{D}_s - \Lambda_s) = 0$. It follows that

$$\dot{W}_1 = \sum_{i=1}^{k_1} \nu_i (z_i^T u_i + \frac{1}{2} x_i^T \left(PA + A^T P\right) x_i + \omega^T B_2^T P x_i), \tag{A.2}$$

consider the term

$$\begin{aligned}\sum_{i=1}^{k_1} \nu_i z_i^T u_i &= \gamma \sum_{i=1}^{k_1} \sum_{j \in \mathcal{E}_i} \nu_i a_{ij} z_i^T \left(z_j^\tau - z_i^\tau\right), \\ &\le \gamma \sum_{i=1}^{k_1} \sum_{j \in \mathcal{E}_i} \nu_i a_{ij} \left(|z_i|^2 + \frac{1}{2}|z_i^\tau|^2 + \frac{1}{2}\left|z_j^\tau\right|^2\right).\end{aligned} \tag{A.3}$$

Define the functional

$$W_2(x_t(\theta)) = \frac{\gamma}{2} \sum_{i=1}^{k_1} \sum_{j \in \mathcal{E}_i} \nu_i a_{ij} \int_{-\tau}^{0} |z_j(t+s)|^2 + |z_i(t+s)|^2 \, ds, \tag{A.4}$$

with $x_t(\theta) = x(t+\theta) \in \mathcal{C}$, $\theta \in [-\tau, 0]$, and $\mathcal{C} = [-\tau, 0] \to \mathbb{R}^{kn}$ the Banach space of continuous functions mapping the interval $[-\tau, 0]$ into $\mathbb{R}^{kn}$. The norm of an element $x_t(\theta) \in \mathcal{C}$ is defined as $|x_t(\theta)| := \sup_{\theta\in[-\tau,0]} |x(t+\theta)|$. Note the abuse of notation, however, no confusion may arise. It follows that

$$\dot{W}_2(x_t(\theta)) = \frac{\gamma}{2}\sum_{i=1}^{k_1}\sum_{j\in\mathcal{E}_i} \nu_i a_{ij}\left(|z_i|^2 + |z_j|^2 - |z_i^\tau|^2 - \left|z_j^\tau\right|^2\right). \tag{A.5}$$

Finally, consider the functional $W_s = W_1 + W_2$, then

$$\begin{aligned}
\dot{W}_s &\leq \sum_{i=1}^{k_1}\nu_i\left(\frac{1}{2}x_i^T\left(PA + A^TP\right)x_i + \omega^TB_2^TPx_i\right) \\
&+ \gamma\sum_{i=1}^{k_1}\sum_{j\in\mathcal{E}_i}\nu_i a_{ij}\left(\frac{3}{2}|z_i|^2 + \frac{1}{2}|z_j|^2\right), \\
&\leq \sum_{i=1}^{k_1}\nu_i\left(\frac{1}{2}x_i^T\left(PA + A^TP\right)x_i + \omega^TB_2^TPx_i\right) \\
&+ \gamma\sum_{i=1}^{k_1}\sum_{j\in\mathcal{E}_i}\nu_i a_{ij}\left(2|z_i|^2 + \frac{1}{2}|z_j|^2 - \frac{1}{2}|z_i|^2\right),
\end{aligned} \tag{A.6}$$

since $\nu^T(\mathcal{D}_s - \Lambda_s) = 0$, it follows that

$$\begin{aligned}
\dot{W}_s \quad &\leq \quad \sum_{i=1}^{k_1}\nu_i\left(\frac{1}{2}x_i^T\left(PA + A^TP + 4\gamma\bar{d}PB_1B_1^TP\right)x_i\right) \\
&+ \sum_{i=1}^{k_1}\nu_i\omega^TB_2^TPx_i.
\end{aligned}$$

Consider now the nodes $\{v_{k_1+1}, ..., v_k\}$ and the positive semidefinite function

$$W_3(x) = \sum_{i=k_1+1}^{k}\underline{\nu}x_i^TPx_i, \tag{A.7}$$

with $\underline{\nu} = \min(\nu_1, ..., \nu_{k_1})$, then

$$\dot{W}_3 = \sum_{i=k_1+1}^{k}\underline{\nu}(z_i^Tu_i + \frac{1}{2}x_i^T\left(PA + A^TP\right)x_i + \omega^TB_2^TPx_i), \tag{A.8}$$

consider the term

$$\sum_{i=k_1+1}^{k} z_i^T u_i = -\gamma z_c^T \left(\mathcal{F} \otimes I_m\right) z_s^\tau - z_c^T \left(L_c \otimes I_m\right) z_c^\tau, \tag{A.9}$$

$$\leq \frac{\gamma \left\|\mathcal{F}\right\|}{2} \left(|z_c|^2 + |z_s^\tau|^2\right)$$

$$+ \frac{\gamma \left\|L_c\right\|}{2} \left(|z_c|^2 + |z_c^\tau|^2\right).$$

Define the functional

$$\begin{aligned} W_4(x_t(\theta)) &= \frac{\gamma \underline{\nu} \left\|\mathcal{F}\right\|}{2} \int_{-\tau}^{0} \left|z_s(t+s)\right|^2 ds \\ &\quad + \frac{\gamma \underline{\nu} \left\|L_c\right\|}{2} \int_{-\tau}^{0} \left|z_c(t+s)\right|^2 ds, \end{aligned} \tag{A.10}$$

with $x_t(\theta) = x(t+\theta) \in \mathcal{C}$ and $\theta \in [-\tau, 0]$. It follows that

$$\dot{W}_4 = \frac{\gamma \underline{\nu} \left\|\mathcal{F}\right\|}{2} (|z_s|^2 - |z_s^\tau|^2) + \frac{\gamma \underline{\nu} \left\|L_c\right\|}{2} (|z_c|^2 - |z_c^\tau|^2). \tag{A.11}$$

Consider the functional $W_c = W_3 + W_4$, then

$$\begin{aligned} \dot{W}_c &\leq \sum_{i=k_1+1}^{k} \underline{\nu} \left(\frac{1}{2} x_i^T \left(PA + A^T P\right) x_i + \omega^T B_2^T P x_i \right) \\ &\quad + \gamma \underline{\nu} \left(\|L_c\| + \|\mathcal{F}\|\right) \sum_{i=1}^{k} |z_i|^2 . \\ &\leq \sum_{i=k_1+1}^{k} \underline{\nu} \left(\frac{1}{2} x_i^T \left(PA + A^T P\right) x_i + \omega^T B_2^T P x_i \right) \\ &\quad + \gamma \underline{\nu} \left(\|L_c\| + \|\mathcal{F}\|\right) \sum_{i=1}^{k} x_i^T P B_1 B_1^T P x_i. \end{aligned} \tag{A.12}$$

Finally, consider the functional $W = W_s + W_c$, it follows that

$$\begin{aligned} \dot{W} &\leq \sum_{i=1}^{k} \underline{\nu} \left(\frac{1}{2} x_i^T \left(PA + A^T P + 2\gamma \bar{a} P B_1 B_1^T P\right) x_i \right) \\ &\quad + \sum_{i=1}^{k} \bar{\nu} \delta \left| B_2^T P x_i \right| , \end{aligned} \tag{A.13}$$

with $\bar{\nu} = \max(\nu_1, ..., \nu_{k_1})$ and $\bar{a} = 2\bar{d} + \|\mathcal{F}\| + \|L_c\|$. By assumption, there exist $\gamma, \beta \in \mathbb{R}_{>0}$ such that

$$PA + A^T P + \beta P B_2 B_2^T P + 2\gamma \bar{a} C_2^T C_2 \quad \leq \quad 0.$$

Let γ_{max} be the largest γ such that the above inequality is satisfied. Then,

$$\dot{W} \leq \sum_{i=1}^{k} \underline{\nu} \left(-\frac{\beta}{2} \left| B_2^T P x_i \right|^2 + \frac{\bar{\nu}\delta}{\underline{\nu}} \left| B_2^T P x_i \right| \right), \tag{A.14}$$
$$\leq -\sum_{i=1}^{k} \underline{\nu} \left| B_2^T P x_i \right| \left(\frac{\beta}{2} ||B_2^T P|| \, |x_i| - \frac{\bar{\nu}\delta}{\underline{\nu}} \right).$$

it follows that, $\dot{W} \leq 0$ for sufficiently large $|x|$. The functional $W(\cdot)$ is positive definite and radially unbounded. Hence, there exists a positive constant $c > 0$ such that $\dot{W}(x) \leq 0$ for c and x satisfying $W(x) \geq c$. Then, solutions starting in the set $\{W(x) \leq c\}$ will remain there for all future time since $\dot{W} \leq 0$ on the boundary $W(x) = c$. Moreover, for any x in the set $\{c < W(x) \leq c^*\}$ for some finite constant $c^* > c > 0$, the function $\dot{W}(x)$ is negative semidefinite, which implies that, solutions starting in this set will be trapped in $\{c \leq W(x) \leq c^*\}$ for all future time. ■

A.2 Proof of Lemma 2.11

The stacked closed loop system (2.1),(2.2),(2.24),(2.25) can be written in terms of the estimation error $\epsilon = \eta - x^{\tau}$ as follows

$$\dot{x} = (I_k \otimes A)x - \gamma(L \otimes B_1 C_2)x^{\tau} - \gamma(L \otimes B_1 C_2)\epsilon + (\mathbf{1}_k \otimes B_2)\,\omega, \tag{A.15}$$
$$\dot{\epsilon} = (I_k \otimes (A + HC_1))\,\epsilon. \tag{A.16}$$

The above system is the cascade of the closed-loop system (2.12) with an exponentially stable estimation error ϵ. It follows that boundedness of (2.12) implies boundedness of (A.15),(A.16) as long as the matrix $(A + HC_1)$ is Hurwitz; therefore, (2.1),(2.2),(2.24),(2.25) possesses bounded solutions if inequality (2.13) stated in Lemma 2.2 is satisfied. ■

A.3 Proof of Lemma 2.14

The closed-loop stacked system (2.1),(2.3),(2.29),(2.30) can be written in terms of the stacked prediction error $\varepsilon = \zeta - x$ as follows

$$\dot{x} = (I_k \otimes A)x - \gamma(L \otimes B_1 C_2)x - \gamma(L \otimes B_1 C_2)\varepsilon + (\mathbf{1}_k \otimes B_2)\,\omega, \tag{A.17}$$
$$\dot{\varepsilon} = (I_k \otimes A)\varepsilon + (I_k \otimes K_1 C_2)\varepsilon^{\tau}, \tag{A.18}$$

which is the cascade of (2.12) with $\tau = 0$ and exponentially stable prediction error ε. Therefore, boundedness of (A.17) for $\varepsilon = \mathbf{0}$ implies boundedness of (A.17),(A.18) as long as the roots of the characteristic equation (2.28) belong to the open left half of the complex plane. Then, we only have to prove boundedness of (A.17) for $\varepsilon = 0$ and $\tau = 0$. First consider the nodes $\{v_1, ..., v_{k_1}\}$, i.e., the iSCC of the connected graph. Consider the storage function

$$W_1(x) = \frac{1}{2}\sum_{i=1}^{k_1} \nu_i x_i^T P x_i, \tag{A.19}$$

where ν_i are the entries of the left eigenvector corresponding to the zero eigenvalue of the Laplacian matrix L_s, i.e., $\nu = (\nu_1, ..., \nu_{k_1})^T$, $\nu^T L_s = \nu^T(\mathcal{D}_s - \Lambda_s) = 0$. It follows that

$$\dot{W}_1 = \sum_{i=1}^{k_1} \nu_i (z_i^T u_i + \frac{1}{2} x_i^T \left(PA + A^T P\right) x_i + \omega^T B_2^T P x_i), \tag{A.20}$$

consider the term

$$\begin{aligned} \sum_{i=1}^{k_1} \nu_i z_i^T u_i &= \gamma \sum_{i=1}^{k_1} \sum_{j \in \mathcal{E}_i} \nu_i a_{ij} z_i^T \left(z_j - z_i\right), \\ &\leq \gamma \sum_{i=1}^{k_1} \sum_{j \in \mathcal{E}_i} \nu_i a_{ij} \left(\frac{1}{2}\left|z_j\right|^2 - \frac{1}{2}\left|z_i\right|^2\right). \end{aligned} \tag{A.21}$$

Since $\nu^T(\mathcal{D}_s - \Lambda_s) = 0$, it follows that

$$\dot{W}_1 \leq \sum_{i=1}^{k_1} \nu_i \left(\frac{1}{2} x_i^T \left(PA + A^T P\right) x_i + \omega^T B_2^T P x_i\right).$$

Consider now the nodes $\{v_{k_1+1}, ..., v_k\}$ and the positive semidefinite function

$$W_2(x) = \sum_{i=k_1+1}^{k} \underline{\nu} x_i^T P x_i,$$

with $\underline{\nu} = \min(\nu_1, ..., \nu_{k_1})$, then

$$\dot{W}_2 = \sum_{i=k_1+1}^{k} \underline{\nu}(z_i^T u_i + \frac{1}{2} x_i^T \left(PA + A^T P\right) x_i + \omega^T B_2^T P x_i), \tag{A.22}$$

consider the term

$$\begin{aligned} \sum_{i=k_1+1}^{k} z_i^T u_i &= -\gamma z_c^T \left(\mathcal{F} \otimes I_m\right) z_s - z_c^T \left(L_c \otimes I_m\right) z_c, \\ &\leq \gamma \left(\|\mathcal{F}\| + \|L_c\|\right) \left|z_c\right|^2 + \frac{\gamma \|\mathcal{F}\|}{2} \left|z_s\right|^2. \end{aligned} \tag{A.23}$$

It follows that

$$\begin{aligned}\dot{W}_2 &\leq \sum_{i=k_1+1}^{k} \underline{\nu}\left(\frac{1}{2}x_i^T\left(PA+A^TP\right)x_i+\omega^T B_2^T P x_i\right)\\ &\quad+\gamma\underline{\nu}\left(\|L_c\|+\|\mathcal{F}\|\right)\sum_{i=1}^{k}|z_i|^2.\\ &\leq \sum_{i=k_1+1}^{k} \underline{\nu}\left(\frac{1}{2}x_i^T\left(PA+A^TP\right)x_i+\omega^T B_2^T P x_i\right)\\ &\quad+\gamma\underline{\nu}\left(\|L_c\|+\|\mathcal{F}\|\right)\sum_{i=1}^{k}x_i^T P B_1 B_1^T P x_i.\end{aligned} \tag{A.24}$$

Finally, consider the function $W = W_1 + W_2$, it follows that

$$\begin{aligned}\dot{W} &\leq \sum_{i=1}^{k} \underline{\nu}\left(\frac{1}{2}x_i^T\left(PA+A^TP+2\gamma\bar{a}PB_1B_1^TP\right)x_i\right)\\ &\quad+\sum_{i=1}^{k}\bar{\nu}\delta\left|B_2^TPx_i\right|,\end{aligned} \tag{A.25}$$

with $\bar{\nu} = \max(\nu_1, ..., \nu_{k_1})$ and $\bar{a} = \|\mathcal{F}\| + \|L_c\|$. Then, by assumption

$$\dot{W} \leq \sum_{i=1}^{k} \underline{\nu}\left(-\frac{\beta}{2}\left|B_2^TPx_i\right|^2+\frac{\bar{\nu}\delta}{\underline{\nu}}\left|B_2^TPx_i\right|\right), \tag{A.26}$$

it follows that $\dot{W} \leq 0$ for sufficiently large $|x|$. Now, the result follows from the same arguments presented in the proof of Lemma 2.2. ∎

A.4 Proof of Theorem 2.8

Boundedness of the solutions follows from Lemma 2.2. Define $T \in \mathbb{R}^{k\times k}$ as

$$T = \begin{pmatrix} 1 & \mathbf{0} \\ \mathbf{1} & -I_{k-1} \end{pmatrix}, \tag{A.27}$$

with $\mathbf{1}_{k-1} = \mathrm{col}(1, ..., 1)$ of dimension $k-1$. Introduce a new set of coordinates $\bar{z} = (T \otimes I_m)z$ and $\bar{\zeta} = (T \otimes I_p)\zeta$. Define $e_z = \mathrm{col}(\bar{z}_2, ..., \bar{z}_k)$ and $e_\zeta = \mathrm{col}(\bar{\zeta}_2, ..., \bar{\zeta}_k)$. Then, the synchronization error dynamics is given by

$$\dot{e}_\zeta = (I_{k-1} \otimes N_1)e_\zeta + (I_{k-1} \otimes N_2)e_z, \tag{A.28}$$

$$\dot{e}_z = (I_{k-1} \otimes M_1)e_\zeta + (I_{k-1} \otimes M_2)e_z + \tilde{u}, \tag{A.29}$$

where $\tilde{u} = \text{col}(u_1 - u_2, ..., u_1 - u_k)$, then

$$\tilde{u}(t) = -\gamma(\tilde{L} \otimes I_m)e_z(t - \tau), \tag{A.30}$$

with

$$TLT^{-1} = \begin{pmatrix} 0 & * \\ \mathbf{0} & \tilde{L} \end{pmatrix}.$$

The matrix $\tilde{L} \in \mathbb{R}^{(k-1)\times(k-1)}$ has eigenvalues $\lambda_2, ..., \lambda_k \in \mathbb{C}_{>0}$. Then, the closed loop system (A.28),(A.29),(A.30) is given by

$$\dot{e}_\zeta = (I \otimes N_1)e_\zeta + (I \otimes N_2)e_z, \tag{A.31}$$

$$\dot{e}_z = (I \otimes M_1)e_\zeta + (I \otimes M_2)e_z - \gamma(\tilde{L} \otimes I_m)e_z^\tau. \tag{A.32}$$

Using continuity properties of the solutions and Leibniz's rule e_z^τ can be written as follows

$$\begin{aligned} e_z^\tau &= e_z - \int_{-\tau}^0 \dot{e}_z(t+s)ds, \\ &= e_z - (I \otimes M_1)\int_{-\tau}^0 e_\zeta(t+s) - (I \otimes M_2)\int_{-\tau}^0 e_z(t+s)ds \\ &+ \ \gamma(\tilde{L} \otimes I_m)\int_{-\tau}^0 e_z(t+s-\tau)ds, \end{aligned} \tag{A.33}$$

it follows that

$$\begin{aligned} \dot{e}_z(t) &= (I \otimes M_1)e_\zeta + (I \otimes M_2)e_z - \gamma(\tilde{L} \otimes I_m)e_z \\ &+ \ \gamma\int_{-\tau}^0 (\tilde{L} \otimes M_1)e_\zeta(t+s) + (\tilde{L} \otimes M_2)e_z(t+s)ds \\ &- \ \gamma^2(\tilde{L}^2 \otimes I_m)\int_{-\tau}^0 e_z(t+s-\tau)ds. \end{aligned} \tag{A.34}$$

By construction $(-\tilde{L})$ is a stable matrix. Under the detectability assumption of the pair (A, C_2), the coordinate transformation can be chosen such that N_1 is a Hurwitz matrix. Then, there exist unique solutions of the Lyapunov equations $(-\tilde{L})Q + Q(-\tilde{L})^T = -2\mu I_{k-1}$ and $N_1R + RN_1^T = -2\alpha I_p$ for some positive definite matrices $R \in \mathbb{R}^{p\times p}$, $Q \in \mathbb{R}^{k-1\times k-1}$ and some constants $\mu, \alpha \in \mathbb{R}_{>0}$. Consider the following Lyapunov function

$$V(e_\zeta, e_z) = \frac{1}{2}e_\zeta^T(I_{k-1} \otimes R)e_\zeta + \frac{1}{2}e_z^T(Q \otimes I_m)e_z.$$

It follows that

$$\begin{aligned}\dot{V} \leq &-\alpha\left|e_\zeta\right|^2-\left(\mu\gamma-\|Q\|\,\|M_2\|\right)\left|e_z\right|^2\\ &+\left(\|R\|\,\|N_2\|+\|Q\|\,\|M_1\|\right)\left|e_\zeta\right|\left|e_z\right|\\ &+\ \gamma\,\|Q\|\,\|M_1\|\,\|\tilde{L}\|\left|e_z\right|\int_{-\tau}^{0}\left|e_\zeta(t+s)\right|ds\\ &+\ \gamma\,\|Q\|\,\|M_2\|\,\|\tilde{L}\|\left|e_z\right|\int_{-\tau}^{0}\left|e_z(t+s)\right|ds\\ &+\ \gamma^2\|\tilde{L}\|^2\left|e_z\right|\int_{-\tau}^{0}\left|e_z(t+s-\tau)\right|ds.\end{aligned} \tag{A.35}$$

Let $V(e_\zeta, e_z)$ be a Lyapunov-Razumikhin function such that if

$$\kappa^2 V(e_\zeta, e_z) < V(e_\zeta(t+\theta), e_z(t+\theta)),$$

for $\theta \in [-2\tau, 0]$ and some $\kappa > 1$ (see, for instance [48], for details about Lyapunov-Razumikhin functions), then

$$\begin{aligned}\dot{V} \leq &-\alpha\left|e_\zeta\right|^2 \qquad\qquad (A.36)\\ &+\left(\|Q\|\,\|M_1\|\left(1+\kappa\gamma\tau\|\tilde{L}\|\right)+\|R\|\,\|N_2\|\right)\left|e_\zeta\right|\left|e_z\right|\\ &+\left(\|Q\|\,\|M_2\|\left(1+\kappa\gamma\tau\|\tilde{L}\|\right)\ +\kappa\gamma^2\tau\|\tilde{L}\|^2-\mu\gamma\right)\left|e_z\right|^2.\end{aligned}$$

Define $\chi = \gamma\tau$, it is easy to verify that (A.36) is negative definite if

$$\gamma > \gamma' := \frac{\left(\|R\|\,\|N_2\|+\|Q\|\,\|M_1\|\right)^2}{4\mu\alpha}+\frac{\|Q\|\,\|M_2\|}{\mu}, \tag{A.37}$$

and

$$\begin{aligned}\frac{(\gamma-\gamma')}{\kappa\|\tilde{L}\|\,\|Q\|} > &\left(\|M_2\|+\frac{\|\tilde{L}\|}{\|Q\|}\gamma\right)\chi\\ &+\left(\frac{\|M_1\|\left(\|R\|\,\|N_2\|+\|Q\|\,\|M_1\|\right)}{2\alpha\mu}\right)\chi\\ &+\ \frac{\kappa\|\tilde{L}\|\,\|Q\|\,\|M_1\|^2}{4\alpha\mu}\chi^2.\end{aligned}$$

Hence, it can be concluded that (A.36) is negative definite if γ is sufficiently large and χ is sufficiently small. Thus, there exist a constant χ' such that (A.36) is negative definite for $\gamma > \gamma'$ and $\gamma\tau < \chi'$. Then, ultimate boundedness of the solutions and the Lyapunov-Razumikhin theorem [48] implies that the set $\{e_\zeta = 0, e_z = 0\}$ is a global attractor for $\gamma > \gamma'$ and $\gamma\tau < \chi'$. ■

A.5 Proof of Theorem 2.12

Boundedness of the solutions follows from Lemma 2.11. The closed-loop stacked system (2.1),(2.2),(2.24),(2.25) can be written in terms of synchronization errors e_ζ, e_z (with e_ζ and e_z as in the proof of Theorem 2.8), and the estimation error $e_\epsilon = \text{col}(\epsilon_1 - \epsilon_2, ..., \epsilon_1 - \epsilon_k)$ as follows

$$\dot{e}_\zeta = (I \otimes N_1)e_\zeta + (I_{k-1} \otimes N_2)e_z, \tag{A.38}$$

$$\dot{e}_z = (I \otimes M_1)e_\zeta + (I \otimes M_2)e_z - \gamma(\tilde{L} \otimes I_m)e_z^\tau - \gamma(\tilde{L} \otimes C_2)e_\epsilon, \tag{A.39}$$

$$\dot{e}_\epsilon = (I \otimes (A + HC_1))\, e_\epsilon, \tag{A.40}$$

which is the cascade of the closed-loop system (A.31),(A.32) with an exponentially stable estimation error e_ϵ. Then, using Theorem 2.8, it can be concluded that exponential stability of (A.31),(A.32) implies exponential stability of (A.38)-(A.40) as long as the matrix $A + HC_1$ is Hurwitz, $\gamma > \gamma'$, and $\gamma\tau < \chi'$ with γ' and χ' as in the proof of Theorem 2.8. ■

A.6 Proof of Theorem 2.15

Ultimate boundedness of the solutions follows from Lemma 2.14. The closed-loop stacked system (2.1),(2.3),(2.29),(2.30) can be written in terms of synchronization errors e_ζ, e_z (with e_ζ and e_z as in the proof of Theorem 2.8), and the prediction error $e_\varepsilon = \text{col}(\varepsilon_1 - \varepsilon_2, ..., \varepsilon_1 - \varepsilon_k)$ as follows

$$\dot{e}_\zeta = (I \otimes N_1)e_\zeta + (I \otimes N_2)e_z, \tag{A.41}$$

$$\dot{e}_z = (I \otimes M_1)e_\zeta + (I \otimes M_2)e_z - \gamma(\tilde{L} \otimes I_m)e_z - \gamma(\tilde{L} \otimes C_2)e_\varepsilon, \tag{A.42}$$

$$\dot{e}_\varepsilon = (I \otimes A)\, e_\varepsilon + (I \otimes K_1 C_2)\, e_\varepsilon^\tau, \tag{A.43}$$

which is the cascade of (A.31),(A.32) with $\tau = 0$ and an exponentially stable prediction error e_ε. Therefore, exponential stability of (A.31),(A.32) for $\tau = 0$ and $e_\varepsilon = 0$ implies asymptotic stability of (A.41),(A.42),(A.43) as long as (A.43) is asymptotically stable. Then, we only have to prove the asymptotic stability of (A.43). Using Leibniz's rule, the error dynamics (A.43) can be written as

$$\begin{aligned} \dot{e}_\varepsilon = \ & (I \otimes A + K_1 C_2)\, e_\varepsilon - (I \otimes K_1 C_2 A) \int_{-\tau}^{0} e_\varepsilon(t+s) ds \\ & - \left(I \otimes (K_1 C_2)^2\right) \int_{-\tau}^{0} e_\varepsilon(t+s-\tau) ds. \end{aligned} \tag{A.44}$$

Under the detectability assumption of the pair (A, C_2), there exists matrix K_1 such that $A + K_1C_2$ is Hurwitz. Then, there exists a unique solution of the Lyapunov equation $(A+K_1C_2)G+G(A+K_1C_2)^T = -2\varkappa I_n$ for some positive definite matrix $G \in \mathbb{R}^{n\times n}$ and some positive constant $\varkappa \in \mathbb{R}_{>0}$. Consider the following Lyapunov function

$$V(e_\varepsilon) = \frac{1}{2}e_\varepsilon^T(I_{k-1} \otimes G)e_\varepsilon,$$

then

$$\begin{aligned}\dot{V} \leq & -\varkappa |e_\varepsilon|^2 + \|G\| \|K_1\| \|C_2\| \|A\| |e_\varepsilon| \int_{-\tau}^{0} |e_\varepsilon(t+s)| \, ds \\ & + \|G\| \|K_1\|^2 \|C_2\|^2 |e_\varepsilon| \int_{-\tau}^{0} |e_\varepsilon(t+s-\tau)| \, ds. \end{aligned} \tag{A.45}$$

Let $V(e_\varepsilon)$ be a Lyapunov-Razumikhin function such that if

$$\kappa^2 e_\varepsilon(t)^T(I_{k-1} \otimes G)e_\varepsilon(t) < e_\varepsilon^T(t+\theta)(I_{k-1} \otimes G)e_\varepsilon(t+\theta),$$

for $\theta \in [-2\tau, 0]$ and some $\kappa > 1$, then

$$\dot{V}(e_\varepsilon) \leq -\left(\varkappa - \tau\kappa c_1 \|G\| \|A\| - \tau\kappa c_1^2 \|G\|\right) |e_\varepsilon|^2 \tag{A.46}$$

with $c_1 = \|K_1\| \|C_2\|$. Straightforward computations show that

$$\tau \quad < \quad \tau' := \frac{\varkappa}{\kappa c_1 \left(\|A\| + c_1\right)}, \tag{A.47}$$

implies that $\dot{V}(e_\varepsilon) \leq -\sigma |e_\varepsilon|^2$ for some $\sigma > 0$. Which proves the asymptotic stability of the set $e_\varepsilon = 0$. Therefore, for $\tau < \tau'$ and $\gamma > \gamma'$ with γ' as in (A.37), all the systems asymptotically synchronize. ■

A.7 Proof of Lemma 3.4

By assumption, each systems is strictly $\mathcal{C}^1$-semipassive with radially unbounded function $V(x_i)$. Consider the function $W_1 \in \mathcal{C}^1(\mathbb{R}^{kn}, \mathbb{R}_{\geq 0})$ defined as

$$W_1(x_i) = \sum_{i=1}^{k} \nu_i V(x_i), \tag{A.48}$$

where ν_i are the entries of the left eigenvector corresponding to the zero eigenvalue of the Laplacian matrix L, i.e., $\nu = (\nu_1, ..., \nu_k)^T$ and $\nu^T L = \nu^T (D - A) = 0$. Since the communication graph is assumed to be strongly connected, it follows that all the entries ν_i of the left eigenvector ν are strictly positive [113, 129]. Then, by assumption (H3.4)

$$\dot{W}_1(x_i) \leq \sum_{i=1}^{k} \nu_i z_i^T u_i - \nu_i H(x_i). \tag{A.49}$$

Consider the term

$$\sum_{i=1}^{k} \nu_i z_i^T u_i = \gamma \sum_{i=1}^{k} \sum_{j \in \mathcal{E}_i} \nu_i a_{ij} z_i^T (\hat{z}_j - \hat{z}_i). \tag{A.50}$$

The observation error (3.11) is given by

$$\epsilon_i = \hat{z}_i - z_i \rightarrow \hat{z}_i = \epsilon_i + z_i, \tag{A.51}$$

substitution of the righthand side of (A.51) in (A.50) yields

$$\sum_{i=1}^{k} \nu_i z_i^T u_i = \gamma \sum_{i=1}^{k} \sum_{j \in \mathcal{E}_i} \nu_i a_{ij} z_i^T (z_j - z_i) + \gamma \sum_{i=1}^{k} \sum_{j \in \mathcal{E}_i} \nu_i a_{ij} z_i^T (\epsilon_j - \epsilon_i). \tag{A.52}$$

Using Young's inequality, we can rewrite (A.52) as follows

$$\begin{aligned} \sum_{i=1}^{k} \nu_i z_i^T u_i \quad &\leq \quad \frac{\gamma}{2} \sum_{i=1}^{k} \sum_{j \in \mathcal{E}_i} \nu_i a_{ij} \left(|z_j|^2 - |z_i|^2 \right) \\ &\quad + \frac{\gamma}{2} \sum_{i=1}^{k} \sum_{j \in \mathcal{E}_i} \nu_i a_{ij} \left(2\,|z_i|^2 + |\epsilon_i|^2 + |\epsilon_j|^2 \right). \end{aligned} \tag{A.53}$$

Since $\nu^T (D - A) = 0$, it follows that

$$\sum_{i=1}^{k} \nu_i z_i^T u_i \leq \frac{\gamma}{2} \sum_{i=1}^{k} \sum_{j \in \mathcal{E}_i} \nu_i a_{ij} \left(2\,|z_i|^2 + |\epsilon_i|^2 + |\epsilon_j|^2 \right). \tag{A.54}$$

By assumption (H3.3), the origin of the estimation error dynamics (3.13) is uniformly asymptotically stable with radially unbounded Lyapunov function $V_0(\epsilon_i)$ such that (3.15) is satisfied. Consider the function $W_2 \in \mathcal{C}^1(\mathbb{R}^{kp}, \mathbb{R}_{>0})$ defined as

$$W_2(\epsilon_i) = \sum_{i=1}^{k} \left(1 + \frac{\gamma}{\kappa} \sum_{j \in \mathcal{E}_i} \nu_i a_{ij} \right) V_0(\epsilon_i), \tag{A.55}$$

it follows that

$$\dot{W}_2(\epsilon_i) \leq - \sum_{i=1}^{k} \left(\gamma \sum_{j \in \mathcal{E}_i} \nu_i a_{ij} \,|\epsilon_i|^2 + \kappa\,|\epsilon_i|^2 \right). \tag{A.56}$$

Finally, define the function

$$W(x_i, \epsilon_i) = W_1(x_i) + W_2(\epsilon_i), \tag{A.57}$$

combining the previous results and after some straightforward computations yields

$$\dot{W} \leq \frac{\gamma}{2}\sum_{i=1}^{k}\sum_{j\in\mathcal{E}_i}\nu_i a_{ij}\left(2\left|z_i\right|^2+\left|\epsilon_j\right|^2-\left|\epsilon_i\right|^2\right)-\sum_{i=1}^{k}\nu_i H(x_i)-\kappa\sum_{i=1}^{k}\left|\epsilon_i\right|^2,$$

since $\nu^T(D-A)=0$, then

$$\dot{W} \leq -\sum_{i=1}^{k}\nu_i\left(H(x_i)-\gamma d_i\left|z_i\right|^2+\kappa\left|\epsilon_i\right|^2\right), \tag{A.58}$$

it follows that $\dot{W}<0$ for sufficiently large $|\varsigma|$ with $\varsigma=\mathrm{col}(x_1,...,x_k,\epsilon_1,...,\epsilon_k)$ and $\kappa>0$. The function W is positive definite and radially unbounded by construction. Hence, there exists a constant $\sigma>0$ such that $\dot{W}(\varsigma)<0$ for σ and ς satisfying $W(\varsigma)\geq\sigma$. Then, solutions starting in the set $\{W(\varsigma)\leq\sigma\}$ will remain there for all future time since $\dot{W}$ is negative on the boundary $W(\varsigma)=\sigma$. Moreover, for any ς in the set $\{W(\varsigma)\geq\sigma^*\}$ with $\sigma^*>\sigma$, the function $\dot{W}(\varsigma)$ is negative, which shows that, in this set, $W(\varsigma)$ will decrease monotonically until the solutions enter the set $\{W(\varsigma)\leq\sigma\}$ again. Therefore, the solutions of the closed-loop system (3.1),(3.2),(3.14) exist and are ultimately bounded for all $\gamma<\gamma_{max}$ and $\kappa>0$. ■

A.8 Proof of Theorem 3.5

The existence and uniqueness of the solutions of the coupled systems follows from smoothness of the righthand side of the closed-loop system. By Lemma 3.4, the solutions are ultimately bounded for all $t\geq 0$, then

$$\begin{aligned}\lim_{t\to\infty}\sup\left|z_i(t)\right| &\leq \mathcal{B}_z,\\ \lim_{t\to\infty}\sup\left|\zeta_i(t)\right| &\leq \mathcal{B}_\zeta,\\ \lim_{t\to\infty}\sup\left|\epsilon_i(t)\right| &\leq \mathcal{B}_\epsilon,\end{aligned} \tag{A.59}$$

for some finite constants $\mathcal{B}_z,\mathcal{B}_\zeta,\mathcal{B}_\epsilon\in\mathbb{R}_{>0}$. Let $\zeta=\mathrm{col}(\zeta_1,\zeta_2,...,\zeta_k)\in\mathbb{R}^{k(n-m)}$ and $\epsilon=\mathrm{col}(\epsilon_1,\epsilon_2,...,\epsilon_k)\in\mathbb{R}^{km}$. Define $M\in\mathbb{R}^{k\times k}$ as

$$M := \begin{pmatrix} 1 & \mathbf{0}_{1\times(k-1)} \\ \mathbf{1}_{(k-1)\times 1} & -I_{k-1}\end{pmatrix}. \tag{A.60}$$

Introduce the new coordinates $\bar{z} := (M \otimes I_m)z$, $\bar{\zeta} := (M \otimes I_{n-m})\zeta$, and $\bar{\epsilon} = (M \otimes I_m)\epsilon$. Notice that $\bar{z}_1 = z_1, \bar{z}_2 = z_1 - z_2, \ldots, \bar{z}_k = z_1 - z_k$, $\bar{\zeta}_1 = \zeta_1, \bar{\zeta}_2 = \zeta_1 - \zeta_2, \ldots, \bar{\zeta}_k = \zeta_1 - \zeta_k$, and $\bar{\epsilon}_1 = \epsilon_1, \bar{\epsilon}_2 = \epsilon_1 - \epsilon_2, \ldots, \bar{\epsilon}_k = \epsilon_1 - \epsilon_k$. Define $\tilde{z} = \mathrm{col}(\bar{z}_2, ..., \bar{z}_k)$, $\tilde{\zeta} = \mathrm{col}(\bar{\zeta}_2, ..., \bar{\zeta}_k)$, and $\tilde{\epsilon} = \mathrm{col}(\bar{\epsilon}_2, ..., \bar{\epsilon}_k)$. Note that $\tilde{z} = \tilde{\zeta} = 0$ implies that the systems synchronize. Assumptions (H3.3) and (H3.5) and Proposition 3.2 imply the existence of positive definite radially unbounded functions $V_1 : \mathbb{R}^{km} \to \mathbb{R}_{\geq 0}$ and $V_2 : \mathbb{R}^{(k-1)(n-m)} \to \mathbb{R}_{\geq 0}$ such that

$$\dot{V}_1(\epsilon, x) \leq -\kappa \left|\epsilon\right|^2 \quad \forall \ \epsilon, x, \tag{A.61}$$

$$\dot{V}_2(\tilde{\zeta}, \tilde{z})\Big|_{\tilde{z}=0} \leq -\alpha|\tilde{\zeta}|^2, \tag{A.62}$$

for some constant $\alpha > 0$ and κ as in (H3.3). Smoothness of the vector fields and boundedness of the solutions of the closed-loop system implies

$$\dot{V}_2(\tilde{\zeta}, \tilde{z}) - \dot{V}_2(\tilde{\zeta}, 0) \leq c_2|\tilde{\zeta}|\,|\tilde{z}|\,, \tag{A.63}$$

for some positive constant c_2. Notice that

$$MLM^{-1} = \begin{pmatrix} 0 & * \\ 0 & \tilde{L} \end{pmatrix},$$

where the matrix $\tilde{L} \in \mathbb{R}^{(k-1)\times(k-1)}$ has eigenvalues $\lambda_2, ..., \lambda_k \in \mathbb{C}_{>0}$. Note that $spec(\tilde{L}) = spec(L)\backslash\{0\}$. The stacked estimation error is defined as $\epsilon = \hat{z} - z$, then the controller (3.14) can be written in matrix form as follows

$$\begin{aligned} u &= -\gamma\left(L \otimes I_m\right)\hat{z} \\ &= -\gamma\left(L \otimes I_m\right)z - \gamma\left(L \otimes I_m\right)\epsilon. \end{aligned} \tag{A.64}$$

Moreover, denote $\tilde{u} = \mathrm{col}((u_1 - u_2), ..., (u_1 - u_k))$, it follows that

$$\tilde{u} = -\gamma\left(\tilde{L} \otimes I_m\right)\tilde{z} - \gamma\left(\tilde{L} \otimes I_m\right)\tilde{\epsilon}, \tag{A.65}$$

and the closed-loop system can be written as

$$\dot{\tilde{z}} = \tilde{a}(\tilde{z}, \tilde{\zeta}, z_1, \zeta_1) - \gamma\left(\tilde{L} \otimes I_m\right)\tilde{z} - \gamma\left(\tilde{L} \otimes I_m\right)\tilde{\epsilon}, \tag{A.66}$$

where

$$\tilde{a}(\tilde{z}, \tilde{\zeta}, z_1, \zeta_1) = \begin{pmatrix} a(z_1, \zeta_1) - a(z_1 - \tilde{z}_1, \zeta_1 - \tilde{\zeta}_1) \\ \vdots \\ a(z_1, \zeta_1) - a(z_1 - \tilde{z}_{k-1}, \zeta_1 - \tilde{\zeta}_{k-1}) \end{pmatrix}. \tag{A.67}$$

Since $\tilde{L}$ is a stable matrix, it follows that there exists a unique solution of the Lyapunov equation $(-\tilde{L})^T\mathcal{P} + \mathcal{P}(-\tilde{L}) + Q = 0$ for some positive definite matrices

$\mathcal{P}, Q \in \mathbb{R}^{(k-1)\times(k-1)}$. Let $\mathcal{P}$ be such that $\|\mathcal{P}\| = 1$ and $(-\tilde{L})^T\mathcal{P} + \mathcal{P}(-\tilde{L}) = -2\mu I$ for some constant $\mu > 0$, and consider the positive definite function

$$V_3(\tilde{z}) = \frac{1}{2}\tilde{z}^T\left(\mathcal{P}\otimes I_m\right)\tilde{z},$$

then

$$\begin{aligned} \dot{V}_3(\tilde{z}) \;\; &\leq \;\; \tilde{z}^T\left(\mathcal{P}\otimes I_m\right)\left(\tilde{a}(\tilde{z},\tilde{\zeta},z_1,\zeta_1) - \gamma\left(\tilde{L}\otimes I_m\right)\tilde{\epsilon}\right) \\ &\quad -\frac{\gamma}{2}\tilde{z}^T\left(\left(\tilde{L}\otimes I_m\right)^T\left(\mathcal{P}\otimes I_m\right) + \left(\mathcal{P}\otimes I_m\right)\left(\tilde{L}\otimes I_m\right)\right)\tilde{z}, \\ &\leq \;\; \tilde{z}^T\left(\mathcal{P}\otimes I_m\right)\left(\tilde{a}(\tilde{z},\tilde{\zeta},z_1,\zeta_1)\right) + \gamma\|\tilde{L}\|\,|\tilde{z}|\,|\tilde{\epsilon}| - \gamma\mu\,|\tilde{z}|^2 . \end{aligned} \tag{A.68}$$

Ultimate boundedness of solutions and smoothness of the vector fields imply

$$\tilde{z}^T\left(P\otimes I_m\right)\left(\tilde{a}(\tilde{z},\tilde{\zeta},z_1,\zeta_1)\right) \leq c_3\,|\tilde{z}|\,|\tilde{\zeta}| + c_4\,|\tilde{z}|^2 , \tag{A.69}$$

for some positive constants c_3 and c_4. Consider the function

$$\mathcal{V}(\epsilon,\tilde{\zeta},\tilde{z}) = V_1(\epsilon) + V_2(\tilde{\zeta}) + V_3(\tilde{z}),$$

then

$$\dot{\mathcal{V}}(\epsilon,\tilde{\zeta},\tilde{z}) \leq -\kappa\,|\epsilon|^2 - \alpha|\tilde{\zeta}|^2 - (\mu\gamma - c_4)\,|\tilde{z}|^2 + (c_2 + c_3)\,|\tilde{z}|\,|\tilde{\zeta}| + \gamma c_5\|\tilde{L}\|\,|\tilde{z}|\,|\epsilon| , \tag{A.70}$$

for some positive constant c_5. Straightforward computations show that

$$\gamma \;\; > \;\; \gamma' := \frac{1}{\mu}\left(\frac{(c_2+c_3)^2}{4\alpha} + c_4\right), \tag{A.71}$$

$$\kappa \;\; > \;\; \kappa' := \frac{\left(c_5\|\tilde{L}\|\right)^2}{4\mu}\left(\frac{\gamma^2}{\gamma - \gamma'}\right), \tag{A.72}$$

implies that

$$\dot{\mathcal{V}}(\tilde{z},\tilde{\zeta},\epsilon) \leq -\sigma\left(|\tilde{z}|^2 + \left|\tilde{\zeta}\right|^2 + |\epsilon|^2\right), \tag{A.73}$$

for some positive constant σ. This proves the Lyapunov stability of the set $\{\mathrm{col}(\tilde{z},\tilde{\zeta},\epsilon) = 0\}$. Moreover, since $\mathcal{V}$ is radially unbounded then $\{\mathrm{col}(\tilde{z},\tilde{\zeta},\epsilon) = 0\}$ is a global attractor for $\gamma > \gamma'$ and $\kappa > \kappa'$. ■

A.9 Proof of Lemma 4.8

First, we prove boundedness of the closed-loop system (4.1),(4.2),(4.21),(4.22). By assumption, each system (4.1),(4.3) is strictly semipassive with radially unbounded function $V(x_i)$. Define the functional

$$W_1(x_t(\theta)) = \sum_{i=1}^{k} \nu_i \big(V(x_i) + \frac{\gamma}{2} \sum_{j \in \mathcal{E}_i} a_{ij} \int_{-\tau}^{0} |z_j(t+s)|^2 \, ds \big),$$

with $x = \text{col}(x_1, ..., x_k)$, $x_t(\theta) = x(t+\theta) \in \mathcal{C}$, $\theta \in [-\tau, 0]$, $\mathcal{C} = [-\tau, 0] \to \mathbb{R}^{kn}$ the Banach space of continuous functions mapping the interval $[-\tau, 0]$ into $\mathbb{R}^{kn}$, and ν_i denoting the entries of the left eigenvector corresponding to the zero eigenvalue of the Laplacian matrix L, i.e., $\nu = (\nu_1, ..., \nu_k)^T$ and $\nu^T L = \nu^T (D - A) = 0$. The graph is assumed to be strongly connected, it follows that the vector ν has strictly positive real entries [29, 129], i.e., $\nu_i > 0$ for all i. Then, by the semipassivity assumption in Lemma 4.8, it follows that

$$\dot{W}_1(x_t(\theta)) \leq \sum_{i=1}^{k} \nu_i \left(z_i^T u_i - H(x_i) \right) + \sum_{i=1}^{k} \nu_i \left(\frac{\gamma}{2} \sum_{j \in \mathcal{E}_i} a_{ij} \left(|z_j|^2 - |z_j^\tau|^2 \right) \right). \quad \text{(A.74)}$$

Define the variable

$$\epsilon_{zi} := \hat{z}_i - z_i = C_2 \left(\hat{x}_i - x_i \right), \quad \text{(A.75)}$$

using (4.11), it follows that

$$\begin{aligned} \epsilon_{zi} &= C_2 \left(N_2 \hat{\rho}_i + N_3 y_i - N_2 \rho_i - N_3 y_i \right), \\ &= C_2 N_2 \left(\hat{\rho}_i - \rho_i \right), \\ &= C_2 N_2 \epsilon_i, \end{aligned} \quad \text{(A.76)}$$

then $\hat{z}_i$ can be written as

$$\hat{z}_i = z_i + C_2 N_2 \epsilon_i. \quad \text{(A.77)}$$

Consider the term

$$\sum_{i=1}^{k} \nu_i z_i^T u_i = \gamma \sum_{i=1}^{k} \sum_{j \in \mathcal{E}_i} \nu_i a_{ij} z_i^T (\hat{z}_j^\tau - \hat{z}_i). \quad \text{(A.78)}$$

substitution of (A.77) in (A.78) yields

$$\begin{aligned} \sum_{i=1}^{k} \nu_i z_i^T u_i \quad = \quad & \gamma \sum_{i=1}^{k} \sum_{j \in \mathcal{E}_i} \nu_i a_{ij} z_i^T (z_j^\tau - z_i) \\ & + \gamma \sum_{i=1}^{k} \sum_{j \in \mathcal{E}_i} \nu_i a_{ij} z_i^T C_2 N_2 (\epsilon_j^\tau - \epsilon_i), \end{aligned} \quad \text{(A.79)}$$

by Young's inequality it follows that

$$\sum_{i=1}^{k} \nu_i z_i^T u_i \leq \frac{\gamma}{2} \sum_{i=1}^{k} \sum_{j \in \mathcal{E}_i} \nu_i a_{ij} \left(|z_j^\tau|^2 - |z_i|^2 \right) + \frac{\gamma c}{2} \sum_{i=1}^{k} \sum_{j \in \mathcal{E}_i} \nu_i a_{ij} \left(2|z_i|^2 + |\epsilon_i|^2 + |\epsilon_j^\tau|^2 \right), \tag{A.80}$$

with $c = \|C_2\| \|N_2\|$. Consider the functional

$$W_2(\epsilon_t(\theta)) = \sum_{i=1}^{k} \nu_i \left(1 + \frac{\gamma c}{\kappa} \sum_{j \in \mathcal{E}_i} a_{ij} \right) V_0(\epsilon_i) + \frac{\gamma c}{2} \sum_{i=1}^{k} \sum_{j \in \mathcal{E}_i} \nu_i a_{ij} \int_{-\tau}^{0} |\epsilon_j(t+s)|^2 \, ds, \tag{A.81}$$

with $V_0(\epsilon_i)$ from (H4.5). Then

$$\dot{W}_2 \leq \sum_{i=1}^{k} \nu_i \Big(-\kappa |\epsilon_i|^2 + \frac{\gamma c}{2} \sum_{j \in \mathcal{E}_i} a_{ij} (|\epsilon_j|^2 - |\epsilon_j^\tau|^2 - 2|\epsilon_i|^2) \Big).$$

Finally, define the functional $W(x_t(\theta), \epsilon_t(\theta)) = W_1 + W_2$. Using the fact that $\nu^T (D - A) = 0$ and combining the previous results yields

$$\dot{W} \leq -\sum_{i=1}^{k} \nu_i \left(H(x_i) + \kappa |\epsilon_i|^2 - \gamma c d_i |z_i|^2 \right). \tag{A.82}$$

Then by assumption (H4.6), $\dot{W} < 0$ for $\kappa > 0$ and sufficiently large $|\varsigma|$ with $\varsigma = \mathrm{col}(x, \epsilon)$. The functional W is radially unbounded by construction. Hence, there exists a constant $\sigma > 0$ such that $\dot{W}(\varsigma) < 0$ for σ and ς satisfying $W(\varsigma) \geq \sigma$. Then, solutions starting in the set $\{W(\varsigma) \leq \sigma\}$ will remain there for all future time since $\dot{W}$ is negative on the boundary $W(\varsigma) = \sigma$. Moreover, for any ς in the set $\{W(\varsigma) \geq \sigma^*\}$ with $\sigma^* > \pi$, the function $\dot{W}(\varsigma)$ is negative, which shows that, in this set, $W(\varsigma)$ will decrease monotonically until the solutions enter the set $\{W(\varsigma) \leq \sigma\}$ again. Therefore, it can be concluded that the solutions of the closed loop system (4.1),(4.2),(4.21),(4.22) exist and are ultimately bounded for all $\tau \geq 0$ and $\gamma < \gamma_{max}$. Now consider the closed-loop system (4.1),(4.2),(4.21),(4.23) and the positive definite functional

$$W = \sum_{i=1}^{k} \nu_i \left(1 + \frac{\gamma c}{\kappa} \sum_{j \in \mathcal{E}_i} a_{ij}\right) V_0(\epsilon_i) + \sum_{i=1}^{k} \nu_i V(x_i) \tag{A.83}$$
$$+ \frac{\gamma c}{2} \sum_{i=1}^{k} \sum_{j \in \mathcal{E}_i} \nu_i a_{ij} \int_{-\tau}^{0} \left(|\epsilon_i(t+s)|^2 + |\epsilon_j(t+s)|^2\right) ds$$
$$+ \frac{\gamma}{2} \sum_{i=1}^{k} \sum_{j \in \mathcal{E}_i} \nu_i a_{ij} \int_{-\tau}^{0} \left(|z_i(t+s)|^2 + |z_j(t+s)|^2\right) ds.$$

Using the same machinery as before an after some straightforward computations yields

$$\dot{W} \quad \leq \quad -\sum_{i=1}^{k} \nu_i \left(H(x_i) + \kappa |\epsilon_i|^2 - \gamma \tilde{c} d_i |z_i|^2\right), \tag{A.84}$$

with $\tilde{c} = \|C_2\|\|N_2\| + 2$. The result follows from the same arguments presented in the first part of the proof. ■

A.10 Proof of Theorem 4.11

First, we prove that the closed-loop system (4.1),(4.2),(4.21),(4.22) asymptotically synchronize. The existence and uniqueness of the solutions follows from smoothness of the right-hand side of the closed loop system. By Lemma 4.8, the solutions exist for all $t \geq 0$ and are ultimately bounded. Let $\zeta = \mathrm{col}(\zeta_1, ..., \zeta_k) \in \mathbb{R}^{k(n-m)}$ and $\epsilon = \mathrm{col}(\epsilon_1, ..., \epsilon_k) \in \mathbb{R}^{kp}$. Define $M \in \mathbb{R}^{k \times k}$ as

$$M := \begin{pmatrix} 1 & \mathbf{0} \\ \mathbf{1} & -I_{k-1} \end{pmatrix}. \tag{A.85}$$

Introduce the set of coordinates, $\bar{z} = (M \otimes I_m) z$, $\bar{\zeta} = (M \otimes I_{n-m}) \zeta$, and $\bar{\epsilon} = (M \otimes I_m) \epsilon$. Note that, $\bar{z}_1 = z_1, \bar{z}_2 = z_1 - z_2, \ldots, \bar{z}_k = z_1 - z_k$, $\bar{\zeta}_1 = \zeta_1$, $\bar{\zeta}_2 = \zeta_1 - \zeta_2, \ldots, \bar{\zeta}_k = \zeta_1 - \zeta_k$, and $\bar{\epsilon}_1 = \epsilon_1, \bar{\epsilon}_2 = \epsilon_1 - \epsilon_2, \ldots, \bar{\epsilon}_k = \epsilon_1 - \epsilon_k$. Define, $\tilde{z} = \mathrm{col}(\bar{z}_2, \ldots, \bar{z}_k)$, $\tilde{\zeta} = \mathrm{col}(\bar{\zeta}_2, \ldots, \bar{\zeta}_k)$, and $\tilde{\epsilon} = \mathrm{col}(\bar{\epsilon}_2, \ldots, \bar{\epsilon}_k)$. Note that $\tilde{z} = \tilde{\zeta} = 0$ implies that the systems synchronize. Assumptions (H4.5) and (H4.2) imply the existence of positive definite radially unbounded functions $V_1 : \mathbb{R}^{kp} \to \mathbb{R}_{\geq 0}$ and $V_2 : \mathbb{R}^{(k-1)(n-m)} \to \mathbb{R}_{\geq 0}$ such that

$$\dot{V}_1(\epsilon, x) \leq -\kappa \left|\epsilon\right|^2, \ \ \forall \ \epsilon, x, \tag{A.86}$$

$$\dot{V}_2(\tilde{\zeta}, \tilde{z})\Big|_{\tilde{z}=0} \leq -\alpha |\tilde{\zeta}|^2, \tag{A.87}$$

for some constant $\alpha > 0$ and κ as in (4.24). Smoothness of the vector fields and boundedness of the solutions of the closed-loop system implies

$$\dot{V}_2(\tilde{\zeta}, \tilde{z}) - \dot{V}_2(\tilde{\zeta}, 0) \leq c_2 |\tilde{\zeta}| \, |\tilde{z}| \, , \tag{A.88}$$

for some positive constant c_2. Notice that

$$MLM^{-1} = \begin{pmatrix} 0 & * \\ 0 & \tilde{L} \end{pmatrix}.$$

Since $spec(\tilde{L}) = spec(L) \backslash \{0\}$, it follows that the matrix $\tilde{L} \in \mathbb{R}^{(k-1)\times(k-1)}$ has eigenvalues $\lambda_2, ..., \lambda_k \in \mathbb{C}_{>0}$, [129]. The stacked estimation error is given by $\epsilon = \hat{\rho} - \rho$, then the controller (4.22) can be written in matrix form as follows

$$\begin{aligned} u = & -\gamma(D \otimes I_m)\hat{z} + \gamma(A \otimes I_m)\hat{z}^\tau \\ = & -\gamma(D \otimes I_m)z - \gamma(D \otimes C_2N_2)\epsilon \\ & + \gamma(A \otimes I_m)z^\tau + \gamma(A \otimes C_2N_2)\epsilon^\tau . \end{aligned} \tag{A.89}$$

Using continuity properties of the solutions, and Leibniz's rule, z^τ and ϵ^τ can be written as

$$z^\tau = z - \int_{-\tau}^{0} \dot{z}(t+s)ds, \quad \epsilon^\tau = \epsilon - \int_{-\tau}^{0} \dot{\epsilon}(t+s)ds, \tag{A.90}$$

it follows that

$$\begin{aligned} u = & -\gamma(L \otimes I_m)z - \gamma(L \otimes C_2N_2)\epsilon \\ & - \gamma \int_{-\tau}^{0} (A \otimes I_m)\dot{z}(t+s)ds + (A \otimes C_2N_2)\dot{\epsilon}(t+s)ds, \end{aligned} \tag{A.91}$$

with Laplacian matrix $L = D - A$. Denote $\tilde{u} = \text{col}((u_1 - u_2), ..., (u_1 - u_k))$, then

$$\begin{aligned} \tilde{u} = & -\gamma(\tilde{L} \otimes I_m)\tilde{z} - \gamma(\tilde{L} \otimes C_2N_2)\tilde{\epsilon} \\ & - \gamma \int_{-\tau}^{0} (\tilde{A} \otimes I_m)\dot{\tilde{z}}(t+s)ds + (\tilde{A} \otimes C_2N_2)\dot{\tilde{\epsilon}}(t+s)ds, \end{aligned} \tag{A.92}$$

with

$$MAM^{-1} = \begin{pmatrix} 0 & * \\ 0 & \tilde{A} \end{pmatrix}.$$

Then, the closed-loop system can be written as

$$\begin{aligned} \dot{\tilde{z}} = & \, \tilde{a}(\tilde{z}, \tilde{\zeta}, z_1, \zeta_1) - \gamma(\tilde{D} \otimes I_m)\tilde{z} - \gamma(\tilde{D} \otimes C_2N_2)\tilde{\epsilon} \\ & + \gamma(\tilde{A} \otimes I_m)\tilde{z}^\tau + \gamma(\tilde{A} \otimes C_2N_2)\tilde{\epsilon}^\tau, \end{aligned} \tag{A.93}$$

$$\begin{aligned} = & \, \tilde{a}(\tilde{z}, \tilde{\zeta}, z_1, \zeta_1) - \gamma(\tilde{L} \otimes I_m)\tilde{z} - \gamma(\tilde{L} \otimes C_2N_2)\tilde{\epsilon} \\ & - \gamma(\tilde{A} \otimes I_m) \int_{-\tau}^{0} \dot{\tilde{z}}(t+s)ds - \gamma(\tilde{A} \otimes C_2N_2) \int_{-\tau}^{0} \dot{\tilde{\epsilon}}(t+s)ds, \end{aligned} \tag{A.94}$$

where

$$\tilde{a}(\tilde{z}, \tilde{\zeta}, z_1, \zeta_1) = \begin{pmatrix} a(z_1, \zeta_1) - a(z_1 - \tilde{z}_1, \zeta_1 - \tilde{\zeta}_1) \\ \vdots \\ a(z_1, \zeta_1) - a(z_1 - \tilde{z}_{k-1}, \zeta_1 - \tilde{\zeta}_{k-1}) \end{pmatrix}.$$

Likewise, $\dot{\tilde{\epsilon}}$ is given by

$$\dot{\tilde{\epsilon}} = \tilde{\phi}(\tilde{\epsilon}, \tilde{x}, \epsilon_1, x_1), \tag{A.95}$$

with

$$\tilde{\phi}(\tilde{\epsilon}, \tilde{x}, \epsilon_1, x_1) := \begin{pmatrix} \phi(\epsilon_1, x_1) - \phi(\epsilon_1 - \tilde{\epsilon}_1, x_1 - \tilde{x}_1) \\ \vdots \\ \phi(\epsilon_1, x_1) - \phi(\epsilon_1 - \tilde{\epsilon}_{k-1}, x_1 - \tilde{x}_{k-1}) \end{pmatrix},$$

and $\phi(\cdot)$ defined in (4.17). Substitution of (A.93) and (A.95) in (A.94) yields

$$\begin{aligned} \dot{\tilde{z}} &= \tilde{a}(\tilde{z}, \tilde{\zeta}, z_1, \zeta_1) - \gamma(\tilde{L} \otimes I)\tilde{z} - \gamma(\tilde{L} \otimes C_2 N_2)\tilde{\epsilon} \qquad \text{(A.96)} \\ &- \gamma(\tilde{A} \otimes I) \int_{-\tau}^{0} \tilde{a}(\tilde{z}, \tilde{\zeta}, z_1, \zeta_1)(t+s)ds \\ &+ \gamma^2(\tilde{A}\tilde{D} \otimes I) \int_{-\tau}^{0} \tilde{z}(t+s) + (I \otimes C_2 N_2)\tilde{\epsilon}(t+s)ds \\ &- \gamma^2(\tilde{A}^2 \otimes I) \int_{-\tau}^{0} \tilde{z}(t+s-\tau) + (I \otimes C_2 N_2)\tilde{\epsilon}(t+s-\tau)ds \\ &- \gamma(\tilde{A} \otimes C_2 N_2) \int_{-\tau}^{0} \tilde{\phi}(\tilde{\epsilon}, \tilde{x}, \epsilon_1, x_1)(t+s)ds. \end{aligned}$$

Without loss of generality, it will be assumed that $\mathcal{D} = I_k$. Then, by construction $\|\tilde{A}\| \leq 1$ and $\|\tilde{D}\| = 1$. Since $\tilde{L}$ is a stable matrix, it follows that there exists a unique solution of the Lyapunov equation $(-\tilde{L})^T P + P(-\tilde{L}) + Q = 0$ for some $P = P^T > 0$ and $Q = Q^T > 0$. Let $(-\tilde{L})^T P + P(-\tilde{L}) = -2\mu I$ for some constant $\mu > 0$, and consider the positive definite function $V_3(\tilde{z}) = \frac{1}{2}\tilde{z}^T (P \otimes I_m) \tilde{z}$. Then

$$\begin{aligned} \dot{V}_3(\tilde{z}) \leq &-\gamma\mu|\tilde{z}|^2 + \tilde{z}^T(P \otimes I)(\tilde{a}(\tilde{z}, \tilde{\zeta}, z_1, \zeta_1) - \gamma(\tilde{L} \otimes C_2 N_2)\tilde{\epsilon}) \\ &+ \gamma\,|\tilde{z}|\,\|P\| \int_{-\tau}^{0} \left|\tilde{a}(\tilde{z}, \tilde{\zeta}, z_1, \zeta_1)(t+s)\right| ds \\ &+ \gamma^2\,|\tilde{z}|\,\|P\| \int_{-\tau}^{0} (|\tilde{z}(t+s)| + c\,|\tilde{\epsilon}(t+s)|)ds \\ &+ \gamma^2\,|\tilde{z}|\,\|P\| \int_{-\tau}^{0} (|\tilde{z}(t+s-\tau)| + c|\tilde{\epsilon}(t+s-\tau)|)ds \\ &+ \gamma c\,|\tilde{z}|\,\|P\| \int_{-\tau}^{0} \left|\tilde{\phi}(\tilde{\epsilon}, \tilde{x}, \epsilon_1, x_1)(t+s)\right| ds, \end{aligned} \tag{A.97}$$

with $c = \|C_2\|\|N_2\|$. In addition, ultimate boundedness of the solutions and smoothness of the functions $a(\cdot)$ and $\phi(\cdot)$ imply that

$$\tilde{z}^T(P \otimes I)\tilde{a}(\tilde{z}, \tilde{\zeta}, z_1, \zeta_1) \leq c_3 |\tilde{z}| |\tilde{\zeta}| + c_4 |\tilde{z}|^2 ,$$
$$\tilde{z}^T(P\tilde{A} \otimes C_2N_2)\tilde{\phi}(\tilde{\epsilon}, \tilde{x}, \epsilon_1, x_1) \leq \tilde{c}_2 |\tilde{z}| |\tilde{\epsilon}| + \tilde{c}_3 |\tilde{z}| |\tilde{\zeta}| + \tilde{c}_4 |\tilde{z}|^2 ,$$

for some positive constants $c_3, c_4, \tilde{c}_2, \tilde{c}_3, \tilde{c}_4 \in \mathbb{R}_{>0}$. Let the function $\mathcal{V}(\epsilon, \tilde{\zeta}, \tilde{z}) := V_1(\epsilon) + V_2(\tilde{\zeta}) + V_3(\tilde{z})$ be a Lyapunov-Razumikhin function such that if $\mathcal{V}(\epsilon, \tilde{\zeta}, \tilde{z}) > \varkappa^2\mathcal{V}(\epsilon(t+\theta), \tilde{\zeta}(t+\theta), \tilde{z}(t+\theta))$ for $\theta \in [-2\tau, 0]$ and some constant $\varkappa > 1$, then

$$\begin{aligned}\dot{\mathcal{V}} \leq& -\kappa |\epsilon|^2 - \alpha|\tilde{\zeta}|^2 - (\mu\gamma - \varkappa c_5\Xi - 2\varkappa \|P\| \gamma\Xi - c_4) |\tilde{z}|^2 \\ &+ \sqrt{k}\left(c \|P\| \|\tilde{L}\|\gamma + 2\varkappa c \|P\| \gamma\Xi + \varkappa c_6\Xi\right) |\epsilon| |\tilde{z}| \\ &+ (c_7 + \varkappa c_8\Xi) |\tilde{\zeta}||\tilde{z}|, \end{aligned} \tag{A.98}$$

for some positive constants $c_5, c_6, c_7, c_8 \in \mathbb{R}_{>0}$ and $\Xi = \gamma\tau$. Some straightforward algebra shows that (A.98) is negative definite if

$$\mu > \mu' := \frac{1}{\gamma}(\frac{(c_7 + \varkappa c_8\Xi)^2}{4\alpha} + \varkappa c_5\Xi + c_4) + 2\varkappa \|P\| \Xi,$$

$$\kappa > \kappa' := \frac{k\left(c \|P\| \|\tilde{L}\|\gamma + 2\varkappa c \|P\| \gamma\Xi + \varkappa c_6\Xi\right)^2}{4\gamma(\mu - \mu')},$$

hence, it can be concluded that (A.98) is negative definite if γ is sufficiently large, Ξ is sufficiently small, and $\kappa > \kappa'$; hence, there exist constants γ', Ξ', and κ' such that (A.98) is negative definite if $\gamma > \gamma'$, $\Xi < \Xi'$ and $\kappa > \kappa'$. Then, ultimate boundedness of the solutions and the Lyapunov-Razumikhin theorem implies that the set $\{\text{col}(\epsilon, \tilde{\zeta}, \tilde{z}) = 0\}$ is a global attractor for $\gamma > \gamma'$, $\Xi < \Xi'$, and $\kappa > \kappa'$. ■

A.11 Proof of Theorem 5.4

The existence and uniqueness of the solutions of the coupled systems follows from smoothness of the righthand side of the closed-loop system. By Lemma 5.2, solutions are ultimately bounded for all $t \geq 0$. If there exists a solution X of the matrix equation $(I_k - \Pi) L = X (I_k - \Pi)$ for a given permutation matrix Π, then the set $\mathcal{N}$ defined in Lemma 5.3 defines a linear invariant manifold for the coupled systems (5.14),(5.15). Define the stacked estimation error $\epsilon := \text{col}(\epsilon_1, \ldots, \epsilon_k) \in \mathbb{R}^{km}$, semipassive output $z := \text{col}(z_1, \ldots, z_k) \in \mathbb{R}^{km}$, and internal state $\zeta := \mathrm{col}(\zeta_1, \ldots, \zeta_k) \in \mathbb{R}^{k(n-m)}$. Note that $z \in \ker\left(I_{km} - \Pi \otimes I_m\right)$ and $\zeta \in \ker\left(I_{k(n-m)} - \Pi \otimes I_{n-m}\right)$ define equations of the form

$$z_i - z_j = 0,\ \zeta_i - \zeta_j = 0, \tag{A.99}$$

for some $i, j \in \mathcal{I}$. Let $\mathcal{I}_\Pi$ be the set of pairs (i, j) for which (A.99) is satisfied. We want to show that $z_i - z_j = 0$, $\zeta_i - \zeta_j = 0$, and $\epsilon_i = 0$ restricted to $\mathcal{I}_\Pi$ are globally asymptotically stable under the conditions supplied in the Theorem 5.4. Define

$$\begin{aligned} \bar{\zeta} \quad &: \quad = \left(I_{k(n-m)} - \Pi \otimes I_{n-m}\right)\zeta, \\ \bar{z} \quad &: \quad = \left(I_{km} - \Pi \otimes I_m\right) z. \end{aligned}$$

Note that (H5.4) implies that the internal dynamics (5.20) are exponentially convergent systems with inputs z_i. Assumptions (H5.1) and (H5.4), smoothness of the vector fields, and boundedness of the solutions of the closed-loop system imply the existence of positive definite radially unbounded functions $V_1(\epsilon)$ and $V_2(\bar{\zeta})$ such that

$$\begin{aligned} &\dot{V}_1(\epsilon, x) \le -\kappa|\epsilon|^2 \ \ \forall\ \epsilon, x, \\ &\dot{V}_2(\bar{\zeta}, \bar{z}) \le -\alpha\left|\bar{\zeta}\right|^2 + c_1|\bar{\zeta}||\bar{z}|, \end{aligned}$$

for some constants $c_1, \alpha \in \mathbb{R}_{>0}$ and κ as in (5.13). Let

$$V_3(z) = \frac{1}{2}\left|\bar{z}\right|^2 = \frac{1}{2}\sum_{(i,j)\in\mathcal{I}_\Pi} |z_i - z_j|^2.$$

By Lemma 5.3, there exists X such that $(I - \Pi)L = X(I - \Pi)$. Then, the time derivative of $V_3(\bar{z})$ along the trajectories of the closed-loop system is given by

$$\begin{aligned} \dot{V}_3(\zeta, z, \epsilon) = &\sum_{(i,j)\in\mathcal{I}_\Pi} |z_i - z_j|^T \left(a(\zeta_i, z_i) - a(\zeta_j, z_j)\right) \\ &- \frac{\gamma}{2}\bar{z}^T((X + X^T)\otimes I_m)\bar{z} - \frac{\gamma}{2}\bar{z}^T((X + X^T)\otimes I_m)\bar{\epsilon}, \end{aligned}$$

with $\bar{\epsilon} = (I_{km} - \Pi \otimes I_m)\epsilon$. Again, using smoothness of the vector fields, ultimate boundedness of the solutions, and assumption (H5.3) it follows that

$$\dot{V}_3 \le (c_2 - \gamma\lambda')|\bar{z}|^2 + c_3|\bar{z}||\bar{\zeta}| + \gamma\bar{\lambda}|\bar{z}||\bar{\epsilon}|,$$

for some constants $c_2, c_3 \in \mathbb{R}_{>0}$, $\bar{\lambda} > 0$ being the largest eigenvalue of the symmetric matrix $\frac{1}{2}(X + X^T)$, and λ' the largest number such that (H5.3) holds. Let $\mathcal{V} = V_1 + V_2 + V_3$, then from the previous results, it follows that

$$\dot{\mathcal{V}} \le (c_2 - \gamma\lambda')|\bar{z}|^2 - \kappa|\epsilon|^2 - \alpha|\bar{\zeta}|^2 + (c_1 + c_3)|\bar{\zeta}||\bar{z}| + \gamma\bar{\lambda}c_4|\bar{z}||\epsilon|, \tag{A.100}$$

for some constant $c_4 \in \mathbb{R}_{>0}$. Straightforward computations show that

$$\gamma \quad > \quad \gamma' := \frac{1}{\lambda'}\left(\frac{(c_1+c_3)^2}{4\alpha} + c_2\right), \tag{A.101}$$

$$\kappa \quad > \quad \kappa' := \frac{\bar{\lambda}^2}{4\lambda'}\left(\frac{\gamma^2}{\gamma-\gamma'}\right), \tag{A.102}$$

implies $\dot{\mathcal{V}} \leq -\sigma(|\bar{z}|^2 + |\bar{\zeta}|^2 + |\epsilon|^2)$, for some positive constant σ. Hence, $\dot{\mathcal{V}}$ is negative definite for $\gamma > \gamma'$ and $\kappa > \kappa'$, and therefore the set $\mathcal{N}$ contains a globally asymptotically stable subset for $\gamma > \gamma'$ and $\kappa > \kappa'$. ■

A.12 Proof of Proposition 6.6

Using continuity of the solutions and Leibniz's rule (see [48] for details), $\tilde{\epsilon}_{1\tau}$ can be written as

$$\tilde{\epsilon}_{1\tau} = \tilde{\epsilon}_1 - \int_{-\tau}^{0} \dot{\tilde{\epsilon}}_1(t+s)ds, \tag{A.103}$$

substitution of (A.103) in (6.32),(6.33) yields

$$\dot{\tilde{\epsilon}}_1 = -\kappa\tilde{\epsilon}_1 + \kappa\int_{-\tau}^{0} \dot{\tilde{\epsilon}}_1(t+s)ds - a\tilde{\epsilon}_1 - b\tilde{\epsilon}_2 - 3cy^2\tilde{\epsilon}_2, \tag{A.104}$$

$$\dot{\tilde{\epsilon}}_2 = \tilde{\epsilon}_1. \tag{A.105}$$

Consider the $\mathcal{C}^1$-function $V : \mathbb{R}^2 \to \mathbb{R}_{\geq 0}$ given by

$$V = \frac{1}{2}\left(\lambda\kappa + \lambda a + b\right)\tilde{\epsilon}_2^2 + \lambda\tilde{\epsilon}_1\tilde{\epsilon}_2 + \frac{1}{2}\tilde{\epsilon}_1^2, \tag{A.106}$$

for some positive constant $\lambda \in (0, \kappa + a]$. Notice that for any λ in this interval, it is ensured that (A.106) is positive definite. It can be proved that $y(t)$ in (6.26), (6.27) is uniform bounded, i.e., there exists a constant $\delta > 0$ such that $|y(t)|^2 < \delta$, for all $t \geq 0$. Then, the derivative of (A.106) along the trajectories of (A.104),(A.105) satisfies

$$\begin{aligned}\dot{V} &= -\left(\kappa + a - \lambda\right)\tilde{\epsilon}_1^2 - 3cy^2\tilde{\epsilon}_1\tilde{\epsilon}_2 - \lambda\left(b + 3cy^2\right)\tilde{\epsilon}_2^2 + \kappa\left(\lambda\tilde{\epsilon}_2 + \tilde{\epsilon}_1\right)\int_{-\tau}^{0} \dot{\tilde{\epsilon}}_1(t+s)ds \\ &\leq -\left(\kappa + a - \lambda\right)\tilde{\epsilon}_1^2 + 3c\delta\left|\tilde{\epsilon}_1\right|\left|\tilde{\epsilon}_2\right| - \lambda b\tilde{\epsilon}_2^2 + \kappa\left(\lambda\tilde{\epsilon}_2 + \tilde{\epsilon}_1\right)\int_{-\tau}^{0} \dot{\tilde{\epsilon}}_1(t+s)ds,\end{aligned} \tag{A.107}$$

substitution of (6.32) in (A.107) yields

$$\dot{V} \leq -(\kappa + a - \lambda)\,\tilde{\epsilon}_1^2 + 3c\delta\,|\tilde{\epsilon}_1|\,|\tilde{\epsilon}_2| - \lambda b\tilde{\epsilon}_2^2 \tag{A.108}$$
$$+ \kappa\,(\lambda\,|\tilde{\epsilon}_2| + |\tilde{\epsilon}_1|)\int_{-\tau}^{0} \kappa\,|\tilde{\epsilon}_1(t+s-\tau)| + a\,|\tilde{\epsilon}_1(t+s)|\,ds$$
$$+ \kappa\,(\lambda\,|\tilde{\epsilon}_2| + |\tilde{\epsilon}_1|)\int_{-\tau}^{0} b\,|\tilde{\epsilon}_2(t+s)| + 3c\delta\,|\tilde{\epsilon}_2(t+s)|\,ds.$$

Let $V(\cdot)$ in (A.106) be a Lyapunov-Razumikhin function such that if $\alpha^2 V(\tilde{\epsilon}(t)) < V(\tilde{\epsilon}(t+\theta))$ for $\theta \in [-2\tau, 0]$ and some $\alpha > 1$ (see [48], for details about Lyapunov-Razumikhin functions), then

$$\begin{aligned}\dot{V} &\leq -(\kappa + a - \lambda)\,\tilde{\epsilon}_1^2 + 3c\delta\,|\tilde{\epsilon}_1|\,|\tilde{\epsilon}_2| - \lambda b\tilde{\epsilon}_2^2 \\ &+ \alpha\kappa\tau\,(\lambda\,|\tilde{\epsilon}_2| + |\tilde{\epsilon}_1|)\,((\kappa+a)\,|\tilde{\epsilon}_1| + (b + 3c\delta)\,|\tilde{\epsilon}_2|) \\ &\leq -(\kappa + a - \lambda - (\kappa+a)\,\kappa\alpha\tau)\,\tilde{\epsilon}_1^2 - (\lambda b - \kappa\alpha\tau\lambda\,(b+3c\delta))\,\tilde{\epsilon}_2^2 \\ &+ ((\kappa+a)\,\kappa\alpha\tau\lambda + (b+3c\delta)\,\kappa\alpha\tau + 3c\delta)\,|\tilde{\epsilon}_1|\,|\tilde{\epsilon}_2|\,.\end{aligned}$$

Define $\chi := \kappa\tau$, then

$$\begin{aligned}\dot{V} \quad \leq \quad & -((\kappa+a)\,(1-\alpha\chi) - \lambda)\,\tilde{\epsilon}_1^2 - \lambda\,(b - \alpha\chi\,(b+3c\delta))\,\tilde{\epsilon}_2^2 \\ & + (3c\delta + \alpha\,(b+3c\delta)\,\chi + \lambda\alpha\,(\kappa+a)\,\chi)\,|\tilde{\epsilon}_1|\,|\tilde{\epsilon}_2|\,,\end{aligned} \tag{A.109}$$

by Young's inequality, it follows that $|\tilde{\epsilon}_1|\,|\tilde{\epsilon}_2| \leq \frac{\varepsilon}{2}\,|\tilde{\epsilon}_2|^2 + \frac{1}{2\varepsilon}\,|\tilde{\epsilon}_1|^2$, for some constant $\varepsilon > 0$, then

$$\begin{aligned}\dot{V} \leq &-\left((\kappa+a)\,(1-\alpha\chi) - \lambda - \frac{1}{2\varepsilon}\,(3c\delta + \alpha\,(b+3c\delta)\,\chi + \lambda\alpha\,(\kappa+a)\,\chi)\right)\tilde{\epsilon}_1^2 \\ &- \lambda\left(b - \alpha\chi\,(b+3c\delta) - \frac{\varepsilon}{2}\,(3c\delta + \alpha\,(b+3c\delta)\,\chi + \lambda\alpha\,(\kappa+a)\,\chi)\right)\tilde{\epsilon}_2^2,\end{aligned} \tag{A.110}$$

taking $\varepsilon = \frac{b}{3c\delta}$ and after some straightforward algebra, it can be concluded that (A.110) is negative definite if the following inequalities are satisfied

$$\begin{aligned}3c\delta &> \chi\left(\alpha\,(b+3c\delta) + \lambda\alpha\,(\kappa+a) + \frac{6\alpha c\delta}{b}\,(b+3c\delta)\right), \\ (\kappa+a) &> \chi(b + 3c\delta + (\kappa+a)\left(\lambda + \frac{2b}{3c\delta}\right))\frac{3c\delta\alpha}{2b} + \lambda + \frac{9c^2\delta^2}{2b}.\end{aligned}$$

It follows that $\dot{V}$ is negative definite if κ is sufficiently large and χ is sufficiently small. Thus, there exist constants $\bar{\gamma}$ and $\bar{\chi}$ such that (A.110) is negative definite if $\gamma > \bar{\gamma}$ and $\kappa\gamma < \bar{\chi}$ and by the Lyapunov-Razumikhin theorem [48], the origin of (6.32),(6.33) is globally asymptotically stable for all τ and κ in this region. ■

A.13 Proof of Lemma 7.2

The boundedness assumption in Lemma 7.2 and smoothness of the right-hand side of the closed-loop system imply that the solutions of (7.4)-(7.6),(7.13)-(7.15) exist and are unique. The prediction error is defined as $\epsilon_i = x_i - \eta_i^{\tau_2}$ and the prediction error dynamics is given by (7.16),(7.17). Assumption (H7.1), Proposition 1.5, smoothness of the functions $a(\cdot)$ and $q(\cdot)$, and boundedness of the solutions imply the existence of a positive definite radially unbounded function $V_0 : \mathbb{R}^{n-m} \to \mathbb{R}_{\geq 0}$ such that

$$\dot{V}_0(\epsilon_{1i}, \epsilon_{2i}) \leq -\alpha|\epsilon_{1i}|^2 + c_0|\epsilon_{1i}|\,|\epsilon_{2i}|\,, \tag{A.111}$$

for some constants $\alpha, c_0 \in \mathbb{R}_{>0}$, see Section 5 in Ref. [104] for further details. Using Leibniz's rule ϵ_{2i}^{τ} can be written as

$$\epsilon_{2i}^{\tau} = \epsilon_{2i} - \int_{-\tau}^{0} \dot{\epsilon}_{2i}(t+s)ds, \tag{A.112}$$

it follows that the prediction error dynamics (7.17) can be written as

$$\begin{aligned}\dot{\epsilon}_{2i} &= a(\zeta_i, y_i) - a(\zeta_i - \epsilon_{1i}, y_i - \epsilon_{2i}) \\ &\quad - \kappa\epsilon_{2i} + \kappa \int_{-\tau}^{0} \dot{\epsilon}_{2i}(t+s)ds,\end{aligned} \tag{A.113}$$

substitution of (7.17) in (A.113) yields

$$\begin{aligned}\dot{\epsilon}_{2i} &= a(\zeta_i, y_i) - a(\zeta_i - \epsilon_{1i}, y_i - \epsilon_{2i}) \\ &\quad - \kappa\epsilon_{2i} - \kappa^2 \int_{-\tau}^{0} \epsilon_{2i}(t+s-\tau)ds \\ &\quad + \kappa \int_{-\tau}^{0} (a(\zeta_i, y_i)(t+s) - a(\zeta_i - \epsilon_{1i}, y_i - \epsilon_{2i})(t+s))ds.\end{aligned} \tag{A.114}$$

Consider the function $V_1(\epsilon_{2i}) = \frac{1}{2}\epsilon_{2i}^T\epsilon_{2i}$. Then

$$\begin{aligned}\dot{V}_1 &\leq \epsilon_{2i}^T\left(a(\zeta_i, y_i) - a(\zeta_i - \epsilon_{1i}, y_i - \epsilon_{2i})\right) \\ &\quad - \kappa\left|\epsilon_{2i}\right|^2 - \kappa^2\epsilon_{2i}^T \int_{-\tau}^{0} \epsilon_{2i}(t+s-\tau)ds \\ &\quad + \kappa\epsilon_{2i}^T \int_{-\tau}^{0} \left(a(\zeta_i, y_i)(t+s) - a(\zeta_i - \epsilon_{1i}, y_i - \epsilon_{2i})(t+s)\right)ds.\end{aligned} \tag{A.115}$$

Ultimate boundedness of the solutions and smoothness of the function $a(\cdot)$ imply that

$$\epsilon_{2i}^T\left(a(\zeta_i, y_i) - a(\zeta_i - \epsilon_{1i}, y_i - \epsilon_{2i})\right) \leq c_1\left|\epsilon_{2i}\right|^2 + c_2|\epsilon_{2i}||\epsilon_{1i}|,$$

for some constants $c_1, c_2 \in \mathbb{R}_{>0}$. Let the function $\mathcal{V}_1(\epsilon_{1i}, \epsilon_{2i}) := V_0(\epsilon_{1i}) + V_1(\epsilon_{2i})$ be a Lyapunov-Razumikhin function such that if $\mathcal{V}_1(\epsilon_i(t)) > \varkappa^2 \mathcal{V}_1(\epsilon_i(t+\theta))$ for $\theta \in [-2\tau, 0]$ and some constant $\varkappa > 1$, then

$$\begin{aligned} \dot{\mathcal{V}}_1 \quad \leq \quad & -\alpha \left|\epsilon_{1i}\right|^2 - \left(\kappa - c_1 - \varkappa\kappa^2\tau - \varkappa\kappa\tau c_1\right)\left|\epsilon_{2i}\right|^2 \\ & + \left(c_0 + c_2 + \varkappa\kappa\tau c_2\right)\left|\epsilon_{1i}\right|\left|\epsilon_{2i}\right|. \end{aligned} \tag{A.116}$$

The constant $\varkappa$ can be arbitrarily close to one as long as it is greater than one. Then, for the sake of simplicity, we take $\varkappa$ on the boundary $\varkappa = 1$ for the rest of the analysis. Some simple algebra shows that (A.116) is negative definite if

$$\left(\kappa - \kappa'\right) - \left(\kappa + \frac{\bar{c}_1}{\bar{c}_2}\right)\kappa\tau - \frac{1}{2\bar{c}_2}(\kappa\tau)^2 > 0, \tag{A.117}$$

with

$$\kappa' := \frac{\left(c_0 + c_2\right)^2}{4\alpha} + c_1, \tag{A.118}$$

$$\bar{c}_1 := \frac{2\alpha c_1 + c_0 c_2 + c_2^2}{c_2^2}, \quad \bar{c}_2 := \frac{2\alpha}{c_2^2}. \tag{A.119}$$

All the constants in (A.117) are positive by construction and κ and τ are nonnegative by definition. Then, a necessary condition for (A.117) to be satisfied is that $\kappa > \kappa'$. After some straightforward computations (A.117) can be rewritten as follows

$$\tau < -\left(\bar{c}_2 + \frac{\bar{c}_1}{\kappa}\right) \pm \sqrt{\left(\bar{c}_2 + \frac{\bar{c}_1}{\kappa}\right)^2 + 2\bar{c}_2\frac{(\kappa - \kappa')}{\kappa^2}}. \tag{A.120}$$

The total time-delay τ is nonnegative by definition. Hence, in order to satisfy (A.120), it is sufficient to consider the possible positive values of the right-hand side of (A.120), i.e., the positive square root. Then, inequality (A.120) amounts to

$$\tau < \varphi(\kappa) := -\left(\bar{c}_2 + \frac{\bar{c}_1}{\kappa}\right) + \sqrt{\left(\bar{c}_2 + \frac{\bar{c}_1}{\kappa}\right)^2 + 2\bar{c}_2\frac{(\kappa - \kappa')}{\kappa^2}}. \tag{A.121}$$

We are only interested in possible values of $\kappa, \tau \in \mathbb{R}_{\geq 0}$ such that (A.121) is satisfied. Then, we restrict the function $\varphi(\kappa)$ to the set $\mathcal{J} := [\kappa', \infty)$. Next, we prove that the function $\varphi : \mathcal{J} \to \mathbb{R}_{\geq 0}$ is unimodal. The function $\varphi(\cdot)$ is continuous and real-valued on $\mathcal{J}$. Moreover, it is strictly positive on the interior of $\mathcal{J}$, it has a root at $\kappa = \kappa'$, i.e., $\varphi(\kappa') = 0$, and

$$\begin{aligned} \lim_{\kappa\to\infty} \varphi(\kappa) &= \lim_{\kappa\to\infty} \frac{2\bar{c}_2\left(\frac{1}{\kappa} - \frac{\kappa'}{\kappa^2}\right)}{\left(\bar{c}_2 + \frac{\bar{c}_1}{\kappa}\right) + \sqrt{(\bar{c}_2 + \frac{\bar{c}_1}{\kappa})^2 + 2\bar{c}_2\left(\frac{1}{\kappa} - \frac{\kappa'}{\kappa^2}\right)}} \\ &= \frac{2\bar{c}_2\,(0)}{(\bar{c}_2 + 0) + \sqrt{(\bar{c}_2 + 0)^2 + 2\bar{c}_2\,(0)}} = \frac{0}{2\bar{c}_2} = 0. \end{aligned}$$

The function $\varphi(\cdot)$ is differentiable on $\mathcal{J}$, then we can compute its local extrema by computing its critical points. It is easy to verify that $\frac{\partial\varphi(\kappa)}{\partial\kappa} = 0$ only for $\kappa = \kappa_1^*$ and $\kappa = \kappa_2^*$ with

$$\kappa_1^* = \left(1 + \frac{1}{1+2\bar{c}_1}\right)\kappa' + \frac{\sqrt{2\bar{c}_1^2\bar{c}_2\kappa'(1+2\bar{c}_1+2\bar{c}_2\kappa')}}{\bar{c}_2(1+2\bar{c}_1)}, \tag{A.122}$$

$$\kappa_2^* = \left(1 + \frac{1}{1+2\bar{c}_1}\right)\kappa' - \frac{\sqrt{2\bar{c}_1^2\bar{c}_2\kappa'(1+2\bar{c}_1+2\bar{c}_2\kappa')}}{\bar{c}_2(1+2\bar{c}_1)}. \tag{A.123}$$

Then, $\kappa = \kappa_1^*$ and $\kappa = \kappa_2^*$ are the critical points of $\varphi(\kappa)$ and $\varphi(\kappa_1^*)$ and $\varphi(\kappa_2^*)$ are the corresponding global extrema. Notice that $\kappa_1^* > \kappa'$; therefore, κ_1^* belongs to the interior of $\mathcal{J}$. It is difficult to visualize from (A.123) whether κ_2^* is contained in $\mathcal{J}$. Then, we rewrite (A.123) in a more suitable manner. After some algebra (A.123) can be written as follows

$$\kappa_2^* = \frac{2\bar{c}_2\kappa' - \bar{c}_1^2}{\bar{c}_2\left(1 + \bar{c}_1 + \bar{c}_1\sqrt{1 + \frac{1+2\bar{c}_1}{\bar{c}_2\kappa'}}\right)}. \tag{A.124}$$

Notice that the denominator of (A.124) is strictly positive, then the sign of κ_2^* is solely determined by the numerator. Substitution of (A.118) and (A.119) in the numerator of (A.124) yields

$$2\bar{c}_2\kappa' - \bar{c}_1^2 = -\frac{4\alpha c_1\left(c_0c_2 + \alpha c_1\right)}{c_2^2}, \tag{A.125}$$

which is strictly negative. It follows that κ_2^* is strictly negative as well; in consequence, κ_2^* is not contained on $\mathcal{J}$, i.e., $\kappa_2^* \notin \mathcal{J}$. Then, the function $\varphi(\cdot)$ has a unique extremum on $\mathcal{J}$ and it is given by $\varphi(\kappa_1^*)$. Finally, given that $\varphi(\kappa') = 0$, $\lim_{\kappa\to\infty}\varphi(\kappa) = 0$, $\phi(\kappa)$ is strictly positive on the interior of $\mathcal{J}$, and $\varphi(\kappa_1^*)$ is the unique extremum on $\mathcal{J}$, it follows that $\varphi(\kappa_1^*)$ is a unique local maximum on $\mathcal{J}$; therefore, it can be concluded that the function $\varphi(\cdot)$ is a *unimodal function* in the sense of Definition 7.1. Hence, (A.116) is negative definite if $\kappa > \kappa'$ and $\tau < \varphi(\kappa)$. Then, ultimate boundedness of the solutions and the Lyapunov-Razumikhin theorem imply that the set $\{\epsilon_i = 0\}$ is a global attractor for $\kappa > \kappa'$ and $\tau < \varphi(\kappa)$. ■

A.14 Proof of Lemma 7.4

By assumption each system (7.4),(7.6) is strictly $\mathcal{C}^1$-semipassive with input $u_i^{\tau_2}$, output y_i, and radially unbounded function $V(x_i)$. Define the function $W_1(x) := \sum_{i=1}^{k}\nu_i V(x_i)$, where $x = \mathrm{col}(x_1, ..., x_k)$ and the constants ν_i denote the entries of the left eigenvector corresponding to the zero eigenvalue of the Laplacian matrix L, i.e., $\nu = (\nu_1, ..., \nu_k)^T$ and $\nu^T L = \nu^T (D - A) = 0$. Note that L is singular by construction. Moreover, since it is assumed that the graph is strongly connected, then the zero eigenvalue is simple. Using the Perron-Frobenius theorem [29], it can be shown that the vector ν has strictly positive real entries, i.e., $\nu_i > 0$ for all i. Then, by assumption

$$\dot{W}_1(x) \leq \sum_{i=1}^{k} \nu_i \left(y_i^T u_i^{\tau_2} - H(x_i) \right). \tag{A.126}$$

Consider the term

$$\sum_{i=1}^{k} \nu_i y_i^T u_i^{\tau_2} = \gamma \sum_{i=1}^{k} \sum_{j \in \mathcal{E}_i} \nu_i a_{ij} y_i^T (\eta_{2j}^{\tau_2} - \eta_{2i}^{\tau_2}), \tag{A.127}$$

using Young's inequality it follows that

$$\sum_{i=1}^{k} \nu_i y_i^T u_i^{\tau_2} \leq \frac{\gamma}{2} \sum_{i=1}^{k} \sum_{j \in \mathcal{E}_i} \nu_i a_{ij} \Big(2\,|y_i|^2 + |\eta_{2j}^{\tau_2}|^2 + |\eta_{2i}^{\tau_2}|^2 \Big).$$

Notice that if $\kappa = 0$ and $u_i = \mathbf{0}$, the predictor dynamics (7.19),(7.20) is the same as (7.4),(7.5) with $u^{\tau_2} = \mathbf{0}$. Therefore, strict $\mathcal{C}^1$-semipassivity of (7.4),(7.5) implies strict $\mathcal{C}^1$-semipassivity of (7.19)-(7.20) with radially unbounded function $V(\eta_i)$, output η_{2i}, and input $w_i = u_i + \kappa y_i^{\tau_1} - \kappa \eta_{2i}^{\tau}$. Define the functional

$$\begin{aligned} W_2(\eta_t(\theta)) = \sum_{i=1}^{k} \nu_i \Bigg(V(\eta_i) &+ \gamma \sum_{j \in \mathcal{E}_i} a_{ij} \int_{-\tau_2}^{0} |\eta_{2i}(t+s)|^2\, ds \\ &+ \frac{\kappa}{2} \int_{-\tau_1}^{0} |y_i(t+s)|^2\, ds + \frac{\kappa}{2} \int_{-\tau}^{0} |\eta_{2i}(t+s)|^2\, ds \Bigg), \end{aligned}$$

with $\eta = \text{col}(\eta_1, ..., \eta_k)$, $\eta_t(\theta) = \eta(t+\theta) \in \mathcal{C}$, $\theta \in [-\tau, 0]$, and $\mathcal{C} = [-\tau, 0] \to \mathbb{R}^{kn}$ the Banach space of continuous functions mapping the interval $[-\tau, 0]$ into $\mathbb{R}^{kn}$. Then, by assumption

$$\begin{aligned} \dot{W}_2 = \sum_{i=1}^{k} \nu_i \Bigg(\eta_{2i}^T w_i - H(\eta_i) &+ \gamma \sum_{j \in \mathcal{E}_i} a_{ij} \Big(|\eta_{2i}|^2 - |\eta_{2i}^{\tau_2}|^2 \Big) \\ &+ \frac{\kappa}{2} \Big(|y_i|^2 - |y_i^{\tau_1}|^2 + |\eta_{2i}|^2 - |\eta_{2i}^{\tau}|^2 \Big) \Bigg). \end{aligned} \tag{A.128}$$

Consider the term

$$\sum_{i=1}^{k} \nu_i \eta_{2i}^T w_i = \sum_{i=1}^{k} \nu_i \left(\gamma \sum_{j \in \mathcal{E}_i} a_{ij} \eta_{2i}^T \left(\eta_{2j} - \eta_{2i} \right) + \kappa \eta_{2i}^T y_i^{\tau_1} - \kappa \eta_{2i}^T \eta_{2i}^{\tau} \right),$$

using Young's inequality it follows that

$$\sum_{i=1}^{k} \nu_i \eta_{2i}^T w_i \leq \sum_{i=1}^{k} \nu_i \left(\frac{\gamma}{2} \sum_{j \in \mathcal{E}_i} a_{ij} \Big(\left| \eta_{2j} \right|^2 - \left| \eta_{2i} \right|^2 \Big) + \kappa \left| \eta_{2i} \right|^2 + \frac{\kappa}{2} \left| y_i^{\tau_1} \right|^2 + \frac{\kappa}{2} \left| \eta_{2i}^{\tau} \right|^2 \right).$$

Finally, define the functional $W(x_t(\theta), \eta_t(\theta)) := W_1 + W_2$, with $x_t(\theta) = x(t+\theta) \in \mathcal{C}$ and $\theta \in [-\tau, 0]$. Then, combining the previous results

$$\begin{aligned} \dot{W} \leq \sum_{i=1}^{k} \nu_i \Bigg(& - H(x_i) - H(\eta_i) + \frac{\kappa}{2} \left| y_i \right|^2 + \gamma \sum_{j \in \mathcal{E}_i} a_{ij} \left| y_i \right|^2 \\ & + \frac{3\kappa}{2} \left| \eta_{2i} \right|^2 + \frac{\gamma}{2} \sum_{j \in \mathcal{E}_i} a_{ij} \Big(2 \left| \eta_{2i} \right|^2 + \left| \eta_{2j} \right|^2 - \left| \eta_{2i} \right|^2 \Big) \\ & + \frac{\gamma}{2} \sum_{j \in \mathcal{E}_i} a_{ij} \left(|\eta_{2j}^{\tau_2}|^2 - |\eta_{2i}^{\tau_2}|^2 \right) \Bigg), \end{aligned} \tag{A.129}$$

using $\nu^T (D - A) = 0$ and $\max_{i \in \mathcal{I}} \sum_{j \in \mathcal{E}_i} a_{ij} = 1$, it follows that

$$\begin{aligned} \dot{W} \leq & \sum_{i=1}^{k} \nu_i \left(-H(x_i) + \left(\gamma + \frac{3\kappa}{2} \right) \left| y_i \right|^2 \right) \\ & + \sum_{i=1}^{k} \nu_i \left(-H(\eta_i) + \left(\gamma + \frac{3\kappa}{2} \right) \left| \eta_{2i} \right|^2 \right). \end{aligned} \tag{A.130}$$

The function $H(\cdot)$ is strictly positive if its argument is sufficiently large. Moreover, by assumption (H7.2), there exists a positive constant $R \in \mathbb{R}_{>0}$ such that $|x_i| > R$ implies that $H(x_i) - \delta |y_i|^2 > 0$ for some $\delta \in \mathbb{R}_{>0}$. Let $\bar{\delta}$ be the largest δ that satisfies (H7.2), then for (γ, κ) satisfying $\gamma + \frac{3\kappa}{2} \leq \bar{\delta}$ and for sufficiently large $|\varsigma|$ with $\varsigma := \mathrm{col}(x, \eta)$, it follows that $\dot{W} < 0$. The functional W is radially unbounded and positive definite by construction. Hence, there exists a constant $\sigma \in \mathbb{R}_{>0}$ such that $\dot{W}(\varsigma) < 0$ for σ and ς satisfying $W(\varsigma) \geq \sigma$. Then, solutions starting in the set $\{W(\varsigma) \leq \sigma\}$ will remain there for future time since $\dot{W}$ is negative on the boundary $W(\varsigma) = \sigma$. Moreover, for any ς in the set $\{W(\varsigma) \geq \sigma^*\}$ with $\sigma^* > \sigma$, the function $\dot{W}(\varsigma)$ is strictly negative, which implies that, in this set, $W(\varsigma)$ will decrease monotonically until the solutions enter the set $\{W(\varsigma) \leq \sigma\}$ again. Therefore, it can be concluded that the solutions of the closed loop system (7.4),(7.5),(7.19)-(7.22) exist and are ultimately bounded for any finite $\tau \geq 0$ and (γ, κ) satisfying $\gamma + \frac{3\kappa}{2} \leq \bar{\delta}$.
■

A.15 Proof of Theorem 7.6

The existence and uniqueness of the solutions follows from smoothness of the right-hand side of the closed-loop system. By Lemma 7.4, the solutions exist for all $t \in [-\tau, +\infty]$ and are ultimately bounded. Let $\zeta = \mathrm{col}(\zeta_1, ..., \zeta_k) \in \mathbb{R}^{k(n-m)}$, $y = \mathrm{col}(y_1, \ldots, y_k) \in \mathbb{R}^{km}$, $\epsilon_1 = \mathrm{col}(\epsilon_{11}, \ldots, \epsilon_{1k}) \in \mathbb{R}^{k(n-m)}$, and $\epsilon_2 = \mathrm{col}(\epsilon_{21}, \ldots, \epsilon_{2k}) \in \mathbb{R}^{km}$. Define $M \in \mathbb{R}^{(k-1)\times k}$ as

$$M := \begin{pmatrix} \mathbf{1}_{(k-1)\times 1} & -I_{k-1} \end{pmatrix}. \tag{A.131}$$

Introduce the set of coordinates $\tilde{\zeta} = (M \otimes I_{n-m})\zeta$, $\tilde{y} = (M \otimes I_m)y$, $\tilde{\epsilon}_1 = (M \otimes I_{n-m})\epsilon_1$, and $\tilde{\epsilon}_2 = (M \otimes I_m)\epsilon_2$. Note that, $\tilde{y}_1 = y_1 - y_2, \ldots, \tilde{y}_{k-1} = y_1 - y_k$, $\tilde{\zeta}_1 = \zeta_1 - \zeta_2, \ldots, \tilde{\zeta}_{k-1} = \zeta_1 - \zeta_k$, $\tilde{\epsilon}_{11} = \epsilon_{11} - \epsilon_{12}, \ldots, \tilde{\epsilon}_{1(k-1)} = \epsilon_{11} - \epsilon_{1k}$, and $\tilde{\epsilon}_{21} = \epsilon_{21} - \epsilon_{22}, \ldots, \bar{\epsilon}_{2(k-1)} = \epsilon_{21} - \epsilon_{2k}$. Then, it follows that $\tilde{y} = \tilde{\zeta} = 0$ implies that the systems are synchronized. Assumption (H7.1), Proposition 1.5, smoothness of the vector fields, and boundedness of the solutions imply the existence of a positive definite function $V_2 : \mathbb{R}^{(k-1)(n-m)} \to \mathbb{R}_{\geq 0}$, $\tilde{\zeta} \mapsto V_2(\tilde{\zeta})$ such that

$$\dot{V}_2(\tilde{\zeta}, \tilde{y}) \leq -\alpha|\tilde{\zeta}|^2 + c_0|\tilde{\zeta}|\,|\tilde{y}|\,, \tag{A.132}$$

for some constants $\alpha, c_0 \in \mathbb{R}_{>0}$, see Section 5 in Ref. [104] for further details. Notice that

$$\tilde{M} = \begin{pmatrix} 1 & \mathbf{0} \\ \mathbf{1} & -I_{k-1} \end{pmatrix} \to \tilde{M}L\tilde{M}^{-1} = \begin{pmatrix} 0 & * \\ \mathbf{0} & \tilde{L} \end{pmatrix}, \tag{A.133}$$

where L denotes the Laplacian matrix. By assumption, the communication graph is *strongly connected* and the interconnections are mutual, i.e., $a_{ij} = a_{ji}$. Then, the Laplacian matrix is symmetric and its eigenvalues are real. Moreover, the matrix L has an algebraically simple eigenvalue $\lambda_1 = 0$ and $\mathbf{1} = \mathrm{col}(1, \ldots, 1) \in \mathbb{R}^k$ is the corresponding eigenvector [29]. Applying Gerschgorin's theorem [138] about localization of eigenvalues, it can be concluded that the eigenvalues of L are nonnegative, i.e., L is positive semidefinite. Since $spec(\tilde{L}) = spec(L)\backslash\{0\}$, it follows that the matrix $\tilde{L} \in \mathbb{R}^{(k-1)\times(k-1)}$ has eigenvalues $\lambda_2, ..., \lambda_k \in \mathbb{R}_{>0}$ with $0 < \lambda_2 \leq \cdots \leq \lambda_k$. The stacked prediction errors are given by $\epsilon_1 = \zeta - \eta_1^{\tau_2}$ and $\epsilon_2 = y - \eta_2^{\tau_2}$ with $\eta_1 = \mathrm{col}(\eta_{11}, ..., \eta_{1k}) \in \mathbb{R}^{k(n-m)}$ and $\eta_2 = \mathrm{col}(\eta_{21}, ..., \eta_{2k}) \in \mathbb{R}^{km}$. Then, the controller (7.21) can be written in matrix form as follows

$$\begin{aligned} u(t) &= -\gamma\,(L \otimes I_m)\,\eta_2(t) \\ &= -\gamma\,(L \otimes I_m)\,y(t+\tau_2) + \gamma\,(L \otimes I_m)\,\epsilon_2(t+\tau_2), \end{aligned} \tag{A.134}$$

where $u = \mathrm{col}(u_1, ..., u_k) \in \mathbb{R}^{km}$. Denote $\tilde{u} := \mathrm{col}((u_1 - u_2), ..., (u_1 - u_k))$, it follows that

$$\tilde{u}(t) = -\gamma\left(\tilde{L} \otimes I_m\right)\tilde{y}(t+\tau_2) + \gamma\left(\tilde{L} \otimes I_m\right)\tilde{\epsilon}_2(t+\tau_2), \tag{A.135}$$

with $\tilde{L}$ as in (A.133). Then, in the new coordinates, the closed-loop system is given by

$$\dot{\tilde{\zeta}} = \tilde{q}(\tilde{y}, \tilde{\zeta}, y_1, \zeta_1), \tag{A.136}$$
$$\dot{\tilde{y}} = \tilde{a}(\tilde{y}, \tilde{\zeta}, y_1, \zeta_1) - \gamma(\tilde{L} \otimes I_m)\tilde{y}(t) + \gamma(\tilde{L} \otimes I_m)\tilde{\epsilon}_2(t), \tag{A.137}$$

where

$$\tilde{a}(\tilde{y}, \tilde{\zeta}, y_1, \zeta_1) = \begin{pmatrix} a(y_1, \zeta_1) - a(y_1 - \tilde{y}_1, \zeta_1 - \tilde{\zeta}_1) \\ \vdots \\ a(y_1, \zeta_1) - a(y_1 - \tilde{y}_{k-1}, \zeta_1 - \tilde{\zeta}_{k-1}) \end{pmatrix}, \tag{A.138}$$

and

$$\tilde{q}(\tilde{y}, \tilde{\zeta}, y_1, \zeta_1) = \begin{pmatrix} q(y_1, \zeta_1) - q(y_1 - \tilde{y}_1, \zeta_1 - \tilde{\zeta}_1) \\ \vdots \\ q(y_1, \zeta_1) - q(y_1 - \tilde{y}_{k-1}, \zeta_1 - \tilde{\zeta}_{k-1}) \end{pmatrix}. \tag{A.139}$$

Since L is symmetric, then there exists a nonsingular matrix $U \in \mathbb{R}^{(k-1)\times(k-1)}$ such that $\|U\| = 1$ and $U\tilde{L}U^{-1} = \Lambda$, where Λ denotes a diagonal matrix with the nonzero eigenvalues of L as entries. Introduce new coordinates $\bar{y} = (U \otimes I_m)\tilde{y}$ and for consistency of notation $\bar{\zeta} = \tilde{\zeta}$. In the new coordinates, the closed-loop system can be written as

$$\dot{\bar{\zeta}} = \bar{q}(\bar{y}, \bar{\zeta}, y_1, \zeta_1), \tag{A.140}$$
$$\dot{\bar{y}} = \bar{a}(\bar{y}, \bar{\zeta}, y_1, \zeta_1) - \gamma(\Lambda \otimes I_m)\bar{y}(t) + \gamma\,(\Lambda \otimes I_m)\,\bar{\epsilon}_2(t), \tag{A.141}$$

where $\bar{\epsilon}_2 = (U \otimes I_m)\tilde{\epsilon}_2$, $\bar{a}(\bar{y}, \bar{\zeta}, y_1, \zeta_1) := (U \otimes I_m)\tilde{a}((U^{-1} \otimes I_m)\bar{y}, \bar{\zeta}, y_1, \zeta_1)$, and $\bar{q}(\bar{y}, \bar{\zeta}, y_1, \zeta_1) := \tilde{q}((U^{-1} \otimes I_m)\bar{y}, \bar{\zeta}, y_1, \zeta_1)$. Notice that $\bar{y} = \bar{\zeta} = 0$ implies that the systems are synchronized because U is nonsingular. Since stability is invariant under a change of coordinates and $\|U\| = 1$, then from (A.132), it follows that there exists a positive definite function $\bar{V}_2 : \mathbb{R}^{(k-1)(n-m)} \to \mathbb{R}_{\geq 0}$, $\bar{\zeta} \mapsto \bar{V}_2(\bar{\zeta})$ such that

$$\dot{\bar{V}}_2(\bar{\zeta}, \bar{y}) \leq -\alpha|\bar{\zeta}|^2 + c_0|\bar{\zeta}|\,|\bar{y}|\,, \tag{A.142}$$

for some constants $\alpha, c_0 \in \mathbb{R}_{>0}$. Consider the function $V_3(\bar{y}) = \frac{1}{2}\bar{y}^T\bar{y}$. Then

$$\dot{V}_3 \leq -\gamma\lambda_2|\bar{y}|^2 + \bar{y}^T(\bar{a}(\bar{y}, \bar{\zeta}, y_1, \zeta_1) + \gamma(\Lambda \otimes I_m)\bar{\epsilon}_2). \tag{A.143}$$

Ultimate boundedness of the solutions and smoothness of the function $a(\cdot)$ imply that

$$\bar{y}^T\bar{a}(\bar{y}, \bar{\zeta}, y_1, \zeta_1) \leq c_1\,|\bar{y}|^2 + c_2\,|\bar{y}|\,|\bar{\zeta}|,$$
$$\gamma\bar{y}^T(\Lambda \otimes I_m)\bar{\epsilon}_2 \leq \gamma\lambda_k\,|\bar{y}|\,|\bar{\epsilon}_2|,$$

for some positive constants $c_1, c_2 \in \mathbb{R}_{>0}$. Consider the function $\mathcal{V}_2(\bar{\zeta}, \bar{y}) = \bar{V}_2(\bar{\zeta}) + V_3(\bar{y})$, then

$$\dot{\mathcal{V}}_2 \leq -(\gamma\lambda_2 - c_1)\,|\bar{y}|^2 + (c_2 + c_0)\,|\bar{y}|\,|\bar{\zeta}| - \alpha|\bar{\zeta}|^2 + \gamma\lambda_k\,|\bar{y}|\,|\bar{\epsilon}_2|.$$

Next, from the proof of Lemma 7.2, consider the function

$$\mathcal{V}_3(\epsilon_1, \epsilon_2) = \sum_{i=1}^{k} \mathcal{V}_1(\epsilon_{1i}, \epsilon_{2i}) = \sum_{i=1}^{k} V_0(\epsilon_{1i}) + V_1(\epsilon_{2i}), \tag{A.144}$$

with $V_0(\cdot)$ and $V_1(\cdot)$ from (A.111) and (A.115), respectively. Let the function $\mathcal{V}_3(\epsilon_1, \epsilon_2)$ be a Lyapunov-Razumikhin function such that if $\mathcal{V}_3(\epsilon_1(t), \epsilon_2(t)) > \varkappa^2\mathcal{V}(\epsilon_1(t+\theta), \epsilon_2(t+\theta))$, for $\theta \in [-2\tau, 0]$ and some constant $\varkappa > 1$, then from the proof of Lemma 7.2, it follows that

$$\begin{aligned}\dot{\mathcal{V}}_3 \leq{}& -\alpha\,|\epsilon_1|^2 - \left(\kappa - c_1 - \varkappa\kappa^2\tau - \varkappa\kappa\tau c_1\right)|\epsilon_2|^2 \\ &+ (c_0 + c_2 + \varkappa\kappa\tau c_2)\,|\epsilon_1|\,|\epsilon_2|\,.\end{aligned}$$

Finally, consider the function $\mathcal{V}(\bar{x}, \epsilon) = \mathcal{V}_2(\bar{\zeta}, \bar{y}) + \mathcal{V}_3(\epsilon_1, \epsilon_2)$ with $\bar{x} = \mathrm{col}(\bar{\zeta}, \bar{y})$ and $\epsilon = \mathrm{col}(\epsilon_1, \epsilon_2)$. Then, using the fact that $|\bar{\epsilon}_2| \leq \|M\||\epsilon_2| = \sqrt{k}|\epsilon_2|$, taking $\varkappa$ on the boundary $\varkappa = 1$, and combining the previous results, it follows that

$$\begin{aligned}\dot{\mathcal{V}} \leq{}& -\alpha|\bar{\zeta}|^2 - (\gamma\lambda_2 - c_1)\,|\bar{y}|^2 + (c_0 + c_2)\,|\bar{y}|\,|\bar{\zeta}| \\ &- \alpha\,|\epsilon_1|^2 - \left(\kappa - c_1 - \kappa^2\tau - \kappa\tau c_1\right)|\epsilon_2|^2 \\ &+ (c_0 + c_2 + \kappa\tau c_2)\,|\epsilon_1|\,|\epsilon_2| + \gamma\sqrt{k}\lambda_k\,|\bar{y}|\,|\epsilon_2|.\end{aligned} \tag{A.145}$$

Some straightforward algebra shows that (A.145) is negative definite if the following inequalities are satisfied

$$\gamma > \gamma' := \frac{1}{\lambda_2}\left(c_1 + \frac{(c_0 + c_2)^2}{4\alpha}\right) = \frac{\kappa'}{\lambda_2}, \tag{A.146}$$

$$\Big(\kappa - \bar{\kappa}(\gamma)\Big) - \left(\kappa + \frac{\bar{c}_1}{\bar{c}_2}\right)\kappa\tau - \frac{1}{\bar{c}_2}(\kappa\tau)^2 > 0, \tag{A.147}$$

with constants $\kappa', \bar{c}_1, \bar{c}_2 \in \mathbb{R}_{>0}$ from the proof of Lemma 7.2, defined in (A.118) and (A.119), and

$$\begin{cases} \bar{\kappa}(\gamma) := \kappa' + \frac{\sigma'\gamma^2}{\gamma - \gamma'}, \\ \sigma' := \frac{k\lambda_k^2}{4\lambda_2}. \end{cases} \tag{A.148}$$

Since the constants in (A.146) and (A.147) are positive by construction and κ, τ, and γ are nonnegative by definition, then a necessary condition for (A.147) to be satisfied is that $\kappa > \bar{\kappa}(\gamma)$. We are only interested in possible values of $\kappa, \tau, \gamma \in \mathbb{R}_{\geq 0}$

such that (A.146) and (A.147) are satisfied. Then, we restrict the function $\bar{\kappa}(\gamma)$ to the set $\Gamma := (\gamma', \infty)$. It is easy to verify that the function $\bar{\kappa} : \Gamma \to [\bar{\kappa}(2\gamma'), \infty)$ is strictly positive, continuous, and real-valued on Γ. Notice that the inequality (A.147) has the same structure as (A.117), which is the inequality that has to be satisfied to render the origin of the prediction error dynamics (7.16),(7.17) asymptotically stable. The only difference between them is that the delay-free term in (A.117) depends solely on κ while in (A.147) depends on both κ and γ. Then, as in the proof of Lemma 7.2, the inequality (A.147) amounts to

$$\tau < \bar{\varphi}(\kappa, \gamma) := -\left(\bar{c}_2 + \frac{\bar{c}_1}{\kappa}\right) + \sqrt{\left(\bar{c}_2 + \frac{\bar{c}_1}{\kappa}\right)^2 + 2\bar{c}_2 \frac{(\kappa - \bar{\kappa}(\gamma))}{\kappa^2}}. \tag{A.149}$$

Again, we are only interested in possible values of $\kappa, \tau, \gamma \in \mathbb{R}_{\geq 0}$ such that (A.146) and (A.147) are satisfied. Then, we restrict the function $\bar{\varphi}(\kappa, \gamma)$ to the set where $\kappa > \bar{\kappa}(\gamma)$ and $\gamma > \gamma'$, i.e., restricted to $\mathcal{K} := \{\kappa, \gamma \in [\bar{\kappa}(2\gamma'), \infty) \times \Gamma \mid \kappa > \bar{\kappa}(\gamma)\ \}$. The function $\bar{\varphi} : \mathcal{K} \to \mathbb{R}_{\geq 0}$ is continuous and real-valued on $\mathcal{K}$. Moreover, it is strictly positive on the interior of $\mathcal{K}$, it is zero on the curve $\kappa = \bar{\kappa}(\gamma)$, i.e., $(\bar{\varphi} \circ \bar{\kappa})(\gamma) = 0$, and $\lim_{\kappa \to \infty} \bar{\varphi}(\kappa, \gamma) = 0$ for all $\gamma \in \Gamma$. The function $\bar{\varphi}(\cdot)$ is differentiable on $\mathcal{K}$, then we can compute its local extrema by computing its critical points. It is easy to verify that $\frac{\partial \bar{\varphi}(\kappa,\gamma)}{\partial \kappa} = 0$ only for $\kappa = \bar{\kappa}_3^*(\gamma)$ and $\kappa = \bar{\kappa}_4^*(\gamma)$ with

$$\bar{\kappa}_3^* = \left(1 + \frac{1}{1 + 2\bar{c}_1}\right) \bar{\kappa}(\gamma) + \frac{\sqrt{2\bar{c}_1^2 \bar{c}_2 \bar{\kappa}(\gamma)(1 + 2\bar{c}_1 + 2\bar{c}_2 \bar{\kappa}(\gamma))}}{\bar{c}_2(1 + 2\bar{c}_1)}, \tag{A.150}$$

$$\bar{\kappa}_4^* = \left(1 + \frac{1}{1 + 2\bar{c}_1}\right) \bar{\kappa}(\gamma) - \frac{\sqrt{2\bar{c}_1^2 \bar{c}_2 \bar{\kappa}(\gamma)(1 + 2\bar{c}_1 + 2\bar{c}_2 \bar{\kappa}(\gamma))}}{\bar{c}_2(1 + 2\bar{c}_1)}. \tag{A.151}$$

Likewise, $\frac{\partial \bar{\varphi}(\kappa,\gamma)}{\partial \gamma} = 0$ only for $\gamma = 0$ and $\gamma = 2\gamma' = \frac{2\kappa'}{\lambda_2}$. Notice that $\bar{\kappa}_3^*(\gamma) > \bar{\kappa}(\gamma)$ for all $\gamma \in \Gamma$; therefore, $\bar{\kappa}_3^*(\gamma)$ belongs to the interior of $\mathcal{K}$. It is difficult to visualize from (A.151) whether $\bar{\kappa}_4^*(\gamma)$ is contained in $\mathcal{K}$. Then, we rewrite (A.151) in a more suitable manner. After some algebra (A.151) can be written as $\bar{\kappa}_4^*(\bar{\kappa}) = A(\bar{\kappa})\bar{\kappa}(\gamma)$ with

$$A(\bar{\kappa}) := \left(1 + \frac{1}{1 + 2\bar{c}_1}\right) - \frac{\bar{c}_1 \sqrt{4 + \frac{2}{\bar{c}_2 \bar{\kappa}(\gamma)} + \frac{4\bar{c}_1}{\bar{c}_2 \bar{\kappa}(\gamma)}}}{1 + 2\bar{c}_1}. \tag{A.152}$$

Hence, if $A(\bar{\kappa}) < 1$ for all $\bar{\kappa} \in [\bar{\kappa}(2\gamma'), \infty)$, it follows that $\bar{\kappa}_4^*(\bar{\kappa}) = A(\bar{\kappa})\bar{\kappa}(\gamma) < \bar{\kappa}(\gamma)$ for all $\gamma \in \Gamma$ and therefore $\bar{\kappa}_4^*(\bar{\kappa}) \notin \mathcal{K}$. It is easy to check that the function $A(\bar{\kappa})$ does not have any critical points, $\lim_{\bar{\kappa} \to 0+} A(\bar{\kappa}) = -\infty$, and $\lim_{\bar{\kappa} \to \infty} A(\bar{\kappa}) = \frac{2}{1+2\bar{c}_1}$. Then, the function $A(\bar{\kappa})$ does not have any local maxima on the interval $(0, \infty)$ and its greatest value occurs at infinity. It follows that $A(\bar{\kappa}) < 1$ for all $\bar{\kappa} \in [\bar{\kappa}(2\gamma'), \infty)$ if $\frac{2}{1+2\bar{c}_1} < 1$, which is trivially true from the definition of $\bar{c}_1$ in (A.119). Hence, it can be concluded that the function $\bar{\varphi}(\kappa, \gamma)$ has a unique extremum on $\mathcal{K}$ and it is given by $\bar{\varphi}(\bar{\kappa}_3^*(2\gamma'), 2\gamma')$. Finally, given that $\bar{\varphi}(\bar{\kappa}(\gamma), \gamma) = 0$, $\lim_{\kappa\to\infty} \bar{\varphi}(\kappa, \gamma) = 0$ for all $\gamma \in \Gamma$, $\bar{\varphi}(\kappa, \gamma)$ is strictly positive on the interior of $\mathcal{K}$, and $\bar{\varphi}(\bar{\kappa}_3^*(2\gamma'), 2\gamma')$ is the unique extremum on $\mathcal{K}$. It follows that $\bar{\varphi}(\bar{\kappa}_3^*(2\gamma'), 2\gamma')$ is the unique maximum on $\mathcal{K}$ and the function $\bar{\varphi}(\kappa, \gamma)$ is concave. Then, ultimate boundedness of the solutions and the Lyapunov-Razumikhin theorem imply that the set $\{\mathrm{col}(\epsilon, \bar{\zeta}, \bar{z}) = 0\}$ (and therefore $\{\mathrm{col}(\epsilon, \tilde{\zeta}, \tilde{z}) = 0\}$ as well) is a global attractor if $\tau < \varphi(\kappa)$, $\gamma > \gamma'$, $\kappa > \bar{\kappa}(\gamma)$, $\tau < \bar{\varphi}(\kappa, \gamma)$, and $(\gamma, \kappa) \in \mathcal{N}$ with $\mathcal{N}$ the boundedness set defined in Lemma 7.4. ■

Appendix B

Auxiliary Technical Results of Chapter 8

B.1 Ultimately Bounded Solutions

In order to have the synchronization problem well-defined, we require the solutions of the time-delayed coupled systems to be bounded on the whole positive time-axis. Using the notion of *semipassivity*, we present conditions at the level of the dynamics of the individual systems that ensure the whole network to have *uniformly ultimately bounded solutions*. We emphasize that these results are non-trivial. Even if the solutions of individual systems are bounded the solutions of (time-delayed) coupled systems may grow unbounded. To simplify notation, we let $x_i := \text{col}(z_i, y_i)$ and rewrite system (8.1) as

$$\begin{cases} \dot{x}_i = f(x_i, u_i), \\ y_i = h(x_i), \end{cases} \tag{B.1}$$

with $i \in \mathcal{I}$, state $x_i \in \mathbb{R}^n$, input $u_i \in \mathbb{R}^m$, output $y_i \in \mathbb{R}^m$, and sufficiently smooth functions $f : \mathbb{R}^n \times \mathbb{R}^m \to \mathbb{R}^n$ and $h : \mathbb{R}^n \to \mathbb{R}^m$.

Definition B.1. [107]. *Consider the system* (B.1) *and a non-negative function* $V \in \mathcal{C}^r(\mathbb{R}^n, \mathbb{R}_{\geq 0})$*, which is called the storage function. Assume that along solutions* x_i *of* (B.1) *for a given input* u_i *defined on* $[t_0, t]$*, we have*

$$V(x_i(t)) - V(x_i(t_0)) \leq \int_{t_0}^{t} \big((y_i^T u_i)(s) - H(x_i(s))\big)\,\mathrm{d}s, \tag{B.2}$$

with $H \in \mathcal{C}(\mathbb{R}^n, \mathbb{R})$*. Then, system* (B.1) *is called:*

1. *$\mathcal{C}^r$-semi-passive, with respect to input u_i and output y_i, if (B.2) is satisfied with the function $H(\cdot)$ non-negative outside some ball $\mathcal{B} = \mathcal{B}(0, R) \subset \mathbb{R}^n$, i.e., $\exists R > 0$ such that $|x_i(t)| > R \to H(x_i(t)) \geq 0$;*
2. *strictly $\mathcal{C}^r$-semi-passive, with respect to input u_i and output y_i, if (B.2) is satisfied with the function $H(\cdot)$ positive outside some ball $\mathcal{B} = \mathcal{B}(0, R) \subset \mathbb{R}^n$.*

Remark B.2. *If the storage function $V \in \mathcal{C}^1$, then* (B.2) *may be replaced by*

$$\dot{V}(x_i(t)) \leq (y_i^T u_i)(t) - H(x_i(t))$$

along solutions x_i of (B.1) *for given input u_i.*

Remark B.3. *System* (B.1) *is $\mathcal{C}^r$-passive (strictly $\mathcal{C}^r$-passive) if it is $\mathcal{C}^r$-semi-passive (strictly $\mathcal{C}^r$-semi-passive) with $H(\cdot)$ being positive semi-definite (positive definite).*

In light of Remark B.3, a (strictly) $\mathcal{C}^r$-semi-passive system behaves like a (strictly) passive system for large $|x_i(t)|$. From a physical point of view, one may think of a semi-passive system as a passive system with a limited amount of free energy. The class of strictly semi-passive systems includes, e.g., the chaotic Lorenz system [104] and many models that describe the action potential dynamics of individual neurons [136].

Theorem B.4. [132]. *Consider a network of k coupled systems (8.1),(8.2) on the simple and strongly connected graph $\mathcal{G} = (\mathcal{V}, \mathcal{E}, A)$. Let $w_1, w_2, w_3 : [0, \infty) \to [0, \infty)$ be strictly increasing functions and $w_1(0) = w_2(0) = w_3(0) = 0$. Suppose that the systems* (8.1) *are strictly $\mathcal{C}^1$-semi-passive with a storage function $V(\cdot)$ satisfying*

$$w_1(|x_i(t)|) \leq V(x_i(t)) \leq w_2(|x_i(t)|),$$

and the function $H(\cdot)$ is such that

$$H(x_i(t)) \geq w_3(|x_i(t)|) - M,$$

for some constant $M \geq 0$. Then, the solutions of the coupled systems (8.1),(8.2) *are uniformly ultimately bounded.*

Theorem B.5. [132]. *Consider a network of k coupled systems* (8.1),(8.3) *on the simple and strongly connected graph $\mathcal{G} = (\mathcal{V}, \mathcal{E}, A)$. Let $w_1, w_2, w_3 : [0, \infty) \to [0, \infty)$ be strictly increasing functions and $w_1(0) = w_2(0) = w_3(0) = 0$. Suppose that the systems* (8.1) *are strictly $\mathcal{C}^1$-semi-passive with a storage function $V(\cdot)$ satisfying*

$$w_1(|x_i(t)|) \leq V(x_i(t)) \leq w_2(|x_i(t)|),$$

and the function $H(\cdot)$ is such that

$$H(x_i(t)) \geq 2\gamma_{\max}|y_i(t)|^2 + w_3(|x_i(t)|) - M,$$

for some constants $\gamma_{\max} > 0$ and $M \geq 0$. Then, the solutions of the coupled systems (8.1),(8.3) *are uniformly ultimately bounded for $\gamma \in [0, \gamma_{\max})$.*

Notice that the conditions for boundedness of the solutions in networks of full delay coupled systems depend directly on the coupling strength γ. We remark that, under the assumptions of Theorem B.5, the solutions of the network of coupled systems (8.1),(8.3) are uniformly bounded for coupling strengths larger than $\gamma_{\max}$ provided that the time-delay τ is sufficiently small. This result, which is partly presented in Ref. [130], is beyond the scope of this paper. In particular, for the systems that we consider in the next sections the constant $\gamma_{\max}$ can be chosen arbitrarily large.

B.2 Necessary Conditions for Partial Synchronization

Proposition B.6. [135]. *Assume that $A = A^T$ is the adjacency matrix of a simple and strongly connected graph, and that the row sums of A all equal 1. Then A has eigenvalues $1 = \lambda_1 > \lambda_2 \geq \ldots \geq \lambda_k \geq -1$. Given a permutation matrix Π that commutes with A, let Λ_Π be the set of eigenvalues of A with eigenvectors in the set $\mathrm{range}(I - \Pi)$. Then*

- *$\gamma^* < \bar{\gamma}$ only if the largest element of Λ_Π is strictly smaller than λ_2;*
- *$\chi^* > \bar{\chi}$ only if all elements of Λ_Π are in absolute value is strictly smaller than $\max\{|\lambda_2|, |\lambda_k|\}$.*

Proposition B.7. [135]. *Suppose that $L = L^T$ is the Laplacian matrix of a simple and strongly connected graph. Then L has eigenvalues $0 = \lambda_1 < \lambda_2 \leq \ldots \leq \lambda_k$. Given a permutation matrix Π that commutes with L, let Λ_Π be the set of eigenvalues of L with eigenvectors in the set $\mathrm{range}(I - \Pi)$. Then*

- *$\gamma' < \bar{\gamma}$ only if the smallest element of Λ_Π is strictly larger than λ_2;*
- *$\chi' > \bar{\chi}$ only if all elements of Λ_Π are strictly smaller than λ_k.*

Bibliography

[1] Focus issue on control and synchronization of chaos. *Chaos: An Interdisciplinary Journal of Nonlinear Science*, 7(4), 1997.

[2] Special issue on chaos synchronization, control, and applications. *IEEE Transactions on Circuit and Systems-I*, 44(10), 1997.

[3] Special issue on control of chaos and synchronization. *Systems and Control Letters*, 31(5), 1997.

[4] Special issue on chaos control and synchronization. *International Journal of Bifurcation and Chaos*, 12(5), 2002.

[5] Focus issue on control and synchronization in chaotic dynamical systems. *Chaos: An Interdisciplinary Journal of Nonlinear Science*, 13(1), 2003.

[6] Special issue on chaos synchronization and control. *Mathematics and Computers in Simulation*, 58(4-6), 2003.

[7] Focus issue on synchronization in complex networks. *Chaos: An Interdisciplinary Journal of Nonlinear Science*, 18(3), 2008.

[8] Focus issue on synchronization and cascading processes in complex networks. *Chaos: An Interdisciplinary Journal of Nonlinear Science*, 21(2), 2011.

[9] S. Adinandra. *Hierarchical Coordination Control of Mobile Robots. PhD Thesis.* Eindhoven University of Technology, Eindhoven. The Netherlands, 2012.

[10] S. Adinandra, J. Caarls, D. Kostić, and H. Nijmeijer. Towards a flexible transportation in distribution centers: A low-level motion control approach. *In proceedings of the 7th International Conference on Informatics in Control, Automation and Robotocs (ICINCO)*, pages 155–169.

[11] S. Adinandra, J. Caarls, D. Kostić, J. Verriet, and H. Nijmeijer. *Flexible transportation in warehouses. In: Hamberg, R., Verriet, J., Automation in Warehouse Development.* Springer, 2012.

[12] D.K. Agrawal, P. Thiruvenkatanathan, Jize Yan, and A.A. Seshia. Electrically coupled mems oscillators. In *Frequency Control and the European Frequency and Time Forum (FCS), 2011 Joint Conference of the IEEE International*, pages 1–5, May, 2011.

[13] I. Aihara, R. Takeda, T. Mizumoto, T. Otsuka, T. Takahashi, and H. Okuno. Complex and transitive synchronization in a frustrated system of calling frogs. *Physical Review E*, 83:031913, 2011.

[14] V. Andrieu and L. Praly. On the existence of a Kazantzis-Kravaris Luenberger observer. *SIAM Journal on Control and Optimization*, 45:432–456, 2006.

[15] D. Angeli. A Lyapunov approach to incremental stability properties. *IEEE Transactions on Automatic Control*, 47:410–421, 2000.

[16] D. Angeli and E.D. Sontag. Forward completeness, unboundedness observability, and their Lyapunov characterizations. *Systems and Control Letters*, 38:209–217, 1999.

[17] A. Astolfi, D. Karagiannis, and R. Ortega. *Nonlinear and Adaptive Control with Applications*. Springer, 2008.

[18] A. Astolfi, R. Ortega, and A. Venkatraman. A globally exponentially convergent immersion and invariance speed observer for mechanical systems with non-holonomic constraints. *Automatica*, 46:182–189, 2010.

[19] I. Belykh, V. Belykh, and M. Hasler. Generalized connection graph method for synchronization in asymmetrical networks. *Physica D*, 224:42–51, 2006.

[20] I. Belykh, M. Hasler, M. Lauret, and H. Nijmeijer. Synchronization and graph topology. *International Journal of Bifurcation and Chaos*, 15:3423–3433, 2005.

[21] N. Belykh, V. Belykh, and M. Hasler. Hierarchy and stability of partially synchronous oscillations of diffusively coupled dynamical systems. *Physical Review E*, 62:6332–6345, 2000.

[22] V. N. Belykh, I. V. Belykh, and M. Hasler. Connection graph stability method for synchronized coupled chaotic systems. *Physica D*, 195:159–187, 2004a.

[23] V. N. Belykh, I. V. Belykh, and M. Hasler. Blinking model and synchronization in small-world networks with a time-varying coupling. *Physica D*, 195:188–206, 2004b.

[24] Michael V.L Bennett and R.Suzanne Zukin. Electrical coupling and neuronal synchronization in the mammalian brain. *Neuron*, 41:495 – 511, 2004.

[25] B. Björn, N. van de Wouw, and M. Mueller. Convergent systems vs. incremental stability. *Systems and Control Letters*, 62:277–285, 2013.

[26] I. I. Blekhman, A. L. Fradkov, H. Nijmeijer, and A.Y. Pogromsky. On self-synchronization and controlled synchronization. *Systems and Control Letters*, 31(5):299–305, 1997.

[27] I. Blekman. *Synchronization in science and technology*. ASME, New York, 1988.

[28] P. Bliman and G. Trecate. Average consensus problems in networks of agents with delayed communications. *Automatica*, 44:1985–1995, 2008.

[29] B. Bollobas. *Modern Graph Theory*. Springer-Verlag, New York, 1998.

[30] F. Cacace and A. Germani. An observer for a class of nonlinear systems with time varying observation delay. *Systems and Control Letters*, 59:305–312, 2010.

[31] J. Cidras and A. Feijoo. A linear dynamic model for asynchronous wind turbines with mechanical fluctuations. *IEEE Transactions on Power Systems*, 17:681–687, 2002.

[32] J. Cidras, A. Feijoo, and C. Gonzalez. Synchronization of asynchronous wind turbines. *IEEE Transactions on Power Systems*, 17:1162–1169, 2002.

[33] C. A. Czeisler, E. D. Weitzman, M. C. Moore-Ede, J. C. Zimmerman, and R. S. Knauer. Human sleep: Its duration and organization depend on its circadian phase. *Science*, 210:1264–1267, 1980.

[34] R. Danbury and M. Jenkinson. Synchronised servomechanisms-the scalar-field approach. *IET Control Theory and Applications*, 141:261–273, 1994.

[35] C. De Persis and B. Jayawardhana. On the internal model principle in the coordination of nonlinear systems. *IEEE Transactions on Control of Network Systems*, 1:272–282, 2014.

[36] P. DeLellis, M. di Bernardo, and G. Russo. On QUAD, Lipschitz, and contracting vector fields for consensus and synchronization of networks. *IEEE Transactions on Circuit and Systems-I*, 58:576–583, 2011.

[37] B.P. Demidovich. *Lectures on Stability Theory*. Moscow. In Russian, 1967.

[38] A. Denasi, D. Kostić, and H. Nijmeijer. Time delay compensation in bilateral teleoperations using impact. *IEEE Transactions on Control Systems Technology*, 21:704–715, 2013.

[39] F. Dorfler and F. Bullo. Synchronization and transient stability in power networks and non-uniform kuramoto oscillators. *SIAM Journal on Control and Optimization*, 50(3):1616–1642, 2012.

[40] F. Dorfler, M. Chertkov, and F. Bullo. Synchronization in complex oscillator networks and smart grids. *Proceedings of the National Academy of Sciences*, 110:2005–2010, 2013.

[41] K. Engelborghs, T. Luzyanina, and G. Samaey. DDE-BIFTOOL v.2.00: a matlab package for bifurcation analysis of delay differential equations. *Department of Computer Science, Katholieke Universiteit Leuven TW Report*, 330, 2001.

[42] M. Fieldler. Algebraic connectivity of graphs. *Czechoslovak Mathematical Journal*, 23:298–305, 1973.

[43] F. Forni and R. Sepulchre. On differentially dissipative dynamical systems. *9th IFAC Symposium on Nonlinear Control Systems*, 2013.

[44] E. Fridman and U. Shaked. On reachable sets for linear systems with delay and bounded peak inputs. *Automatica*, 39:2005–2010, 2010.

[45] C.M. Gray. Synchronous oscillations in neuronal systems: Mechanisms and functions. *Journal of Computational Neuroscience*, pages 11–38, 1994.

[46] V. Guillermin and A. Pollack. *Differential Topology*. Prentice-Hall, Englewood, 1974.

[47] J. Hale. Diffusive coupling, dissipation, and synchronization. *Journal of Dynamics and Differential Equations*, 9, 1997.

[48] J. Hale and S. Verduyn Lunel. *Introduction to functional differential equations, Applied Mathematical Sciences*. Springer-Verlag, 1993.

[49] A. Hamadeh, G.-B. Stan, R. Sepulchre, and J. Gonçalves. Global state synchronization in networks of cyclic feedback systems. *IEEE Transactions on Automatic Control*, 57:478 – 483, 2012.

[50] D. Heck, C. Heemskerk, J. Koning, A. Abbasi, and H. Nijmeijer. Robust haptic large distance telemanipulation for iter. *Fusion Engineering and Design*, 89:197–210, 2011.

[51] J. Hindmarsh and R. Rose. A model for neuronal bursting using three coupled differential equations. *Proceedings of the Royal Society of London, Series B*, 221:87–102, 1984.

[52] F. Hoppensteadt and E. Izhikevich. Synchronization of mems resonators and mechanical neurocomputing. *IEEE Transactions on Circuit and Systems-I*, 48(2):133–138, 2001.

[53] F. Hutu, S. Cauet, and P. Coirault. Robust synchronization of different coupled oscillators: Application to antenna arrays. *Journal of the Franklin Institute*, 346:413–430, 2009.

[54] C. Huygens. In martinus nijhoff. *Editor, Oeuvres completes of Christiaan Huygens*, 17:156 – 189, 1660.

[55] A. Isidori, L. Marconi, and G. Casadei. Robust output synchronization of a network of heterogeneous nonlinear agents via nonlinear regulation theory. *IEEE Transactions on Automatic Control*, 59:2680–2691, 2014.

[56] D. Karagiannis, D. Carnevale, and A. Astolfi. Invariant manifold based reduced-order observer design for nonlinear systems. *IEEE Transactions on Automatic Control*, 53:2602–2614, 2008.

[57] D. Karagiannis, M. Sassano, and A. Astolfi. Dynamic scaling and observer design with application to adaptive control. *Automatica*, 45:2883–2889, 2009.

[58] N. Kazantzis and C. Kravaris. Nonlinear observer design using Lyapunov's auxiliary theorem. *Systems and Control Letters*, 34:241–247, 1998.

[59] N. Kazantzis and R. Wright. Nonlinear observer design in the presence of delayed output measurements. *Systems and Control Letters*, 54:877–886, 2005.

[60] A. Krener and A. Isidori. Linearization by output injection and nonlinear observers. *Systems and Control Letters*, 3:47–52, 1983.

[61] A. Krener and W. Respondek. Nonlinear observers with linearizable error dynamics. *SIAM Journal on Control and Optimization*, 23:197–216, 1985.

[62] N. Leonard. Multi-agent system dynamics: Bifurcation and behavior of animal groups. *Annual Reviews in Control*, 38:171–183, 2014.

[63] T. Lewis and J. Rinzel. Dynamics of spiking neurons connected by both inhibitory and electrical coupling. *Journal of Computational Neuroscience*, 14:283–309, 2003.

[64] T. Li and J. Zang. Consensus conditions of multi-agent systems with time-varying topologies and stochastic communication noises. *IEEE Transactions on Automatic Control*, 55:2043–2057, 2010.

[65] Z. Li, Z. Duan, G. Chen, and L. Huang. Consensus of multiagent systems and synchronization of complex networks: A unified viewpoint. *IEEE Transactions on Circuit and Systems-I*, 57:213–224, 2010.

[66] S. Lichiardopol, N. van de Wouw, and H. Nijmeijer. Robust disturbance estimation for human-robotic co-manipulation. *International Journal of Robust and Nonlinear Control*, 24:1772–1796, 2014.

[67] Y. Liu and J. Zhao. Generalized output synchronization of dynamical networks using output quasi-passivity. *IEEE Transactions on Circuit and Systems-I*, 59:1290–1298, 2012.

[68] W. Lohmiller and J. Slotine. On contraction analysis for nonlinear systems. *Automatica*, 34:683–695, 1998.

[69] D. Luenberger. Observing the state of a linear system. *IEEE Transactions on Military Electronics*, 8:74–80, 1964.

[70] L. Marquez-Martinez, C. Moog, and M Velasco-Villa. Observability and observers for nonlinear systems with time delays. *Kybernetika*, 4:445–456, 2002.

[71] W. Michiels, K. Engelborghs, P. Vansevenant, and D. Roose. Continuous pole placement for delay equations. *Automatica*, 38:747–761, 2002.

[72] W. Michiels and S. Niculescu. *Stability and stabilization of time-delay systems. An eigenvalue based approach*. SIAM Publications, Philadelphia, 2007.

[73] L. Moreau. Stability of multiagent systems with time-dependent communication links. *IEEE Transactions on Automatic Control*, 50:169–182, 2005.

[74] U. Münz, A. Papachristodoulou, and F. Allgöwer. Delay robustness in consensus problems. *Automatica*, 46:1252–1265, 2010.

[75] C. Murguia, R.H.B. Fey, and H. Nijmeijer. Immersion and invariance observers with time-delayed output measurements. *Communications in Nonlinear Science and Numerical Simulation, submitted*.

[76] C. Murguia, R.H.B. Fey, and H. Nijmeijer. Network synchronization using invariant-manifold-based diffusive dynamic couplings with time-delay. *Automatica, accepted*.

[77] C. Murguia, R.H.B. Fey, and H. Nijmeijer. Network synchronization by dynamic diffusive coupling. *International Journal of Bifurcation and Chaos*, 23:1350076–1350088, 2013.

[78] C. Murguia, R.H.B. Fey, and H. Nijmeijer. Synchronization of identical linear systems and diffusive time-delayed couplings. *IEEE Transactions on Circuit and Systems-I*, 61:1801–1814, 2014.

[79] C. Murguia, R.H.B. Fey, and H. Nijmeijer. Network synchronization of time-delayed coupled nonlinear systems using predictor-based diffusive dynamic couplings. *Chaos: An Interdisciplinary Journal of Nonlinear Science*, 25:023108, 2015.

[80] C. Murguia, R.H.B. Fey, and H. Nijmeijer. Partial network synchronization using diffusive dynamic couplings. *Proceedings of the 19th World Congress of The International Federation of Automatic Control (IFAC)*, Cape Town, South Africa, 2014.

[81] C. Murguia and H. Nijmeijer. Controlled synchronization in networks of nonlinear systems via dynamic coupling. In *3rd IFAC Conference on Analysis and Control of Chaotic Systems*, pages 261–266, June, 2012.

[82] P. Neefs, E. Steur, and H. Nijmeijer. Network complexity and synchronous behavior an experimental approach. *International Journal of Neural Systems*, 20:233–247, 2010.

[83] S. Niculescu. *Delay Effects on Stability: A Robust Control Approach*. Springer-Verlag, New York, 2001.

[84] H. Nijmeijer and M. Mareels. An observer looks at synchronization. *IEEE Transactions on Circuit and Systems-I*, 44:295–319, 1997.

[85] H. Nijmeijer and A. Rodriguez. *Synchronization of mechanical systems*. World Scientific, London, 2003.

[86] E. Nuño, R. Ortega, and L. Basañez. An adaptive controller for nonlinear teleoperators. *Automatica*, 46:155–159, 2010.

[87] E. Nuño, R. Ortega, L. Basañez, and D. Hill. Synchronization of networks of nonidentical Euler-Lagrange systems with uncertain parameters and communication delays. *IEEE Transactions on Automatic Control*, 56:935–941, 2011.

[88] T. Oguchi. Finite spectrum assignment for nonlinear time-delay systems using synchronization-based predictor. *In the Proceedings of the 51st IEEE Conference on Decision and Control*, 2012.

[89] T. Oguchi and H. Nijmeijer. Prediction of chaotic behavior. *IEEE Transactions on Circuits and Systems-I*, 11:2464–2472, 2005.

[90] T. Oguchi and H. Nijmeijer. A synchronization condition for coupled nonlinear systems with time-delay: A frequency domain approach. *International Journal of Bifurcation and Chaos*, 21:2525–2538, 2011.

[91] T. Oguchi, H. Nijmeijer, and T. Yamamoto. Synchronization in networks of chaotic systems with time-delay coupling. *Chaos: An Interdisciplinary Journal of Nonlinear Science*, 18:037108, 2008.

[92] R. Olfati-Saber and M. Murray. Consensus problems in networks of agents with switching topology and time-delays. *IEEE Transactions on Automatic Control*, 49:1520–1533, 2004.

[93] S. Ostojic, N. Brunel, and V. Hakim. Synchronization properties of networks of electrically coupled neurons in the presence of noise and heterogeneities. *Journal of Computational Neuroscience*, 26:369–392, 2008.

[94] A. Pavlov, A.Y. Pogromsky, N. van de Wouw, and H. Nijmeijer. Convergent dynamics, a tribute to Boris Pavlovich Demidovich. *Systems and Control Letters*, 52:257–261, 2004.

[95] J. Peña. *Huygens synchronization of dynamical systems: beyond pendulum clocks. PhD Thesis.* Eindhoven University of Technology, Eindhoven. The Netherlands, 2013.

[96] J. Peña, R.H.B. Fey, and H. Nijmeijer. Synchronization of weakly nonlinear oscillators with Huygens' coupling. *Chaos: An Interdisciplinary Journal of Nonlinear Science*, 23:033118, 2013.

[97] J. Peña, R.H.B. Fey, and H. Nijmeijer. On phase synchronization of oscillators mounted on a movable support. *Proceedings of the 7th European Nonlinear Dynamics Conference (ENOC)*, Rome, 2011.

[98] J. Peña Ramirez, K. Aihara, R.H.B. Fey, and H. Nijmeijer. An improved model for the classical Huygens' experiment on synchronization of pendulum clocks. *Journal of Sound and Vibration*, 333:7248–7266, 2014.

[99] L. Pecora and T. Carroll. Synchronization in chaotic systems. *Physical Review Letters*, 64:821–824, 1990.

[100] Alberto E. Pereda, Sebastian Curti, Gregory Hoge, Roger Cachope, Carmen E. Flores, and John E. Rash. Gap junction-mediated electrical transmission: Regulatory mechanisms and plasticity. *Biochimica et Biophysica Acta (BBA) - Biomembranes*, 1828(1):134 – 146, 2013.

[101] C.S. Peskin. Mathematical aspects of heart physiology. *(Courant Institute of Mathematical Sciences, New York University)*, pages 268–278, 1975.

[102] A. Pikovsky, M. Rosenblum, and J. Kurths. *Synchronization: A universal concept in nonlinear Science*. Cambridge University Press, Cambridge, 2001.

[103] J. Ploeg, N. van de Wouw, and H. Nijmeijer. Lp string stability of cascaded systems : application to vehicle platooning. *IEEE Transactions on Control Systems Technology*, 22:786–793, 2014.

[104] A.Y. Pogromsky. Passivity based design of synchronizing systems. *International Journal of Bifurcation and Chaos*, 8:295–319, 1998.

[105] A.Y. Pogromsky. A partial synchronization theorem. *Chaos: An Interdisciplinary Journal of Nonlinear Science*, 18:037107, 2008.

[106] A.Y. Pogromsky. Erratum: A partial synchronization theorem, chaos 18, 037107 (2008). *Chaos: An Interdisciplinary Journal of Nonlinear Science*, 19:049901, 2009.

[107] A.Y. Pogromsky, T. Glad, and H. Nijmeijer. On diffusion driven oscillations in coupled dynamical systems. *International Journal of Bifurcation and Chaos*, 9:629–644, 1999.

[108] A.Y. Pogromsky and H. Nijmeijer. Coorperative oscillatory behavior of mutually coupled dynamical systems. *IEEE Transactions on Circuit and Systems-I*, 48:152–162, 2001.

[109] A.Y. Pogromsky, G. Santoboni, and H. Nijmeijer. Partial synchronization: From symmetry towards stability. *Physica D*, 172:65–87, 2002.

[110] K. Pyragas. Continuous control of chaos by self-controlling feedback. *Physics Letters A*, 170:421, 1998.

[111] W. Qin and G. Chen. Coupling schemes for cluster synchronization in coupled josephson equations. *Physica D*, 197:375–391, 2004.

[112] W. Ren. On consensus algorithms for double-integrator dynamics. *IEEE Transactions on Automatic Control*, 53:1503–1509, 2008.

[113] W. Ren and E. Atkins. Distributed multi-vehicle coordinated coordinated control via local information exchange. *International Journal of Robust and Nonlinear Control*, pages 1002–1033, 2007.

[114] W. Ren and R. Beard. Consensus seeking in multiagent systems under dynamically changing interaction topologies. *IEEE Transactions on Automatic Control*, 50:655–661, 2005.

[115] W. Ren and R. Beard. *Distributed Consensus in Multi-vehicle Cooperative Control*. Springer-Verlag, London, 2008.

[116] A. Rodriguez and H. Nijmeijer. Coordination of two robot manipulators based on position measurements only. *International Journal of Control*, 74:1311–1323, 2001.

[117] N.F. Rulkov. Images of synchronized chaos: Experiments with circuits. *Chaos: An Interdisciplinary Journal of Nonlinear Science*, 6:262–279, 1996.

[118] A. Sarlette and R. Sepulchre. Control limitations from distributed sensing: theory and extremely large telescope application. *Automatica*, submitted, 2013.

[119] L. Scardovi and R. Sepulchre. Synchronization in networks of identical linear systems. *IEEE Transactions on Automatic Control*, 57:2132–2143, 2010.

[120] C. Scherer and S. Weiland. *Linear matrix inequalities in control.In W.S. Levine (Ed.), The Control Systems Handbook, Second Edition: Control System Advanced Methods*. CRC Press, London, 2011.

[121] S. Shafi, M. Arcak, M. Jovanovic, and A. Packard. Synchronization of diffusively-coupled limit cycle oscillators. *Automatica*, 49:3613 – 3622, 2013.

[122] U. Shaked, I. Yaesh, and E. de Souza. Bounded real criteria for linear time-delay systems. *IEEE Transactions on Automatic Control*, 43:1016–1022, 1998.

[123] S. Sheikholeslam and A. Desoer. Longitudinal control of a platoon of vehicles with no communication of lead vehicle information: A system level study. *IEEE Transactions on Vehicular Technology*, 42:546 – 554, 1993.

[124] W. Singer. Neuronal synchrony: A versitile code for the definition of relations. *Neuron*, 24:49 – 65, 1999.

[125] R. Sipahi, S. Niculescu, C. T. Abdallah, W. Michiels, and K. Gu. Stability and stabilization of systems with time delay. *IEEE Control Systems Magazine*, 31(1):38–65, 2011.

[126] G. Söhl, S. Maxeiner, and K. Willecke. Expression and functions of neuronal gap junctions. *Nature Reviews Neuroscience*, 6:191–200, 2005.

[127] M. Spivak. *A Comprehensive Introduction to Differential Geometry, vol. 1*. Publish or Perish, Inc., 1999.

[128] S. Stankovic, M. Stanojevic, and D. Siljak. Decentralized overlapping control of a platoon of vehicles. *IEEE Transactions on Control Systems Technology*, 8:816 – 832, 2000.

[129] E. Steur. *Synchronization Behavior in Networks of Coupled Systems. PhD Thesis.* Eindhoven University of Technology, Eindhoven. The Netherlands, 2012.

[130] E. Steur, W. Michiels, H. Huijberts, and H. Nijmeijer. Networks of diffusively time-delay coupled systems:conditions for synchronization and its relation to the network topology. *Physica D*, 277:22–39, 2014.

[131] E. Steur, C. Murguia, R.H.B. Fey, and H. Nijmeijer. Synchronization and partial synchronization experiments with networks of time-delay coupled hindmarsh-rose neurons. *International Journal of Bifurcation and Chaos, submitted*.

[132] E. Steur and H. Nijmeijer. Synchronization in networks of diffusively time-delay coupled (semi-)passive systems. *IEEE Transactions on Circuit and Systems-I*, 58(6):1358–1371, 2010.

[133] E. Steur, T. Oguchi, C. van Leeuwen, and H. Nijmeijer. Partial synchronization in diffusively time-delay coupled oscillator networks. *Chaos: An Interdisciplinary Journal of Nonlinear Science*, 22:043144, 2012.

[134] E. Steur, T. Oguchi, C. van Leeuwen, and H. Nijmeijer. Partial synchronization in diffusively time-delay coupled oscillator networks. *Chaos: An Interdisciplinary Journal of Nonlinear Science*, 22:043144, 2012.

[135] E. Steur, T. Oguchi, C. van Leeuwen, and H. Nijmeijer. Partial synchronization in diffusively time-delay coupled oscillator networks. *Chaos: An Interdisciplinary Journal of Nonlinear Science*, 22:043144, 2012.

[136] E. Steur, I. Tyukin, and H. Nijmeijer. Semi-passivity and synchronization of diffusively coupled neuronal oscillators. *Physica D*, 238:2119–2128, 2009.

[137] E. Steur, C. van Leeuwen, and W. Michiels. Partial synchronization manifolds for linearly time-delayed coupled systems. In *21th International Symposium on Mathematical Theory of Networks and Systems (MTNS 2014), Groningen, the Netherlands*, 2014.

[138] G.W. Stewart and J. Sun. *Matrix Perturbation Theory*. NY: Academic, New York, 1990.

[139] S. Strogatz. *Sync: the emerging science of spontaneous Order*. Hyperion, New York, 2003.

[140] Y. Tang, F. Qian, H. Gao, and J. Kurths. Synchronization in complex networks and its application: A survey of recent advances and challenges. *Annual Reviews in Control*, 38:184–198, 2014.

[141] J.R. Terry, K.S. Thornburg, D.J. DeShazer, G.D. VanWiggeren, S. Zhu, P. Ashwin, and R. Roy. Synchronization of chaos in an array of three lasers. *Physical Review E*, 59:4036–4043, 1999.

[142] H. Ünal and W. Michiels. Prediction of partial synchronization in delay-coupled nonlinear oscillators, with application to Hindmarsh-Rose neurons. *Nonlinearity*, 26:3101–3126, 2013.

[143] H. U. Voss. Anticipating chaotic synchronization. *Physical Review E*, 61:5115–5119, 2000.

[144] P. Wieland, R. Sepulchre, and F. Allgöwer. An internal model principle is necessary and sufficient for linear output synchronization. *Automatica*, 5:1068–1074, 2011.

[145] A.T. Winfree. *The geometry of biological time, Interdisciplinary Applied Mathematics, 2nd ed.* Springer, 2001.

[146] C. Wu, J. Lai, H. Yang, G. Turner, L. Chen, and A. Chiang. Heterotypic gap junctions between two neurons in the drosophila brain are critical for memory. *Current Biology*, 21(10):848 – 854, 2011.

[147] C. W. Wu and L. O. Chua. Synchronization in an array of linearly coupled dynamical systems. *IEEE Transactions on Circuit and Systems-I*, 42:430–447, 1995.

[148] S. Yanchuk, Y. Maistrenko, and E. Mosekilde. Partial synchronization and clustering in a system of diffusively coupled chaotic oscillators. *Mathematics and Computers in Simulation*, 54:491–508, 2001.

[149] M. Zanin, J. Buldu, and S. Boccaletti. Networks of springs: A practical approach. *International Journal of Bifurcation and Chaos*, 20:937–942, 2010.

[150] D. Zhao, C. Li, and J. Ren. Speed synchronisation of multiple induction motors with adjacent cross-coupling control. *IET Control Theory and Applications*, 4:119–128, 2009.

[151] J. Zhou, J. Lu, and J. Lü. Pinning adaptive synchronization of a general complex dynamical network. *Automatica*, 44:996–1003, 2008.

Samenvatting

Geregelde Synchronisatie in Netwerken van Diffusief Gekoppelde Dynamische Systemen

Er zijn minimaal twee cruciale aspecten die in beschouwing moeten worden genomen wanneer synchronisatie in netwerken van dynamische systemen wordt bestudeerd. Ten eerste moet de dynamica van de individuele systemen worden bekeken, bijvoorbeeld hun ingangs-uitgangsstabiliteit of hun mate van homogeniteit. Ten tweede moet de uitwisseling van informatie tussen deze systemen worden beschouwd, m.a.w. er moet worden bekeken hoe de systemen in het netwerk informatie over hun toestand communiceren met aangrenzende systemen. Dit proefschrift bestudeert de relatie van deze twee aspecten tot het optreden van synchroon gedrag in netwerken van gekoppelde dynamische systemen. In het bijzonder wordt voor bepaalde klassen van systemen onderzocht welke netwerkstructuren en koppelingen leiden tot synchronisatie van de onderling verbonden systemen. In een netwerk resulteert informatie uitwisseling tussen de systemen onvermijdelijk in tijdsvertragingen vanwege de tijd die nodig is om gegevens te verzenden van het ene systeem naar het andere systeem. Het effect van deze door het netwerk geïnduceerde tijdvertragingen op voorgestelde synchronisatie schema's wordt onderzocht.

Allereerst wordt gefocust op synchronisatie in netwerken van lineaire tijdinvariante systemen. Van ieder systeem in het netwerk wordt aangenomen dat het passief en detecteerbaar is met betrekking tot de koppelingsvariabelen (de meetbare uitgang). De systemen zijn diffusief gekoppeld met een tijdvertraging. Dat wil zeggen dat zij gekoppeld zijn via gewogen, vertraagde verschillen van hun uitgang. We leiden voorwaarden af die ultieme begrensdheid van de oplossingen van de gekoppelde systemen garanderen gebruik makend van de passiviteit van de individuele systemen en Lyapunov-Krasovskii functionalen. Als detecteerbaarheid wordt aangenomen en wordt aangenomen dat aan een aantal andere milde voorwaarden is voldaan wordt bewezen dat er altijd een gebied bestaat in de parameterruimte opgespannen door de koppelingssterkte en de tijdvertraging, het zogenaamde synchronisatiegebied, waarbij de systemen synchroniseren. Vervolgens worden voorspellings-gebaseerde diffusieve dynamische koppelingen voorgesteld die nog steeds synchroon gedrag laten zien als tijdvertragingen in de communicatie toenemen. Anders gesteld, door voorspellingen te introduceren in de koppelingen wordt bewezen dat het synchronisatiegebied kan worden vergroot. Bovendien worden waarnemer-gebaseerde diffusieve dynamische koppelingen voorgesteld om de klassen van synchroniserende systemen uit breiden. Door waarnemers in de gesloten lus op te nemen is de aanname van passiviteit m.b.t. de meetbare uitgang niet meer nodig zolang passiviteit gegarandeerd is m.b.t. een andere uitgangsfunctie.

Vervolgens worden een aantal van deze resultaten uitgebreid naar een bepaalde klasse van niet-lineaire systemen. De begrippen passiviteit en detecteerbaarheid die worden gebruikt bij lineaire systemen worden vervangen door respectievelijk semi-passiviteit en convergentie voor het niet-lineaire geval. Semi-passiviteit en convergentie worden hierbij niet aangenomen m.b.t. de meetbare uitgang. Dit wordt verondersteld te gelden m.b.t. een andere uitgangsfunctie die niet direct wordt gemeten. Indien er echter een niet-lineaire waarnemer bestaat die de semi-passieve uitgang schat op basis van metingen van de beschikbare uitgang, kan deze worden gebruikt om een waarnemer-gebaseerde diffusieve dynamische koppeling te construeren om de systemen onderling te verbinden. Een algemene aanpak is ontwikkeld om de waarnemer dynamica te construeren door gebruik te maken van de begrippen immersie en invariantie. Voldoende voorwaarden worden afgeleid m.b.t. de systemen, de koppelingen, de convergentiesnelheid van de waarnemer en de tijdvertraging die begrensdheid van de oplossingen alsmede synchronisatie van de gekoppelde systemen garanderen.

Het mogelijk optreden van gedeeltelijke synchronisatie wordt ook bestudeerd. Gedeeltelijke synchronisatie is het verschijnsel, waarbij een aantal, minimaal twee, systemen in het netwerk synchroniseren maar niet met ieder systeem in het netwerk. Door gebruik te maken van symmetrieën in het netwerk kunnen lineair invariante hypervlakken van de gekoppelde systemen worden geïdentificeerd. Indien deze hypervlakken aantrekkend zijn, kunnen de systemen in het netwerk gedeeltelijke synchronisatie vertonen. Bewezen wordt dat een lineaire invariant hypervlak gedefinieerd door een symmetrie in het netwerk aantrekkend is, als de interactie tussen de systemen voldoende sterk is en de convergentiesnelheid van de waarnemer hoog genoeg is. Vervolgens wordt een resultaat m.b.t. netwerk synchronisatie gepresenteerd voor het geval dat er een andere tijdvertraging optreedt bij het meten van de uitgang als bij de datatransmissie van de regelaars. Voorspeller-gebaseerde diffusieve dynamische koppelingen gebaseerd op het concept van anticiperende synchronisatie worden voorgesteld om de systemen te verbinden. Aangetoond wordt dat de tijdvertraging bij deze koppelingen toe kan nemen terwijl synchroon gedrag behouden blijft. Dit betekent dat het mogelijk is om het synchronisatiegebied significant uit te breiden door voorspellers te gebruiken.

In het laatste deel van het proefschrift worden een aantal experimentele resultaten gepresenteerd m.b.t. synchronisatie in een netwerk met diffusieve statische koppelingen met tijdvertraging. Hierbij is gebruik gemaakt van een experimentele opstelling bestaande uit een elektronisch equivalent van een aantal gekoppelde zenuwcellen gebaseerd op het Hindmarsh-Rose model. Het is belangrijk om op te merken dat in een praktische situatie niet verwacht kan worden dat de dynamica van de systemen in het netwerk volledig identiek is. De informatie die wordt uitgewisseld tussen de systemen zal vervuild zijn met een zekere mate van ruis en de systemen zelf zullen onderling ook (kleine) verschillen vertonen. Vanwege deze inherente imperfecties kan niet verwacht worden dat de verschillen tussen de toestanden van de systemen naar nul convergeren. Het is noodzakelijk om een verschil tussen deze toestanden toe te staan. Dit verschil moet uiteraard klein genoeg zijn om te kunnen constateren dat deze systemen 'praktisch gesynchroniseerd' zijn. Daarom wordt het begrip (gedeeltelijke) praktische synchronisatie ingevoerd. Dit begrip drukt uit dat in experimenten systemen (gedeeltelijk) gesynchroniseerd genoemd mogen worden indien de verschillen tussen hun uitgangen klein genoeg zijn op een lang, maar eindig, tijdinterval. Eerst wordt praktische synchronisatie van twee diffusief gekoppelde elektronische Hindmarsh-Rose circuits bestudeerd. Vervolgens worden drie experimentele studies gepresenteerd m.b.t. gedeeltelijke praktische synchronisatie. Ten slotte wordt de relatie tussen de voorwaarden voor synchronisatie van symmetrisch gekoppelde systemen en de netwerktopologie experimenteel onderzocht.

Acknowledgements

After more than four years of hard work, I am very glad to have finished my Ph.D. thesis. I would never have been able to complete my dissertation without the guidance and support of several people. First and foremost, I would like to express my deepest and most sincere gratitude to my parents, siblings, and fianceé. I owe them everything.

Gracias mamá y papá por el apoyo ilimitado e incondicional que siempre me han brindado. Gracias a su arduo trabajo tuve la motivación, medios y recursos necesarios para terminar mis estudios profesionales y continuar desarrollándome en mi camino como investigador. Gracias mamá por siempre cuidar de mi salud, tu esfuerzo constante por mejorarla fue parte esencial para alcanzar mis metas profesionales y personales. Gracias papá por enseñarme a ser responsable y que el trabajo duro es la única forma de salir adelante. A mis hermanos Lore, Paty y Quique. Gracias por su motivación constante, por estar en todo momento conmigo. Muy especialmente les agradezco el esfuerzo que han hecho por atender a mi defensa de doctorado.

To my beloved Laura, my gorgeous fianceé. Without Laura, none of this would ever have been possible. At the dark times when we questioned whether coming to the Netherlands was the right decision, when unexpected health problems threatened our future, Laura was always there, and always supported me unconditionally. Laura, thanks for your love and encouragement, for standing beside me throughout all my professional career, for all the late nights and early mornings, and for keeping me sane over the past few years. Thank you for being my muse, editor, proofreader, and sounding board. But most of all, thank you for being my best friend.

I would like to express my special appreciation and gratitude to my supervisor Professor Henk Nijmeijer. Dear Henk, you have been a tremendous mentor for me. I thank you for accepting me into your group, encouraging my research, supporting my attendance at various conferences, and engaging me in new ideas. I enjoyed all our discussions and countless meetings. Thanks for teaching me how to conduct research.

Next, I want to thank my co-supervisor Rob Fey. Dear Rob, I am grateful for having had the opportunity of working with you. Thanks for your guidance and constant support during the last three years of my Ph.D. research. I can never repay you for all the time you spent carefully reading all my manuscripts. Thanks for having been critical, you always made valuable suggestions for improving our results.

I am most grateful to the professors that participated in the committee, Cees van Leeuwen, Lorenzo Marconi, Claudio De Persis, Nathan van de Wouw, and Rutger van Santen. Thanks for their critical reading and evaluation of my thesis and for their valuable comments and feedback.

My gratitude is further extended to the Mexican Council for Science and Technology (CONACYT) for the partial financial support to conduct my Ph.D.

I would like to thank Erik Steur for our collaboration on experimental synchronization, for his help in getting familiarized with the operation of the experimental setup, and for all the technical discussions related to my work. In a direct or indirect way, Erik greatly contributed to my Ph.D. thesis. Likewise, I express my gratitude to Toshiki Oguchi for our collaborations with students. Dear Toshiki, thanks for your friendship and for always having provided insightful comments about my work.

Regarding administrative matters, I want to express my gratitude to Thea Weijers and Hetty van Neerven for their help in getting my residence permit. Likewise, I would like to thank Geertje Janssen-Dols and Petra Aspers for always solving my administrative problems in a friendly way.

Thanks to all the colleagues at the Eindhoven University of Technology, in the D&C and CST groups, with whom I had chats at the coffee corner during many small breaks. Likewise, I would like to extend this gratitude towards Alejandro Alvarez, Juan Francisco Flores Resendiz, Sisdarmanto Adinandra, Eric van den Hoven, Roel Pieters, Alejandro Rodriguez-Angeles, Zhenyu Ye, America Morales, Haitao Xing, Erandi Miranda, Anggera Bayuwindra, Nikolaos Kontaras, Menno Lauret, Roy Canela, Fabiola Gutiérrez, Victor Marin, Simon Chen, Liya Wang, Chia-yu Chang, Janet Chao, Finie Winata, Ying Zhao, and Jingjing Lv with whom I shared lunch, coffee breaks, and many other memorable times including outside the work environment.

Special thanks goes to my housemate César López who shared his friendship with me beyond the scientific environment. Next in line are my office-mates, who are also my friends. Dear Alper and Isaac, thanks for our many discussions, for stimulating conversations, and for all the fun we had at practising sports. This also applies to my former roommates and friends Jonatán Peña Ramírez and Behnam Asadi. Dear Jonatán, thank you for the good times we spent together, for all the help you gave me at my arrival to the Netherlands, and for always being there for me as a selfless friend.

Finally, I would also like to thank my dear friends in México. To Angel González Mendoza, Gerardo Rodriguez Blanca, Leopoldo Martin del Campo, Rogelio Portillo, Eduardo Cruz, Arturo Rivera, Ricardo Guadarrama, Daniel Melendez, Miguel Zepeda, Donovan Rodriguez, and Aquiles Rodriguez. I feel very fortunate to have them as friends.

Carlos Gerardo Murguía Rendón
Eindhoven, The Netherlands
April, 2015.

Curriculum Vitae

Carlos Murguia was born on May 18th 1984 in Mexico City, Mexico. In September 2003, he started his undergraduate education at the Autonomous Metropolitan University (UAM), Mexico City, Mexico. He received his Bachelor degree in Mechanical Engineering in 2007. He continued his education at the Center for Research and Advanced Studies of the National Polytechnic Institute (CINVESTAV), Mexico City, Mexico, where he obtained a Master's degree in Electrical Engineering in 2009, specializing in mechatronics. His master's thesis was entitled "*Lateral Dynamics Control of a Single Rotor Airship*".

In November 2010, Carlos started his PhD research in the Dynamics and Control group at the Department of Mechanical Engineering of Eindhoven University of Technology, working on *controlled synchronization in networks of diffusively coupled nonlinear systems.* The main results of his PhD research are presented in this dissertation. His research interests include nonlinear dynamics, nonlinear control, synchronization, consensus, observer design, and time-delayed systems.